TECHNISCHE UNIVERSITÄT WIEN

DISSERTATION

Energy storage - optimisation of the placement and operation (in a Distribution Grid)

ausgeführt zum Zwecke der Erlangung des akademischen Grades eines Doktors der technischen Wissenschaften

unter der Leitung von
Univ.-Prof. Dr.-Ing. Wolfgang Gawlik
Institut für Energiesysteme und Elektrische Antriebe

eingereicht an der Technischen Universität Wien
Fakultät für Elektrotechnik und Informationstechnik

von
Dipl.-Ing. Markus Heimberger, MA
Matr.-Nr. 0425837
Am Langen Felde 21/1/20
1220 Wien

Wien, Dezember 2015

Markus Heimberger

Contents

Kurzfassung

Die starke Integration von volatilen, erneuerbaren, dezentralen Erzeugungsanlagen in das Stromnetz, kann das elektrische System an seine Grenzen bringen. Durch Kopplung vorhandener Infrastrukturen (Strom-, Gas-, Fernwärmenetz) kann einerseits eine Entlastung des Stromsystems erreicht werden. Andererseits kann eine Reduktion des Primärenergiebedarfs für den Strom- und Wärmebedarf ermöglicht werden. Zusätzlich stellen Speicher ein probates Mittel zum Energie- und Leistungsausgleich zwischen volatiler, erneuerbarer Erzeugung und dem Verbrauch dar.
Diese beiden Ansätze sollen in einer Modellregion, die die österreichischen Gebäude-, Wohnverhältnisse und Energieinfrastrukturmerkmale abbildet, untersucht werden.
Das Ziel dieser Arbeit besteht in der optimalen Platzierung und dem optimalen Betrieb von Speicher- und Umwandlungstechnologien.
Dafür werden in dieser Arbeit folgende Punkte berücksichtigt bzw. erarbeitet:

- Die Modellierung von Strom-, Gas- und Fernwärmenetzen wird so gestaltet, dass sie den in Österreich üblichen Strukturen entsprechen. Für das Stromnetz wird die Direct Current Load Flow (DCLF)-Berechnung (lineare LF-Berechnung) verwendet. Für die Massenströmungsnetze (Gas, Fernwärme) erfolgt die Netzdarstellung so, dass damit ebenso die DCLF-Methode angewandt werden kann. Die lineare Lastflussberechnung hat den Nachteil, dass Netzverluste nicht direkt berücksichtigt werden können. Dies wird in der vorliegenden Arbeit mit einer zusätzlichen Linearisierung der Verluste gelöst.
- Basierend auf statistischen Parametern wird jedem einzelnen Gebäude in der Modellregion ein Gebäudetyp (Ein-, Zwei-, Mehrfamilienhäuser, Wohnanlagen und Landwirtschaft) und ein Errichtungsjahr zugeordnet. Die verschiedenen Gebäudetypen werden in der Region so angeordnet, dass damit städtische und ländliche Gebiete repräsentiert werden (z.B. aufgrund der Leitungslängen und Lastdichten).

- Realistische Verbrauchskurven werden erreicht, indem für jedes Gebäude ein individuelles, elektrisches und thermisches Lastprofil erzeugt wird, das auf statistischen Verbrauchsparametern basiert.
- Für die Produktion wird das maximale Photovoltaik (PV)-Potential der Dachflächen und das maximale Biomassepotenzial in der Modellregion ermittelt und für die Optimierung herangezogen.

Die optimale Platzierung und der optimale Betrieb der Speicher- und Umwandlungstechnologien wird mittels einjährigem Betrachtungszeitraum ermittelt. Dadurch können Langzeit- (saisonaler Ausgleich) und Kurzzeiteffekte (Tagesausgleich) gleichermaßen berücksichtigt werden. Für die Umsetzung der Ganzjahressimulation werden drei repräsentative Wochen (Sommer, Winter und Übergangszeit) generiert und in der Optimierung verwendet.
Die untersuchten Szenarien sind so gestaltet, dass drei Grundfälle berücksichtigt werden:

- "technische"-Sicht: es werden nur die technischen Limitierungen betrachtet und der Speicher- und Umwandlungstechnologiebedarf aufgrund dieser Limitierungen ermittelt (z.B. thermische Leitungsgrenzströme, maximale Transformatorauslastung).
- "gesamte Region": hierbei werden zusätzlich zu den technischen Limitierungen Kosten und Erlöse für den Energieimport bzw. -export am Bilanzknoten einbezogen.
- "nachhaltige Region": dieser Grundfall ist mit jenem der "gesamten Region" vergleichbar. Einzig die Kosten für Energiebezüge sind um den Faktor 100 erhöht. Dadurch soll der gesamte Energiebezug durch die Optimierung minimiert werden, damit ein Maximum der regenerativ erzeugten Energie verwendet wird, die innerhalb der Modellregion erzeugt wird.

Insgesamt werden 31 Szenarien untersucht. Diese Szenarienvariationen werden durch Abänderung verschiedener Parameter generiert. Die geänderten Parameter sind zum Beispiel: Kosten von Speichern oder Umwandlungstechnologien oder Berücksichtigung/ Variation von technischen Limitierungen (z.B. thermischer Grenzstrom von Leitungen, maximale Trafoauslastung).
Szenarien, in denen Ergebnisse einen besonderen Einfluss auf das elektrische Energiesystem haben, werden hochgerechnet. Dabei werden die energetischen und leistungsmäßigen Charakteristika der Modellregion mit dem Einwohnerverhältnis (zwischen Österreich und der Modellregion) auf die Größe von Österreich skaliert und Auswirkungen auf das österreichische Elektroenergiesystem ermittelt.

Abstract

The strong integration of volatile, renewable, decentralized production into the electricity grid, can bring the electrical system to its limits. On the one hand, by coupling existing infrastructures (electric-, gas-, district heating-networks), relief on the electrical system can be achieved. On the other hand, a reduction in the primary energy demand for the electricity and heating demand can be realised. In addition, storages provide an effective option to balance energy and power between the volatile, renewable production and consumption.
These two approaches are investigated in a region, which is modelled in a way to represent the Austrian building-, living- and energy infrastructure-characteristics. Alternatively this region is called "model region". The goal of this work is the optimal placement and optimal operation of storage and conversion technologies.
Therefore in this work the following parts are taken into account or are elaborated:

- The modelling of electric-, gas- and district heating-networks will be designed in a way so that they represent commonly used structures in Austria. For the electricity grid the DCLF-calculation is used, for mass flow networks (gas, district heating), the network representation is carried out in a way so that the DCLF method can be applied too. The linear load flow calculation has the disadvantage in that power losses cannot be considered directly; this problem is solved in this work with an additional linearisation of the losses.
- Based on statistical parameters each individual building is assigned to a building type (single-, double-, multi-family houses, apartment buildings and agriculture) and a construction year. The different building types are located within the region in a way that the structure represents an urban and rural area (e.g. line lengths and load densities).

- Realistically load profiles are achieved by an individual, annual, electrical and thermal load profile generation for each building, these profile generations are based on statistical parameters.
- For the production, the maximum roof Photovoltaic (PV)-potential and biomass-potential in the model region is determined and used in the optimisation.

The placement and operation of the storage- and conversion-technologies will be optimised for a one year period. As a result, long-term (seasonal balancing) and short-term effects (daily balancing) are considered. For the implementation of a whole year simulation, three representative weeks (summer, winter and transitional period) are generated and used in the optimisation.
The investigated scenarios are designed in a way, that three basic cases are considered:

- "technical"-case: only the technical limitations are considered and the storage- and conversion technology-demands are determined according these technical limitations.
- "whole region": in addition to the technical limitations, costs and revenues for the energy import or export at the slack node are considered.
- "ecological region": this case is similar to the "whole region". Only the energy import costs are increased by a factor of 100. The aim is, that the optimisation shall minimise energy imports and maximise the usage of the renewable produce energy within the region.

A total of 31 scenarios are examined. These scenario variations are generated by changing various parameters. For example, the modified parameters are: costs of storage- or conversion-technologies, or consideration/variation of technical limitations (e.g. thermal line currents, maximum transformer loads).
For those scenarios where the results have an particular influence at the electrical power system, results are up-scaled. Therefore the population ratio (between Austria and the model region) is used and energetic and power characteristics of the model region are scaled to the size of Austria and the impact on the Austrian electrical power system is determined.

1 Motivation

The motivation for this research approach will be deduced step-by-step. The need for renewable energy production and energy savings will be aligned. This will be followed by Austrian political targets, which are derived from these energy saving needs. Finally, it will be pointed out why private households and different building standards are important to reach these targets.

1.1 Energy Costs

The entire living standard is based on the permanent presence of energy – whether for daily transportation, heating or the production of goods.
It is of great relevance how our enormous energy needs are satisfied and with which resources. Figure 1.1 shows that Austria, with a renewable energy usage of 27 percent, is already very sustainable. This is due to the heavy use of hydro power, which can be more easily used in Austria than in other European countries. However, further expansion into this energy area is only possible with great difficulty, as the potential of hydro power is reached in most areas.
Still, three quarters of the total gross energy consumption comes from fossil fuels. With 39 percent, oil represents the largest share. In this context, the question of peak oil often arises, and opinions on this often differ. Peak oil describes the moment, where the global oil production reaches its maximum point and the global delivery rate decreases. The question of whether peak oil has already been reached is difficult to answer, but there may be some developments which can be observed [1, p. 51]:

- All major oil fields were discovered more than 50 years ago.
- Since the 1960s, a reduction in oil discovery has been identified.
- Since 1980, the annual consumption has exceeded the annual discoveries.
- Until now over 47 000 deposits have been discovered and the 400 largest fields contain more than 75 percent of the discovered petroleum.

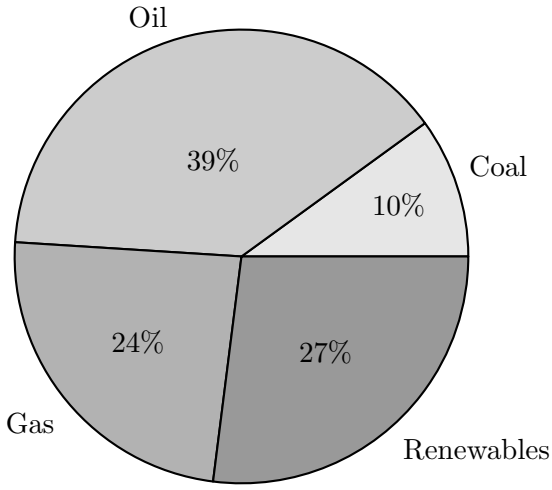

Figure 1.1: Gross energy consumption in Austria; Modified according to [2]

In the last decade, energy prices have risen sharply. This is due to several factors, but have been primarily driven by the depletion of fossil fuels [1, p. 13]. Figure 1.2 shows the oil price trends for the last 100 years. An enormous increase is expected over the next 30 years. This future price development might be seen as a very extreme forecast, however these values are from Gege [3, p. 29]. Currently, the price per barrel is around USD 50. According to Gege [3, p. 29], even though the oil price has been around USD 100 per barrel in the last years, it estimates that there will be a price increase of up to 250 percent over the next 25 years (fig. 1.2). However at the moment, due to shale gas exploration there is an opposite trend. Despite this, it still might be a question of when and not if a price increase will occur. In any case, it is not sure whether such a price development will happen. A discussion about a price increase is not the subject of this work and it is only considered as a possible development. The prices of many other primary resources such as gas and coal are correlated to oil prices, and therefore an increase in the prices of these resources cannot be dismissed. The price of electricity was not related to the price of other primary energy sources. Likewise, for electric power companies in the long term it might not be possible to keep the prices of electric

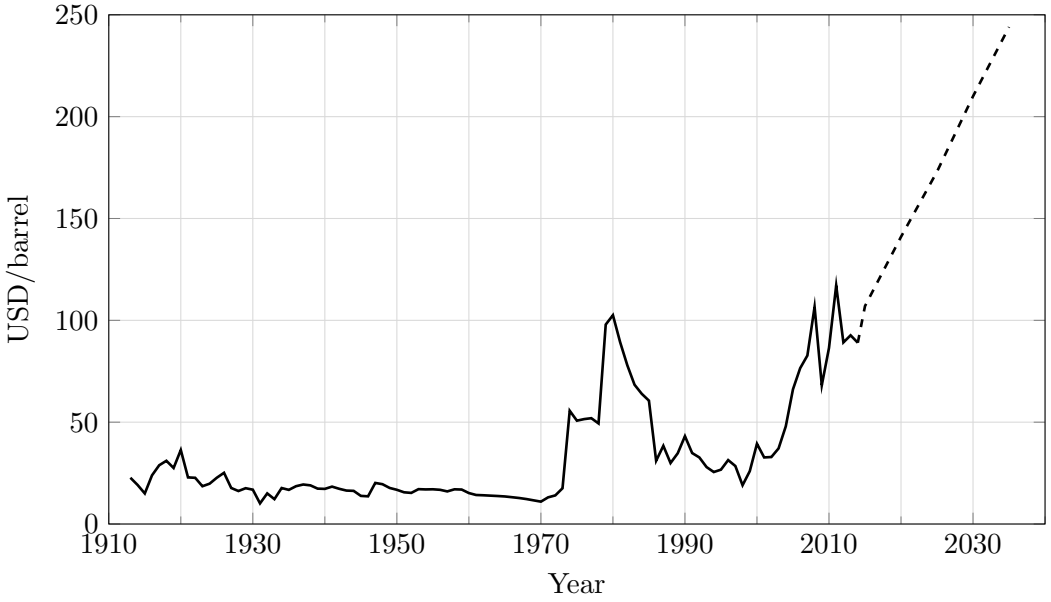

Figure 1.2: USD/barrel for crude oil, historical data (continuous line) are inflation-adjusted (2014=1); Modified according to [4], [3, p. 29]

energy at such a low level. This is due to the ceasing of nuclear energy production in some countries and the strong production dependency on fossil fuels (coal and gas power plants).
These indicators lead to the following conclusion. If there are no structural changes to the energy system, an energy price raise can be expected, but there is another major drawback with the current structure: the environmental issues due to major CO_2-emissions.

1.2 Political Targets

Because of the shortage of reserves/resources and the ecological impact of fossil fuels, European policies state that there should be a drastic reduction in consumption of these energy sources.
The dependence on energy resources, which are not sufficiently available in the European Union (EU), and therefore are often imported from politically unstable countries, should be reduced. This is necessary because a future destabilisation of prices and reliability is likely. This was the case in 2009 with the gas supply from Russia because of the dispute with the Ukraine. Furthermore, by the reduction of fossil fuels usage the anthropogenic

(caused by humans) CO_2-emissions and hence the negative impact on the climate should be reduced, to make sure that the temperature increase stays within the 2 °C range. This is shown apposite in the World Energy Outlook 2008:

> "The world's energy system is at a crossroads. Current global trends in energy supply and consumption are patently unsustainable – environmentally, economically, socially. But that can — and must — be altered; there's still time to change the road we're on. It is not an exaggeration to claim that the future of human prosperity depends on how successfully we tackle the two central energy challenges facing us today: securing the supply of reliable and affordable energy; and effecting a rapid transformation to a low-carbon, efficient and environmentally benign system of energy supply. What is needed is nothing short of an energy revolution [5, p. 39]."

As a result, with the Strategic Energy Technology (SET)-Plan the European Commission has set the 20/20/20 targets [6, p. 2]. These suggest that by 2020

- a reduction in greenhouse gas emissions of 20 percent,
- 20 percent of renewable energy sources in the EU energy mix,
- and a reduction in the EU global primary energy use of 20 percent should be reached.

If these EU targets are allocated to Austria, the following targets have to be achieved [7, p. 18]:

- An increase in the production of renewable energies of up to 34 percent, and usage for transport of up to 10 percent by 2020.
- Greenhouse gas reductions in sectors which are not subject to emissions trading, of at least 16 percent by 2020 relative to the emissions in 2005. For sectors which are subject to the EU emissions trading scheme, an EU-wide reduction of 21 percent was decided.
- An improvement in energy efficiency of 20 percent by the year 2020 based on a baseline scenario was converted directly.

With these requirements, a more sustainable energy supply should be ensured. This is the case when the long term energy usage is less than the supply, and it is socially and economically acceptable. Additionally the living conditions, by taking future energy production into account, would not be deteriorated. [7, p. 25]

Preliminary Research question: What is the most sustainable and/or cost efficient energy supply for Austria?

1.3 Contribution of private households

Of course each sector, e.g. production, transportation and private households have to contribute to reach those goals. For the contribution of the transportation sector, electric vehicles and other alternative transportation methods are being researched extensively [8], [9]. Even the interaction between cars and the grid, and therefore the usage of car batteries as distributed storage with the concept Vehicle-to-Grid (V2G) is being broadly investigated [10].
The production sector varies a lot. Not only between sectors, but even within the same industries, huge differences in energy saving potentials are possible. That is why a general investigation of the whole production sector is not feasible. It might be even necessary to analyse companies individually.
The question is, why should private households be focused on? As shown in figure 1.3, the final energy demand of households in Austria is 26 percent of the total energy demand. After transportation and production, private households are the third largest sector. This is why the focus of this work has led to households. However if there are differences in energy consumption from household to household, they are more homogeneous than the production sector.

Preliminary Research question: What is the most sustainable and/or cost efficient energy supply for private households in Austria?

Figure 1.4 looks at the household energy usage in more detail. If the energy consumption for the annual transportation needs – with a car – is included, the car contributes 33 percent to the total household energy demand. This is in contrast to the total final energy consumption in Austria (fig. 1.3), where transportation was the highest. In households, heating consumption is the highest with almost half of the energy demand (fig. 1.4a). If the energy requirement for transportation with a car is excluded from the household energy needs, heating represents nearly three quarters of the total demand (fig. 1.4b).
The ratio "Hot Water" with 8 or 12 percent should not be disregarded. This category includes the overall energy demand for water heating, including hot water for dishwashers

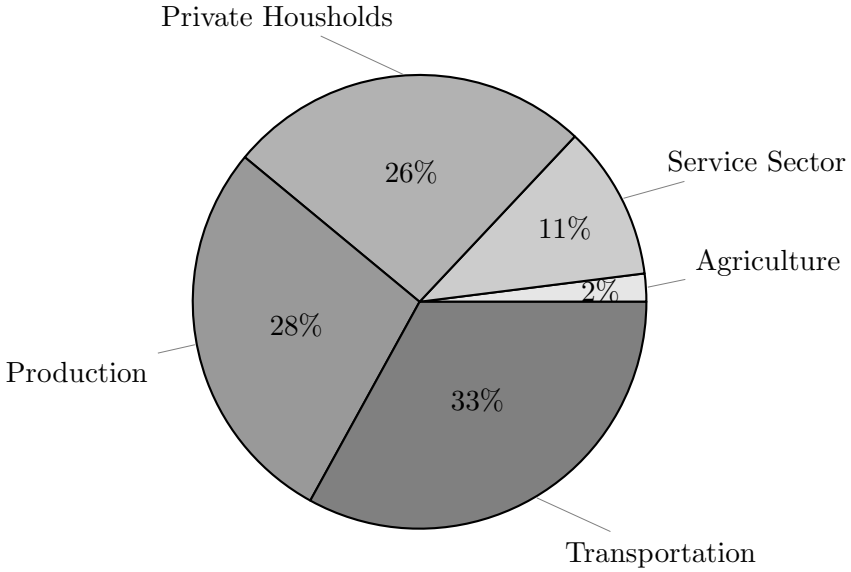

Figure 1.3: Energetic final energy consumption by sectors in Austria; Modified according to [2]

and washing machines. The energy to run these machines is allocated to "Mechanical Energy". This also includes the energy required to run all the electric engines, e.g. for refrigerators and freezers.
With "Process Heat" the energy needed for cooking, drying, ironing and so on is subsumed.
"Inform. & Commun." which means Information and Communication, represents the demand for computers, peripheral equipment and devices for telecommunication and consumer electronics.

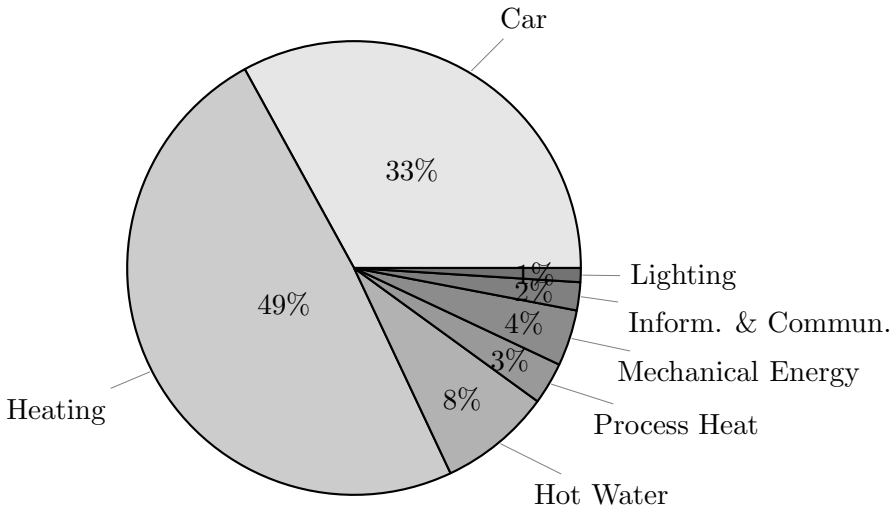

(a) Data including cars

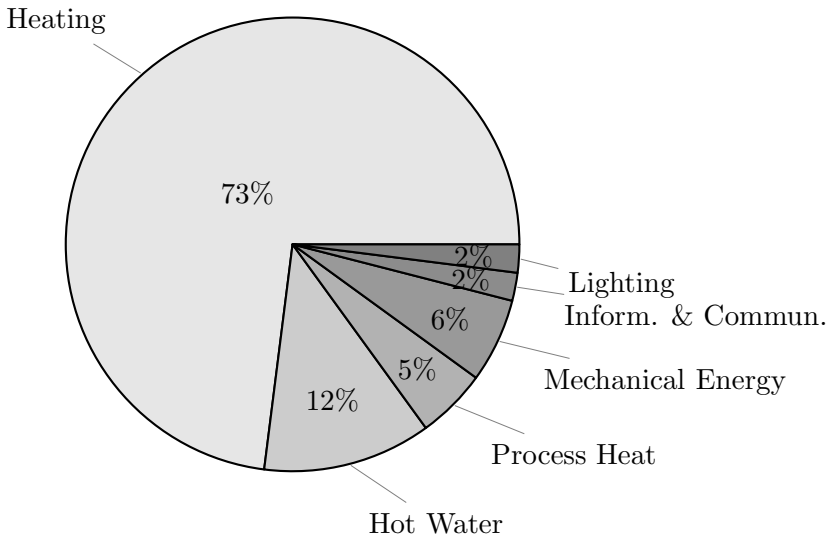

(b) Data without cars

Figure 1.4: Energy consumption in households for different categories; Modified according to [11, p. 9]

The energy demand for heating in households is the highest (fig. 1.4) – regardless whether additional consumption for transportation via a car is taken into account or not. Future developments of this sector have a major impact on how the energy demand for heating is fulfilled best, for example heating directly through electricity or through the use of heat pumps, or even with a separate infrastructure as right now via gas or district heating.

The Austrian standard "OENORM H 5055" [12, p. 7] separates the heating demand of households in nine segments (tab. 1.1). The building classification for passive-, lowest- and low energy house is according to [13]. The spread from old unrenovated buildings to the passive house standard is almost a factor 20. Because of this big difference this is an important factor and has been taken into account.

Table 1.1: Heat demand for different building types; Modified according to [14, p. 140], [12, p. 7], [13]

Heating Demand$_{BGF,Ref}$ [1]		Category	Building Standard
-	$\leq 10\,kWh/m^2a$	A++	Passive House
$> 10\,kWh/m^2a$	$\leq 15\,kWh/m^2a$	A+	Lowest Energy House
$> 15\,kWh/m^2a$	$\leq 25\,kWh/m^2a$	A	
$> 25\,kWh/m^2a$	$\leq 50\,kWh/m^2a$	B	Low Energy House
$> 50\,kWh/m^2a$	$\leq 100\,kWh/m^2a$	C	Conventional new Building
$> 100\,kWh/m^2a$	$\leq 150\,kWh/m^2a$	D	Old unrenovated Buildings
$> 150\,kWh/m^2a$	$\leq 200\,kWh/m^2a$	E	
$> 200\,kWh/m^2a$	$\leq 250\,kWh/m^2a$	F	
$> 250\,kWh/m^2a$	-	G	

Preliminary Research question: What is the most sustainable and/or cost efficient energy supply for private households in Austria, dependent on different building scenarios?

Austria has roughly 2 000 000 buildings [15], it would not be possible to model or optimise the whole building structure. That is why a model region designed for the project "aktives Demand-Side-Management durch Einspeiseprognose (aDSM)"[2] is used [16]. Statistically this region represents the Austrian building circumstances. The model region used, shown in figure 1.5 is described in more detail in section 3.1. The whole optimisation process is carried out for this model region.

Preliminary Research question: What is the most sustainable and/or cost efficient energy supply for a model region, dependent on different building types?

[1] BGF German for: Gross Floor Area (GFA); "Ref" indicates the usage of the reference climate

[2] aDSM – Aktives Demand-Side-Management durch Einspeiseprognose is German for: active Demand-Side-Management through feed-in forecast

Figure 1.5: Model region which is used for the optimisation and represents the Austrian building structure; Modified according to [16, p. 19]

1.4 Decentralised Production

To reduce the dependencies on fossil fuels, a change to a more sustainable energy production would be a solution. This means, producing energy with renewable sources such as PV-systems or wind turbines. In electric systems a balance between production and demand is always necessary. The electricity demand was freely set by individual demands and "conventional" power plants (e.g. gas-, coal- and nuclear-plant) followed this demand. This guaranteed the balance between production and demand. Renewable sources like wind and PV adhere the disadvantage of fluctuated production. They can only produce energy if the sun is shining or wind is blowing. Since both sides in the system are no longer controllable, other solutions are needed to balance the gap between production and demand. One solution is the use of battery storages, another is the uni-, or bidirectional coupling between different energy systems (electric-, gas- and district heating-grid) to achieve more flexibility in production and demand.

All of the aforementioned approaches lead to the following final research question:

What is the most sustainable and/or cost efficient energy supply for a model region? What is the dependency on different building types and what is the best placement and operation of batteries and coupling technologies for different objectives (e.g. sustainability, price)?

2

State of the Art

This chapter gives an overview of related works. Firstly works who describe and model Hybrid Renewable Energy System (HRES) are mentioned, followed by literature where the approach of energy hubs is describes concluded with sources who describe Hybrid Energy Storage System (HESS) and the optimisation of hybrid energy systems.

The work of Deshmukh [17] is a meta-analysis and describes methodologies to model HRES-components, HRES designs and their evaluation. The term HRES is used to describe energy systems with more than one generator type, usually a conventional generator powered by diesel, and a renewable energy source such as PV and wind turbine. It describes usual modelling techniques for PV-, wind energy-, diesel generators and battery-systems gathered from a literature survey. Different methods for HRES evaluations are listed, such as energy to load ratio, battery to load ratio, and non-availability of energy. To select an optimal combination of a HRES to meet the demand, evaluations on reliability and economics of power supply are carried out. For the probability the Loss of Load Probability (LOLP) is used as an indicator, which describes how many hours in a given period cannot be supplied with the renewable sources and the battery system. For the cost criteria the resulting energy production costs are taken as an indicator. The results are:

- A low LOLP results in high system costs and vice versa.
- HRES are mainly suitable for remote area power applications and are cost-effective where expensive grid extension would be necessary.
- Although, there has been an encouraging cost and technological development of HRES in recent years, they remain an expensive source of power.

From [17] some of the mentioned modelling approaches for batteries and PV-systems are used at this work. In the current work, there is also the goal of a cost optimal solution to meet the energy demand of a model region. Additionally to [17] this work optimises the energy demand with different networks and different energy sources (electricity, gas, district heating).

From the scope of the current work [18–23] go one step further as [17], they optimise HRES systems. If two systems are hybridised with storage provision, the reliability can be increased significantly. Even in such cases, sufficient battery bank capacity is required to provide power on extended cloudy and non-windy days. Therefore the optimal system component sizing represents an important part of hybrid power system.
[18–20] are meta-studies, which summarise recent research developments. Physical modelling and several optimisation criteria and optimisation tools are discussed. One mathematical modelling option for PV, wind turbine and engine generators is listed. Various optimisation techniques such as graphical construction, probabilistic approach, iterative technique, Artificial Intelligence (AI), dynamic programming, linear programming, multi-objective and available simulation tools such as "HOMER", "HYBRID2", "INSEL", "RAPISM", "SOLISM", etc. are analysed and compared.
In [21] Particle Swarm Optimisation (PSO) is used as an optimisation algorithm due to its advantages over the other techniques for reducing the Levelised Cost of Energy (LCE). LCE is the price at which energy has to be sold to break even over the lifetime of the technology. For one special system which contains PV, wind turbine, battery bank and one load the optimisation is carried out and the optimal size for the production and storage technologies is derived.
Sharafi [22] uses the ε-constraint method to minimise simultaneously the total system cost, unmet load, and fuel emission. To tackle the multi-objective optimisation problem also a PSO-approach is used. The approach is tested on a case study including a wind turbine, PV-panels, diesel generator, batteries, fuel-cell, electrolyser and hydrogen tank. A comparison of the optimised solutions with the original previous method shows that an improvement in the total cost can be obtained while the same fuel emissions are achieved. A sensitivity analysis indicates that a reduction of battery life time or interest rate increases the total cost and the system is very sensitive to the allowable level of CO_2 emissions, compared to other variables.
All of these five works [18–22] consider HRES systems and their optimisation. Some works [18–20] mention possible optimisation methods and tools, but actually do not optimise HRES systems. The mentioned use of the software GAMS for optimising HRES

systems is realised at this work. [21, 22] optimise only an electric system of PV, wind turbine and battery or an electric- and hydrogen-network. Instead of optimising the size of decentralised productions, in the current work the demand and production are specified. Instead the network(s) (electricity, gas, district heating) and the thermal demand/system are taken into account and the placement and operation of storage- and conversion-technologies of a model region is optimised.

The previous mentioned works consider different energy production sources only for the electricity system. The works [24–27], [28, 29] in [30], [31] in [32] and [33] in [34] deal with multi-carrier energy systems (multi-carrier energy networks). With multi-carrier energy systems, the consideration of electricity-, gas-, and district heating-networks is meant.
All of these works consider this approach from the perspective of "energy-hubs". An example of an energy hub with three input paths (electricity, natural gas and district heating) and two output paths (electricity and heat) is shown in fig. 2.1. Energy hubs

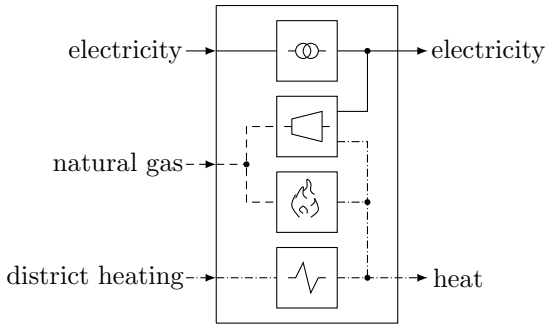

Figure 2.1: Energy hub with three input paths (electricity, natural gas and district heating) and two output paths (electricity and heat); Modified according to [29, p. 2]

are interfaces between energy producers, consumers, and networks. From a system point of view, an energy hub is a unit that provides in- and output, conversion, and storage of multiple energy carriers. Energy hubs serve as interfaces between different infrastructures and network participants (producers, consumers). All works use the modelling concept of $\boldsymbol{L} = \boldsymbol{C} \cdot \boldsymbol{P}$, or enhanced versions, where $\boldsymbol{L}$ represents the output parameters, $\boldsymbol{P}$ the input parameters and $\boldsymbol{C}$ is the coupling matrix, which describes the coupling technologies, e.g. gas burner, micro turbine, etc. The optimisation approaches are either a topological optimisation, an optimisation of the used technologies at the energy hub (coupling matrix) or combinations of both.

Conclusions are:

- The flexible combination of different energy carriers using conversion and storage technology brings the potential for overall energy cost reduction and emission reductions.
- The supply reliability is increased because of the power and network diversification.
- Integration of larger amounts of variable renewable electricity production is possible, compared to an electric-only grid connection.

In [35] each node (building) also contains an energy hub, but the goal is the optimisation from a cost optimal network design perspective. The cost optimal network design is represented via ideal cable or pipe connections and dimensions. The investment costs for the cable or pipe installations and the operation costs for the consideration period are included. Because of the appropriate design decisions, as well as the detailed description of flow dynamics for the different networks, the result is a Mixed Integer Nonlinear Optimisation Problem (MINLOP). Piecewise linearisations are used to transform the MINLOP to a Mixed Integer Linear Optimisation Problem (MILOP). The load-flow of the electric network, which is fully described with the AC Load Flow (ACLF), is approximated with the Power Resistance (PR)-model. This model only considers the active power flow and the real part of the line impedances. The DCLF used at this work is mentioned in [35], but was no option, since it does not include network losses, which are important if it comes to network design optimisations. The gas- and district heating-network are modelled with node pressures u_μ for each node μ, and the load flows $f_{\mu\nu}$ at the branches from node μ to ν. For the calculation of the pressure losses due to pipe friction the "Darcy-Weisbach-equation" is used. The optimisation results for a radial network with 16 nodes (single- and multi-family houses) shows that the energy demand is satisfied exclusively with electricity purchase and the heat production with boilers. No district heating system is installed. Due to the network coupling with a Combined Heat and Power plant (CHP), the objective function can be reduced by 39 %, compared to the decoupled option. This saving has to cover the investment- and operating-costs of the CHP.
The purpose of this work and [35] is different: for this work the networks are specified; it is not part of the optimisation to determine the network topology and branch dimensions, but the optimisation has to place and operate storage- and conversion technologies, to minimise the total costs of the model region.

In [36] the optimal sizing of a HESS is the goal. The HESS is a combination of a Lithium battery and Ultra-Capacitor (UC), which is useful for high energy and high power applications such as Hybrid Electric Vehicles (HEVs) and renewable energy. The used dynamic programming method to optimise the Power Distribution Control Strategy (PDCS) increases the battery life compared to the conventional PDCS. The HESS optimum sizing strongly depends on the load profile. The current work includes the optimal battery placement and sizing in a distribution network, whereas [36] is specially oriented on the sizing for electric vehicles.

[37] is the most relevant work and [38] mentions some of the used modelling strategies. The idea of [37] is to examine whether the integration of decentralised storage technologies and decentralised coupling of existing energy supply infrastructures can obtain new storage potentials in order to assist the massive integration of regenerative producers and relieves higher-level grid structures and units. The impact of the optimal storage operation on the electrical grid operation is as well identified in the project. All analyses are made on two selected model regions (rural and urban) considering the entire estimated regions regenerative potential. The regions energy networks, storage and conversion technologies are implemented in a linear optimisation model. The network calculations shows that massive integration of renewable generation units in the Medium Voltage Grid (MVG) is only possible with additional actions. In both model regions decentralised short-term storages (Li-Ion- and Lead-Acid-batteries) are preferred storage technologies. A tremendous reduction of decentralised storages (85 % to 97 %) in the rural model region is achieved by cutting off just a small quantity of regenerative energy generation (4 % to 5 %). Different scenarios where each represented a different stakeholder are analysed, and depending on the scenario a CO_2 emission saving from 17 % to 62 % is possible.
The differences between this work and [37] are,

- the combination of both regions (urban, rural) in one model region in this work,
- the investigation of the Low Voltage Grid (LVG) instead of the MVG, which has different requirements,
- and most importantly the linear load-flow implementation for a gas- and district-heating-network in this thesis.

3

Method – Model Region

In this chapter the configuration of the model region is described. Firstly the region set-up, such as considered building types and the building arrangement is described. This is then followed by the description of the network modelling for the electric-, gas- and district heating-network. Followed by the description on how the electric and thermal load is modelled. Finally, the modelling of the decentralised production such as PV and biomass is outlined.

3.1 Model Region

The model region used in this thesis was designed in the project aDSM[1] [16]. The aim of the project was the better utilisation of the Low Voltage Grid (LVG) capacities using Demand Side Management (DSM). Therefore typical network cases for Austria had to be found. Although the aim of this thesis is different, it is necessary to use typical network structures. Since an up-scaling of the results to Austria is considered, it is useful to use the same network structures as in aDSM. Two options are possible:

1. The use of one real typical distribution network for an urban and a rural region.
2. Synthetic distribution networks which represents the different network types.

The use of a real network has the advantage, that simulation results can be verified by measurements. The disadvantage of this approach is due to the selection of a typical distribution network. Especially for the rural area, there is a risk that the network features specific characteristics, which do not allow for a generalisation of the results.

[1] aDSM – aktives Demand-Side-Management durch Einspeiseprognose is German for: active Demand-Side-Management through feed-in forecast

When using synthetic networks it is possible to represent different network situations in one area. Furthermore, a freely selected region cross-section is possible and referring to this, a "typical" situation can be modelled. Because of this, a generalisation of the model results is easier. That is why a synthetic network approach was used for aDSM and is also used for this thesis [16, p. 14].
Also, the goals while creating the region will be described. The goal was to represent Austrian living conditions with a virtual region. The "Gebäude- und Wohnugngszählung"[2] was the basis for the region configuration [39]. The "Gebäude- und Wohnugngszählung" provides data for [16, p. 15]:

- Number of buildings per building category.
- Number of households per building category and household size.
- Number of people per building category and household size.

The following building categories are separated [16, p. 15]:

- Residential buildings with associated farm (Agriculture).
- Residential buildings with 1 or 2 apartments (Single-, Double-family House).
- Residential buildings with 3 to 10 apartments (Multi-family House).
- Residential buildings with 11 or more apartments (Apartment Building).
- Residential buildings with additional other usage.
- Non-residential buildings.

The term "apartment" used by Statistics Austria is herein subsequently used as "households". The category "Residential buildings with associated farm" describes both farms and houses with a small farm operated as a sideline. The category "Residential buildings with 1 or 2 apartments" is interpreted subsequently as a combination of single- and double-family houses. Other buildings types would be possible too, which contain only one or two households. However, these should only be constituted as an exception [16, p. 15].
The two categories "residential building with additional other usage" and "non-residential buildings" cannot be associated with a typical building type. The absolute number of principal residences in these two building categories is comparatively low. Therefore, these types of buildings are not considered.
From the raw data, the values of "households per building", "people per household" and

[2] Gebäude- und Wohnugngszählung is German for: building- and apartment counting

"people per building" were calculated for each building category. Furthermore, the relationship between the categories was determined. By following the population definition of the model region, all other characteristics of the region can be calculated. For the size of the aDSM model region the following targets were considered:

- "Reasonable" low voltage network size,
- small rounding error and
- integer numbers for easy scaling.

Table 3.1 lists the results for the model region with the specification of 300 residents and in fig. 3.1 the region mixture is shown graphically.

Table 3.1: Configuration of the aDSM region; Modified according to [16, p. 15]

	Agriculture	Single-, Double-family House	Multi-family House	Apartment Building	Sum
Buildings	8	45	5	2	60
Households (HH)	9	52	27	38	126
People (PPL)	31	137	57	75	300
HH per Building	1.1	1.2	5.4	19.0	2.1
PPL per Household	3.4	2.6	2.1	2.0	2.4
PPL per Building	3.9	3.0	11.4	37.5	5.0

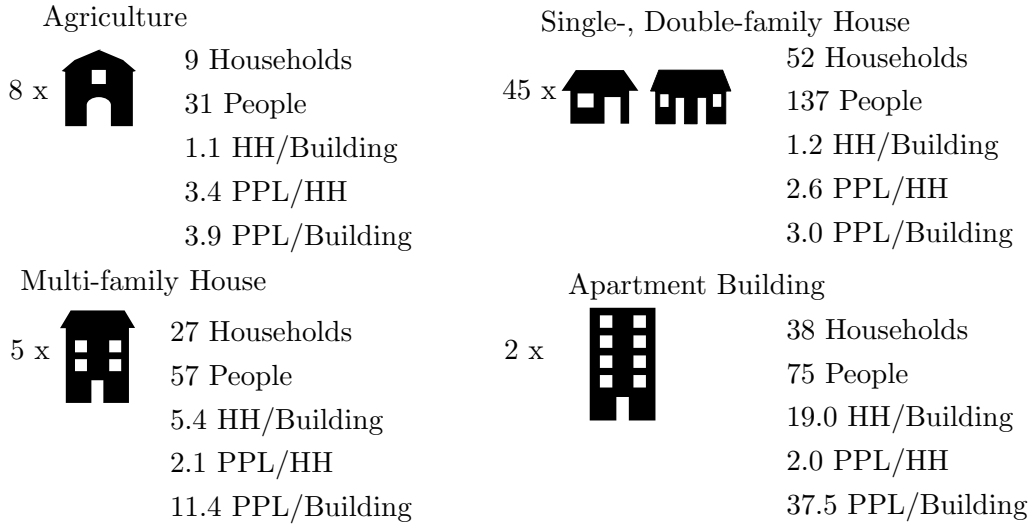

Figure 3.1: Graphical description of the aDSM region configuration; Modified according to [16, p. 15]

Once the configuration of the model region is defined it is necessary to geographically arrange the different buildings. Therefore, experiences in how electric networks are structured were used. These experiences consider typical typologies of LVG, average line length, cable cross sections and load densities. The structure of the grids is substantially depending on the parameter "load density". This parameter describes the sum of all loads in reference to the area. For low load densities, which are typical for rural areas, radial networks are common. Areas with higher load density are often supplied via open rings to allow higher reliability. Since the model region should represent the Austrian circumstances, both regions rural and urban have to be represented; therefore both topologies are used in the model region. The two topologies are shown in fig. 3.6 and are described in more detail at sec. 3.2.1. With this topology approach, the geographical relation between some buildings is already defined in a certain way. The joining link between the electric network characteristics (e.g. cable length and typology) and the geographical arrangement is the building area that is contemplated for each building type. On the one hand, this was used to show that the estimated practical experience of cable lengths fits to a spatial arrangement of the building. On the other hand this helped in creating a fictitious scaled map, in order to create a more accurate picture of the model region.
Single-family houses with a property dimension of $25\,\mathrm{m} \times 25\,\mathrm{m} = 625\,\mathrm{m}^2$ were considered. Double-family houses were modelled using $30\,\mathrm{m} \times 30\,\mathrm{m} = 900\,\mathrm{m}^2$. Residential complexes with three and more households in urban areas were also considered with $30\,\mathrm{m} \times 30\,\mathrm{m}$. The average road width was deposited with 10 m. For the "agriculture" category, different ground areas were taken into account, with a range from $60\,\mathrm{m} \times 60\,\mathrm{m} = 3\,600\,\mathrm{m}^2$ up to $150\,\mathrm{m} \times 150\,\mathrm{m} = 2.25\,\mathrm{ha}$. Here, the complete agricultural land has not been taken into account. The two farms with the largest area are placed at the edge of the model region (top left and bottom left), see fig. 3.4. Thus, the agricultural area theoretically can be extended. [16, p. 18]
All of this leads to the model region shown in fig. 3.2. The open ring – the network area with high load density – contains the two apartment buildings with 11 or more households and most of the multi-family houses that contain 3 or more households. The right bottom corner represents a village area. This occurs in a mixture of relatively densely built single-family houses and smaller farms. As mentioned earlier, the area on the left represents agriculture that is located further away.

The goal of this work is to optimise the placement and operation of storages and conversion technologies. Experiences in the project "SYMBIOSE" [37] showed that high numbers of nodes can cause problems computing the optimisation on regular PC's, from

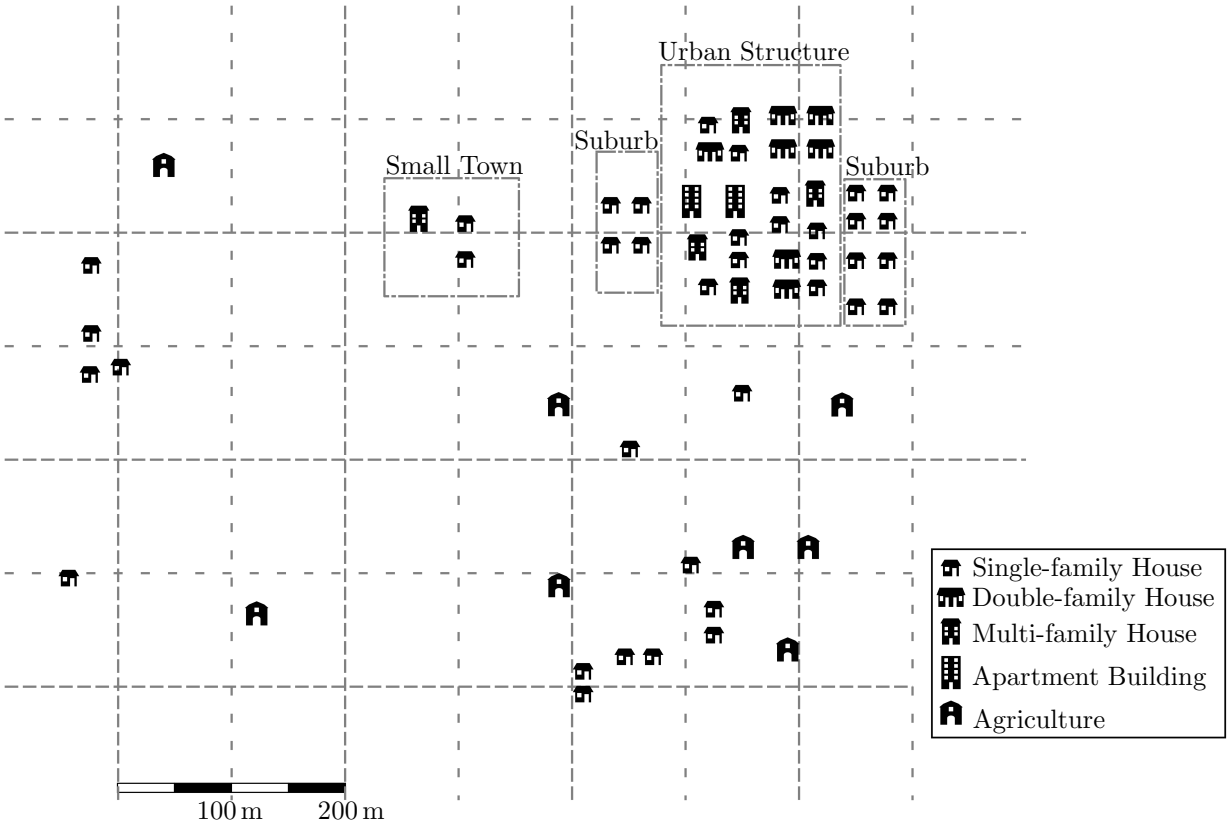

Figure 3.2: The original aDSM region which was used for the node reduction; Modified according to [16, p. 19]

a calculation time purpose, as well as from Random Access Memory (RAM) usage, which can easily exceed the need of 64 GB. Each building or junction between line intersections represents a node. One solution to overcome this problem is a network reduction. This is equivalent to a node number reduction. Since each building is represented as a node, the amount of separated buildings is reduced. Of course this is afflicted with certain information loss. For example, if two buildings are combined, they are placed at the position where originally the furthest away building was placed. Furthest away position means the position furthest from a network perspective. Figure 3.3 illustrates this for the Small Town. On the left, the building structure before the reduction is displayed. For example, if the three lines have the length a, b and c then the line length on the right side is $a + b + c$ and the two single-family houses and the multi-family house are located at the original position of the multi-family house. Even if information is lost,

this approach has the advantage that the circumstances in the network are worst case. If the optimisation finds a solution for the reduced network, this will also work in the not reduced version. That is why this approach is appropriate for the needs of this work.

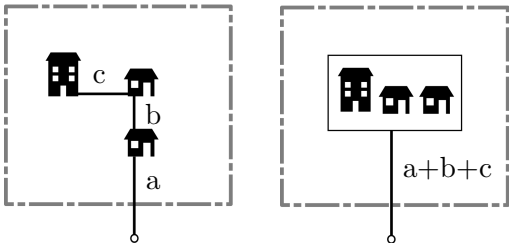

(a) before reduction (b) after reduction

Figure 3.3: Network reduction on the example of the small town

If this reduction is carried out for all buildings, fig. 3.2 leads to the system mentioned at fig. 3.4. The total number of nodes, from originally 72 is reduced to 35. The building distribution and the geographical arrangement of the buildings defined at the next page (fig. 3.4), is used for all further steps.

Figure 3.4: Model region which represents the Austrian building structure and is used for the optimisation; Modified according to [16, p. 19]

3.2 Networks

In this section, the three different network types (electric, gas and district heating) are discussed. For each network type, a general overview about the structure and how the networks are operated is given. Followed by a detailed description of network structures used in the model region and how the networks are modelled for further use in the optimisation.

3.2.1 Electric network

A typical power system basically contains [40, pp. 2–3]:

- production,
- an interface and
- loads.

Such a system with different network levels is shown in figure 3.5. The generation and

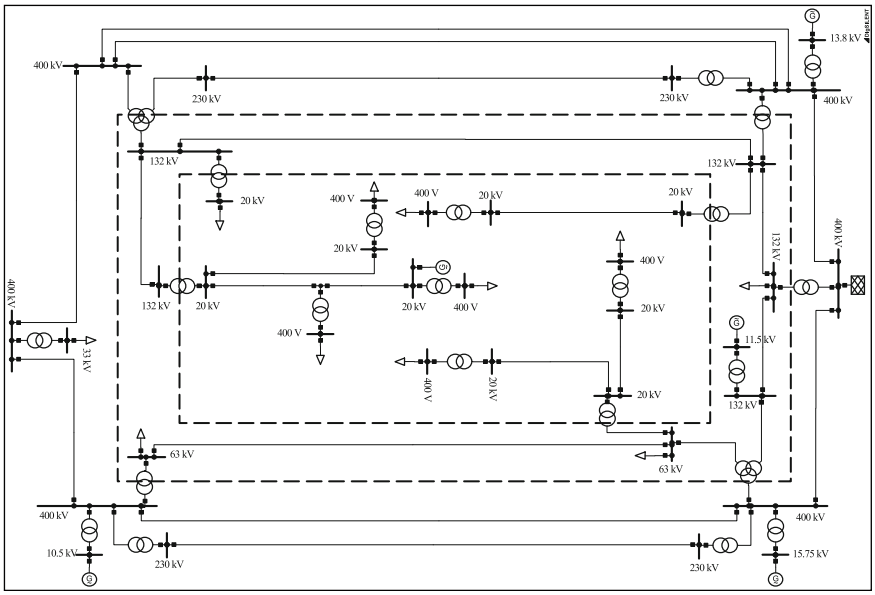

Figure 3.5: A typical electric power system; [40, p. 3]

loads are geographically distributed; therefore the interface represented as a network of lines or cables is needed to transfer the generated power to the loads. The generation can be from a small solar cell on the roof of a house up to a large water, gas, coil or nuclear power plant. Also the loads start from small single family houses up to huge industrial consumers such as paper producers. Due to this variation in production and consumption sizes it is not useful to produce, transport and consume the electricity at the same – or even at only one – voltage level. Therefore the special task, e.g. production is done at the most suitable voltage level, afterwards it is transformed to voltages which suit the transportation. For long distance transportation, voltage levels up to several hundred kilovolts are used. The consumption of electricity at such high voltage levels would not be possible, and therefore the voltage is transformed down again, for small

consumers down to 400 V. Due to the variation of voltage levels, the total power system is categorised in seven classes, the classification is shown in table 3.2 [41, p. 26]. Voltage levels of 66 kV or higher are generally classified as part of the transmission system, levels 1-4 belong to this system. Such high voltage levels are used to transport energy over long distances, which is why it is called transmission system. Voltages of less than 66 kV are categorised at distribution level (Level 5-7), because the energy at this voltage level can only be transported over small distances and is used to transport the energy over the "last mile". For a functional electric power system many more components are needed, for example, control or protection devices to protect the system and more importantly to protect people.
Talking about all of this would go too far within this work. The aim of this work is

Table 3.2: Classification of the electric power system; Modified according to [41, p. 26]

Level	Nominal Voltage	Name
1	380 kV or 220 kV	supergrid (SG)
2	380 kV or 220 kV/110 kV	transformer SG-HVG
3	110 kV	high-voltage grid (HVG)
4	110 kV/ 10 kV or 20 kV or 30 kV	transformer HVG-MVG
5	10 kV or 20 kV or 30 kV	medium-voltage grid (MVG)
6	10 kV or 20 kV or 30 kV/0.4 kV	transformer MVG-LVG
7	0.4 kV	low-voltage grid (LVG)

to energetically optimise a model region. Because of this it is not possible or useful to consider the whole network structure as shown in figure 3.5. This would go beyond the scope of the work for two reasons. The first is the lack of information gain, if several, similar model regions are optimised at the same time. The other is limited computing resources; it is not possible to model the whole network system in detail. It is possible either to model a limited area or network topology in detail or to model the whole system with reduced modelling details and compute in adequate time.
For this work, the detailed modelling of a limited region is used. All of the lines to each house, the different cable cross sections and so on are considered. Figure 3.6 shows the electric system used for the model region. The electric system only contains levels 6 and 7, i.e. the low voltage transformer and the 400-V-grid. The feeding network is not modelled and considered as slack node (hatched square). For the urban structure and the main branches 150 mm^2 aluminium cables are used, the side branches – connections of just one or only a few buildings – due to the reduced load a 50 mm^2 aluminium cable is sufficient. Since the urban typology is an open ring, the typology of the whole region

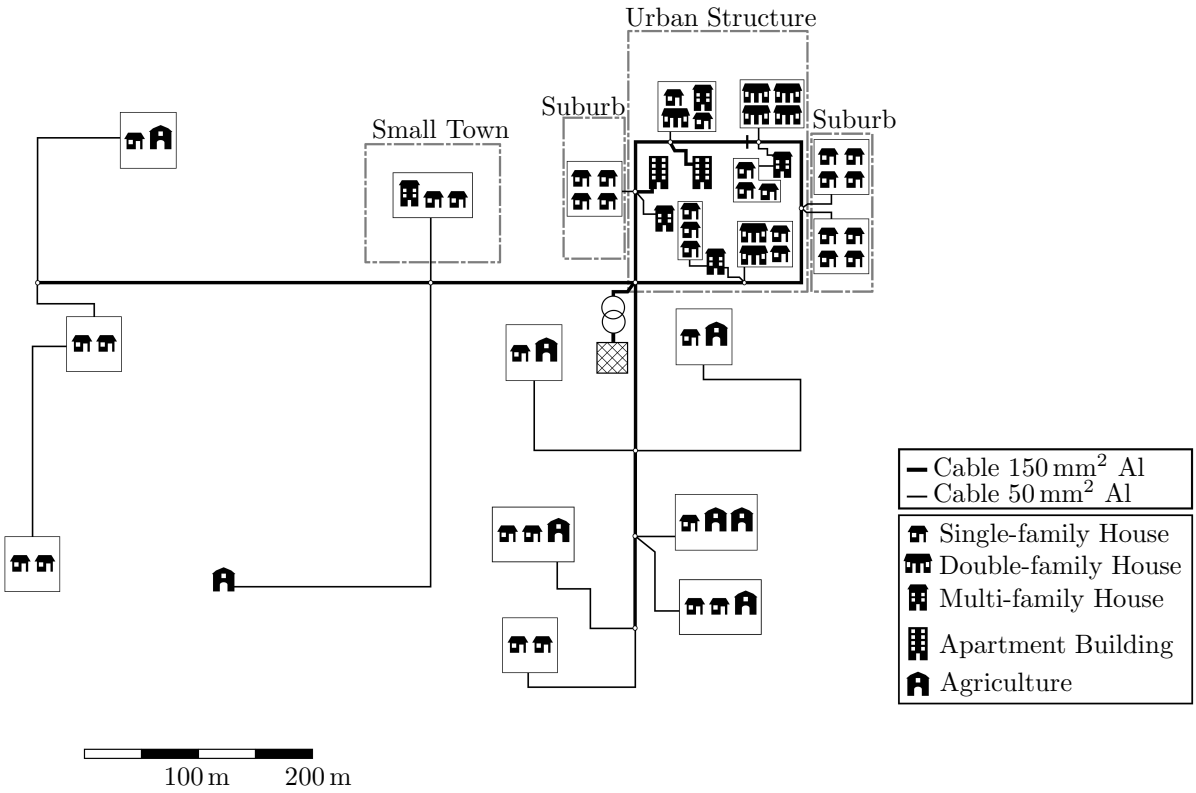

Figure 3.6: Electric network for the model region

results in a radial distribution system.
To be able to calculate the line loads for each time step, a load flow calculation has to be carried out.
For the classic load flow problem, four variables have to be considered for each bus [40, p. 245]. These variables are (counted positive if the active power flow or active current flow is towards the bus):

1. P_ν : Net active power injection
2. Q_ν : Net reactive power injection
3. $|\underline{V}_\nu|$: Voltage magnitude
4. ϑ_ν : Voltage angle

The active and reactive power injections can be calculated as followed (this circumstance is shown in fig. 3.7)

$$P_\nu = P_{G\nu} - P_{D\nu} \tag{3.1}$$

$$Q_\nu = Q_{G\nu} - Q_{D\nu} \tag{3.2}$$

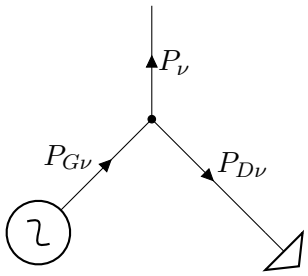

Figure 3.7: Node power split for node ν

$P_{G\nu}$ and $Q_{G\nu}$ are active and reactive power generations at bus ν, whereas $P_{D\nu}$ and $Q_{D\nu}$ are active and reactive power demands at this bus.
If Kirchhoff's law is taken into account

$$\boldsymbol{I} = \boldsymbol{Y}\boldsymbol{V} \tag{3.3}$$

$$\underline{I}_\nu = \frac{(P_\nu - jQ_\nu)}{|\underline{V}_\nu|} e^{j\vartheta_\nu} \tag{3.4}$$

with

$\underline{I}_\nu$	:	Net injected current at bus ν
V	:	Vector of bus voltages
I	:	Vector of injected currents at the buses
Y	:	Bus admittance matrix of the system

(3.1) and (3.2) can be written as following, if (3.4) is used to replace **I** from (3.3); n_k represents the number of nodes at the network and $\delta_{\nu\mu}$=$arg(\underline{Y}_{\nu\mu})$:

$$P_\nu = \sum_{\mu=1}^{n_k} |\underline{Y}_{\nu\mu}||\underline{V}_\nu||\underline{V}_\mu| \cos(\vartheta_\nu - \vartheta_\mu - \delta_{\nu\mu}) \tag{3.5}$$

$$Q_\nu = \sum_{\mu=1}^{n_k} |\underline{Y}_{\nu\mu}||\underline{V}_\nu||\underline{V}_\mu| \sin(\vartheta_\nu - \vartheta_\mu - \delta_{\nu\mu}) \tag{3.6}$$

If (3.5) and (3.6) are presented at a different form, it is possible to write them as (3.7) and (3.8). The factor 3 is caused from the three phases which are used at three-phase electric power system.

$$P_\nu = 3 \sum_{\mu=1}^{n_k} \Re \left\{ \underline{V}_\nu \cdot \underline{V}_\mu^* \cdot \underline{Y}_{\nu\mu}^* \right\} \tag{3.7}$$

$$Q_\nu = 3 \sum_{\mu=1}^{n_k} \Im \left\{ \underline{V}_\nu \cdot \underline{V}_\mu^* \cdot \underline{Y}_{\nu\mu}^* \right\} \tag{3.8}$$

The voltage $\underline{V}_\nu$ describes the node voltage at node ν in relation to the earth potential. The element of the node admittance matrix $\underline{Y}_{\nu\mu}$ is calculated from the branch impedance matrix with the following rules [42, p. 42], [43, p. 125]:

$$\begin{aligned} \underline{Y}_{\nu\mu} &= -\frac{1}{\underline{Z}_{\nu\mu}} \qquad \text{if } \nu \neq \mu \\ \underline{Y}_{\nu\nu} &= -\sum_{\substack{\mu=1 \\ \mu\neq\nu}}^{n_k} \underline{Y}_{\nu\mu} \end{aligned} \tag{3.9}$$

The element of the node admittance matrix $\underline{Y}_{\nu\mu} = |\underline{Y}_{\nu\mu}| \mathrm{e}^{j\delta_{\nu\mu}} = G_{\nu\mu} + jB_{\nu\mu}$ is derived from the network topology and line parameters, the matrix completely describes the network. For the creation of the matrix, the branch admittance has to be known, this is guaranteed since the length of each cable and its parameters are known. The main diagonal contains the sum of the conductances of all connected branches. At the secondary diagonal, the Matrix $Y_{\nu k}$ contains the branch admittance with a negative value [43, p. 125].

The drawback with this load flow simulation in respect to the purposes of this work is, the non-linearity and that two of the four variables have to be known in advance. Therefore only a iterative solution method is possible, e.g. a Newton-Raphson-algorithm [40, p. 246].

To overcome this problem, a Direct Current Load Flow (DCLF) can be carried out. It provides an estimation of line power flows in Alternating Current (AC) systems. DCLF only takes the active power flow into account and neglects the reactive power flow; it is a linear load flow calculation. Therefore it is absolute convergent but less accurate than a AC Load Flow (ACLF) [40, p. 246]. For this linearisation from AC to DCLF, a few assumptions are necessary [42, pp. 42–43], [40, p. 246]:

- The line impedances have a small R/X-ratio, i.e. the real part of the impedances are much smaller than the imaginary part (R $\ll$ X).
- The voltage angles ϑ_ν referred to the reference voltage are much smaller than 90°, i.e. $\cos\vartheta_\nu \approx 1$ and $\sin\vartheta_\nu \approx \vartheta_\nu$
- The bus voltage magnitudes are almost the same as the nominal voltage, i.e:

$$\Re\{\underline{V}_\nu\} = V_\nu \cos\vartheta_\nu \approx V_\nu \approx V_n \tag{3.10}$$

$$\Im\{\underline{V}_\nu\} = V_\nu \sin\vartheta_\nu \approx V_\nu\vartheta_\nu \approx V_n\vartheta_\nu \tag{3.11}$$

- The network does not contain any phase-angle regulating transformers

With these assumptions a linear correlation between the active power P and the node voltage angle ϑ can be approximated [43, p. 126]:

$$P_\nu = -V_n^2 \sum_{\mu=1}^{n_k} \Im\{\underline{Y}_{\nu\mu}\}\ \vartheta_\mu \tag{3.12}$$

(3.12) at matrix notation can be written as follows

$$\boldsymbol{p} = -V_n^2 \cdot \boldsymbol{B} \cdot \boldsymbol{\vartheta} \tag{3.13}$$

The dimension of the node power vector $\boldsymbol{p}$ and the voltage angle vector $\boldsymbol{\vartheta}$ is the node number n_k. The matrix $\boldsymbol{B}$ describes the imaginary part of the node admittance matrix and has a dimension of $n_k \times n_k$. According to its structure (3.11) the Matrix $\mathbf{B}$ is singular. Because of this the form $\boldsymbol{B}^{-1}$ cannot be calculated, but it is necessary to calculate the inverse for solving the load flow problem. An option to overcome the problem of the singularity is to eliminate one node. It is advisable that this eliminated node is the slack node. This elimination causes a modified vector $\boldsymbol{p'}$ and $\boldsymbol{\vartheta'}$. The dimension of these vectors is now $n_k - 1$. In the matrix $\boldsymbol{B}$, because of the slack node elimination the corresponding row and column are removed. The result is a reduced node susceptance matrix $\boldsymbol{B'}$ with the dimension $(n_k - 1) \times (n_k - 1)$. This matrix is no longer singular and the inverse can be calculated.
Since the network shown in figure 3.6 is always the same, the inverse of $\boldsymbol{B'}$ only has to be calculated once. With this inversion, (3.13) can be reformulated as shown in (3.14) [43, pp. 126–127].

$$\boldsymbol{\vartheta'} = -\frac{1}{V_n^2}\boldsymbol{B'^{-1}} \cdot \boldsymbol{p'} \tag{3.14}$$

If the node voltage angles ϑ_ν are used, the branch loads can be calculated (3.15).

$$P_{\nu\mu} = -V_n^2 \Im\{\underline{Y}_{\nu\mu}\}(\vartheta_\nu - \vartheta_\mu) \tag{3.15}$$

It is not necessary to calculate (3.15) for all indices. It can be seen, that $P_{\nu\mu} = P_{\mu\nu}$ and because of an angle difference of $\vartheta_\nu - \vartheta_\nu = 0$, $P_{\nu\nu}$ must be zero. If a network is just weakly meshed, a major computing speed improvement is possible, if the load flow only for branches $P_{\nu\mu}$ is calculated, which are connected.
For this, the branch-node incidence matrix $\boldsymbol{A}$ is used. This matrix describes which nodes are connected via which branches. The elements of the matrix are 0 if there is no connection or otherwise ± 1, since the connection has a direction (beginning and end). The rows of the matrix represent the branches and the columns the nodes. At each row there are exactly two elements different from zero. One value is +1 this represents the start node and one value is -1 this represents the end node [43, p. 128]. Because of the reduction of the slack node for e.g. $\boldsymbol{B}$, the branch-node incidence matrix $\boldsymbol{A}$ has to be reduced as well. This means, that the corresponding column has to be removed. The dimension of the reduced matrix $\boldsymbol{A'}$ is $n_l \times (n_k - 1)$, where n_l is the branch number.
If the vector of the node angles $\boldsymbol{\vartheta'}$ is multiplied from the left side with the reduced branch-node incidence matrix, the angle differences $\boldsymbol{\Theta_l}$ are calculated. This means multiplying (3.14) from the left side with $\boldsymbol{A'}$, which results in (3.16).

$$\boldsymbol{\Theta}_l = \boldsymbol{A'} \cdot \boldsymbol{\vartheta'} = -\frac{1}{V_n^2} \boldsymbol{A'} \cdot \boldsymbol{B'^{-1}} \cdot \boldsymbol{p'} \tag{3.16}$$

The branch load is calculated via the multiplication of the branch susceptance and the angle difference between the beginning and end of the branch. Therefore the branch susceptance matrix $\boldsymbol{B_l}$ is used. This is a diagonal matrix with the dimension $n_l \times n_l$, the main diagonal elements consist of the susceptance of the respective branch. With this convention, it is possible to calculate the load flow for exactly the branches that contain a real connection. Equation (3.14) can be written as (3.17) [43, p. 129].

$$\boldsymbol{p}_l = -V_n^2 \boldsymbol{B_l} \cdot \boldsymbol{\Theta_l} = -V_n^2 \boldsymbol{B_l} \cdot \boldsymbol{A'} \cdot \boldsymbol{\vartheta'} \tag{3.17}$$

By transforming and inserting (3.14) in (3.17), it is possible to calculate the branch loads depending on the node loads. This is the result of the DCLF:

$$\boldsymbol{p}_l = \boldsymbol{B_l} \cdot \boldsymbol{A'} \cdot \boldsymbol{B'^{-1}} \cdot \boldsymbol{p'} \tag{3.18}$$

If there is no change in the network topology, the three matrices $\boldsymbol{B_l}$, $\boldsymbol{A'}$ and $\boldsymbol{B'}$ are constant. It is possible to calculate all the matrices before the optimisation and just use the electric load flow matrix $\boldsymbol{L_e} = \boldsymbol{B_l} \cdot \boldsymbol{A'} \cdot \boldsymbol{B'}^{-1}$ to calculate the branch loads according to the node loads. The matrix $\boldsymbol{L_e}$ is used during the optimisation to calculate the branch load depending on the node loads for each time step. There are a few limitations which have to be kept in mind when the load flow from the non-linear form (3.7) is approximated with the DCLF [42, p. 44]. These limitations are:

- The network losses are zero.
- There is no information about the reactive power or the node voltages.
- The branch load flows are generally underestimated, because of the lack of reactive power transport.

There are two reasons why in context of this work these limitations are no problem. The purpose of a annual energetic optimisation is the first reason. The other reason is, that after the linear optimisation with the results, a non-linear load flow calculation is carried out, to check if there is no overstepping of any boundaries. If there are violations, the boundaries are set with new threshold values and the optimisation is carried out again. This process is carried out until all the limits are complied. If for example the control calculation results in an overload of lines, the new threshold for the maximal allowable line loads for the DCLF are set a few percentage points lower and the linear optimisation is carried out again with the new line thresholds. The non-linear control calculation is done with a simulation software, e.g. PSS©SINCAL [44].

3.2.2 Gas network

Compared to the electric system for the gas system it is necessary to consider several different aspects. One is the type of gas or the composition which is used in the system. The other aspect is the network itself.
First we look at the classifications and the different types of gas and the compositions. Combustion gases are gases or mixtures of gases containing different flammable and non-flammable elements. They can be classified differently, e.g. by specific characteristics, by its source, by usage, etc.
The classification according the standard DIN 1340 is by *characteristics*, the groups are separated by calorific value ranges (tab. 3.3).

Table 3.3: Classification of Combustible according DIN 1340; Modified according to [45, p. 70], [46, p. 7]

Group	Combustible $H_{s,n}$ MJ/m^3	Major Components	Usage as Combustible in
1	≤ 10	N_2, CO, H_2	Industry
2	$10 \ldots 30$	CO, H_2, CH_4, N_2, CO_2	Industry, Public facilities
3	$\approx 30 \ldots \approx 75$	CH_4, C_nH_m	Industry, Commerce,
4	> 75	C_nH_m	Public facilities, Households

Another classification is according to the German Technical and Scientific Association for Gas and Water (DVGW) with the technical rule DVGW G 260 [47] (tab. 3.4). Gas family 1 is not distributed in the Austrian and German gas system any more. Gas family 2 contains methane-rich gases, either from natural appearing gas or Synthetic Natural Gas (SNG) and conditioned biogas. The third gas family contains liquefied gases.

Table 3.4: Classification of Combustible according DVGW-G 260; Modified according to [47, p. 10], [45, p. 71]

Gas Family	Major Component	Group
1	Hydrogen H_2	A: illuminating gas B: coke oven gas
2	Methan CH_4	L: natural gas L[3] H: natural gas H
3	Propane C_3H_8, Butane C_4H_{10}	1. propane 2. propane/butane mixture

[3] L and H are classified with the Wobbe-Index; H: $W_{s,n} \leq 12\,\mathrm{kWh/m^3}$, L: $W_{s,n} \leq 10\,\mathrm{kWh/m^3}$

An important aspect of the DVGW G 260 is the characteristics declaration of natural gas, especially for gas family 2. In Austria, natural gas requirements are regulated by the Austrian Association for Gas and Water (OVGW) in the specification OVGW G 31. The infeed of electric surplus energy with an attached electrolysis (and methanation) process, or biogas from biomass power plants into the gas grid, is one option. Therefore the produced gases have to fulfil the corresponding requirements. For such applications the DVGW and OVGW have additionally released feed in requirements of gases like SNG or biogas.
The relevant regulations are DVGW G 262 and OVGW G 33. According to these regulations a direct H_2 infeed is allowed, but only up to a level, where the H_2 concentration does not exceed the +4% limit at any point in the network.

As mentioned earlier, the network itself is the second important part considering the gas network. Similar to the electric grid, where the system is managed in seven voltage levels (tab. 3.2), the gas system, according to safety-related purposes, is managed in the three following pressure levels [45, p. 58]:

- High Pressure (HP): $p_e > 1\,\text{bar}$
- Medium Pressure (MP): $p_e > 100\,\text{mbar}$ and $\leq 1\,\text{bar}$ ($\leq 4\,\text{bar}$ for gas-transport)
- Low Pressure (LP): $p_e \leq 100\,\text{mbar}$

After the exploration, normally the gas is transported in HP-gas pipelines with a common pressure of 67.5 bar to 80 bar. HP-pipe lines are often used for national transmission systems. This system feeds into regional MP structures. Small end consumers such as households are mostly fed by LP systems, larger consumers are usually supplied via MP- or even HP-systems [45, pp. 177–178].
To comply with the different needs, like economic efficiency or supply reliability, various network typologies are possible (fig. 3.8). Since there is an opposing trend between economic efficiency and supply reliability, the best compromise has to be found for all individual situations. For the network in figures 3.8a and 3.8b, each point can be supplied over one path only, for the other typologies more paths are possible.

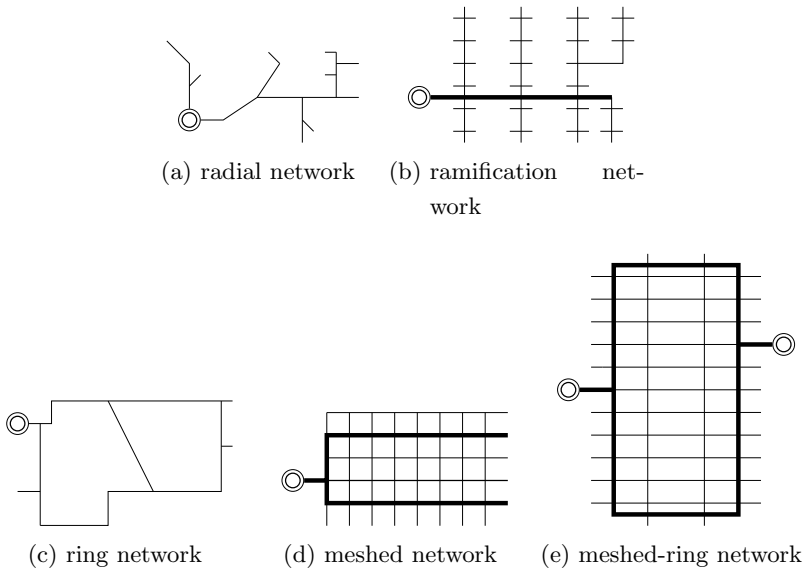

(a) radial network (b) ramification network

(c) ring network (d) meshed network (e) meshed-ring network

Figure 3.8: Different gas grid topologies; Modified according to [45, p. 159]

The gas network for the model region was designed in close collaboration with an Austrian gas provider. At the design process of the gas network the electric network is the initial system. Based on the electric load density and load types (e.g. single-family house, double-family house, etc.) the maximal gas demand is estimated. For this estimation the usually used gas meters for each load type are selected, such as G4 to G65. For each meter type the maximal possible flow rate is taken as maximal possible gas demand. This approach provides the worst case.gch A G4 meter used for single-, double-family houses has a maximal flow rate of 6 m/s ($\approx$ 65 kW). Usually the flow rate for this building types is within 1.5 Nm^3/h to 2 Nm^3/h. Based on the maximal demands for each node, the typology and the dimensions of the gas pipes are selected. The dimensioning of the pipes depends on [48]. From the possible topologies, mentioned in figure 3.8 the gas network in the model region only consists of radial structures and a ring in the urban region. The ring in the urban region is chosen due to higher reliabilities. The whole network is a LP-system operated with 75 mbar at the infeed point. For the pipe dimensioning two parameters are relevant, the maximal flow speed and the maximal pressure drop in the system. The flow rate, for systems designed with a Maximum Operating Pressure (MOP) $\leq$ 100 mbar should not exceed 5 m/s to 7 m/s [49, p. 6]. The general operating pressure level for LP-systems is between 45 mbar to 100 mbar, the gas provider who was involved in the network designing process tries not to underrun 30 mbar.
There are numerous pipe materials, steel, Polyvinyl Chloride (PVC), Polyethylene (PE)

and various dimensions of pipes available, for example from Diameter Nominal (DN) 50 to 600. DN means Diamètre Nominal the American equivalent is Nominal Pipe Size (NPS). The number after DN represents roughly the inner diameter in millimetre. For the model region, there are only PE-pipes with three different dimensions used. The PE Durchmesser Außen (DA)[4] 160, 110 and 63, where the dimensions 160 and 110 are designed for a Standard Dimension Ratio (SDR)[5] 17.6 whereas the DA 63 pipe is designed for SDR 11. The consideration of all this design rules results in the network shown in fig. 3.9.

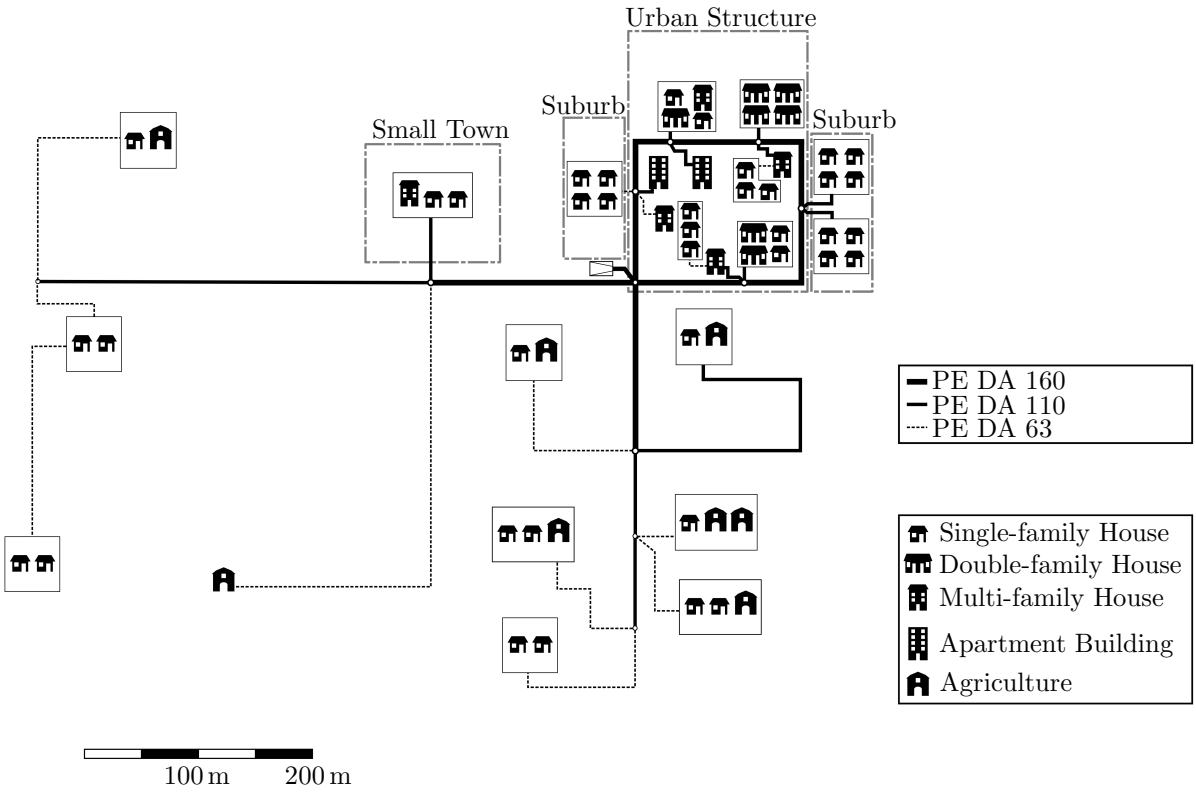

Figure 3.9: Gas network for the model region

[4] "Durchmesser Außen" is german for "Diameter Outside"
[5] $SDR = \frac{\text{Outside pipe diameter}}{\text{thicknes}}$

Since the parameters for the gas composition and the network typology are determined it is necessary to ascertain how a load flow calculation can be performed. For material flow calculations, three aspects need to be considered, the law of conservations of mass, the law of conservation of energy and the law of conservation of impulse.
The law of conservation of mass is described as follows [50, pp. 5–8]

$$\frac{d\,(dm)}{dt} = 0 \tag{3.19}$$

If m is considered as ρAx (fig. 3.10) and $dm = \rho A dx$, (3.19) can be written in its most general form (3.20). This form is valid for steady-state and non-steady state flow, for incompressible or compressible fluids. The gas may be ideal or real, this means, the flow can be lossy or lossless and the system can be adiabatic or non-adiabatic [50, p. 7].

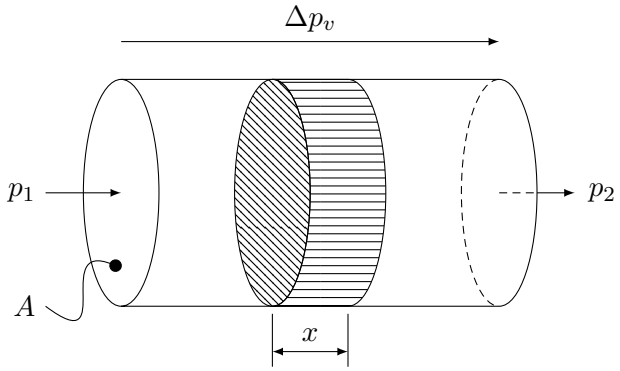

Figure 3.10: Geometric context and pressure distribution for the gas system

$$\left(\frac{\partial\,(\rho A)}{\partial t}\right)_x + \left(\frac{\partial\,(\rho A v)}{\partial x}\right)_t = 0 \tag{3.20}$$

If the system is considered in steady-state conditions the time derivative in (3.20) is zero. With the definition of the mass flow $\dot{m} = \frac{dm}{dt}$, the equation can be simplified to (3.21).

$$\dot{m} = \rho A v \tag{3.21}$$

This is equivalent to $\dot{m} = \rho A v = const.$ If the fluid is considered incompressible ($\rho = const.$) the mass flow can be expressed as volume flow:

$$\dot{V} = Av = const. \tag{3.22}$$

The conservation of energy describes, that the energy content of a fluid element only changes when energy is supplied or removed. The kinetic energy is not considered, since this energy is described with the equations of motion [50, p. 15]. The energy change over time of a fluid element $d\dot{E}_i$ is equal to the sum of the supplied or dissipated power $dP_{su/di}$:

$$d\dot{E}_i = \sum dP_{su/di} \tag{3.23}$$

The detailed deduction of all relevant powers/energies can be found at [50, pp. 15–24]. The following list shows the relevant powers/energies:

- Internal energy
- Power for volume change
- Dissipation power
- Resistance power due to wall friction
- Volume friction power
- Internal heat flow rate
- Outer heat flow rate
- Mechanical power

The law of conservation of impulse (3.24) will be described in more detail since this law describes the square correlation between fluid speed and pressure loss inside of pipes $\Delta p_v \propto v^2$. For the linear optimisation carried out in this work, such a correlation is not feasible and solutions to overcome this problem are described. The law of conservation of impulse means, that the variation of impulse I over time is equal to the sum of all forces F acting on it:

$$\frac{dI}{dt} = \sum F \tag{3.24}$$

To set up the equation of motion, the sum of all forces acting on a fluid particle has to be determined, the deduction of the equations can be found at [50, pp. 10–15]. The following itemisation lists the different forces:

- compressive force: $dF_p = -A\frac{\partial p}{\partial x}dx$
- wall friction: $dF_w = -A\frac{\lambda}{D_{hydro}}\frac{\rho}{2}v|v|dx$
- gravitation: $dF_g = -A\rho g \sin\vartheta dx$
- internal friction: $dF_i = Ak_v\frac{\partial\left(\eta\frac{\partial u}{\partial x}\right)}{\partial x}dx$

All this parts lead to the detailed law of impulse:

$$\rho A \frac{dv}{dt} dx = -A \frac{\partial p}{\partial x} dx - A \frac{\lambda}{D_{hydro}} \frac{\rho}{2} v|v| dx - A\rho g \sin\vartheta dx + A k_v \frac{\partial}{\partial x} \left(\eta \frac{\partial v}{\partial x} \right) dx \quad (3.25)$$

where ρ is the fluid density, A the cross section area according fig. 3.10, v is the fluid speed, p the pressure, λ is the friction coefficient, D_{hydr} is the equivalent circle diameter for any arbitrary pipe cross section $\left(\frac{4 \cdot Area}{Circumference}\right)$, ϑ is the horizontal inclination, k_v is a coefficient for internal friction and η is the dynamic viscosity.
After a few transformations and the discard of the internal friction (3.25) results at the "Bernoulli's equation" [50, pp. 43–44]. If further $\rho = const.$ is assumed and the pressure at two points is considered (fig. 3.10) this leads to the following type of the Bernoulli equation, where the index 1 represents one point/side and the index 2 the second point/side at the pipe. l represents the distance between the two points and d the pipe diameter.

$$\frac{\rho}{2} \cdot v_1^2 + p_1 + \rho \cdot g \cdot h_1 = \frac{\rho}{2} \cdot v_2^2 + p_2 + \rho \cdot g \cdot h_2 + \lambda \frac{l}{d} \frac{v^2}{2} \rho \quad (3.26)$$

The different parts represent [50, p. 44]

- $p_{kin} = \frac{\rho}{2} \cdot v^2$: the *dynamic* pressure caused by the speed of the fluid.
- $p = p_{stat}$: the *static* pressure. This is the pressure inside the fluid if the fluid would be motionless.
- $p_h = \rho \cdot g \cdot h$: the *geodetic* pressure due to the difference in elevation.
- $\Delta p_v = \lambda \frac{l}{d} \frac{v^2}{2} \rho$: the pressure *loss* because of the pipe-friction.

The last part is the equation of "Darcy" which represents the earlier mentioned relation $\Delta p_v \propto v^2$. Its calculation is essential for gas network calculations. This relation is the equivalent of Ohm's law in the electric network, but the relation there is linear $R = V \cdot I \rightarrow R \propto I$.
To calculate gas networks as well as for all network calculations a convenient way of representing the topology is necessary. The topology describes the nodes and the edges. In gas networks the nodes represent feed-in- and load-points. The edges represent the pipes which connect the different nodes. The network description can be done with two different approaches. The graph theory description or via a mathematical description.
For a simplified description the real gas network can be mapped to a network graph, this abstraction represents the relations between nodes and edges without representing the real proportions.

The mathematical description uses topology matrices and vectors [50, p. 77]. For this work the mathematical description is used, because of its simple network description via matrices. A correlation between the node power and the branch volume flow needs to be determined, to make sure that the optimisation keeps the maximum flow rates within its boundaries, as mentioned earlier, between 5 m/s to 7 m/s. Therefore a resistance value for each pipe (index k) has to be calculated [50, p. 107]:

$$a_k = \lambda_k \frac{l_k}{d_{ik}^5} \frac{8 \cdot \rho}{\pi^2} \tag{3.27}$$

λ_k	:	pipe-friction coefficient	$[-]$
l_k	:	pipe length	$[m]$
d_{ik}	:	inner pipe diameter	$[m]$
ρ	:	mass density	$\left[\frac{kg}{m^3}\right]$

For this calculation the pipe-friction coefficient λ is needed, this factor depends on the Reynolds' number Re_k.

$$Re_k = \frac{m \cdot a_{a,k}}{A_k \cdot \eta \cdot \left(\frac{v_k}{l_k}\right)} \tag{3.28}$$

η	:	dynamic viscosity	$[Pa \cdot s] = \left[\frac{kg}{m \cdot s}\right]$
A_k	:	pipe cross section	$\left[m^2\right]$
m	:	mass	$[kg]$
$a_{a,k}$	:	acceleration	$\left[\frac{m}{s^2}\right]$
v_k	:	flow velocity	$\left[\frac{m}{s}\right]$
l_k	:	pipe length	$[m]$

For the flow in pipes this equation can be simplified to [50, p. 48]

$$Re_k = \frac{\bar{v}_k \cdot d_{ik}}{\nu} \tag{3.29}$$

$\bar{v}_k$	:	average flow velocity	$\left[\frac{m}{s}\right]$
d_{ik}	:	inner pipe diameter	$[m]$
ν	:	kinematic viscosity[6]	$\left[\frac{m^2}{s}\right]$

[6] for natural gas it is $\approx 14.13 \times 10^{-6}\,\mathrm{m}^2/\mathrm{s}$ [51]

Measurements showed for a Reynolds' number range from 2 300 to 2 600 a flow change from laminar to turbulent takes place, and Reynolds' numbers of >2320 are used to indicate turbulent flows [50, p. 55]. The Reynolds' number for the gas network in the model region for the maximum load is for all pipes >2320, this implies a turbulent flow in all pipes. Because of this, the differentiation between a hydraulic bare pipe or not is relevant. If a pipe is hydraulic bare the pipe roughness k [mm] is covered completely with a laminar flow and the turbulent flow slides over this laminar layer. A system is hydraulic bare when $Re \cdot \frac{k}{d} < 65$, for all the used pipes in the network this is the case. With all this conditions λ for all pipes k can be calculated as followed [50, p. 62]:

$$\lambda_k = 0.3164 \cdot Re_k^{-0.25} \tag{3.30}$$

Since λ_k is determined all the parameter for (3.27) are known and it is possible to calculate all the resistances a_k.

For electrical systems the nodal analysis is one method for analysing networks. With this analysis it is possible to calculate the branch current $\boldsymbol{I}$ in dependence of the node source currents $\boldsymbol{I}_{qn}$. This approach is used here to calculate the branch volume flow in dependence of the node volume flow/demand. Therefore the node equations for (n-1) nodes are formed. The currents in this node equations are determined from the branch voltages and the susceptances of the branches. To be able to determine the branch voltage, for the (n-1) nodes the node voltage is needed. These are calculated from the node potential φ_ν and a reference potential. The node voltage $V_{\nu 0}$ for the node ν is calculated via the node potential φ_ν and the potential of the reference node φ_0, $V_{\nu 0} = \varphi_\nu - \varphi_0$. If the reference potential is set to zero the node voltage is:

$$V_{\nu 0} = \varphi_\nu \tag{3.31}$$

With this assumption it is possible to determine the voltage drop across a branch between node ν and μ:

$$V_{\nu\mu} = V_{\nu 0} - V_{\mu 0} = \varphi_\nu - \varphi_\mu \tag{3.32}$$

Furthermore applies the following for the nodal analysis (3.33) [52, pp. 7–27]. At this part no differentiation between complex ($\underline{Z} = R + jX$) and non complex parameters shall be made, since at the end, for the gas flow calculation there are no complex values.

$$\boldsymbol{V} = \boldsymbol{A}^T \cdot \boldsymbol{V}_n \tag{3.33}$$

where $\boldsymbol{A}$ is the branch-node incidence matrix, $\boldsymbol{V}$ the branch- and $\boldsymbol{V}_n$ the node-voltage. $\boldsymbol{V}_n$ is the equivalent to $V_{\nu 0}$, which is not written in matrix notation. The branch voltage can be expressed via the branch impedance $\boldsymbol{Z}$ and the branch current $\boldsymbol{I}$.

$$\boldsymbol{V} = \boldsymbol{Z} \cdot \boldsymbol{I} = \boldsymbol{Y}^{-1} \cdot \boldsymbol{I} \Rightarrow \boldsymbol{I} = \boldsymbol{Y} \cdot \boldsymbol{V} \tag{3.34}$$

The source currents at the nodes $\boldsymbol{I}_{qn}$ can be determined with the node admittance matrix $\boldsymbol{Y}_n$ and the node voltage $\boldsymbol{V}_n$.

$$\boldsymbol{I}_{qn} = \boldsymbol{Y}_n \cdot \boldsymbol{V}_n \tag{3.35}$$

If it is assumed that the impedance $\boldsymbol{Z}$ only has a real part $\boldsymbol{R}$, $\boldsymbol{Y} = \boldsymbol{Z}^{-1}$ results in $\boldsymbol{Y} = \boldsymbol{G}$. The following applies to $\boldsymbol{G}$, this is similar to (3.9).

$$\begin{aligned} G_{\nu\mu} &= -g_{\nu\mu} \qquad \text{if } \nu \neq \mu \\ G_{\nu\nu} &= \sum_{\substack{\mu=1 \\ \mu\neq\nu}}^{n_k} g_{\nu\mu} \end{aligned}$$

With this assumption and if (3.33) and (3.34) are inserted in (3.35), the before mentioned dependency between the branch current and the node current can be calculated.

$$\boldsymbol{G}^{-1} \cdot \boldsymbol{I} = \boldsymbol{A}^T \cdot \boldsymbol{G}_n^{-1} \cdot \boldsymbol{I}_{qn} \tag{3.36}$$

or explicit for $\boldsymbol{I}$:

$$\boldsymbol{I} = \boldsymbol{G} \cdot \boldsymbol{A}^T \cdot \boldsymbol{G}_n^{-1} \cdot \boldsymbol{I}_{qn} \tag{3.37}$$

If it is assumed that $I \equiv \dot{V}$ and $U \equiv \Delta p$, the calculation approach of the electric system can be used for the gas network calculation too. But a few restrictions are necessary:

1. The quadratic correlation between Δp and $\dot{V}$ must be assumed to be linear.
2. For the resistance a_k in the gas system (3.27), has to be assumed that it is the same for all flow rates $\rightarrow \lambda_k = const.$

For the gas network shown in fig. 3.9 for maximum gas loads the pressure drop between the infeed node and the other nodes never exceeds 3 mbar, this is a relative value of 3 mbar/75 mbar = 4%. Since the aim of this work is no accurate gas network calculation, but a annually energetic optimisation of a model region, the above mentioned limitations are accepted. With this limitations $\boldsymbol{G}$ in (3.37) can be assumed to be $g_k = 1/a_k$ from (3.27) and therefore the following equation for the gas load flow can be formed; where $\dot{\boldsymbol{V}}$ represents the pipe volume flow and $\dot{\boldsymbol{V}}_{qn}$ the node volume flow:

$$\dot{\boldsymbol{V}} = \boldsymbol{G} \cdot \boldsymbol{A}^T \cdot \boldsymbol{G}_n^{-1} \cdot \dot{\boldsymbol{V}}_{qn} \tag{3.38}$$

Since the topology doesn't change the matrix $\boldsymbol{A}$ is always the same and the two matrices $\boldsymbol{G}$ and $\boldsymbol{G}_n^{-1}$ do not change either, because of the accepted limitations. Therefore the matrix $\boldsymbol{L}_g = \boldsymbol{G} \cdot \boldsymbol{A}^T \cdot \boldsymbol{G}_n^{-1}$ can be calculated once before the optimisation process. This is the same as for the electric system and (3.18).

3.2.3 District Heating network

For the dimensioning of the district heating system it is necessary to know the maximum power demand for heating and for hot water for each building. All the heating systems, such as gas burner, wood firing or domestic heating systems must be designed for this maximal power demand to fulfil the heating needs.
According to the standard DIN EN 12828 [53, p. 14] the total power demand for the heating system is as following:

$$\Phi_{SU} = f_{HL} \cdot \Phi_{HL} + f_{DHW} \cdot \Phi_{DHW} + f_{AS} \cdot \Phi_{AS} \tag{3.39}$$

The design of the heating system takes three parts into account; the demand for room heating, for hot water production and for other affiliated systems.

Φ_{SU}	:	power of the heat production system	[kW]
f_{HL}	:	design factor for the heating demand	[-]
Φ_{HL}	:	power for the heating demand, see (3.40)	[kW]
f_{DHW}	:	design factor for the hot water demand	[-]
Φ_{DHW}	:	power for the hot water demand	[kW]
f_{AS}	:	design factor for other affiliated systems	[-]
Φ_{AS}	:	power of other affiliated systems	[kW]

According to the standard DIN EN 12831 [54, pp. 28–29] the (standard) heating demand for a building unit or a building is calculated according (3.40)gg. The index i refers to the heated rooms.

$$\Phi_{HL} = \sum \Phi_{T,i} + \sum \Phi_{V,i} + \sum \Phi_{RH,i} \tag{3.40}$$

Φ_{HL}	:	heating load for a building unit or a building	[kW]
$\sum \Phi_{T,i}$	:	transmission heating losses of all heated rooms; without taking the heat flow rate between building units or buildings into account	[kW]
$\sum \Phi_{V,i}$	:	ventilation loss of all heated rooms; without taking the heat flow rate between building units or buildings into account	[kW]
$\sum \Phi_{RH,i}$	:	the sum of all additionally heating needs due to heating breaks	[kW]

To be able to calculate the heating demand it would be necessary to know the building cubature and the building arrangement. For example, calculating the transmission heating losses $\sum \Phi_{T,i}$, the following terms are relevant (3.41) [54, p. 15]. This illustrates that the building has to be designed in detail to be able to calculate all the relevant terms.

$$\Phi_{T,i} = (H_{T,ie} + H_{T,iue} + H_{T,ig} + H_{T,ij}) \cdot (\vartheta_{int,i} - \vartheta_e) \tag{3.41}$$

$H_{T,ie}$	:	transmission heating loss coefficient between the heated room i and the outside environment e through the building envelope	[W/K]
$H_{T,iue}$	:	transmission heating loss coefficient between the heated room (i) and the outside environment e through the unheated room u	[W/K]
$H_{T,ig}$	:	stationary transmission heating loss coefficient between the heated room i and the soil g	[W/K]
$H_{T,ij}$	:	transmission heating loss coefficient between the heated room i and a next door heated room j which is kept at a significant different temperature level	[W/K]
$\vartheta_{int,i}$	:	standard internal temperature of room i	[°C]
ϑ_e	:	standard ambient temperature	[°C]

It is not the aim of this work to model each building in detail and create floor plans, since this would not increase the benefits of this work. That is why another approach is used to calculate the heating demand.
In section 3.3.2, the calculation of the Annual Heating Demand (AHD) is described in detail. A few parts of the calculation principle from this section are used here to determine the heating demand.
This principles are the Heating Degree Days (HDD) and the AHD. If the annual ambient temperature profile – or representatively the HDD $[Kd]$ – and the AHD $[Wh]$ are known, it is possible to calculate an average thermal transmittance $\bar{U}'$ for a building.

$$\bar{U}' = \frac{\text{AHD}}{\text{HDD}} \tag{3.42}$$

The U-value is defined as following: $U = \frac{\Phi}{A \cdot (T_1 - T_2)}$, the dimension is $\left[\frac{W}{m^2 K}\right]$. The dimension of $\bar{U}'$ is $\left[\frac{Wh}{Kd}\right]$ simplified $\left[\frac{W}{K}\right]$, it is independent of the surface area and represents the transmission value of the whole building. That is why the apostrophe is used to emphasize this difference.
As shown in (3.41) for the heating demand calculation the ambient temperature ϑ_e is needed. The definition for this temperature is as following: *The standard outside temperature can be represented by the value of the lowest temperature of an average over two days, which was measured at least 10 times in 20 years* [54, p. 13]. This temperature is of course depending on the geographical location. For Austria it is within the range of $-12\,°\text{C}$ to $-22\,°\text{C}$ [55]. The fact the model region shall represent Austria, the average value of $-17\,°\text{C}$ is used for this work.
Since the average thermal transmittance, the ambient temperature and the average room temperature of $22\,°\text{C}$ (see section 3.3.2) are known it is possible to calculate the (maximal) heating demand with the following equation:

$$\Phi_{HL} = (22\,°\text{C} - (-17\,°\text{C})) \cdot \bar{U}' \tag{3.43}$$

The maximal power demand for the hot water production is calculated via tap profiles. It is assumed that there is no thermal hot water storage within the buildings and the power demand for the hot water production has to be delivered from the district heating grid directly via a flow heat exchanger. This has two reasons, one is, the network itself works as a storage and due to the connection of many consumers to the system the simultaneity is less than one and the system has not to be designed for the maximal power. For single-family houses the use of a hot water boiler decreases the maximal

power demand of the heating system, among other causes this is why boilers are used. In order to link the temporally resolved heating demand of a building to a temporally resolved heat requirement to the heating network, is the other reason why boilers have been omitted. Otherwise a time correlated demand between household and network would not be possible, because of the storage characteristics of the boiler. For a thermal energy supply with a district heating network, it is possible to have a system without hot water storages within the buildings. The standard DIN 4708-2 [56, p. 4] uses a demand factor N as indicator to determine the power demand for hot water production. For this demand factor a standard household is defined with 3.5 persons and 4 rooms. The definition with 3.5 persons per household is used to determine the maximal tap flow rate using the tool DHWcalc [57] (for more details see section 3.3.2). According DHWcalc this results in a maximal tap flow rate for one household of 629 l/h. With (3.51) and the values used there (e.g. 40 K temperature raise of the water) this results in a maximal power demand of Φ_{DHW}=29.26 kW per household. Not each household will use its maximal power demand for the hot water production at the same time. The Simultaneity Factor (SF) defines how much load is used at the same time, it is defined as following:

$$\mathrm{SF} = \frac{P_{maxDH}}{\sum_{i=1}^{n} P_{maxHH}} \tag{3.44}$$

SF	:	between 0 to 1; 0...no demand at the same time, 1... all the demand at the same time	[-]
$\sum_{i=1}^{n} P_{maxHH}$	:	sum of the maximal power of all households n at the district heating system	[kW]
P_{maxDH}	:	actual maximal power demand at the district heating system $P_{maxDH} \leq \sum_{i=1}^{n} P_{maxHH}$	[kW]

For the heating power a SF of 1 is assumed because of the similarity of the weather in the model region. For the hot water demand a value of 0.5 is used, because there are more than 35 households in the region of the district heating system (fig. 3.11). This leads to the following power demand per household for hot water production Φ_{DHW} =14.63 kW. According (3.39) this value is added to the maximal heating power Φ_{HL}. It is assumed that no other affiliated systems with heating demands are existing and all the design factors are one.

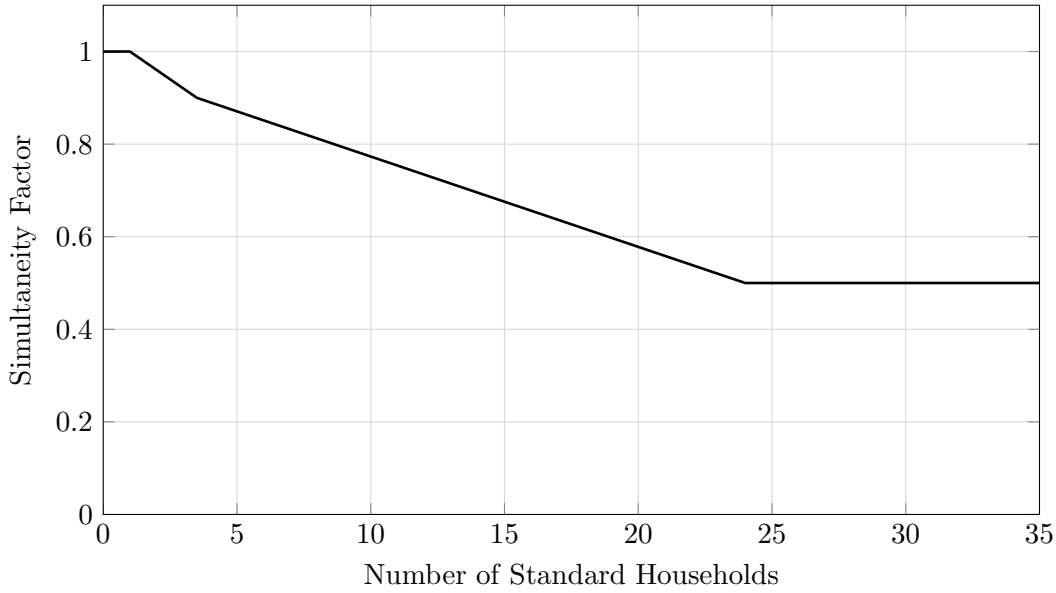

Figure 3.11: Simultaneity Factor for the district heating demand; Modified according to [58, p. 7]

To be able to design the network it is necessary to know which topologies are commonly used. District heating systems are constructed with the following topologies (fig. 3.12) [59, pp. 25–26]. They are similar to the gas network topologies.
There are two basic types, the radial network (fig. 3.12a) and the meshed network (fig. 3.12b). A characteristic of the second one is multiple supply paths and therefore higher security of supply. Due to the higher costs, in residential and industrial areas mostly radial networks are constructed. The line network (fig. 3.12c) is a special type of radial network. It contains only one supply path with rather short branch lines to the loads. Correspondingly the ring network is a supply system with only one mesh/loop and the attached branch lines.

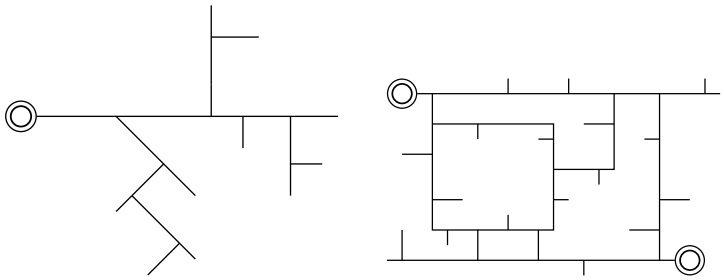

(a) radial network (b) meshed network

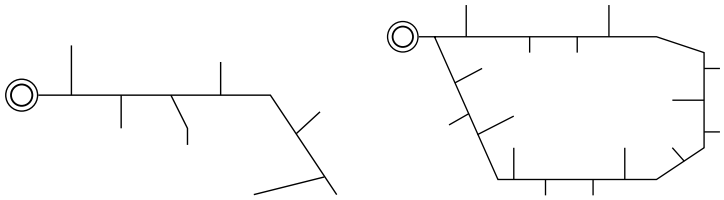

(c) line network (d) ring network

Figure 3.12: Different heating grid topologies; Modified according to [59, pp. 25–26]

From the usually used network types, for the model region the ring network for the "Urban Structure" and the line network for the "Small Town" is used. The ring structure has higher reliabilities, that is why it is chosen for the urban region, this is in dependence on the primary district heating system in Vienna. The "Small Town" represents a less spread area with smaller load density, for such structures radial or line networks are common solutions.

For the pipe dimensioning, it is important to know the demand and temperature spread $\Delta\vartheta$ between forward and return flow of the supplied area. The necessary temperature spread is dependent on the building standard. As mentioned in subsection 3.3.2, three different thermal load scenarios are considered. For the default and usual refurbished scenario the model region contains old buildings which need a higher temperature level for heating. For these two scenarios, the temperature curves shown in fig. 3.13 are used. The minimal forward temperature for an ambient temperature of $-17\,°C$ is $65\,°C$. The maximal return flow temperature at an ambient temperature of $-17\,°C$ is $35\,°C$. The grey highlighted area is roughly the possible temperature spread. At some points it is less than $30\,°C$, and reaches a spread of $20\,°C$. The network has to be designed for the worst case, that is why $20\,°C$ is used for $\Delta\vartheta$, for these two scenarios.

In the "Urban Structure", there is a maximum thermal power demand of 2.3 MW, in the "Small Town" the maximum demand is 188 kW. With the spread of $20\,°C$, and the data from tab. 3.5, for the ring at the "Urban Structure" a DN150 and for the line network

to the "Small Town" a DN50 is used, because this dimensions are capable to transport the maximum power demand. To keep the amount of different pipe types limited, this is usual in practice, otherwise the store-keeping would be complicated and expensive. That is why, DN50 is used as branch lines to supply the individual buildings in the "Urban Structure", if this dimesnion is sufficient. Some nodes (e.g. apartment buildings) require higher dimensions such as DN65. In total, the three dimensions DN150, DN65 and DN50 are used.

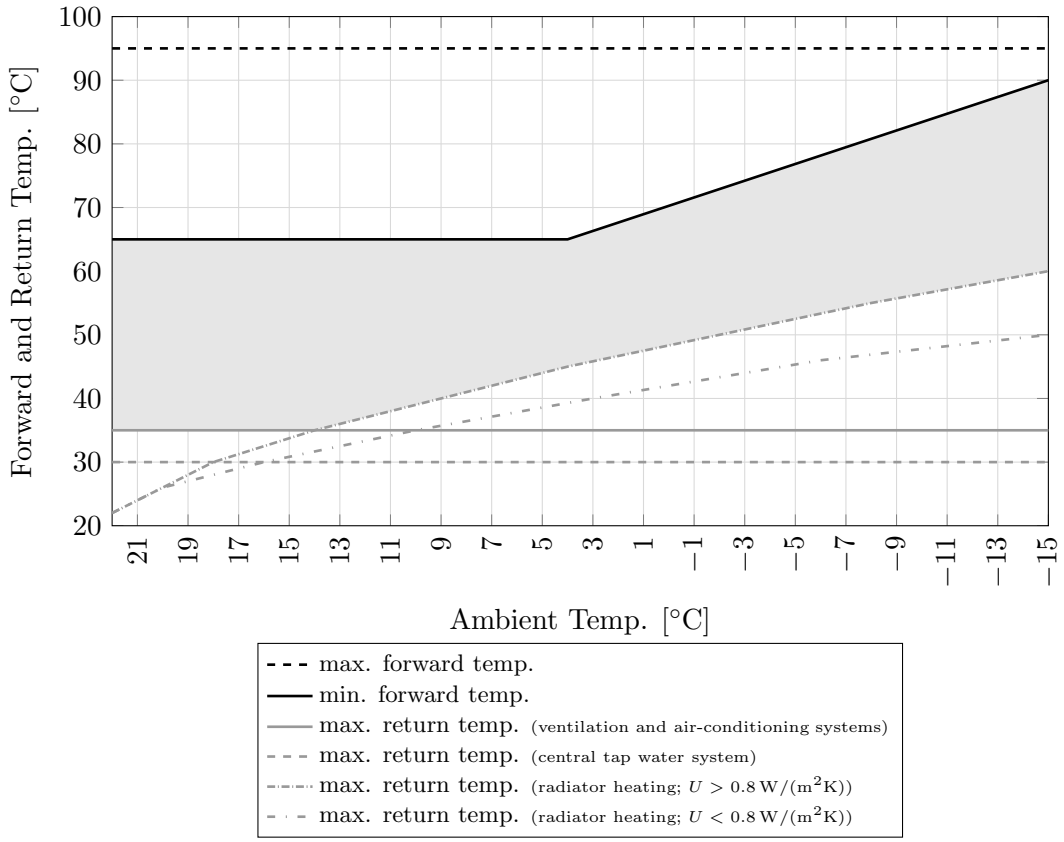

Figure 3.13: Forward and return flow temperature for different usages for the default and refurbished scenario. The gray area represents the minimal possible temperature spread; Modified according to [60, p. 18]

For the default and refurbished scenario, the same network is used. It is assumed that the district heating grid is designed for the building stock of the default scenario and gradually all the buildings are refurbished. This is why there is no redesign in the network. It is not possible to refurbish buildings from an old conventional building standard to the standard of a low-, lowest- or passive houses. That is why it is assumed that such

an urban area would be a new development area and the district heating network is especially designed for this case. Because of low temperature heating systems modern building standards have different temperature level requirements. The district heating temperature range for such a case is shown in fig. 3.14. The minimal practically used forward temperature is 65 °C. The grey area highlights again the possible temperature spread. In consultation with an Austrian district heating provider, a temperature spread of 30 °C is chosen for this case.

For this scenario, the maximal demand at the "Urban Structure" is 1.5 MW and 124 kW

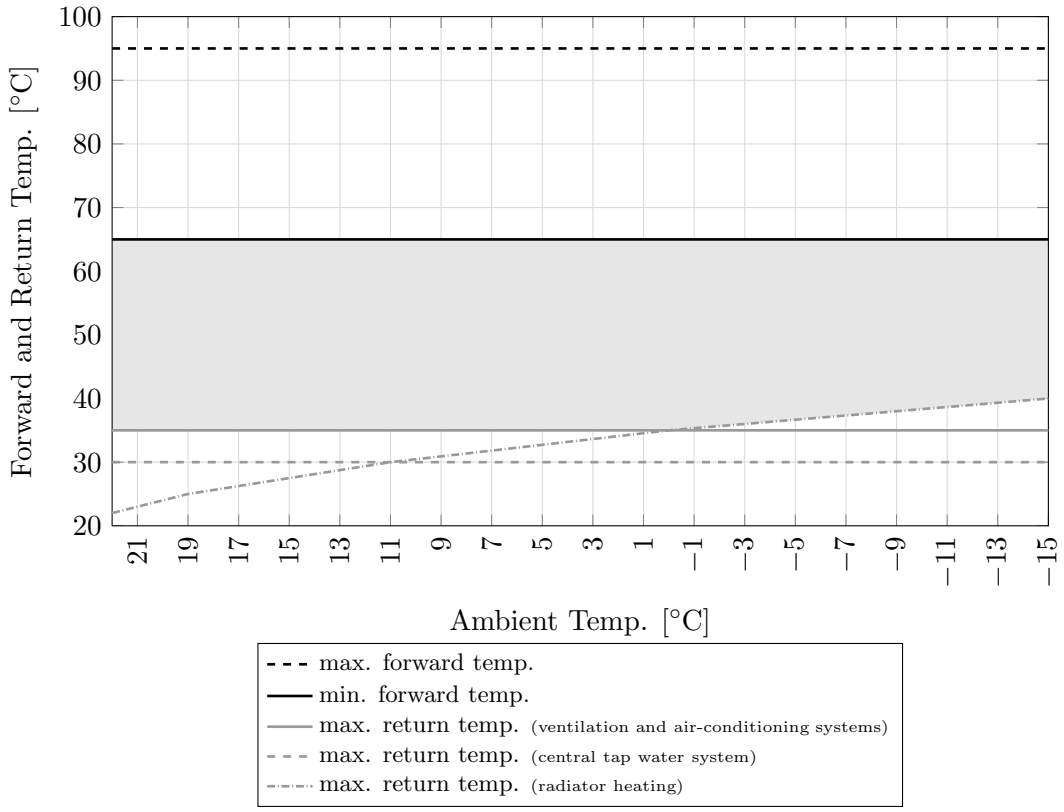

Figure 3.14: Forward and return flow temperature for different usages for the minimal scenario. The gray area represents the minimal possible temperature spread; Modified according to [60, p. 17]

at the "Small Town". With the spread of 30 °C, and the data from tab. 3.5, for the ring at the "Urban Structure" a DN100 and for the supply of the "Small Town" a DN40 pipe is used. DN40 is used as branch lines, if it is sufficient. For the apartment buildings, because of a maximal demand of more than 220 kW a higher dimensions such as DN50 is needed. This results in the following three dimensions DN100, DN50 and DN40 for

this scenario.

All the assumptions lead to the two district heating networks shown in fig. 3.15.

Table 3.5: Transmission Capacity for different pipe dimensions and $\Delta\vartheta$ between forward and return flow; Modified according to [61, p. 2/14]

$\varnothing_N$	Volume Flow [m³/h]		Flow Velocity [m/s]		Transmission Capacity [kW] at $\Delta\vartheta$					
					20 °C		30 °C		40 °C	
DN	from	to	from	to	from	to	from	to	from	to
32	2.348	4.695	0.6	1.2	55	109	82	164	109	218
40	3.151	6.303	0.6	1.2	73	147	110	220	147	293
50	5.879	11.757	0.7	1.4	137	273	205	410	273	547
65	9.781	19.563	0.7	1.4	228	455	341	683	455	910
80	15.395	30.791	0.8	1.6	358	716	537	1074	716	1432
100	25.945	51.891	0.8	1.6	604	1207	905	1811	1207	2414
125	49.639	89.350	1.0	1.8	1155	2078	1732	3118	2309	4157
150	87.185	152.573	1.2	2.1	2028	3549	3042	5324	4056	7098

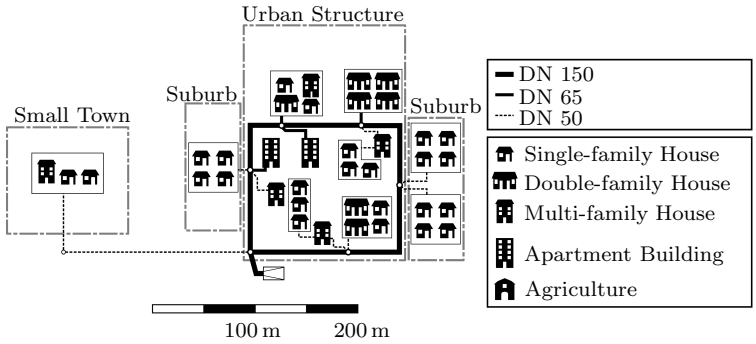

(a) default/refurbished

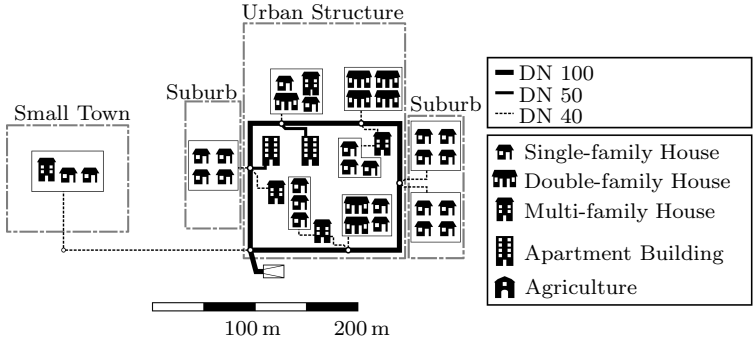

(b) minimal

Figure 3.15: District heating network for the model region for the default/refurbished and minimal scenario

For the load flow calculation of the district heating network, basically the same approach as for the gas network is used. This is because both systems are mass flow networks. The difference is the incompressibility of water compared to methane. Since the pressure drop in the gas network never exceeds 4% it was assumed as incompressible too. That is why it is possible to use the same approach. For the basic calculation principle, it is referred to section 3.2.2.
The difference is how the variables a_k, Re and λ are calculated. For the district heating calculation, the same approach as in the PSS©SINCAL simulation software is used [44]. It is outlined below how these three variables ((3.45), (3.46), (3.47)) are calculated for the district heating system.

$$a_k = \rho \cdot \lambda_k \cdot l_k \frac{1}{d_{ik}^5} \cdot K_1 \cdot K_3 \tag{3.45}$$

a_k	:	line resistance of pipe k	[kg/m^7]
ρ	:	density	[t/m^3]
λ_k	:	pipe-friction coefficient of pipe k	[-]
l_k	:	pipe length of pipe k	[m]
d_{ik}	:	inner pipe diameter of pipe k	[mm]
K_1	:	$\frac{8}{g \cdot \pi^2} \cdot 10^9$	[s^2/m]
K_3	:	$\frac{g}{100}$	[s^2/m]
g	:	gravitational force	[m/s^2]

$$Re_k = K_2 \cdot |Q_{Fk}| \frac{1}{d_{ik} \cdot \nu} \tag{3.46}$$

Re_k	:	Reynolds number of pipe k	[-]
K_2	:	$\frac{4}{\pi} \cdot 10^6$	[-]
Q_{Fk}	:	amount of flow at pipe k	[l/s]
d_{ik}	:	inner pipe diameter of pipe k	[mm]
ν	:	kinematic viscosity (see tab. 3.6)	[mm^2/s]

The kinematic viscosity of water depends on the pressure and temperature. Table 3.6 shows the important range for district heating networks. Since the temperature of the network is between 50 °C to 160 °C, in this work an average value of $0.374\,10^{-6}$m^2/s is used.

Table 3.6: Kinematic Viscosity ν [10^{-6}m^2/s] of water for different pressures and temperatures; Modified according to [62, p. 8]

		T [°C]		
		50	100	150
p [bar]	5	0.550	0.291	0.197
	10	0.550	0.292	0.198
	50	0.549	0.292	0.198

$$\begin{aligned} &\frac{1}{\sqrt{\lambda_k}} = -2 \cdot \log\left(\frac{k_{sk}}{3.71 \cdot d_{ik}} + \frac{2.51}{Re_k} \cdot \frac{1}{\sqrt{\lambda_k}}\right) && \text{if } Re_k > 4000 \\ &\lambda_k = 0.03 && \text{if } Re_k = 0 \\ &\lambda_k = \frac{64}{Re_k} && \text{if } 0 < Re_k \leq 2320 \end{aligned} \tag{3.47}$$

λ_k	:	pipe-friction coefficient of pipe k	[-]
Re_k	:	Reynolds number of pipe k	[-]
d_{ik}	:	inner pipe diameter of pipe k	[mm]
k_{sk}	:	pipe roughness of pipe k	[mm]

The pipe roughness of steel pipes is dependent on the production method. The roughness varies from 0.01 mm to 0.05 mm if they are new. If they are used the value can increase to a range from 0.15 mm to 0.20 mm [63, p. 532]. To not under or overestimate pressure drops significantly because of too high or low roughness value the average of 0.1 mm is used.
Since all parameters for determining a_k are defined it is possible to use (3.38) and calculate the corresponding equivalent load flow matrix $\boldsymbol{L}_h = \boldsymbol{G} \cdot \boldsymbol{A}^T \cdot \boldsymbol{G}_n^{-1}$ for the district heating system. With the matrix $\boldsymbol{L}_h$, it is possible again to calculate the branch loads depending on the node loads. The matrix is determined once before the optimisation and then used to calculate the branch load for each time step, to ensure there are no overloads. At this point, the limitations for the use of this approach shall be mentioned again, which are accepted for the purpose of this work.

1. The quadratic correlation between Δp and $\dot{V}$ must be assumed to be linear.
2. For the resistance a_k, it has to be assumed that it is the same for all flow rates, this is equivalent to $\lambda_k = const.$

The consequences of 1. is an underestimation of Δp. The pressure drop in the whole district heating network for the maximum demand never exceeds 5% ($\frac{p_{infeed}-p_{min}}{p_{infeed}} = \frac{10\,\text{bar}-9.5\,\text{bar}}{10\,\text{bar}}$). Because of the linearisation the calculated pressure drop is <5%. Both values are low, compared to pressure changes because of geological unevennesses. If a hight rise of 40 m is assumed, this result in a pressure change of 4 bar. A detailed geological modelling of the model region is not sufficient, since this would not cause any information gain in context of this work. That is why the region is assumed flat and there is no pressure change due to hight in- or decrease. The error due to the linearisation in this context is therefore negligible. a_k or equivalent λ_k is determined for the maximum heat demand, this results in the maximum possible λ_k for each pipe. (3.26) shows that $\Delta p \propto \lambda$, with assumption 2. the pressure loss in the pipes is overestimated, because normally λ decreases with lower flow rates. 1. and 2. have opposing effects on the calculation of the pressure difference, that is why the resulting error due to the linearisation is expected negligible compared to effectively geological caused pressure changes.

3.3 Loads

The set up of the model region is described at the beginning of this chapter. The 126 households are located at 25 nodes. To be able to perform annual load flow calculations, it is necessary to assign each household with an annual load profile. This is described in this section for the electricity and thermal demand.

3.3.1 Electric loads

When using synthetic profiles two approaches are possible. One is the use of standardised VDEW profiles [64]. The H0 profile which represents the energy demand of households is shown in fig. 3.16. The profile differentiates between three types of days (Weekday, Saturday, Sunday) and three different seasons (summer, winter and transition, which represents spring and autumn). The power values shown here are for an average annual energy consumption of 1 000 kWh. This profile is the result of averaging a huge number of households. This has the disadvantage that each household has the same profile and random differences in device usages, and therefore profile variations are missed. Because of this disadvantage another approach is used. At this approach a different synthetic profile for each household is created. How the profiles are derived is explained here.

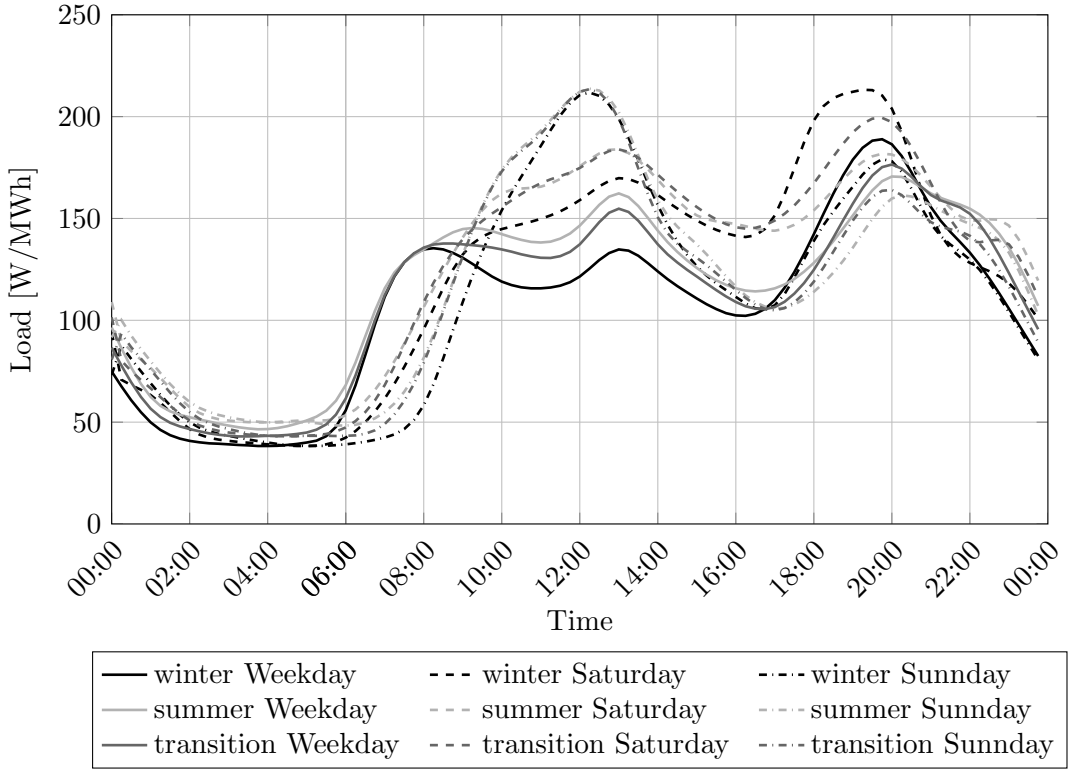

Figure 3.16: VDEW H0 profile for different days and seasons for an annual energy consumption of 1 000 kWh; Modified according to [64, p. 26]

The electric load profiles were generated for the project "aktives Demand-Side- Management durch Einspeiseprognose" aDSM [16, pp. 22–74]. The profile generation is based on an extensive process. Only some detailed parts of this process are highlighted here, for more details to [16], [65] and [66] is referred.
The profile generation is based on the work Zeilinger carried out in his Master thesis [65]. For the profile generation, the number of devices per appliance category (e.g. thermal storage, scheduled operation, constant operation, etc.) for different households is relevant. Likewise, the number of people living in the aDSM region and people per household are needed. Based on these numbers the average operating time and thus the average annual energy consumption per device category is determined.
As a data basis for this study a survey which was carried out for the project "Autonome Dezentrale Regenerative Energie Systeme (ADRES)"[7] [67] was used. Therefore the results of 3 832 questionnaires were analysed and information about living-, employment

[7] Autonome Dezentrale Regenerative Energie Systeme is german for: autonomous decentralised renewable energy systems

conditions, the amount of electrical equipment and the annual energy consumption for different households was gathered.
Households with homogeneous electric appliances were grouped. This grouping had to fulfil certain criteria. There should not be more than 10 groups, each household should be distinctly assigned to one group, each group should contain a useful number of households and the groups must be distinguished according to their appliances. The classifications in tab. 3.7 follow these requirements. Since the households are grouped,

Table 3.7: Classification of of household groups; Modified according to [16, pp. 21–22], [39]

Class	Building Type	Persons	Distribution	Quantity in aDSM
H1	House	1	11%	13
H2	House	2	14%	17
H3	House	3	9%	12
H4+	House	4+	15%	19
A1	Apartment	1	23%	29
A2	Apartment	2	15%	19
A3	Apartment	3	7%	9
A4+	Apartment	4+	7%	8
			100%	126

it is possible to assign the amount of different electric appliances to each household group. This was done with data from the "Strom- und Gastagebuch 2008"[8] [68]. This data was adjusted with the survey results from ADRES. Table 3.8 shows the assigned appliances to each group. The first column lists the household classification, followed by the absolute number of households in the aDSM region. The remaining columns list the relative device numbers for each household category. In the second last row, the average device number for the whole region is listed. For certain devices like "Fridge", "TV" and "PC", the average household has more than one device. The last row lists the average device number per person, this results in an average person number per household of 2.38.

[8]Strom- und Gastagebuch 2008 is german for: electricity- and gas diary 2008

Table 3.8: Average number of devices per household group; Modified according to [67]

Cat.	Quant.	Average number of device per household							Heating		Circ.-pump	Hot Water	
		Fridge	Freezer	Washing-machine	Dryer	Dish-washer	TV	PC	Heat-pump	Radiator		electric Boiler	flow Heater
H1	13	105.8%	59.9%	91.2%	11.8%	49.6%	161.8%	48.2%	0.0%	12.5%	69.2%	29.2%	8.3%
H2	17	157.8%	97.4%	93.8%	35.8%	80.7%	200.1%	84.9%	5.1%	2.6%	85.7%	22.2%	2.8%
H3	12	183.4%	111.2%	92.3%	42.4%	81.4%	282.1%	161.2%	4.8%	14.3%	72.0%	43.5%	4.3%
H4+	19	186.7%	119.8%	91.3%	44.1%	86.8%	262.3%	212.7%	9.3%	4.7%	85.1%	30.0%	3.3%
A1	29	108.6%	26.3%	82.5%	9.0%	50.3%	112.4%	70.0%	0.0%	13.2%	19.6%	45.8%	8.3%
A2	19	124.8%	53.7%	86.2%	12.5%	69.3%	155.4%	116.5%	0.0%	8.1%	39.5%	41.2%	2.9%
A3	9	123.1%	47.8%	90.5%	19.8%	77.7%	188.2%	176.5%	0.0%	0.0%	37.5%	43.8%	0.0%
A4+	8	135.3%	56.4%	86.9%	26.5%	76.9%	206.2%	206.0%	0.0%	0.0%	21.4%	66.7%	6.7%
Avg. tot. region		138.7%	69.0%	88.6%	23.7%	69.2%	185.6%	123.1%	2.5%	7.9%	52.9%	38.8%	4.9%
Avg. p. Pers.		58.3%	29.0%	29.0%	10.0%	29.1%	78.0%	51.7%	1.1%	3.3%	22.2%	16.3%	2.1%

Since the amount of electric devices for the whole model region is estimated, it is necessary to associate each household with its actual amount of equipment and the behaviour of each device. Therefore each of the 126 household is randomly associated to one of the eight classes mentioned in tab. 3.7. The result of this association is the assignment of the 126 households to one of the 60 buildings. This sets the spatial distribution, the assignment to the building type (single-family house, double-family house, etc.) and leads to the number of electric devices for each device type, e.g. "TV".
For the electric device assignment to each household a probabilistic approach was used. This approach associates each household with an integer number for each device, e.g. 1 "TV", 2 "PC's" and so on. [16, p. 23]
So far each household is associated to a building in the aDSM region and each household is associated with its electric appliances. It is essential to allocate each electric device with an individual annual load profile. To model individual devices, a bottom-up approach was chosen. This was done by simulating a huge number of the same devices with its probabilistic characteristics, e.g. 5 000 TVs. The probabilistic characteristics are for example, average annual energy consumption per device, runtime, standby-, running-power and so on.
From the random parameter set, which describes a device class each single device is associated with concrete values for the load flow calculation. The sum load profile of all devices of one class is compared to a comparative profile. This comparative profile for example is derived from the literature [69]. In an adjustment process, the set of random parameters for the whole device class is then modified to fit the sum profile best to the comparative profile. The following figure (fig. 3.17) shows the power consumption for the class Audio-Video-devices, for a summer workday. The number of devices used by 5 000 people was simulated for this purpose. Cycle one and four of the parameter improvements and the comparative data is displayed. Even if the differences are marginal, with each cycle from 1 to 4 the data fits better with the comparative data. For cycle 1 there is a maximum deviation of 5% for cycle 4 the maximum deviation is 2.47%. 2.5% is the target criteria which shall not be exceeded. In total the following 28 different devices are considered:

- Fridge
- Freezer
- Desktop PC
- Notebook
- Monitor for PC
- Laser Printer
- Ink-jet Printer
- Various Office Equipment
- TV
- Set-Top Box
- Video Equipment
- Game Console
- Hi-Fi Device
- Radio
- Lighting
- Washing Machine
- Dishwasher
- Dryer
- Circulation Pump
- Various Devices
- Stove
- Oven
- Microwave
- Various Kitchen Equipment
- Flow Heater
- Hot Water Boiler
- Radiator
- Heat pump

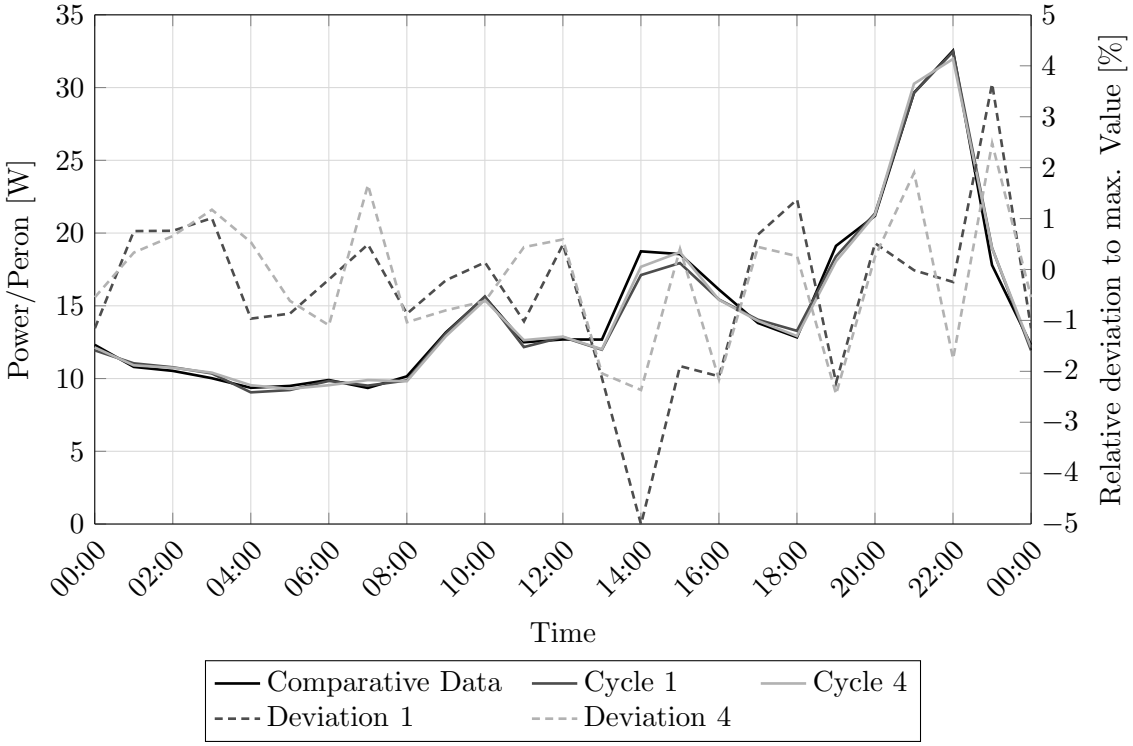

Figure 3.17: Parameter finding for the class Audio-Video-devices. The parameter fit for cycle 1 and 4 is shown, the deviation is between the current simulated value and the maximum value of the comparative data; Modified according to [16, p. 62]

Such a parameter fit is done for each device category, e.g. "TV", "Fridge", and so on. For the profile generation of the total household, one profile for each device was randomly taken from the profile pool for these device types. For example if a household contains two devices from the group Audio-Video-devices, from the load profiles generated for several e.g. 5 000 Audio-Video-devices two profiles are chosen and allocated to the two devices. In figure 3.18, a daily profile for a summer Sunday of one household from the category "H2" is shown. The household contains 30 different devices, for clarity only a few exemplary devices and the sum profile are shown. The household profile is the sum of all devices which the household contains. The generated profiles are annual profiles with a resolution of 1 minute. This results in 525 600 power values for just one household for the period of a whole year. For the 126 households this results in 66 225 600 values, just for the electric loads. Even if the optimisation might be able to handle such huge data, 15 min average values are used. This averaging involves information loss but not in context of this work, because dynamic investigations are not the aim of this work. The aim is the optimisation of the annual energy consumption and therefore 15 min average values are sufficient enough. But even this leads to 131 400 values for one household for

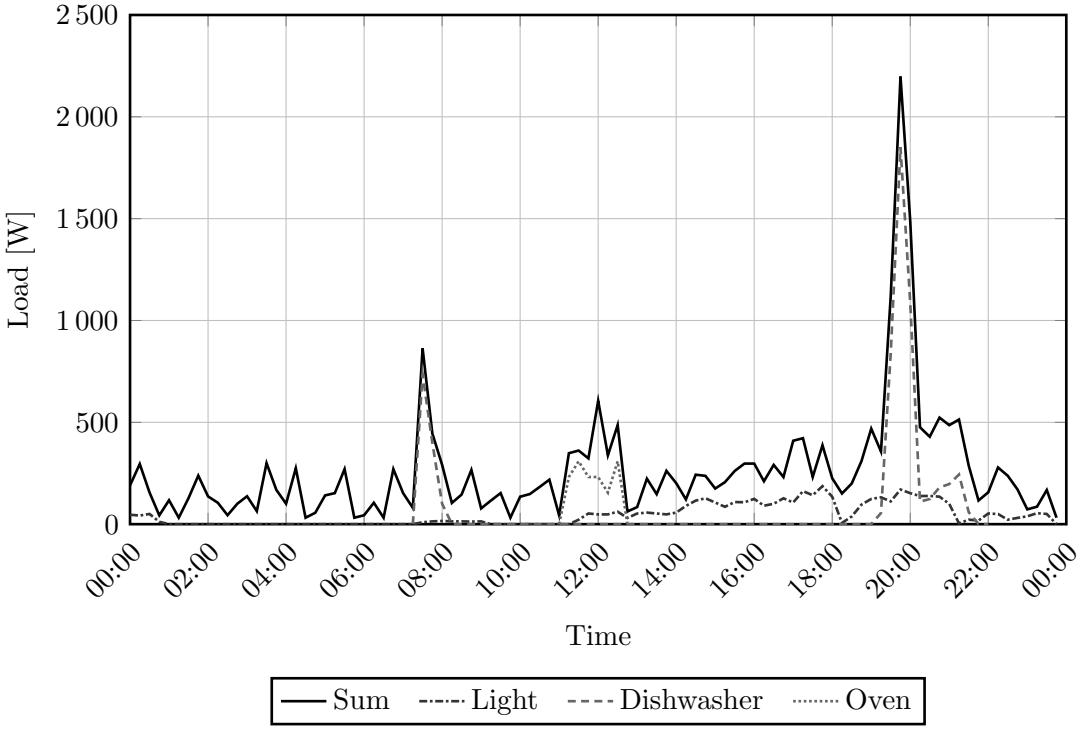

Figure 3.18: Day profile of one household of the group "H2" for a summer Sunday; Modified according to [16, p. 72]

the period of a whole year. According to Verband der Elektrizitätswirtschaft (VDEW)[9] [64] the year is represented with three seasons, summer, winter and a transitional period (spring, autumn). The detailed classification for the year 2013 is shown in table 3.9. The first column lists the "three" seasons, followed by the date range, the allocation of the total amount of days, weeks, Saturdays, Sundays and Weekdays (Monday-Friday). For

Table 3.9: VDEW classification of the seasons. SA...Saturday, SU...Sunday, WD...Weekday; Modified according to [64], [16, p. 27]

	VDEW classification	Days	Weeks	SA	SU	WD
Summer	05/15/ - 09/14/	123	17.57	18	17	88
Transition	03/21/ - 05/14/ & 09/15/ - 10/31/	102	14.57	14	15	73
Winter	11/01/ - 03/20/	140	20.00	20	20	100
		365	52.14	52	52	261

a further data reduction, only one representative sample week for each VDEW period is taken. Summer, transition and winter are represented each time with 7 days. With this approach, it is possible to reduce the total amount of investigated days to 21 instead of 365.

[9] Verband der Elektrizitätswirtschaft is German for: Electricity Association

Following the reduction approach is described, this approach was used by [70]. Several steps are carried out, to achieve the reduction [70, pp. 28–29]:

1. First according to table 3.9 the year is split in its seasons.
2. Determination and allocation of the days (Weekday, Saturday, and Sunday).
3. Separation of working days in five groups (Monday to Friday); Saturdays or Sundays are separate groups (this provides a total of seven groups).
4. Each of the seven groups is sorted in ascending order, according to the daily energy consumption.
5. The number of weekdays must be divisible by five. If this is not the case the amount of weekdays is reduced until it is divisible by five. Therefore alternatively one weekday at the left (maximum daily energy) and the right (minimum daily energy) is removed (see fig. 3.19). A maximum of four days is removed.
6. With a optimisation process, from each of the seven groups (five weekdays, Saturday and Sunday) one day is selected. The objective function is the minimisation of the energetic difference. The energetic difference is between the energy consumption of the household for the original VDEW season, e.g. summer 05/15/ - 09/14/ and the representative sample week times its amount of weeks in this period, e.g. 17.57 for summer.
7. Finally, the determined representative sample weekdays are arranged in random order, followed by the determined Saturday and Sunday.

For one household this process is illustrated in figure 3.19. The transition period is illustrated larger to be able to clearly see the selection details. The other two seasons are shown for comparison purpose. According to the aforementioned step 3, the days are separated in seven segments, the 5 weekday segments are marked with horizontal dashed lines. The Saturday and Sunday segments are marked with dotted lines. Depending on step 4, each group is ordered in an ascending way (Weekdays, Saturdays and Sundays). Since the number of weekdays of the transition period is not divisible by 5, two days on the left and one day on the right of the weekday range are excluded from further calculations (equivalent to step 5). Those are the days represented with white bars. The grey highlighted bars are the ones chosen from the selection/optimisation process. The household illustrated has a heat pump, and this is why there is such a big difference in the electric energy consumption between the seasons. For a household with no electric heating system there is no distinct difference between the seasons. That is why such a household was chosen and why the energy consumption for the heat pump was kept for this illustration purpose.

Otherwise all electric heating systems are excluded from the data since it is an option for the optimisation to choose what the best way for heating is. That means that the optimisation can choose if a heat pump, district heating – if possible – or some other heating option should be used. For more information see chapter 4. This means from the original 28 different electric devices the four following devices for heating purposes are removed:

- Flow Heater
- Hot Water Boiler
- Radiator
- Heat pump

This does not mean that the power demand for heating is ignored. The demand is derived in the next section, just independently from the form of producing the energy for the heating demand.

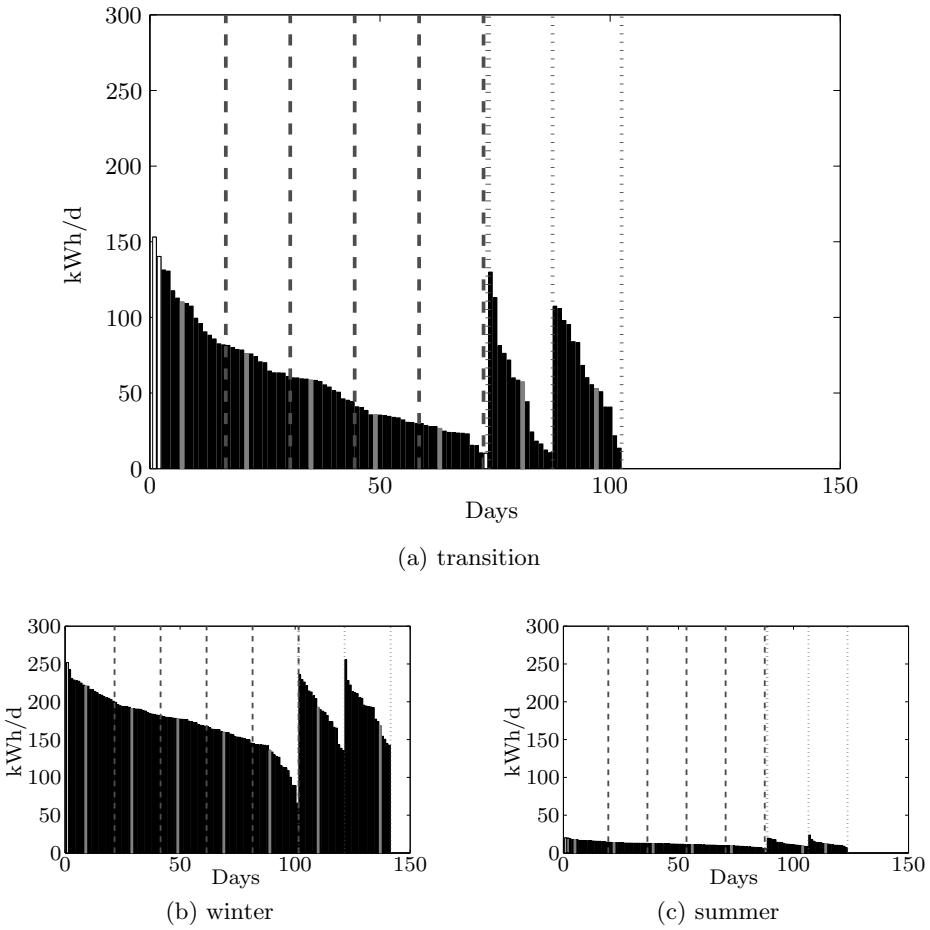

(a) transition

(b) winter

(c) summer

Figure 3.19: Visualisation of the selection process on how the representative electric load sample weeks are obtained. The dashed horizontal lines represent the separation between weekdays, the dotted lines are separations between Saturday and Sunday. The weekdays highlighted with white bars are excluded from further selection processes. The grey bars are the chosen days. Modified according to [70, p. 31]

Since the electric load profiles for each household are determined and each household is allocated to one of the 25 nodes, the profiles for each node are determined too. Figure 3.20 shows the maximum and minimum power consumption of the whole model region for the representative summer sample week. The minimal energy consumption is one of conspicuousness. From the 25 nodes there is always at least one, which has no or almost no power consumption. Besides the peak on the 6th day the maximum power is mostly around 8 kW to 13 kW. The power consumption of all nodes is permanently within the grey area. Figure 3.27 shows the equivalent for the PV production for the summer week. The maximum PV power exceeds the maximum load power by a factor of 3 to 6.

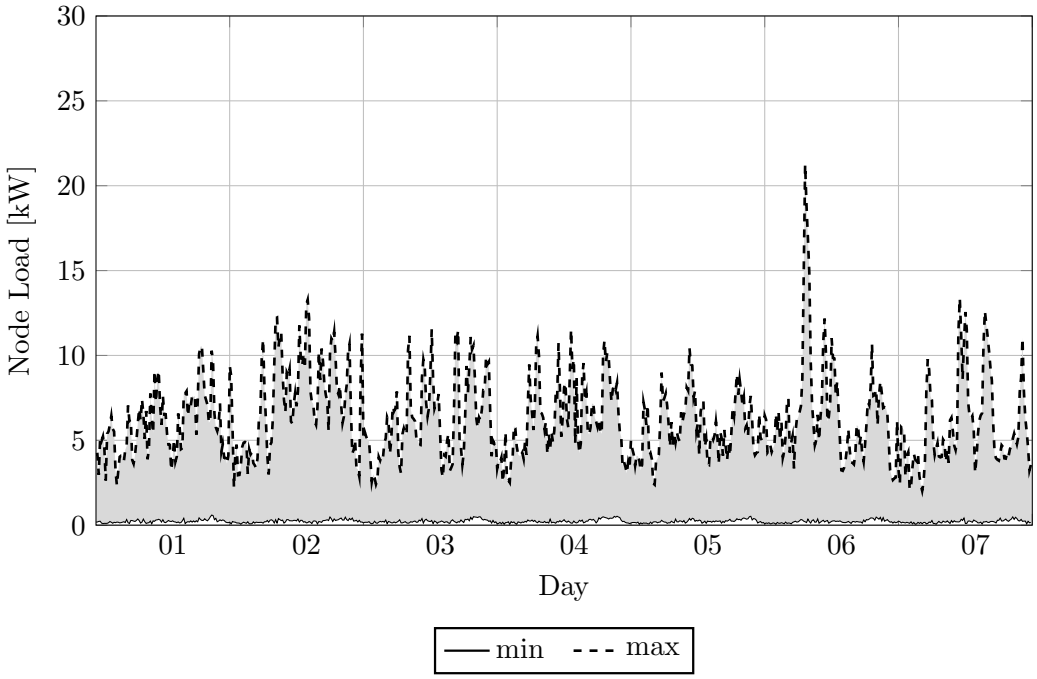

Figure 3.20: Summer load profile for the representative sample week for all nodes. The load power consumption for each node is within the grey area.

With this selection approach, the worst error for one season and one household is 0.19 % and the average error rate for the whole region and all seasons is 0.000 47 %. The error rate is the difference between the energy consumption of one representative sample week up-scaled to the duration of the season (e.g. transition week times 14.57) and the original energy consumption for this season. Because of these very low deviations, this approach is considered admissible and the set of 126 times 3 weeks respectively 25 (number of nodes) times 3 is taken for further investigations.

3.3.2 Thermal loads

The thermal demand in the residential sector is driven by two needs. One is space heating and the other is hot water production. As shown in (3.39), the heating demand consists of three different types: heating, hot water and affiliated systems. As mentioned in section 3.2.3 the demand for affiliated systems is not taken into account. The two remaining needs are combined into one final thermal demand profile. Firstly, it is described how the demand for space heating is calculated followed by the energy calculation for hot water production.
For the energy calculation for space heating it is necessary to determine the heating demand for each building. This is done by calculating the size of each apartment or household. Table 3.10 shows the number – in thousands – of apartments in Austria in relation to different building and apartment sizes [71]. For the model region, each household is located in a specific building, for instance, in a single-family house or in an apartment building with >10 apartments. According to its location (which determines the column) each household is randomly associated to one of the eight groups (rows), always in accordance with the statistical distribution given by the numbers in tab. 3.10. After the group association, the size is randomly chosen between the minimum and maximum square metre range m^2_{min}, m^2_{max}. Each household is now associated with a size.

Table 3.10: Number of apartments in Austria – in thousands – for different building and apartment sizes; and the minimum and maximum square metres for each group. Apt...Apartment; Modified according to [71]

(Apt) Size	Building Size				m^2_{min}	m^2_{max}
	1 Apt	2 Apt	3-9 Apt	≥10 Apt		
<35 m^2	3.2	3.3	24.9	80	25	34
35 m^2 to 44 m^2	5.2	6.5	40.3	118.2	35	44
45 m^2 to 59 m^2	18	26.8	132.1	269.1	45	59
60 m^2 to 89 m^2	146.2	139.2	367.1	518.6	60	89
90 m^2 to 109 m^2	180.8	91.9	102.2	153.4	90	109
110 m^2 to 129 m^2	258.3	73.5	36.2	44.2	110	129
130 m^2 to 149 m^2	260.8	49.4	17.6	15.5	130	149
>150 m^2	431.1	72.9	21.7	13.9	150	170

Because of this it is necessary to determine the heating demand per square metre.
The TABULA project [72] delivers data containing the heating demand for buildings constructed before 1919 to 2009. It is possible to choose various countries from Europe, however for this work the data for Austria are taken. The data provided is for different building types, including single-family houses to apartment buildings. The energy demand kWh/(m^{2}a) is provided for three different building settings. The "Existing State", the "Usual Refurbishment" and the "Advanced Refurbishment". A single-family house, built before 1919, has for example one of the following three average energy demands 399.2 kWh/(m^{2}a), 166.0 kWh/(m^{2}a) or 96.0 kWh/(m^{2}a). In this work, the energy de-

mand only for the "Existing State" and the "Usual Refurbishment" is considered. Additionally the heating demand for modern buildings is taken into account. These buildings' standards are "low energy"-, "lowest energy"- and "passive"-house, the necessary heating demand per square metre is provided at [13]. The heating demands for the different building types and construction years/standards for the "Existing State" are shown in fig. 3.21. For low, lowest and passive houses there is no differentiation in the energy consumption between different building types, since [13] only mentions one general value independent of whether it is a family house, multi-family house or an apartment building.

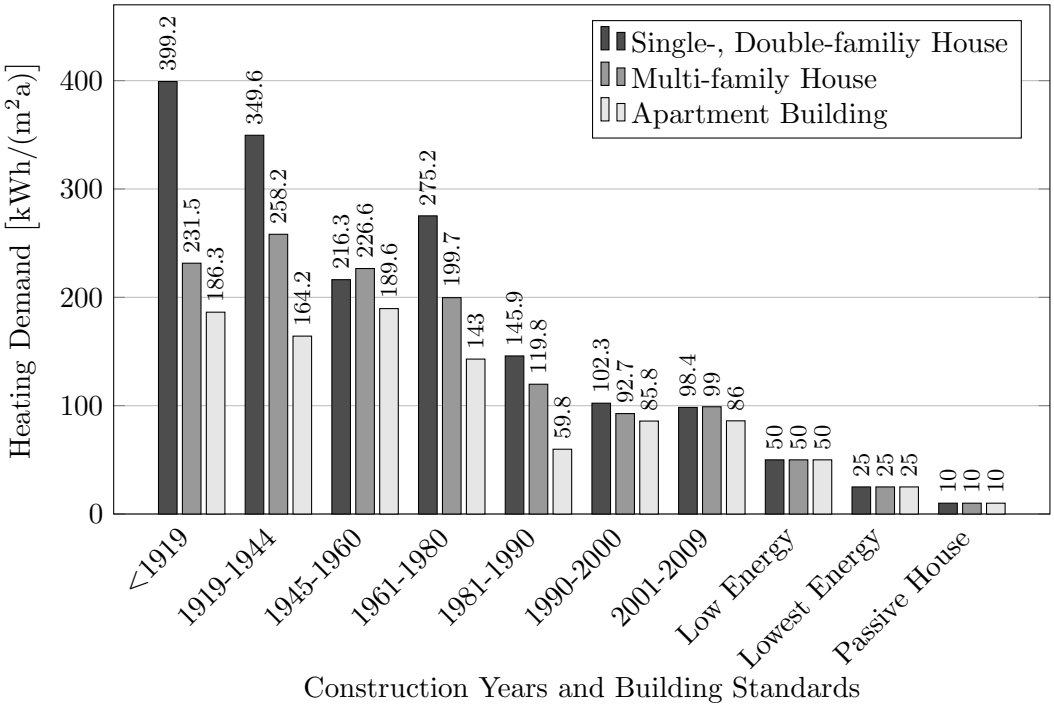

Figure 3.21: The heating demand for different construction years, building standards and building types where no refurbishment was done so far ("Existing State"); Modified according to [13], [72]

For the usual refurbished states the demands are shown in fig. 3.22. For the historical constructed buildings there is a huge potential of heating demand reduction. Since low, lowest and passive house standards are rather new, there is no improvement potential because of refurbishment. Buildings constructed with one of these three standards are rather new and a refurbishment is not necessary, neither from an energetic nor economical improvement. That is why the data is the same in both figures (fig. 3.21 and fig. 3.22). So far square metre are associated to each household and the heating demand for different construction years or building standards are determined. To be able to associate the annual heating demand of each household it is still necessary to determine the construction year or building standard of each building. For this the data shown

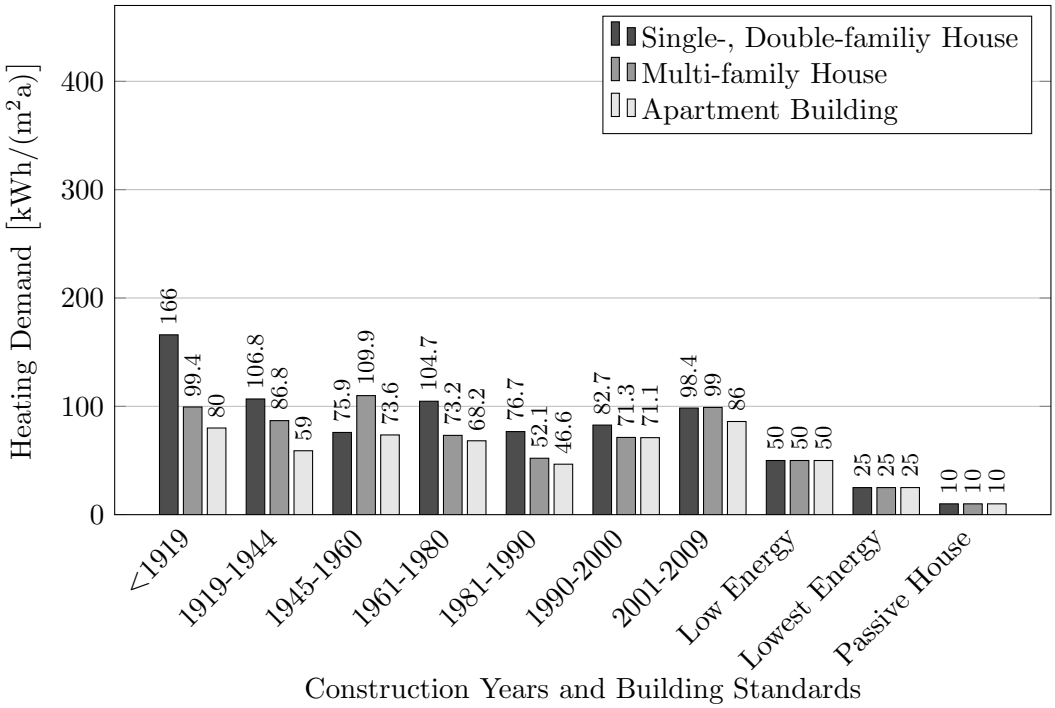

Figure 3.22: The heating demand for different construction years, building standards and building types where the usual refurbishment was done; Modified according to [13], [72]

in tab. 3.11 is used. The table shows the number of buildings constructed at different time periods. According to the relative occurrence each building in the model region is assigned to one construction period.

Table 3.11: Quantity of buildings constructed at specific year ranges and relative number of buildings at specific range; Modified according to [71]

Construction Year	Quantity	Relative Occurrence
<1919	327 350	14.9%
1919-1944	165 930	7.6%
1945-1960	243 616	11.1%
1961-1970	283 271	12.9%
1971-1980	325 343	14.8%
1981-1990	305 125	13.9%
1991-2000	264 146	12.1%
>2001	276 499	12.6%
total	2 191 280	100%

For the heating demand three scenarios are differentiated. For comparability reasons the square metre size of the households is kept the same for all scenarios.

1. **Default** Demand: for this scenario the construction year is assigned randomly according to tab. 3.11. As an annual heating demand, the values for "Existing State" from fig. 3.21 are used.
2. **Refurbished** Demand: for this scenario the construction year is kept the same as at the "Default Demand" scenario. The only difference is the usage of the "Usual Refurbishment" data from fig. 3.22 for the annual heating demand.
3. **Minimal** Demand: for this scenario it is assumed that each building in the model region is built to the newest standards (low-, lowest- or passive-house). [71] does not give statistical data about construction distributions for any of these new building types as seen in tab. 3.11. That is why the three types are equally distributed to the 60 buildings and the corresponding annual heating demand is taken.

The results of the annual heat demand determination for all three scenarios are shown in tab. B.2–B.5 in the appendix.
The annual heating demand is an accumulated value over the whole year. For the optimisation process it is necessary to derive 15 min load profiles from the accumulated values. This is derived using a calculation process based on Heating Degree Days (HDD). The HDD calculation according to the standard "OENORM B 8135" is shown in (3.48) [73, p. 2]. The 20/12 indicates a average room temperature of 20 °C and a ambient limit temperature of 12 °C.

$$\mathrm{HDD}_{20/12} = \sum_{n=1}^{z} (20\,^{\circ}\mathrm{C} - \vartheta_{em}) \tag{3.48}$$

ϑ_{em}	:	average daily temperature	[°C]
z	:	Number of days where ϑ_{em} <12 °C during the period from the 1st of October to the 30th of April	[-]

The standard room temperature for apartments is between 19 °C to 25 °C [54, p. 35]. That is why 22 °C is used as average room temperature and (3.48) is modified to the following version:

$$\mathrm{HDD}_{22/12} = \sum_{n=1}^{z} (22\,^{\circ}\mathrm{C} - \vartheta_{em}) \tag{3.49}$$

For the outside temperature profile the long-term (1978–2007) half synthetic climate data for Vienna, Klagenfurt, Innsbruck and Malnitz are available [74, pp. 39–47]. The HDD-sum of Innsbruck fitted best with the sum of the Austria reference climate, that is why the data of Innsbruck are used and the HDD result in about 3 400 Kd.

The following equation is used to calculate the heating demand profiles from the HDD and AHD:

$$\begin{aligned} P_{heat_i} &= \frac{(22\,^{\circ}\mathrm{C} - \vartheta_{out_i})}{\sum_{n=1}^{z}(22\,^{\circ}\mathrm{C} - \vartheta_{em})} \cdot \mathrm{AHD} && \text{if } \vartheta_{em} \leq 12\,^{\circ}\mathrm{C} \;\&\; i{=}1^{\mathrm{st}}\text{Oct. to } 30^{\mathrm{th}}\text{ Apr.} \\ P_{heat_i} &= 0 && \text{if } \vartheta_{em} > 12\,^{\circ}\mathrm{C} \;||\; i \neq 1^{\mathrm{st}}\text{Oct. to } 30^{\mathrm{th}}\text{ Apr.} \end{aligned} \tag{3.50}$$

P_{heat_i}	:	heating power demand for time step i	[kW]
$\sum_{n=1}^{z}(22\,^{\circ}\mathrm{C} - \vartheta_{em})$	:	is the $\mathrm{HDD}_{22/12}$ from (3.49)	[Kd]
ϑ_{out_i}	:	outside air temperature for the specific time step i	[°C]
AHD	:	multiplication of the apartment size $[m^2]$ and the heat demand shown in fig. 3.21 or fig. 3.22	[kW]

Hot Water

As mentioned at the beginning of this subsection, the second part of the thermal heat demand is the demand for hot water production. How the calculation of this demand is derived is described here.

An average person needs between 30 l/d to 60 l/d of hot water [75, p. 1923]. The tap profiles form the basis for this calculation. The tool DHWcalc [57] is used to generate an average tap profile for the whole model region with an average daily hot water consumption of 45 l/pers. The setting which is used to generate the tap profile is listed in the appendix. To associate the tap profile for one person the total tap profile is divided by the total population of the model region, which is 300 people. The people per household association was already done for the electric load calculation in the previous section. This association is used to determine the tap profile for each household. To derive power values from the tap profile the following equation and values are used [76, p. 65]:

$$P_{HW_i} = \frac{\dot{V}_{tap_i} \cdot c_{p,H_2O} \cdot \Delta\vartheta}{3600\frac{s}{h}} \tag{3.51}$$

P_{HW_i}	:	power for the hot water demand for the time step i	[kW]
$\dot{V}_{tap_i}$	:	flow rate from the tap profile for the time step i	[l/h]
c_{p,H_2O}	:	specific thermal capacity (4.187 kJ/(kgK))	[kJ/(kgK)]
$\Delta\vartheta$	:	temperature difference between the cold tapped water and the average target hot water temperature; 40 °C is used	[°C]

Figure 3.23 shows the selection process of the representative sample weeks for the total thermal energy demand. The total thermal energy demand combines the energy demand

for heating and hot water in one profile. It can be seen, that the transition period contains some days which still need some heating (energy demand >20 kWh/d) and some days where no heating is needed. Even during the winter period at the end of the week range there are a few days without any heating demand. During summer there is only a hot water demand.

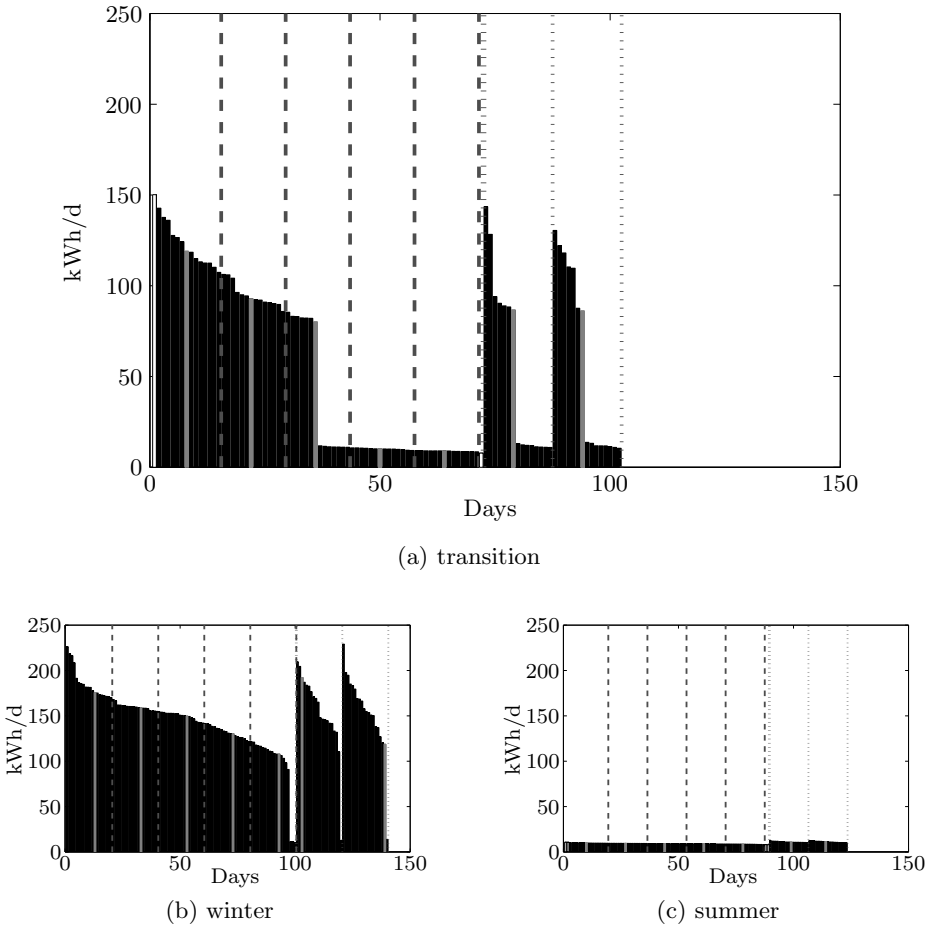

(a) transition

(b) winter

(c) summer

Figure 3.23: Visualisation of the selection process for the representative thermal sample weeks. The dashed horizontal lines represent the separation between the weekdays, the doted lines the separation between Saturday and Sunday. The weekdays highlighted with white bars are excluded from further selection processes. The gray bars are the chosen days.

The selection process for the three different scenarios (default, refurbished and minimal) for the representative winter week is shown in fig. 3.24. There are some differences in the chosen days. The motivation for this figure is not the difference between the chosen days, it is to illustrate the different energy needs for the three scenarios. From the default to

the minimal scenario it can be seen, that the energy demand for heating is decreased by a factor 2 to 2.5. The hot water demand was kept equal in all scenarios, that is why the energy demand around day 100 is the same in all scenarios.

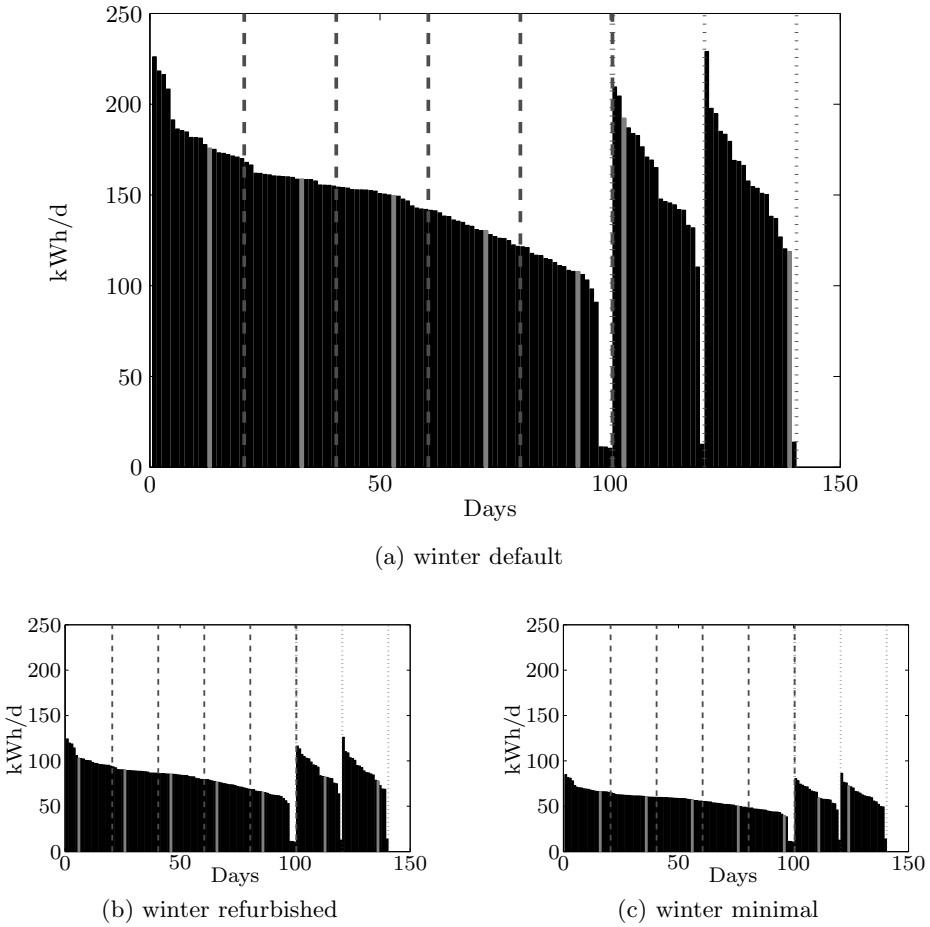

(a) winter default

(b) winter refurbished

(c) winter minimal

Figure 3.24: Comparison of the selection process between the different thermal scenarios; default, refurbished and minimal.

The total thermal load profile (heating and hot water) for the winter week and the three different scenarios is shown in fig. 3.25. Additionally the profile for the hot water demand is shown, this is the same for all three scenarios. The hot water demand has two peaks, one in the morning and one in the evening. During the day the demand is rather constant. This is an averaging result of the water demand of many people, since this is the demand for the whole model region. How distinct the two peaks are in the total demand is dependent on the scenario. In the minimal scenario, it is possible to recognise peaks in the total demand. In the total demand of the default scenario, there are also peaks. The hot water demand raises them, but not in such a distinct amount as the heat demand.

The total demand variations for the default scenario are more distinct because of heating demand variations caused by the daily ambient temperature variations. Because of the worse insulation compared to the minimal scenario, the temperature variation has a higher influence on the heating demand.
The generated profiles, as a result of the processes described in this subsection are used at the optimisation as thermal load profiles.

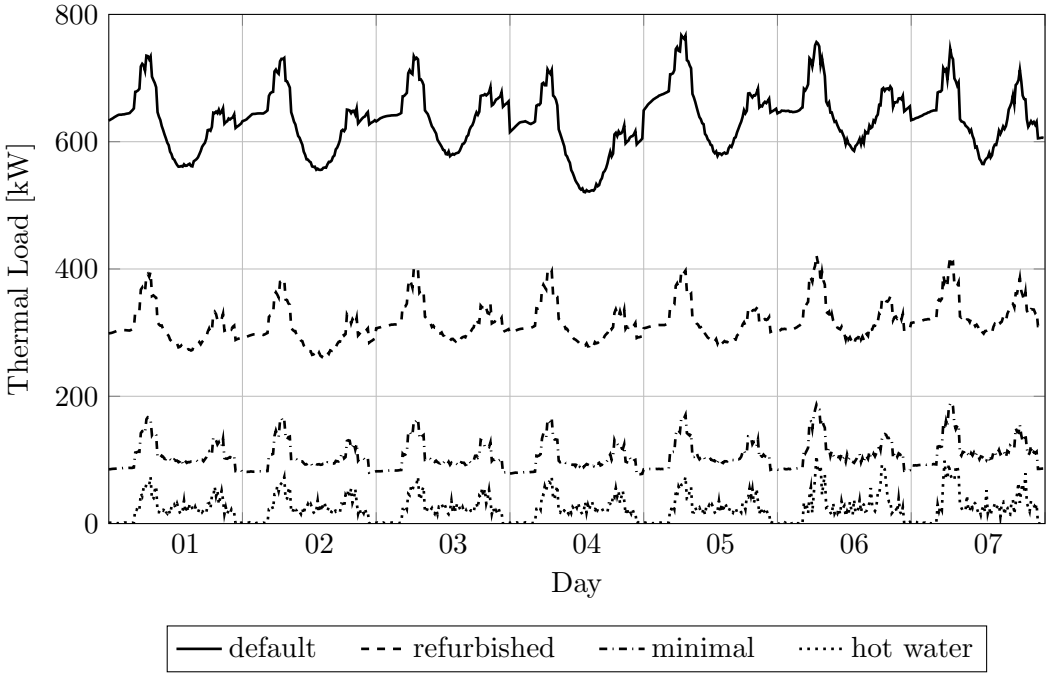

Figure 3.25: Comparison of the total thermal demand (heating & hot water) of the whole model region for the representative winter sample week between the three different scenarios and the energy demand for the hot water supply.

3.4 Decentralised/Renewable Production

For the calculation of the decentralised energy production potential, two approaches are used. If possible a direct approach is used to calculate the production potential for each node. If this approach is not sufficient, the total Austrian potential is taken and downscaled to the model region, since the region should represent the Austrian circumstances. The different approaches are used for different technologies or types of renewable energy productions. For PV systems the direct approach is used, because the type of building is known and therefore it is possible to estimate the PV system directly for each building. Biomass is for example a renewable source, where such an approach is not reasonable, that is why downscaling is used.

3.4.1 Electricity production

The electric grid in the model region represents a Low Voltage Grid (LVG). Wind turbines are often located in the Medium Voltage Grid (MVG) and that is why they are not modelled within the region. Only PV systems are considered.
In [77, pp. 47–49] the PV potential for Austria is integrated in the systems. With the population ratio between Austria and the aDSM region, the PV potential is downscaled, the result is shown in tab. 3.12.

Table 3.12: PV potential in Austria and the aDSM region downscaled with the population ratio; Modified according to [16, p. 105]

PV power	Austria	aDSM
Building	21.4 GW	813 kW
Free Space	11.2 GW	426 kW
Total	32.6 GW	1 239 kW

This approach is sufficient in gathering the amount of the total PV potential for the whole model region. Since it is necessary to know the potential for each individual node/household a "Bottom-Up" approach is used. With the two different approaches, it is also possible to check if they deliver similar results.
For the "Bottom-Up" approach, the PV potential for each building type according to its roof size is determined. Therefore the building classifications shown in tab. 3.1 are used. Furthermore, a division between buildings in the rural and (sub)urban areas is carried out. The survey [78] shows that roughly 45% of the population live in cities. This proportion is allocated to the 300 inhabitants of the model region. It is assumed that farm buildings are exclusively in rural areas and apartment buildings are only found in urban areas. Additionally, a separation between small and large agriculture is done. All these assumptions result in a building distribution shown in tab. 3.13. For the data

Table 3.13: PV installation per building type, separated between the urban and rural region; Modified according to [16, p. 105]

	Large Agric.	Small Agric.	Single- Double House	Multi-fam. House	Apart. Build.	Sum
Buildings - total	2	6	45	5	2	60
Building - urban	0	0	5	4	2	11
Building - rural	2	6	40	1	0	49
PV per Building	43 kW_p	12 kW_p	12 kW_p	17 kW_p	28 kW_p	-
PV total	87 kW_p	69 kW_p	519 kW_p	83 kW_p	55 kW_p	813 kW_p

in tab. 3.13 the following roof sizes are used. In the work [79, p. 7], the average usable roof area for residential buildings is 83 m^2 and 315 m^2 for agricultural buildings. In the work [80, pp. 7–9], the average roof area for houses is determined. For multi-family

houses, the size is roughly 120 m^2 and 200 m^2 for an apartment building.
With the given number of buildings and the calculated roof area, the average PV plant efficiency is determined with 13.8 %, which is a realistic value. With this efficiency, the "Top-Down" and the "Bottom-Up" approach results in exactly the same number of installable PV power for the whole model region, which is 813 kW_p. The detailed PV power assignment of each building is shown in tab. B.1 in the appendix.
Since the PV power for each household is determined it is necessary to allocate each household to a PV production profile. This process is similar to the one carried out for the electric load profile allocation. But there are some differences. For the household loads, a random individual annual load profile is generated. From these profiles, the representative sample days for each household and each season are selected. For the PV profiles, the process between individual profiles and day selection is reversed. Firstly, the representative solar radiation sample days for all three seasons are selected and this 3×7 irradiation days are than used to calculate the individual PV production profile for each node. For this the radiation profile [W/m^2] is multiplied with the installable PV size for each household [m^2]. This is possible since the model region has a limited dimension and therefore it is assumed that the weather data (solar irradiation) at each time step is the same at each node. This results in the same PV production profile for each node.
The irradiation profile is based on measurement data gathered at a test facility in Zwentendorf [81]. The profile is an annual profile, with a minute time resolution, for a south oriented system with a tilt of 30°. Because of the large amount of data of the annual profile the optimisation would face the same problems as the original data base for electric loads. This is why a reduction process with representative sample week selection for each season is necessary. The process is similar to the one shown for electric load separation (fig. 3.19). For weather data, there is no differentiation between weekdays and weekends, and that is why each day is treated equally. Besides this the selection process is equal to the one of the electric load: split year into seasons, sort in descending order, remove days if not dividable by 7 and so on. The result for the representative PV sample week selection is shown in fig. 3.26. It illustrates the selection process for each of the three seasons. The days marked with white bars are removed to obtain a day number for the selection process which is divisible by seven. The horizontal lines are the separations between the seven day groups and the grey bars represent the selected days. In the final step these days are arranged in random order.

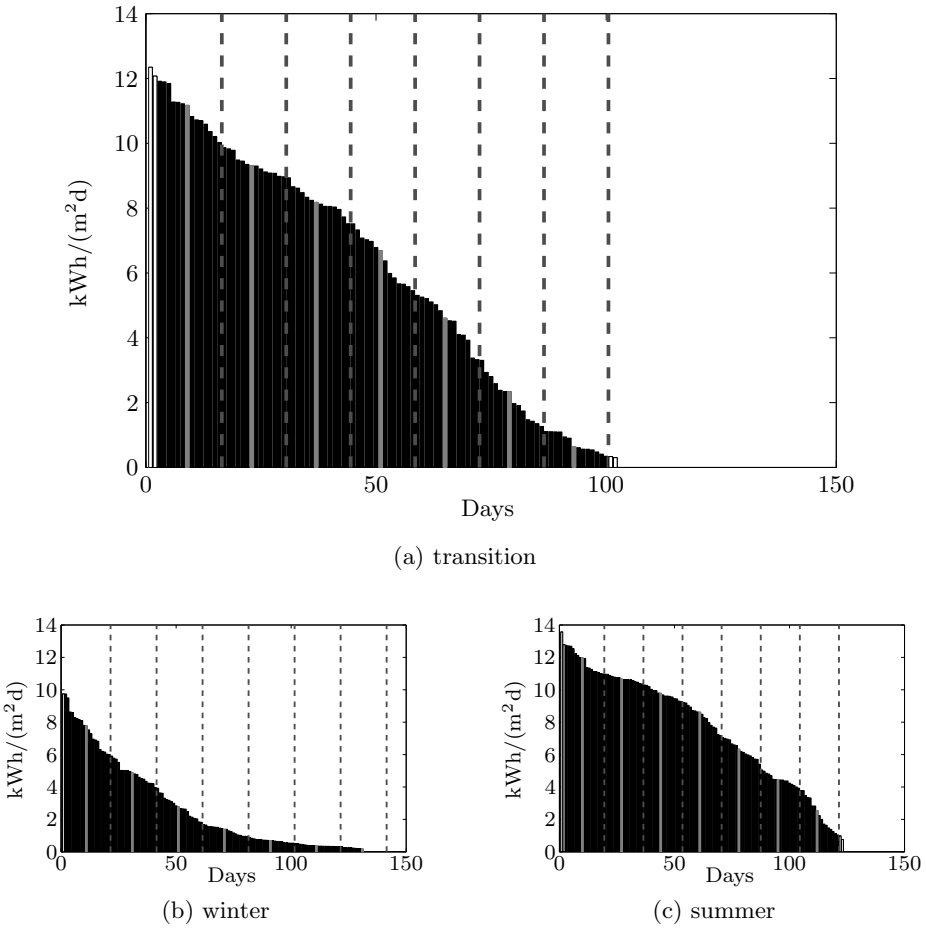

(a) transition

(b) winter

(c) summer

Figure 3.26: Selection of representative PV profile weeks for each season. The dashed lines represent the separation between the seven groups for each representative sample day. The white bars are excluded days (for more information see fig. 3.19) and the chosen days are highlighted in grey; Modified according to [70, p. 14]

The above selection process only delivers 15 min profiles for south oriented systems with a tilt of 30°. In regards to the orientation, in reality not every house will have these ideal conditions. Such as no direct south facing roof area, or no possibility in tilting the system with 30°. To overcome this problem, a system variation is implemented. This variation contains 65 different orientations, an azimuth variation from −30° to 30° in 5° steps, where a azimuth of 0° as a direct south orientation and −30° is an east facing system. The tilt range is from 20° to 40°, also in 5° steps, a horizontal surface is equivalent to a tilt of 0°. For the latitude location of Austria, a south oriented system with a tilt of approximately 30° produces the most energy. That is why a Gaussian distribution – the ideal orientation is the mean value – is taken to select the other orientations.

The allocation of each household to its specific orientation is shown in tab. B.1 at the appendix. With the PV system size and its orientation, it is possible to calculate the profile for each household. Furthermore, because of the allocation of the households to a specific node it is possible to calculate the sum PV profile for each node. The PV profile of the representative summer week is shown in fig. 3.27. The maximum is the maximum for all nodes, the same for the minimum. Because of this, the production of all nodes is within these two boundaries, highlighted with the grey area. There is a big spread between the minimum and maximum values. Around noon for example, some nodes have an infeed power of 6 kW whereas some have more than nine times the power. As mentioned at the subsection "Electric loads" (sec. 3.3.1) the maximum PV power exceeds the maximum load power by a factor up to six. Since the electric network is designed for the maximum load power, the maximum PV power might bring the system to its boundaries. It is a task of the optimisation to clear this problem if it occurs. For more information see chapter 4.
The profiles shown in fig. 3.27 and the corresponding profiles for the winter and transition week are used as input parameter for the optimisation.

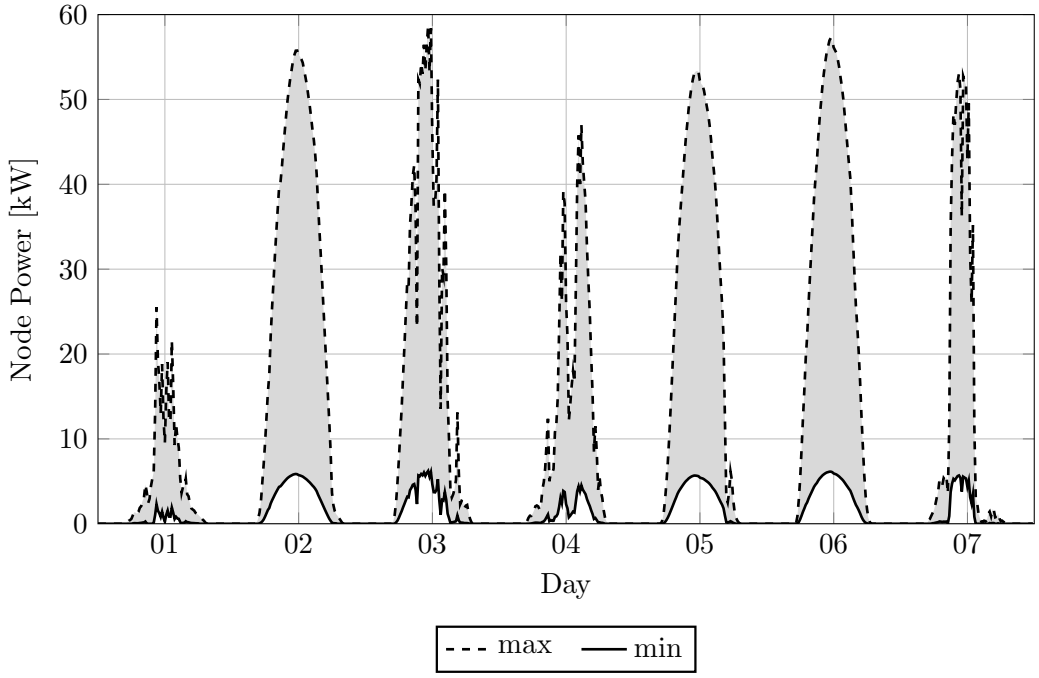

Figure 3.27: Summer PV profile for the representative sample week for all nodes. The PV power production for each node is within the grey area.

3.4.2 Thermal production

In the rural areas, thermal needs are mostly satisfied with decentralized productions. These productions for example are heat pumps, gas burners or wood firing. Some of them are renewable some are not. For urban and suburban regions there is the additional option of a district heating system, but no wood firing is assumed. Many power plants used for heat production produce electricity too. Since the main part of the output energy is heat, they are listed in this subsection. This section describes how the individual potentials and parameters for the decentralised thermal productions are derived.

Since in the urban region a district heating system can be selected as heating form from the optimisation, the question is: which primary sources are used to produce the energy for the district heating system? In Austria, most of the residual waste is burned and the energy is often used to run district heating or co-generation power plants. According to [82, pp. 38–39] in Vienna in the year 2011/2012 1 820 MWh electricity and 1 474 161 MWh heat from waste burning, including clearing sludge, was produced. For this 900 000 t of waste, hazardous waste and clearing sludge were burned. According to Statistik Austria, 2011 Vienna had an average population of 1 708 614 [83]. This results in an average annual energy production from waste of 0.864 MWh/person, and an amount of produced waste of 527 kg/(person $\cdot$ a). The aDSM model region has 300 inhabitants. If this value is taken, an energy production (electricity and heat) of 259 MWh/a from waste is possible. If it is assumed that the heat production from waste is a base load and therefore constantly producing the whole year long (hot water in summer), a producible power of 29.6 kW can be achieved. If the ratio between the annual produced electricity and heat is derived (1 820 MWh/1 474 161 MWh), this results in a rather low ratio of electricity production of 0.1%. If the power 29.6 kW is split according this ratio, this would result in an electric power production of 36 W. This value is negligible and it is assumed that the total power from burning waste is only used for heat production. Because waste originates independently of the utilisation no costs for the production of this amount of energy are assumed.

Another primary energy source is the use of renewable energies such as wood or other biomass. It is necessary to derive the corresponding area for the model region. This area can be used for harvesting wood and other biomass resources. One way for achieving this is the area ration between Austria and the model region. Austria covers an area of roughly 84 000 km^2 [84]. For the model region, an area of 800 m $\times$ 800 m can be assumed. This would mean, that the model region fits 131 061 times into the area of Austria. Another way is the population ratio, between Austria and the model region. Austria has a population of 8 507 786 [84], whereas the region has a population of 300. This leads to a ration of 28 359. The two approaches lead to completely different numbers, if the first one is used Austrian would have a population of over 39 000 000. This means that the average Austrian population density is lower as in the model region. This is due to mountains, lakes and agricultural areas. The conclusion is: the agricultures located at the model region have harvesting areas which exceeds the 800 m $\times$ 800 m limit of the region. Because of this the second approach with the population ratio is used to derive the renewable potential of the model region.

The data for the biomass potential for Austria are taken from [85]. They separate between three different types of potential:

1. The technical potential: this potential describes the maximum amount of resources which can be used with the current state of the art. For this approach each renewable potential is considered individually. It represents the maximum possible potential.
2. The reduced technical potential: this is basically the technical potential with consideration of usage restrictions and the production competition between individual renewable energy technologies. For example between PV and solar thermal.
3. Existence: this scenario describes the currently used potential.

In this work, the reduced technological potential is used. Table 3.14 lists the potentials for three different renewable energy sources, forest, field[10] and grassland. For the energy

Table 3.14: Renewable potential in Austria and the model region; Modified according to [85, pp. 84–94]

Potential	Forest	Field	Grassland
Austria	40 482 GWh	7 300 GWh	8 186 GWh
Model Region	1.427 GWh	0.257 GWh	0.289 GWh

production with wood, a process including a steam turbine is assumed. For the resources from field and grassland a biogas process with a combustion engine is considered. Since the urban and suburban regions contain a district heating system, the power plants are located at the "slack" node. This increases the economy of the power plants with the usage of the waste heat. This slack node is the node where the infeed of all three energy sources from the overall networks takes place (transformer, or infeed of the gas and heating system). For the two power plant types, the following characteristics are used, which lead to the following thermal and electric energy and power production (tab. 3.15).

[10] resources such as corn

Table 3.15: Thermal and electric energy production from renewable sources, forest, field and grassland

	Forest	Field	Grassland
	Steam Turbine	Combustion Engine	
	1.427 GWh	0.257 GWh	0.289 GWh
η_{th}	50%	50%	
η_{el}	20%	30%	
full load hours	6 000 h	5 000 h	
W_{th}	714 MWh	128.5 MWh	145 MWh
W_{el}	285 MWh	77 MWh	87 MWh
P_{th}	119 kW	25.7 kW	28.9 kW
P_{el}	48 kW	15.4 kW	17.3 kW

For the steam turbine, with its 6 000 full load hours, a 100% operation during winter and transition is assumed. For the combustion engine this is not possible and would exceed the 5 000 full load hours. Because of this a 100% operation during winter and a 67% operation for the transition period is assumed. Both power plant types are not operated during summer. This leads to the following power at the slack node (tab. 3.16). Often the feed-in tariff of renewable power plants is governmentally funded. They try to operate as much as possible at nominal power to maximise the annual energy production. That is why the power production within one season is constantly assumed. For example, all seven representative winter sample days have a thermal production power of 174 kW. These profiles are used as thermal and electric slack infeed profiles from biomass production for the optimisation.

Table 3.16: Renewable energy production from biomass at the slack node

	thermal	electric
Winter	174 kW	80 kW
Transition	156 kW	70 kW
Summer	0 kW	0 kW

4

Method – Optimisation

In this chapter, firstly, the common basics of optimisation problems are described. This is then followed by an overview of different optimisation methods. Secondly, it is explained why the linear approach is used and this is followed by an explanation on how storage and conversion technologies are modelled and implemented. Finally, it is explained how all of the parts – from the previous chapter 3 and the storage and conversion technologies from this chapter – are combined and implemented in the optimisation and which constraints and objective functions are used.

Considering Austria's electricity system, all results for storage and conversion technology placements derived from this thesis, are decentralised solutions. Furthermore, large pumped storage power plants represent centralised storage technologies.
Note, that within this work the terms "centralised" and "decentralised" are defined as follows:

- **"centralised"** technologies can be located only at the slack node of the model region, e.g. Redox-Flow batteries or Power-to-Gas whereas
- **"decentralised"** technologies can be located at each node in the model region, e.g. Li-Ion or Lead-Acid batteries.

4.1 Theory

There are many different optimisation approaches. A short overview will be given later in this section.
They all have the same goal, to find the best solution, or a solution that is better than a certain threshold, for example better than the current situation. The best solution is often to minimise or maximise an evaluation function. This function is defined on the selected evaluation criteria.
Usually it is not possible to freely choose from all available decision alternatives. There are constraints that restrict the selectable options [86, p. 8]. Optimisation problems have the following characteristics [86, p. 8]:

- Different decision alternatives are available.
- Constraints limit the available decision alternatives.
- Each decision alternative can have different impacts on the optimised system.
- An evaluation function, which is defined on the decision alternatives, describes how the different decision alternatives are affected.

For an optimisation problem, a decision alternative that considers all available constraints and minimises or maximises the evaluation function, should be chosen. To fulfil these requirements a systematic, rational and theory-guided planning process is used. This process consists of the following steps [86, pp. 8–13]:

- **Problem recognition:** For this step, it is necessary to notice that there are different alternatives. For example, using new technologies or different business approaches which are more efficient. In relationship to this work, this was determined as a priority since the whole aim is to optimise the energy supply of a model region.
- **Problem definition:** If the problem, or the existence of more efficient solutions is identified, it is necessary to formulate different decision alternatives. This includes determining constraints; choosing different alternatives and determining the goal(s) of the process. These goals are either an optimal solution or a solution that is better than a certain threshold. The selection of relevant decision alternatives is an important aspect. There is a trade-off between the number of decision alternatives and the difficulty of the problem. Because of this, it is important to neglect all aspects which have no direct impact on the goal of the planning process. The problem has to be defined both: large enough to ensure that it yields some benefits and small enough to be able to solve it.

- **Model construction:** In this step, reality is modelled with mathematical models. It is not possible to represent the reality with all its characteristics. That is why aspects of reality have to be idealised (e.g. linearisation of the load flow) or neglected (e.g. levels of voltages). What aspects have to be considered or can be neglected is dependent on the goal of the optimisation problem.
  The different decision alternatives are usually described by using a set of variables $\{x_1, \ldots, x_n\}$. Normally more than one decision variable is used to model different alternatives. Constraints are used to restrict the model in necessary ways (e.g. $x_1 + x_2 \leq 2$). The objective function assigns objective values to each decision alternative and measures the quality of the different alternatives (e.g. $f(x) = 2x_1 + 2x_2^2$). A solution is one possible decision alternative, which is represented by different values for the decision variables.
- **Model solving:** Usually this is done by an algorithm. An algorithm starts at an initial state and terminates at a defined end state. If an algorithm can solve a problem without any problem-specific adjustments, it is called a black-box algorithm. Between tractability and specificity there is a trade-off. For an optimisation method to perform well for a specific problem, it usually needs to be adapted.
- **Validation of the obtained solution:** If an optimal or near-optimal solution is found they have to be evaluated. This can be done with a sensitivity analysis, to see how the solution depends on the variation of the model. Retrospective tests are another option. For these tests, historical data is used and it is evaluated to see how the model and the resulting solution would have performed if they had been used in the past. In this work, a post calculation with the optimisation result is used. This post calculation is performed with especially designed network calculation tools such as NEPLAN or PSS©SINCAL.
- **Implementation:** There are two options for how the solutions can be implemented. First, a solution is implemented only once. The outcome of the optimisation process for example replaces an existing solution. Second, the model is solved repeatedly. An example is a system for optimal route finding for delivery services. The problem continuously changes (different customers, trucks, loads) therefore it is better to find continuous solutions instead of implementing a solution only once. Result implementation is not part of this work.

The problem difficulty is an important indicator when it comes to optimisation problems. It describes how difficult it is to find the optimal solution. Problem difficulty is defined independently of the used optimisation method. The algorithm complexity is the effort (usually solving time or memory) that is needed to solve a problem. The effort is dependent on the input size. This is equal to the problem size n. Generally the necessary effort to solve a optimisation problem of the size n, is determined by the time complexity (how many iterations or search steps are necessary) and space complexity (usually memory on a computer – e.g. RAM). Both time- and space-complexity normally depend on the input size n. The lowest necessary effort to solve the problem is the difficulty or complexity of a problem. Because of this, problem difficulty is related

closely to the algorithms complexity. If there is a known algorithm that can solve the problem, the upper bound on the difficulty is the complexity of the algorithm. Finding lower bounds is more difficult. For this the algorithm which needs the least effort to solve the problem has to be found [86, pp. 22–29].
For lower bound finding it is possible to group the optimisation problems in complexity classes. For more information refer to [86, pp. 27–28].
If the "Landau Notation" is used, a big O notation represents the asymptotic upper bound. As mentioned before this is the complexity of an algorithm that can solve the problem, and Ω represents the asymptotic lower bound. For optimisation problem solving, the running time is interesting. In general, a differentiation between polynomial and exponential running time is possible. Problems that can be solved using a polynomial-time algorithm are tractable. Such algorithm have an upper bound $O(n^k)$ on the running time, with $k = const.$ Tractable problems are usually easy to solve, because of low running time increase with lager input size n. Finding the lowest element in an unsorted list with the size n could be such an example. There are algorithms with a complexity of $O(n)$. If the list is twice as large $2n$, the algorithm needs twice as much effort for solving.
The other group are intractable problems. They cannot be solved by a polynomial-time algorithm and there is a lower running time bound which is $\Omega(k^n)$. $k > 1$ and $const.$ and n is the problem size. Guessing the combination of a digital door lock with n digits is such a problem. The necessary time for finding the correct key is $\Omega(10^n)$. Using one more digit $n+1$, increases the required search steps by a factor of 10. For this problem, the problem size is n whereas the search space size $|X| = 10^n$. The key finding effort depends on n and increases with the same rate as the size of the search space. For some common functions the growth rate is listed in tab. 4.1 [86, pp. 28–29].
The optimisation carried out in this work has the structure of an intractable problem. The problem increases with several input parameters, such as numbers of nodes, or time steps and in context of problem size they are potency dependent.

Table 4.1: Growth rate of some optimisation functions; Modified according to [86, p. 29]

polynomial	constant	$O(1)$
	logarithmic	$O(\log n)$
	linear	$O(n)$
	quasilinear	$O(n \log n)$
	quadratic	$O(n^2)$
	polynomial (of order c)	$O(n^c)$, $c > 1$
expo-nential	exponential	$O(k^n)$
	factorial	$O(n!)$
	super-exponential	$O(n^n)$

4.1.1 Classification

There are several options how optimisations can be classified. One option is the classification according the optimisation problem. There are many ways, how optimisation problems can be classified: by constraints types, by nature of design variables, by physical structure of the problem, by nature of the involved equations, or by the number of objective functions, just to mention a few [87, p. 2].
One of the most important is the classification according to the nature of involved equations. Based on the nature of objective function and constraint equations, optimisation problems can be classified as linear, nonlinear, geometric or quadratic problems.
The classifications of the optimisation methods are another option. Here, basically between two approaches can be differed: "Exact"-methods which guarantee finding an optimal solution and "Heuristic"-methods, which do not guarantee finding the optimal solution [86, p. 45].
Figure 4.1 lists some optimisation methods and classifies them according exact or heuristic solutions. Figure 4.1 is not intended to be exhaustive. There are many more methods. To list all of them would go beyond the scope of this work. Also to describe all of them, representative one of each group is described. For more information to [86] is referred.

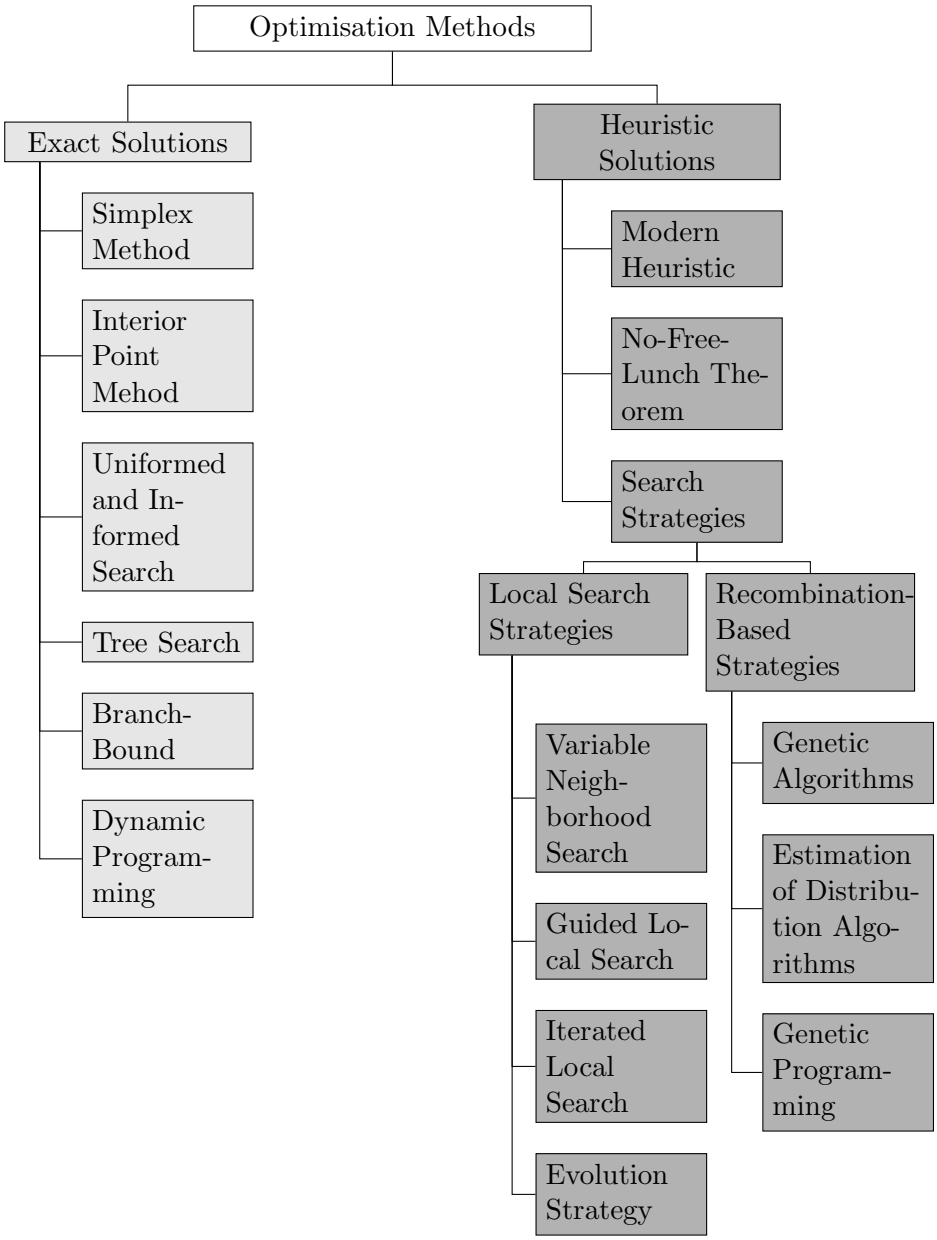

Figure 4.1: Overview of different optimisation methods; Modified according to [86, p. 45–155]

Simplex Method
The simplex method takes a Linear Optimisation Problem (LOP) in standard form (for more information see next subsection) as input and returns an optimal solution. Its worst-case time complexity is exponential, but in practice it is very efficient. It is possible to make use of the fact, that a linear inequality splits an n-dimensional search space in two halves (half-spaces). One half-space contains feasible solutions, whereas the other does not (infeasible). If the constraints are linear, the feasible region of any linear problem is always a convex set. The feasible, convex region forms a simplex which is the simplest possible polytope in a space of size n. The name simplex derives from the simplest possible polytope. Solutions located on the border of the feasible region (simplex) are boundary points. Interior points are solutions that are feasible but without boundary points. Feasible points that are boundary points and located on the intersections of n half-spaces are called corner points or vertices of the simplex. The set of solutions for which the objective function obtains a specific value is a hyperplane with the dimension $n - 1$. If a bounded optimal solution exists, the optimal solution of the linear problem is one of the corner points. Because the set of feasible solutions is a convex set and the objective function is linear, optimal solutions can be found by examining all corner points (vertices) of the simplex and then choosing the one(s) where the objective function becomes a maximum or minimum. Figure 4.2 illustrates the simplex process for the objective function $f(x) = x_1 + 2x_2$ and the constraints $x_1, x_2 > 0$, $-2x_1 + x_2 \leq 1$, $x_2 \leq 3$ and $3x_1 + x_2 \leq 9$. [86, p. 52–53]

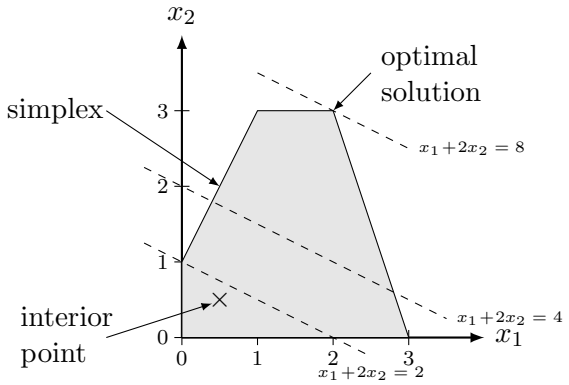

Figure 4.2: Illustration of the simplex method; Modified according to [86, p. 53]

Genetic Algorithm (GA)
Genetic algorithms imitate basic principles of nature. They are based on four basic principles:

1. There is a population of solutions. The solution properties are evaluated based on the phenotype, and variation operators are applied to the genotype. If an upper population limit is exceeded, some of the solutions are removed.
2. New solutions are created with variation operators. The new solutions have similar properties to existing solutions. In GAs, the main search operator is recombination and mutation. In evolution strategies, the situation is reversed.
3. Each decision alternative can have different impacts on the system which is optimised.
4. The selection process selects high-quality individuals more often.

The selection process is used to distinguish high-quality from low-quality individuals and selects promising solutions. Proportionate selection and tournament selection are popular methods.
For proportionate selection, the number of copies of a solution in the next population is proportional to its fitness. The recombination chance of a solution x_i is

$$\frac{f(x_i)}{\sum_{n=1}^{N} f(x_n)}$$

where N represents the population size and $i = 1, \ldots, N$. With increasing fitness, an individual is chosen more often for reproduction.
When tournament selection is used a tournament between s randomly chosen different individuals from the population P is held, and the one with the highest fitness is added to the mating pool M. The mating pool M consists of all solutions which are chosen for recombination. When using tournament selection, there are no copies of the worst solution, and either an average of s copies (with replacement), or exactly s copies (without replacement) of the best solution.
Sexual reproduction is imitated by crossover operators. They are applied to all $x \in M$. Usually, crossover produces two new offspring from two parents by exchanging substrings. The mutation operator is important for local search. It slightly changes the genotype of a solution $x \in P'$. Previously lost solution properties can be reanimated by mutation. The probability of mutation must be at a low level because otherwise mutation would randomly change too many characteristics and new solutions would have nothing in common with their parents. This could lead to a random search.
In GAs, intensification is a result of the selection process. As only high-quality solutions are chosen in a selection step, the average fitness of a population increases. After a number of generations due to selection, the population converges. The initial population is the main source of diversification. Therefore, often large population sizes of a few hundreds or even thousands of solutions are used [86, pp. 147–150].
The parametrisation of the algorithm is important, and there is no guarantee, that after

a specified number of steps an optimal solution is found. Depending on the optimisation problem, there is no guarantee that a found solution is a global, or just a local optimum. It is possible that several optimisation cycles deliver different solutions for the same problem.

If a solution is found, it should be guaranteed, that it is an exact optimum and not an optimum, maybe not even near the optimal point. With this limitation only exact methods are possible. Furthermore if a solution is found, it shall be guaranteed, that this solution is a global optimum and not just a local one. This additional restriction limits the optimisation problem to a linear optimisation. To linearly model the problem has the advantage that many solvers are capable in solving the problem.
The next section describes some basics about linear optimisation or Linear Optimisation Problems.

4.1.2 Linear Optimisation Problem

There are many different forms of Linear Optimisation Problems (LOPs). If the (decision) variables (x_j) have to be integer values, the problem is called Integer Linear Optimisation Problem (ILOP). It is called a Binary Linear Optimisation Problem (BLOP) if the variables are binary, either 0 or 1. This is a special form of an ILOP. If some variables have to be an integer and some can have any value from $\mathbb{R}$ then it is called Mixed Integer Linear Optimisation Problem (MILOP). When the game theory is taken into account it is called Game Linear Optimisation Problem (GLOP) [88, p. viii].

X is the set of all feasible solutions $x \in X$. And f is the evaluation function that assigns a real value to every element of x of the search space $f : X \to \mathbb{R}$ [86, p. 14]. The definition of all possible $x \in X$ and each evaluation function separately for all x would be too extensive. That is why a more elegant way of representing optimisation problems is used. The following way is such an elegant representation option. A general linear programming problem or LOP consists of three parts: The objective function, the constraints and the non-negativity constraints. These three properties can be formulated as follows in matrix form [43, p. 60], [88, p. 9]:

$$\begin{array}{lrcl} \text{Min.} & z & = & \boldsymbol{c}^T\boldsymbol{x} \\ \text{subject to} & & & \boldsymbol{A}\boldsymbol{x} \leq \boldsymbol{b} \\ \text{and} & & & \boldsymbol{x} \geq \boldsymbol{0} \end{array} \tag{4.1}$$

Sometimes for explanations the summation form is used. (4.1) looks then as following:

$$\begin{array}{lll} \text{Min. } z & = & \sum_{j=1}^{n} c_j x_j \\ \text{s.t.} & & \sum_{j=1}^{n} a_{i,j} x_j \leq b_i \quad \text{for} \quad 1 \leq i \leq m \\ \& & & x_j \geq 0 \qquad\qquad \text{for} \quad 1 \leq j \leq n \end{array} \tag{4.2}$$

The matrix $\boldsymbol{A} \in \mathbb{R}^{m \times n}$ and the vector $\boldsymbol{b} \in \mathbb{R}^{m \times 1}$ describe the constraints. The vector $\boldsymbol{x} \in \mathbb{R}^{n \times 1}$ describes the decision variables and the vector $\boldsymbol{c} \in \mathbb{R}^{n \times 1}$ represents the objective function [43].
(4.1) or (4.2) are called "Standard Form". It is possible to transform each optimisation problem to the standard form [88, p. 8]. For example equalities like $\sum a_j x_j = b$ can be replaced by $\sum a_j x_j \leq b$ and $\sum a_j x_j \geq b$. The second pair $\sum a_j x_j \geq b$ can be reversed using $\sum -a_j x_j \leq -b$, to get the standard form for both therms. It is also possible to convert any inequalities to equalities using slack variables s. This leads to the form $\sum a_j x_j + s = 0$. s itself must be non-negative.
It is also possible to transform non-negative constraint to the form $x_j \geq 0$. If for example the non-negative constraint has an explicit lower bound $x_j \geq l$. This can be transformed to the non-negative form $x'_j \geq 0$ using $x'_j = x_j - l$. The same can be carried out if x_j has an upper bound. For this case the transformation from $x_j \leq l$ to $x'_j = l - x_j \geq 0$ is used. In all this cases x_j is called restricted. If it neither has an upper or lower bound it is called free. In this case the substitution $x_j = x_j^+ - x_j^-$ with $x_j^+ \geq 0$ and $x_j^- \geq 0$ can be used.
With all this approaches it is possible to transform any linear problem to a standard form.

An optimisation problem is called feasible if $\boldsymbol{x}$ satisfies all the problem and non-negativity constraints and infeasible otherwise [88, p.10]. An infeasible problem is one which has no feasible points, the constraints are unsolvable. An unbounded problem is a feasible problem with no optimum.

There is another differentiation at the standard form. It either can be a minimisation $\min_{\boldsymbol{x}}$ or maximisation $\max_{\boldsymbol{x}}$ problem. One is the "Primal" and the other the "Dual" form [88, p. 11]. It does not matter which is defined as which, since both can be converted to the other form. For example, if the primal optimisation problem is a maximisation it is possible to convert it to the dual form which is then a minimisation problem and vice versa. If for example $v = -z$ then $\min z = -\max v$. For the standard form the relation between primal and dual form looks as following:

	Primal			Dual	
Min.	$z = \sum_{j=1}^{n} c_j x_j$		Max.	$w = \sum_{i=1}^{m} b_i y_i$	
s.t.	$\sum_{j=1}^{n} a_{i,j} x_j \leq b_i$	$(1 \leq i \leq m)$	s.t.	$\sum_{i=1}^{m} a_{i,j} y_i \geq c_j$	$(1 \leq j \leq n)$
&	$x_j \geq 0$	$(1 \leq j \leq n)$	&	$y_i \geq 0$	$(1 \leq i \leq m)$

For every primal-feasible x and dual-feasible y this leads to the "Weak Duality Theorem" (4.3) [88, p. 11].

$$z = \sum_{j=1}^{n} c_j x_j \leq \sum_{j=1}^{n} \left(\sum_{i=1}^{m} a_{i,j} y_i \right) x_j = \sum_{i=1}^{m} \left(\sum_{j=1}^{n} a_{i,j} x_j \right) y_i \leq \sum_{i=1}^{m} b_i y_i = w \tag{4.3}$$

In matrix notation this is expressed as the following:

$$z = \boldsymbol{c}^T \boldsymbol{x} \leq \boldsymbol{y}^T \boldsymbol{A} \boldsymbol{x} \leq \boldsymbol{y}^T \boldsymbol{b} = w \tag{4.4}$$

This inequality is only valid if both $\boldsymbol{x}$ and $\boldsymbol{y}$ are feasible. If a particular feasible point of the function $z(x)$ is called z^*, then $z^* \geq z(x)$ for all feasible x. Further with $z \leq w$ this leads to $z^* \leq w^*$, because the inequality holds for every pair of feasible solutions. If $\boldsymbol{x}$ and $\boldsymbol{y}$ satisfy the relation $\boldsymbol{c}^T \boldsymbol{x} = \boldsymbol{y}^T \boldsymbol{b}$, then z^* and w^* are found by just solving one of the two forms (either the primal or dual). This consequence is often used by algorithms to solve optimisation problems.

The convexity is an important indicator. With this indicator it is possible to determine if a local minimum is a global minimum too. A set ($C \subset \mathbb{R}^n$) is convex, if for every pair of points – located within the region C – a straight line between the two points is within the region too (fig. 4.3). Or mathematically expressed [89, p. 14]:

$$x_1, x_2 \in C \Rightarrow x(\sigma) \in C \quad \forall \sigma \in [0, 1],$$

at which

$$x(\sigma) = \sigma x_1 + (1 - \sigma) x_2 \tag{4.5}$$

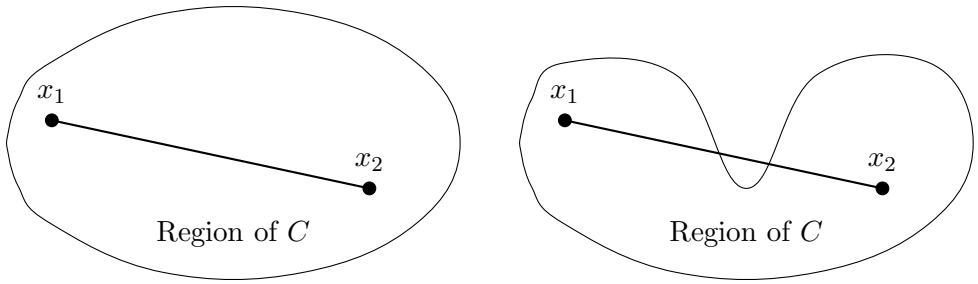

(a) convex (b) not convex

Figure 4.3: Convexity for the set C; the set on the left is convex, the set on the right is not convex; Modified according to [89, p. 14]

The intersection of two convex sets is also convex. This characteristic has relevance in connection with the permissible range of optimisation problems. If the sets defined by different constraints are convex, then the intersection set is convex too. This is important in context of this work, since many different systems are modelled (networks, storages, etc.) in a convex way.
Beside the convexity of sets it is important to know if functions are convex within the range of the convex set. A function $f(x), x \in C$ with the convex set C is convex when for each pair $x_1, x_2 \in C$ the following applies [89, p. 14]:

$$f(x(\sigma)) \leq \sigma f(x_1) + (1 - \sigma) f(x_2) \quad \forall \sigma \in [0, 1] \tag{4.6}$$

$x(\sigma)$ is defined as in (4.5). If (4.6) is valid for all $\sigma \in [0, 1]$, then the function is called strictly convex. A function is concave or strictly concave, if the function $-f(x)$ is convex or strictly convex.

A convex function has the following characteristics [89, pp. 15–16]:

1. If the functions $f_i(x)$ are convex at C and $\alpha_i \geq 0$, $i = 1, \ldots, N$ then the totalling function
$$f(x) = \sum_{i=1}^{N} \alpha_i f_i(x)$$
is convex too.
2. If the function $f(x)$ is convex at C and $x_1, x_2 \in C$, then $\varphi(\sigma) = f(x(\sigma))$, with $x(\sigma)$ from (4.5) is convex too for $\sigma \in [0, 1]$.
3. If the function $f(x)$ is convex, then the set $\{x|f(x) \leq 0\}$ is convex too. If the set $\{x|f(x) \leq 0\}$ is convex, the function $f(x)$ is not necessarily convex (fig. 4.4).

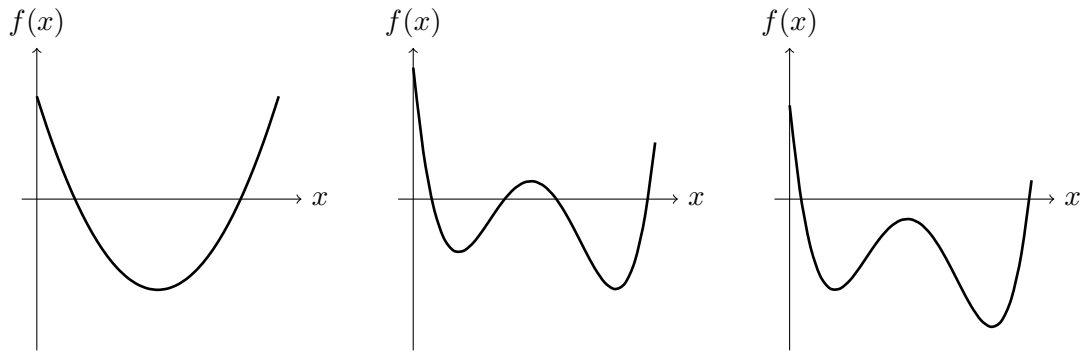

(a) conv./conv. (b) not conv./not conv. (c) not conv./conv.

Figure 4.4: Characterisation if a function and/or set is convex. The left side of the subfigure caption mentions, if the function $f(x)$ is convex or not and the right side defines, if the set $\{x|f(x) \leq 0\}$ is convex or not. For fig. 4.4a the local minimum is a global minimum too. For the situation in fig. 4.4b and 4.4c this has not necessarily to be the case; Modified according to [89, p. 15]

4. The function $f(x)$ is continuously differentiable. The same function $f(x)$ is convex at C, if for all $x_1, x_2 \in C$
$$f(x_2) \geq f(x_1) + (x_2 - x_1)^T \nabla f(x_1)$$
5. The function $f(x)$ is twice continuously differentiable. This function is convex at C, when the Hessian matrix $\nabla^2 f$ for all $x \in C$ is positive semi-definite. A strict convexity of the function does not imply a positive definite Hessian matrix, e.g. the function $f(x) = x^4$ is convex, but $f''(0) = 0$.

A general optimisation problem as defined at (4.1) or (4.2) is called convex, if the allowable range X is a convex set and the power function $f(x)$ is convex.
As mentioned earlier for a convex optimisation problem a local minimum/maximum is

a global minimum/maximum too. For this proof it is assumed that $\hat{x}$ is a local and x^* a global minimum. This results in $f(x^*) \leq f(\hat{x})$. Because of the convexity of the power function this is valid for all $x \in [\hat{x}, x^*]$ and $\sigma \in [0, 1]$ [89, p. 16]

$$f(x) = f(\sigma\hat{x} + (1-\sigma)x^*) \leq \sigma f(\hat{x}) + (1-\sigma)f(x^*) \leq \sigma f(\hat{x}) + (1-\sigma)f(\hat{x}) = f(\hat{x}) \quad (4.7)$$

(4.7) ends up showing $f(x) \leq f(\hat{x})$. Since $\hat{x}$ was assumed as local minimum, this is only possible if $f(x) = f(\hat{x}) = f(x^*)$ for all $x \in [\hat{x}, x^*]$. The latter proves, that $\hat{x}$ is a global minimum.
At a strict convex optimisation problem a local minimum is definitely a global minimum. To proof this, a contradiction is formed, in the way, that x^* is assumed a global minimum and there shall be another (local or global) minimum $\hat{x}$. According to (4.7) it applies that $f(x^*) = f(\hat{x}) = f(x), \forall x \in [x^*, \hat{x}]$. Because of the strict convexity of the power function for all $x \in [\hat{x}, x^*]$ and $\sigma \in (0, 1)$ the following applies:

$$f(x) = f(\sigma\hat{x} + (1-\sigma)x^*) < \sigma f(\hat{x}) + (1-\sigma)f(x^*) < \sigma f(\hat{x}) + (1-\sigma)f(\hat{x}) = f(\hat{x}) \quad (4.8)$$

Finally $f(x) < f(\hat{x})$ applies. This is a contradiction, the result is, that beside x^* there cannot be another minimum.

This is relevant for the optimisations in this work, to ensure that the found solution is the best solution and there is no other point, which is better.

4.2 Storage and Conversion Technologies

The purpose of the optimisation is the placement and the operation of storage and conversion technologies. Firstly, in this section characteristics of storage- and conversion-technologies are mentioned. This is followed by, how these characteristics are used to model the technologies in ways usable for the linear optimisation. Used characteristics are efficiency, energy content, minimum/maximum power, number of storage cycles, charge or discharge -speed and -behavior and costs.
Basically storage technologies integrated in this work can be classified in the following three main groups:

1. mechanical storage systems,
2. electro-chemical storage systems and
3. thermal storage systems.

Figure 4.5 lists technologies and classifies them into the three groups.
Mechanical storage technologies store energy with kinetic-, potential-energy, or pressure difference of mediums. Flywheels for example use the kinetic energy of a rotating disc, the stored energy is $E_{kin} = \frac{1}{2}I\omega^2$, where I represents the moment of inertia and ω the angular velocity. Pumped storage technologies use the potential energy $E_{pot} = mgh$

of water to generate energy, where m represents the object mass, g the acceleration of gravity and h is the height attained due to the objects displacement.
Electro-chemical storage systems use chemical changes to store energy. The energy is stored at chemical compounds, these compounds change during the charge or discharge process. There are two groups of electro-chemical storage systems. In one group, the storage medium and the converter are integrated into one unit and they are operated within this single unit. The power-energy-ratio of such systems is linked. Lithium-Ion or Lead-Acid batteries belong to this type. In the other group the storage medium and the converter are physically separated. There is no coupling between the power and energy of such storage technologies. Redox-Flow batteries and hydrogen production and storage belong to this type of storage system.
Thermal storage systems store thermal energy. Depending on the storing effect, it is possible to differentiate between different types. Sensible storage systems use a temperature change to store or withdraw energy $E_{th} = mc_p\vartheta$, where m represents the object mass, c_p the specific heat coefficient at constant pressure and ϑ the object temperature. Regular water boilers belong to this group. If the thermal energy is stored, using changes between different phases of a medium, they are called latent storage systems, since the energy change cannot be felt (ideally no temperature change). For example a storage system that works only around 0 °C and uses the phase change from solid state to liquid state of water is such a storage type.

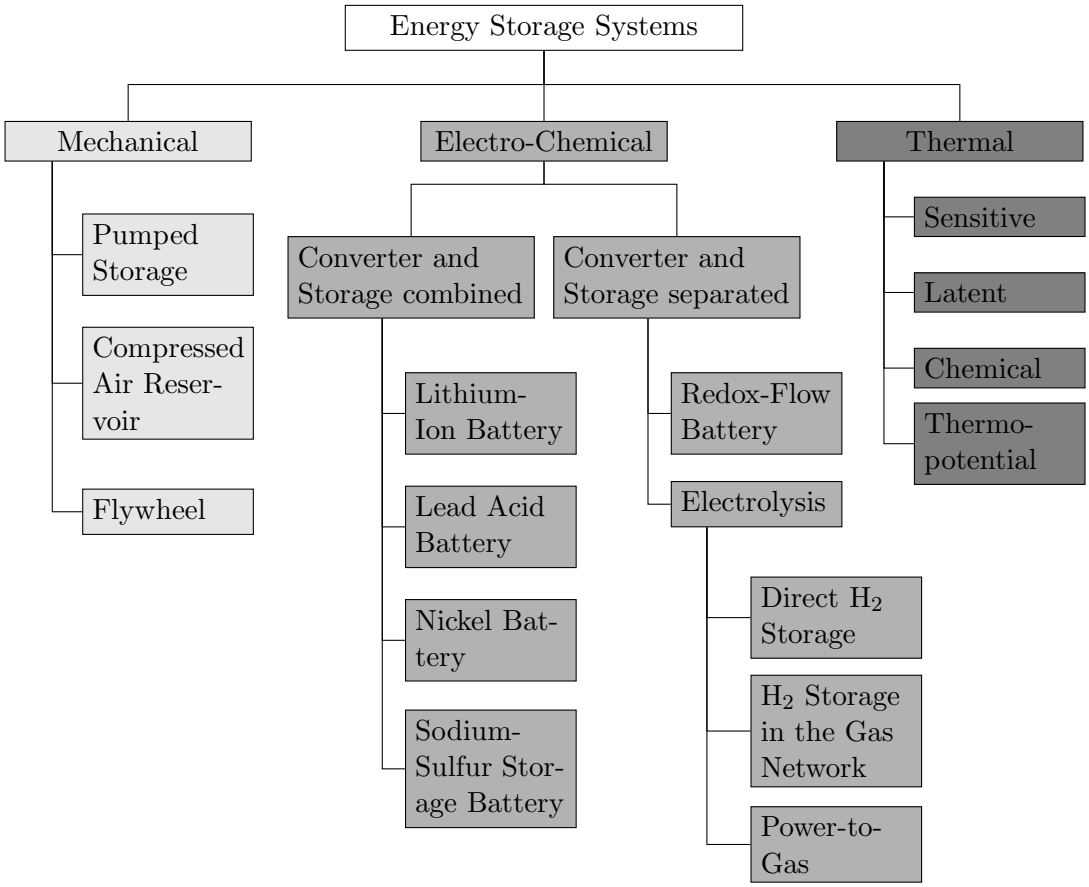

Figure 4.5: Overview of storage and conversion technologies; Modified according to [37, p. 39], [90, pp. 197–531]

Figure 4.5 does not claim to be complete; there are many more types available. From the listed technologies the following ones are used in this work:

- Lithium-Ion battery
- Lead-Acid battery
- Redox-Flow battery
- Power-to-Gas
- Thermal Storage (sensible)
- Heat Pumps

The characteristics for each technology are listed in the following subsections.

4.2.1 Lithium-Ion Battery

Li-Ion batteries consist of two electrodes and an electrolyte. The negative electrode (anode) consists mainly of carbon. The components of the positive electrode (cathode) are usually oxides, such as cobalt oxide and manganese oxide. Dissolved Li-salts act in organic solvents as electrolyte [91, p. 161]. The energy storage principle is based on the transport of Li-Ions between anode and cathode. During the discharge process electrons are released at the negative electrode and the free positive Li-Ions migrate to the positive electrode. There they are neutralised with electrons [92, pp. 104–105]. The most important characteristics are listed in tab. 4.2.

Table 4.2: Overview of typical Li-Ion battery characteristics; Modified according to [92–96]

Characteristics	Dimension	Value
Volumetric Energy Density	Wh/l	360
Gravimetric Energy Density	Wh/kg	150–200
Power Density	W/kg	3 500
max. installable Power	kW	2 000·n
typical Energy Range	kWh	100/0.5·n
Efficiency (System's Efficiency)	%	90–95
Efficiency Charging	%	94–96
Efficiency Discharging	%	96–98
Efficiency Storage	%	100
Self-Discharge	%	0.01
Nominal Voltage/Cell	V	3.6
End-of-Charge Voltage	V	4.2
Open-Circuit Voltage	V	3.6
Cut-Off Voltage (SOC 100%)	V	2.7-3
Internal Resistance	mΩ	25–40
Number of Cycles	–	3 000
Lifetime	a	6–15
min. Discharge Duration	h	0.1
max. Discharge Duration	h	12
Investment Costs	€/kWh	500–1 200
Peripheral Costs	€/kW	20

The charge characteristics shown in fig. 4.6, are for a Li-Ion battery from the company "Saft". It is an Evolion® battery (48 V, 77 Ah), with an end-of-charge voltage of 55 V. For this stack size 13 single Li-Ion batteries are serial connected. First the battery is charged with the constant current mode until the battery voltage reaches the end-of-charge voltage (time from 0 h to 2.2 h). From this point on, the battery is charged with a constant voltage mode until it reaches its full capacity.

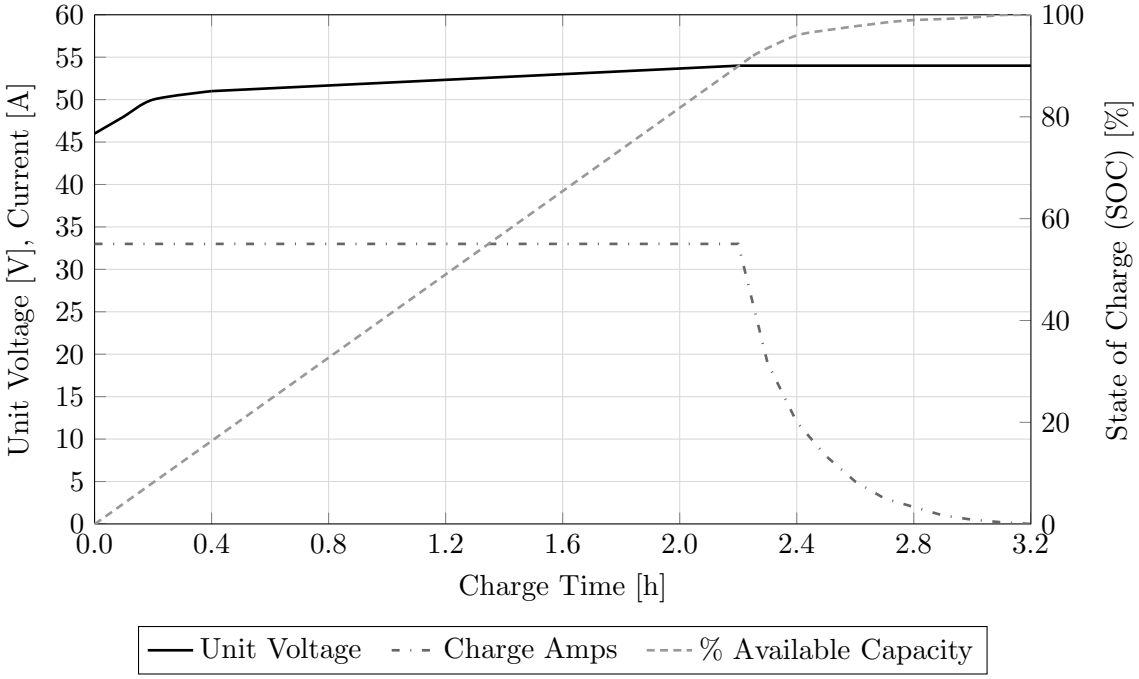

Figure 4.6: Li-Ion battery charge characteristics. The voltage, current and SOC is shown. The first part is the constant current charge section followed by the constant voltage charge section; Modified according to [97, p. 5]

It is possible to get different voltage, current and capacity values if this battery is connected in serial or parallel. This makes it possible for the optimisation to place different battery sizes at different nodes.

4.2.2 Lead-Acid Battery

The Lead-Acid battery is one of the first and most developed accumulator systems. The active material of the negative electrode is made of lead (Pb) and the positive electrode of lead dioxide (PbO_2). In order to achieve a large surface area (small internal resistance), the active material has a porous structure [92, pp. 34–35]. Water, dilute sulphuric acid (H_2SO_4) or a tied variant can act as electrolyte. In the tied case the electrolyte is fixed in a gel form or in a fibreglass structure between the electrodes [91, pp. 154–155]. These battery systems are called "gas-tight batteries". In this work, this type of battery is used. Compared to Lead-Acid batteries with a liquid electrolyte the gas-tight versions have lower energy densities and lower lifetimes. But they are safer, because of the avoidance of detonating gas while overcharging and they have lower maintenance costs.
As before for the Li-Ion technology the important typical characteristics of this battery type are listed at the next page (tab. 4.3). If the Li-Ion and Lead-Acid batteries are compared, a few differences are noticeable. One is the power or energy density of the

Li-Ion battery. The energy density compared to Lead-Acid is approximately 4 to 8 times higher and the power density is roughly 10 times higher. This is why Li-Ion batteries are popular in mobile applications. The other noticeable difference between these two types is the price. For the same storage capacity Lead-Acid cost roughly 1/2 to 1/12 of Li-Ion batteries.

Table 4.3: Overview of typical Lead-Acid battery characteristics; Modified according to [92–95, 98, 99]

Characteristics	Dimension	Value
Volumetric Energy Density	Wh/l	75–120
Gravimetric Energy Density	Wh/kg	25–40
Power Density	W/kg	75–300
max. installable Power	kW	50 000
typical Energy Range	kWh	1–40 000
Efficiency (System's Efficiency)	%	80
Efficiency Charging	%	88–92
Efficiency Discharging	%	90–92
Efficiency Storage	%	100
Self-Discharge	%	0.1–0.2
Nominal Voltage/Cell	V	2
End-of-Charge Voltage	V	2.4
Open-Circuit Voltage	V	1.93/2.15 (0%/100% SOC)
Internal Resistance	mΩ	4–8
Number of Cycles	–	2 000
Lifetime	a	6–12
min. Discharge Duration	h	0.006
max. Discharge Duration	h	10
Investment Costs	€/kWh	100–300
Peripheral Costs	€/kW	20

Figure 4.7 shows the charge characteristics of a battery with an end-of-charge voltage of 7.2 V. Because one single cell has an end-of-charge voltage of 2.4 V, for the shown characteristics three cells are connected in serial. The charge characteristics are similar to the Li-Ion battery. First there is a constant current-, followed by a constant voltage-mode.

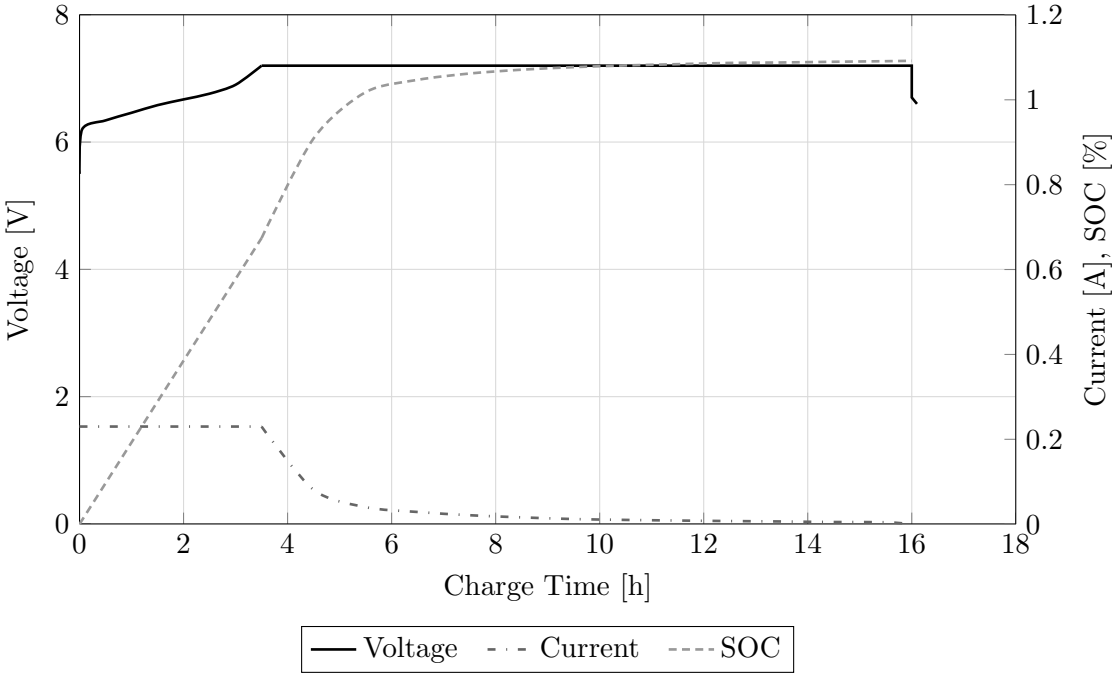

Figure 4.7: Lead-Acid battery UI-charging characteristics. The voltage, current and SOC is shown; Modified according to [92]

4.2.3 Redox-Flow Battery

The name "Redox" refers to the reduction and oxidation process/reaction to store the energy in liquid electrolytes, which flows through cells/membranes during the charge and discharge process.
The energy storage in Redox-Flow batteries does not take place by the reaction of the active material, which is placed on the electrodes of the battery cells, as is the case with the before described storage technologies. The energy-storing material of the Rodox-Flow battery is located in separate tanks and flows through the electrodes during the charge- or discharge-process. Catalysts are positioned on the electrodes to stimulate the chemical conversion of the energy-storing material. The starting material is again fed to the same tank as before having undergone the chemical conversion. The energy-material consists of metal salt solutions and electrolytes. The electrolytes are a dilute sulphuric acid [91, pp. 169–170]. Each electrode is assigned to a tank with the energy-storing material.
The Vanadium-Redox-Flow battery is used as a representative of the Redox-Flow batteries.
The chemical conversion (charge/discharge) is based on valence changes of the energy-storing fluids. Depending on whether the battery is charged or discharged, the anode is flown through by Vanadium V^{3+} or V^{2+}. On the other hand, the cathode is flown through with V^{4+} or V^{5+}. The two electrolyte circulations are separated by a proton

conductive membrane. The energy density of this technology is in the range of Lead-Acid batteries, because the solubility of metal salt in the electrolyte is not very good [93, p. 91].
Redox-Flow batteries are resistant to depth discharge. They have greater cycle numbers (charge/discharge) and longer life times as "conventional" electrochemical storage systems.
The most important typical characteristics of this battery type are listed in tab. 4.4.

Table 4.4: Overview of typical Redox-Flow battery characteristics; Modified according to [95, 98, 100–103]

Characteristics	Dimension	Value
Volumetric Energy Density	Wh/l	10
Gravimetric Energy Density	Wh/kg	20
max. installable Power	kW	10 000 per unit
min. installable Power	kW	10
typical Energy Range	kWh	500–5 000
Efficiency (System's Efficiency)	%	>75
Efficiency Charging	%	70–82
Efficiency Discharging	%	85–90
Efficiency Storage	%	100
Self-Discharge	%	0.1–0.2
Open-Circuit Voltage	V	1.3 (SOC 50%)
Charging Resistance	Ω/cm^2; Stack >80 cm^2	3.12/0.039
Discharging Resistance	Ω/cm^2	2.96/0.037
avg. Current Density/Cell	mA/cm^2	50
Number of Cycles	–	>10 000
Lifetime	a	>20
min. Discharge Duration	h	1
max. Discharge Duration	h	10
Investment Costs	€/kWh	150–500
Peripheral Costs	€/kW	550–1 400

Figure 4.8 shows the charge and discharge characteristic of a Redox-Flow battery with a nominal power of 10 kW (maximum possible discharge power), depending on the SOC. The data represented with the continuous lines are form [104] and the dashed lines are interpolated to get the SOC-range from 0 % to 100 %. The maximum charge power is higher because of several losses (converter, etc.). From a SOC greater 25% the battery can be discharged with its nominal power, below this SOC the power drops linear. The

charging with maximum power is possible up to a SOC of 45% and decreases linearly afterwards.

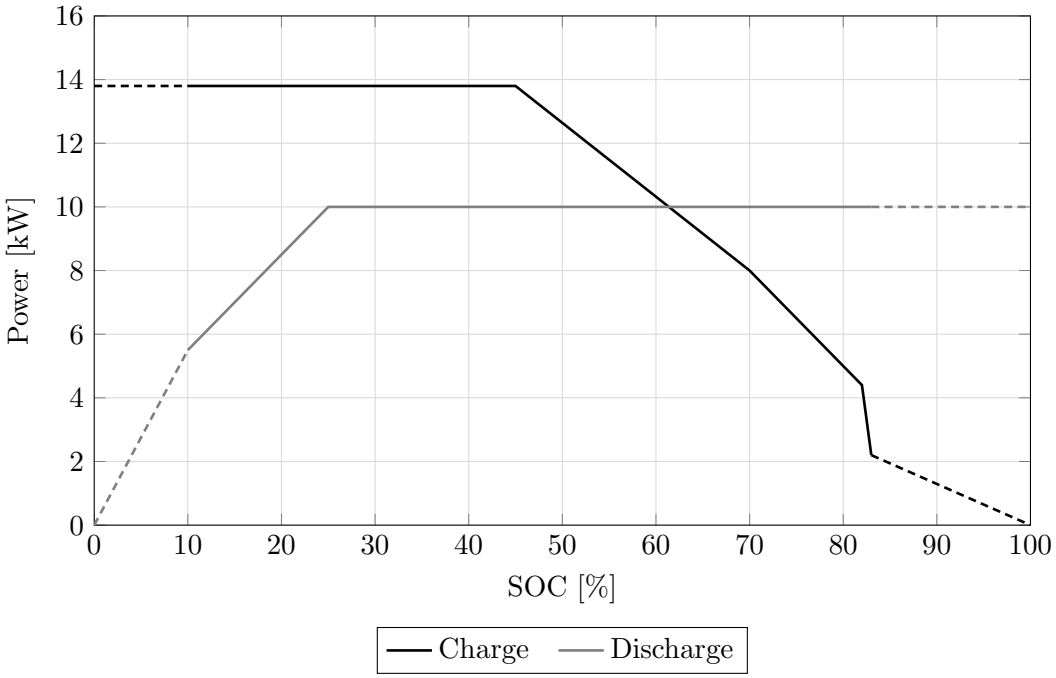

Figure 4.8: The charge and discharge characteristics of a Redox-Flow battery with a nominal power of 10 kW. The continuous lines are form [104] and the dashed lines are interpolated to get the SOC-range from 0 % to 100 %; Modified according to [104]

4.2.4 Thermal Storage (sensible)

As mentioned at the beginning of this section it is possible to separate between different types of thermal storage systems (sensible, latent, etc.). In this work, only sensible systems are used and there are some distinctions too. The heat transfer medium and the temperature range at which the storage system is used are distinguishing characteristics for these storage types. The application ranges from low temperature storage for domestic heating up to high-temperature storage systems for solar power plants (several hundred degrees Celsius). As heat transfer medium salt melts, water or oil are typically used [105] in [106], [107] in [108], [109]. The following table lists typical characteristics of three different sensible storage technologies.

Table 4.5: Typical characteristics of sensible storage technologies, tmp...temperature; Modified according to [107] in [108], [110, p. 110]

Characteristics	Dimension	Value		
		High tmp Oil	Low tmp Rock	Low tmp Water
Volumetric Energy Density	Wh/m^3	27 778	8 333	10 000–50 000
Volumetric Power Density	kW/m^3	10	3	-
Specific Energy Density	Wh/kg	27.78	2.78	-
max. Specific Power Density	kW/kg	0.01	0.001	-
Storage Time	–	Days	Days	Days-Year
Typical Discharge Time	s	10^4 - 10^5	10^4 - 10^5	-
Efficiency	%	70	-	50–90
Life Time	a	20	20	-
Costs	$/kW	400	200	0.1 €/kWh

4.2.5 Power-to-Gas

The purpose of the Power-to-Gas approach is to transform electric energy to energy gases, such as hydrogen (H_2) or methane (CH_4). This process consists of three steps and for each step different technologies are existing [90, pp. 412–416]. The •-symbol indicates technology only used at the power-to-hydrogen path, the –-symbol is used for power-to-methane processes only and technologies marked with a ⋆ are used, or can be used for both paths.

1. To roll-in
   - ⋆ Alkaline Electrolysis (AEL)
   - ⋆ Proton Exchange Membrane Electrolysis (PEMEL)
   - ⋆ High Temperature Electrolysis (HTEL)
   - – Chemical Methanation
   - – Biological Methanation
2. Store
   - ⋆ Gas Network
   - ⋆ Cavern Storage
   - ⋆ Gas-Oil-Deposits
   - ⋆ Overground Storage

3. To roll-out
    - ⋆ Fuel Cell
    - ⋆ Gas Turbine, Combined Heat and Power Plant
    - ⋆ Gas Heating, Gas heat Pump, Cooling Unit
    - • Fuel Cell Vehicle
    - – Gas Vehicles, Plains and Ships
    - ⋆ Material Use

In this work from all the possible storage options only the direct infeed of H_2 or Synthetic Natural Gas (SNG) CH_4 into the "Gas Network" and the storage of H_2 in separate tanks (Overground Storage) is used, because it is hard to estimate the potential of Cavern-, or Gas-Oil-Storages for a region with limited dimensions. Due to this restriction, the driving forces, when it comes to efficiencies, are the "roll-in" and "roll-out" process. That is why, in context of this work relevant "roll-in" and "roll-out" technologies are briefly described and typical parameters for efficiency, power and so on are mentioned.

Alkaline Electrolysis (AEL)
The two regions of the electrolyser are separated via an ion conduction membrane. Water – with an increased conductivity, by adding 20 wt% to 40 wt% potassium hydroxide – is injected in both halves. This reduces the internal cell resistance and increases the efficiency. On both sides, electrodes are located and ideally a voltage which is the decomposition voltage of water (1.23 V) is applied to the electrodes. On the cathode side, the water is split in hydrogen (H_2) and hydroxide (OH_-). The H_2 molecules are segregated and the hydroxide ions diffuse through the membrane and react in the anode reaction to oxygen and water [90, pp. 320–322]. Table 4.6 lists typical characteristics of this technology.

Table 4.6: Overview of typical Alkaline Electrolysis (AEL) characteristics; Modified according to [90, p. 329]

Characteristics	Dimension	Value
Working Temperature	°C	40–90
Pressure	bar	1–30
Efficiency	%	62–82
Active Cell Area	m^2	0.1–4
Current Density	A/cm^2	0.2–0.45
Cell Voltage	V	<2.4
Cells per Stack	–	<700
Hydrogen Production Rate	m^3/h	1–760
Electric Power	kW	5–3 400
Energy	$kWh_{el}/m^3_{H_2}$	4.5–7
Investment Costs	€/kWh	800–1 500

Proton Exchange Membrane Electrolysis (PEMEL)
The membrane electrolysis, also PEM electrolyser, has its origins in the fuel cell technology and is based on the inverse fuel cell process. This electrolyser is more suitable for dynamic operations than the AEL. A PEM electrolysis cell consists of a proton-conducting membrane (Proton Exchange Membrane, PEM), which is usually on both sides connected with electrodes. Onto the electrodes, a Solid Polymer Electrolyte (SPE) such as Nafion is stacked. This SPE is highly porous and accomplishes the current flow from the bipolar plates to the electrode and the transport of water toward the electrode and the product gases away from the electrode. In its functionality the PEM differs from the AEL. Water is supplied to the anode and with the decomposition voltage it is separated to atomic oxygen and two protons. The oxygen combines to O_2 molecules and is segregated, while the H^+-ions diffuse through the membrane to the cathode, where in the cathode reaction with two electrons they react to hydrogen [90, pp. 322–323]. Table 4.7 lists typical characteristics of this technology.

Table 4.7: Overview of typical Proton Exchange Membrane Electrolysis (PEMEL) characteristics; Modified according to [90, p. 329]

Characteristics	Dimension	Value
Working Temperature	°C	20–100
Pressure	bar	30–50
Efficiency	%	67–82
Active Cell Area	m^2	0.001–0.075
Current Density	A/cm^2	<2.5
Cell Voltage	V	<2.2
Cells per stack	–	<120
Hydrogen Production Rate	m^3/h	0.01–30
Electric Power	kW	0.5–160
Energy	$kWh_{el}/m^3_{H_2}$	4.5–7.5
Investment Costs	€/kWh	2 000–6 000

High Temperature Electrolysis (HTEL)
At the high temperature electrolysis (High Temperature Electrolysis of Steam, HTES) or steam electrolysis, a part of the separation energy for the separation of oxygen and hydrogen, is provided via high-temperature heat (700 °C to 1 000 °C). Thus, the cell voltage compared to the PEMEL and AEL can be reduced by more than 0.5 V to less than 1 V, to achieve higher current-related efficiencies. The function of the high-temperature electrolysis is based on the inversion of the solid oxide fuel cell reactions (Solid Oxide Fuel Cell, SOFC). Both half cells are separated with an O_2-ion conductive solid electrolyte and the electrodes are applied on both sides. On the cathode side superheated steam is supplied, which reacts with two electrons to hydrogen and O_2-ions. The hydrogen is segregated and the O^{2-}-ions diffuse through the electrolyte to the anode. There they react with electron release to oxygen O_2 [90, pp. 324–325]. Table 4.8 lists typical characteristics of this technology.

Table 4.8: Overview of typical High Temperature Electrolysis (HTEL) characteristics; Modified according to [90, p. 329]

Characteristics	Dimension	Value
Working Temperature	°C	700–1 000
Pressure	bar	approx. 30
Efficiency	%	65–82
Active Cell Area	m^2	<0.01
Current Density	A/cm^2	0.3–3.0
Cell Voltage	V	-
Cells per stack	–	-
Hydrogen Production Rate	m^3/h	5.7 (at 18 kW)
Electric Power	kW	-
Energy	$kWh_{el}/m^3_{H_2}$	3.2 $\left(0.6\,kWh_{th}/m^3_{H_2}\right)$
Investment Costs	€/kWh	-

All of the above mentioned electrolysis technologies have basically the following, total (anode and cathode) reaction, where l means liquid and g gaseous:

$$2H_2O(l) \rightarrow 2H_2(g) + O_2(g) \tag{4.9}$$

Chemical Methanation
The Sabatier process forms the basis for this conversion. With a catalytic reaction CO_2 (or CO) and H_2 are converted to CH_4. In the chemical methanation two reversible balancing reactions are necessary. The water gas shift reaction, is to separate the weak reactive CO_2 and is performed before the methanation [90, pp. 338–341]. The CO-methanation is the second and main reaction. In this reaction CO is hydrated.

Biological Methanation
The biological methanation is the so-called methanogenesis. The biological methanation is based – in analogy to the chemical methanation – on the reaction of CO_2 and hydrogen to methane. This reaction is done by organisms from the domain "Archaea". This reaction uses catalysts too. The difference is, that the catalysts are embedded in enzymes and the bacteria as organic livings control the reaction [90, pp. 346–347].

Typical characteristics of both methanation processes are listed in tab. 4.9.

Table 4.9: Overview of typical methanation characteristics; Modified according to [90, p. 347], [111, p. 46]

Characteristics	Dimension	Value	
		Ch. Meth.	Bio. Meth.
Working Temperature	°C	200–600	40–60
Pressure	bar	1–3	5–80
Efficiency	%	75–80	75–80

Basically the total reaction of methanation processes is:

$$4H_2 + CO_2 \rightarrow CH_4 + 2H_2O \tag{4.10}$$

Fuel Cell
The fuel cell process is the inverse process of the electrolysis. It consists of two electrodes, which are porous (gas permeable) and catalytically active. Catalytically means that the activation energy of the reaction is lowered because of the properties of the electrode material. The anode at which the electron release occurs (oxidation) is circulated by pure hydrogen or a hydrogen-containing gas. The oxidant, either pure oxygen O_2 or air (approximately 21 vol% O_2) is located at the cathode. The two electrodes are separated by an electrolyte, which is essential for a controlled chemical reaction. The electrolyte is gas impermeable and ion-conductive to avoid a mixture of the two gases and an uncontrollable oxyhydrogen gas reaction.
At the beginning at the anode hydrogen releases its electrons and is ionized into H^+-ions. The freed electrons travel through an electrical conductor from the anode to the cathode where the current source can be attached to a load. At the anode electrons cause a splitting of oxygen molecules in O^{2-}-ions. Depending on the type of fuel cell, O_2-ions move either through the electrolyte to the anode where they react with H^+-ions to water (H_2O), or vice versa [90, pp. 391-392]. The total reaction is:

$$2H_2 + O_2 \rightarrow 2H_2O \tag{4.11}$$

Depending on the reaction gases, the electrolyte and the operation temperature, it is possible to classify the following fuel cell types:

Table 4.10: Fuel Cell classification; Modified according to [90, p.392]

Type	Name	Reductive	Electrolyte	Temp. [°C]	Oxidant
AFC	Alkaline FC	H_2	Caustic Potash	20–90	O_2
DM-FC	Direct Methanol FC	CH_4O	Proton Conductive Membrane	60–130	O_2, Air
MC-FC	Molten Carbonate FC	H_2, CH_4	Li_3CO_3, K_2CO_3	60–130	O_2, Air
PA-FC	Phosphoric Acid FC	H_2	H_3P_4	160–220	O_2, Air
PEM-FC	Proton Exchange Membrane FC	H_2, H_2 cont. gas	Proton Conductive Membrane	60–120	O_2, Air
SO-FC	Solid Oxide FC	H_2, CH_4	Ceramics ZrO_2/Y_2O_3	800–1 000	O_2, Air

4.2.6 Heat Pump

The compression heat pump is the most common type. With this type a refrigerant flows through a closed cycle, where the refrigerant repeatedly changes the state between liquid and gaseous form. The ideal process is a left turning Clausius-Rankine process; it is the complementary of a compression refrigeration machine. Thermal energy at a lower temperature level, by adding power, can be converted to thermal energy available at a higher temperature level. The thermodynamic cycle is shown in fig. 4.9. From the point 1 to 2 the refrigerant ideally is adiabatically compressed (no heat transfer). Because of this the temperature is increased. From 2 to 3 the gaseous refrigerant condenses isobarically while thermal energy is dissipated. This energy is used for heating. From 3 to 4 the refrigerant is adiabatically expanded. 4 to 1 is a isobaric heat absorption up to the evaporation point. The heat energy can be taken from the ground or air.

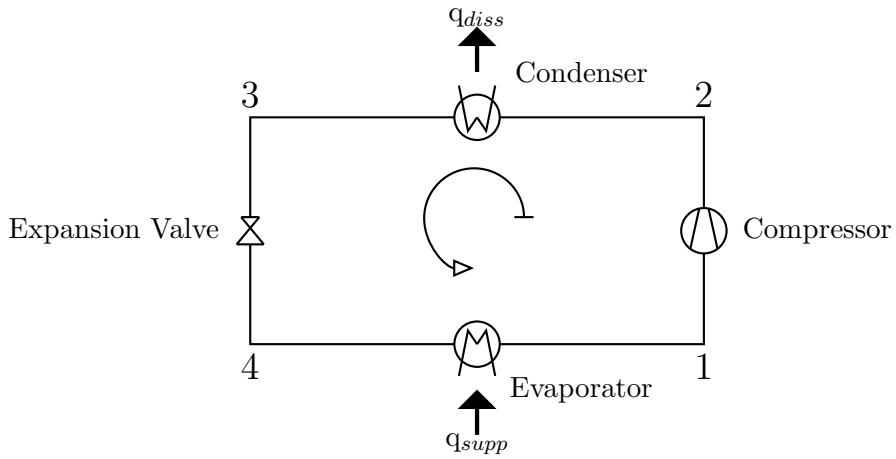

Figure 4.9: Thermodynamic cycle of a compression heat pump; Modified according to [112, p. 12]

There are two important indicators for heat pumps. One is the Coefficient of Performance (COP) and the other is the Seasonal Performance Factor (SPF). The COP indicates the performance at a specific operation point. The coefficient is the ratio between the heat power $\dot{Q}_H$ and the necessary electric power P_{el}, shown in (4.12). The COP is determined on a test rig (under standard conditions) at a steady state. The operating point for the source (supply) and drain (dissipation) is described via a letter (type of medium: B-Brine, W-Water, A-Air and E-earth-coupled humidifier) and a number (temperature), e.g. B0/W35, represents an operating point, where the Brine has a temperature of 0 °C and the water at the supply side has a temperature of 35 °C [112, p. 17].

$$COP = \frac{\dot{Q}_H}{P_{el}} \tag{4.12}$$

More important is, how the heat pump performs at different operating points, since the conditions are not always ideally. This changes the efficiency. The SPF is the relationship between benefits and input over a year, i.e. the ratio of delivered heat in one year to the required operating power (electric energy) in one year [112, p. 17]:

$$SPF = \frac{\int\limits_{Year} \dot{Q}_H}{\int\limits_{Year} P_{el}} = \frac{Q_{H,Year}}{W_{el,Year}} \tag{4.13}$$

One option to determine the SPF, is a simulation of the heating system. The other option is to measure the performance over one or more years. The COP is mostly higher than the SPF and they can vary considerably.
Depending on legislation in different states, the installation of heat pumps is subsidised, but for that they have to fulfil SPF-requirements [113]. The SPF-range for funding is between 3.5 to 4, depending on the technology. It is usually electric compression heat

pumps. Technology in this context means the medium of the source (where the heat is taken from, e.g. brine) and the supply medium (where the heat is supplied to, e.g. water). Because no definition of a specific technology should be done in this work the average SPF of 3.75 is used.

4.2.7 Gas Heating

Here with "Gas Heating" a system is meant, that burns gas for hot water production or room heating. Such a system is often used in houses in form of a gas-central-heating or gas-warm-water-boiler. In its basic form it consists of a burner and a heat exchanger to transfer the heat from the hot air to another medium, mostly water.
Depending on the size of the unit (in Watt), different burner types are used. For this work the efficiencies are the only important aspect of this technology. According to [114, p.33], the efficiency of gas-central-heating systems varies between 92 % to 99 % (based on the net calorific value). This is depending on the forward and return flow temperatures of the water. Especially for heating, this temperature depends on the building type, e.g. conventional buildings or new building standards (low-, lowest- or passive-house). The building structure in the model region is a mixture of all types. That is why the average efficiency of 95 % is used.

4.3 Implementations

The approach in this work is to solve a Linear Optimisation Problem. In this section, it is described how all the components are implemented in the optimisation. First the implementation of the grids mentioned in chapter 3 is described, followed by the implementation of the storage and conversion technologies.
Figure 4.10 shows how all the technologies interact and between which networks and at which nodes they can be placed. The left grey filed area represents a rural node without a connection to the district heating grid; the right filed area represents a node, located at urban or suburban area, where a district heating system is available. At the household nodes, different storage types (Li-Ion and Lead-Acid), heat-pumps and gas-burners are optional; they are placed as part of the optimisation.

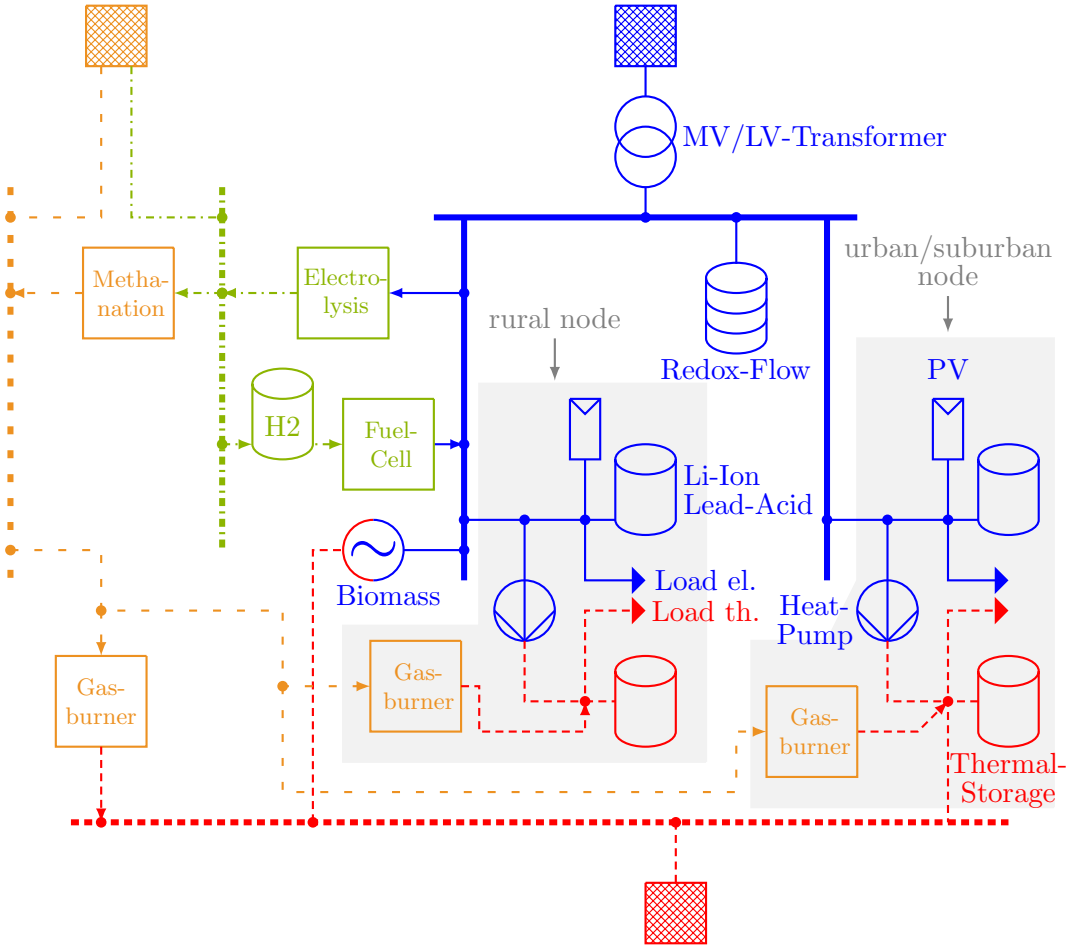

Figure 4.10: Storage- and conversion-technology implementation in the model region

4.3.1 Electric Network - Implementation

In section 3.2.1 it is described how the original non-linear electric load flow calculation is modelled in a linear way and which limitations this linearisation causes. These limitations include the negligence of line losses and reactive power flow. Furthermore no results about resulting level of voltages at the different nodes are possible. To overcome the level of voltage problems, the following workaround is used.
With the tool PSS©SINCAL [44] an AC-load flow calculation is carried out. With this load flow calculation, the maximum allowable node load or load infeed is determined, which causes no violation of the level of voltages in the LVG. The resulting active power values are used in the optimisation as load and infeed limit. If there would be a violation of this limit – exceedance – the optimisation places, dimensions and operates storages to avoid this exceedances.

The standard OENORM EN 60038 [115, p. 12], defines for networks with a nominal voltage of 230 V or 400 V a voltage limit of ±10%. The strong implementation of PV systems and the simultaneous energy production is a problem regarding the upper voltage limit. Even if the voltage band is ±10%, not the whole range is available in the LVG, because higher voltage levels have some voltage variations too. Figure 4.11 shows the level of voltage split for different parts in the distribution grid. The lower continuous, black line is the worst case for load situations, as shown, there is a buffer of 5 % in the LVG. If all the infeeds are excluded and the load flow calculation, only with the loads, is carried out, the maximum voltage drop is 2 % to 3 %. The maximum load case is therefore never a problem for the level of voltages in the model region. The upper continuous line represents the worst case for the infeed situation. In the LVG is a buffer of 3 %. This voltage limit is used by the AC-load flow, for determining the active power limits, for the infeed situation. This constraint is used in addition to ensure there is no voltage violation at the nodes.

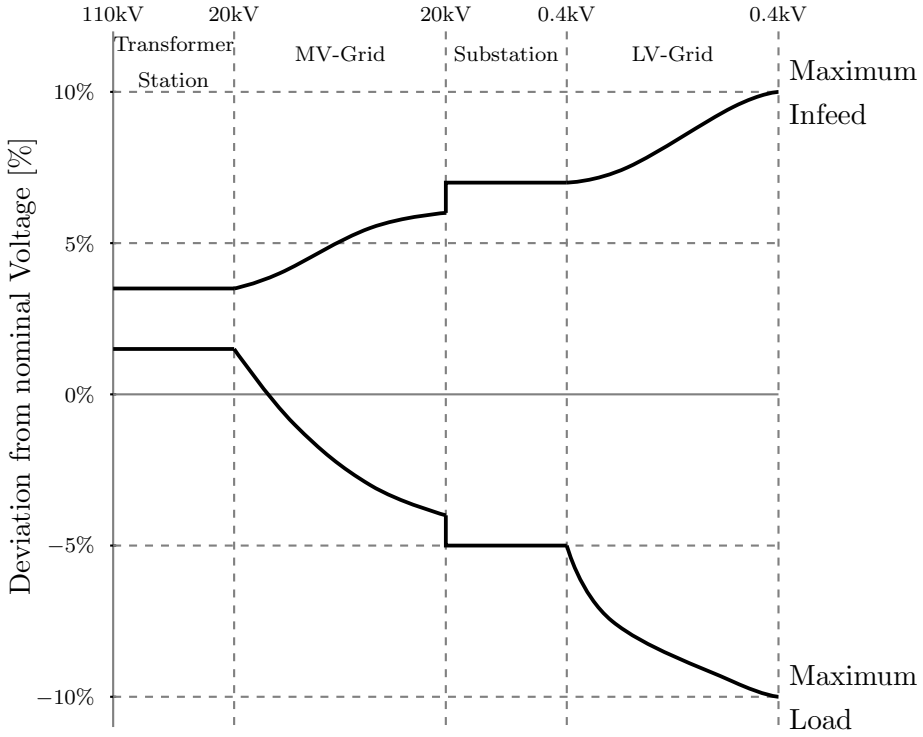

Figure 4.11: Voltage level split at the distribution grid, according to the standard DIN EN 50160 [116]; Modified according to [117, p. 10]

Additionally the Direct Current Load Flow (DCLF) is used by the optimisation to make sure there is no exceedance of the thermal limit current at the lines. If this would happen without any interventions, the optimisation places storages, or limits the infeed to overcome this problem. The resulting power time series of each node is used to

calculate with a AC-load flow calculation the previous neglected reactive power flows and node voltages.
For the Direct Current Load Flow (DCLF) calculation the already mentioned $\boldsymbol{L}_e$ matrix is used. The following equation is used to calculate the line load for each time step depending on the node loads (4.14). $P_{l,e}(t)$ represents the line load, $P_{i,e}(t)$ the node load and it is summed over all nodes n_k except the reference node (slack).

$$P_{l,e}(t) = \sum_{\substack{i=1 \\ i \neq \text{ref}}}^{n_k} L_{e_{li}} \cdot P_{i,e}(t) \leq P_{l,e_{max}} \tag{4.14}$$

As mentioned earlier, with the DCLF it is not possible to calculate network losses. However, the results of the line loads allow an estimate of the network losses. During operation, the resulting line losses can be roughly divided into three categories [118, p. 2]:

1. Voltage-dependent losses (no-load loss)
2. Compensation losses
3. Current-dependent losses (load losses)

Voltage-dependent losses occur as soon as the line is energised. The reason is the non-ideal insulation of electrical conductors between the lines and to ground. They are load independent. Compensation losses occur especially in cable systems because of the reactive power compensation of reactive power compensation coils. The current-dependent losses are caused by the ohmic line resistances. They only occur under load. They are calculated according to equation (4.15) [118, p. 2]. $P_{loss,cur}$ is the power loss at the line, R' the resistance load per unit length, l the line length, V the line-line voltage and S the apparent power.

$$P_{loss,cur} = R' \cdot l \cdot \left(\frac{S}{V}\right)^2 \tag{4.15}$$

The current-dependent losses are added to the optimisation via an additional term. In (4.14) they are not included, because one restriction of the DCLF calculation is the negligence of losses. In the optimisation, this lost term is implemented as cost parameter in the objective function. With this implementation, it is also possible to optimise the operation of storage-, conversion- and production-technologies in a way to minimise the line losses.
For the calculation of the current-dependent losses, another linearisation is necessary, since the losses $P_{loss,cur}$ are quadratically depending on the apparent power S. The following idealisation is used to overcome this issue:

$$S = \sqrt{P^2 + Q^2} \approx P + k \cdot Q$$

The exact calculation of the apparent power in the context of linear optimisations is not possible, since this requires squaring the active and reactive power. In the case of $P \gg Q$

the linear approximation causes relatively small errors. In the present implementation the reactive power is neglected, this results in $S = P$.
The problem $P \propto S^2$ is addressed with the linearisation of the quadratic term of the apparent power. For this, related values are used $p_{rel} = \frac{P_{load,max}}{P_{th,max}}$. All line loads are normalized to the respective, thermal, maximum permissible value $P_{th,max}$. At higher voltage levels, for reliability reasons the related value is usually smaller than the thermal limit (e.g. 65%). Since the network in the model region is a LVG, 100 % of the thermal limit is used, because these networks are usually not operated at a $n-1$ reliability point. Thus, the approximation of the losses for the point $S = 0$ and $S = S_{max}$ coincides exactly to the values without linearisation and results in the following equation (4.16). This linear interpolation between the two points $S = 0$ and $S = S_{max}$ causes an overestimation of network losses, because the losses between these two points is approximated with a straight line instead of the real quadratic correlation.

$$P_{loss,cur} = R' \cdot l \cdot \left(\frac{P}{V}\right)^2 \approx R' \cdot l \cdot \left(\frac{P}{V \cdot V} \cdot p_{rel} \cdot P_{max}\right) \tag{4.16}$$

4.3.2 Gas Network - Implementation

If leakage is not considered, gas networks do not have losses in the form ($P_{loss} \propto P_{transport}$). The load-dependent losses are because of pipe friction. These losses result in pressure drops. To overcome this drop, higher pressure at the infeed node is necessary. In Low Pressure (LP)-networks this is mostly ensured via pressure reduction stations. These stations reduce the pressure from the Medium Pressure (MP)-network to the level of the LP-network. Therefore no energy for compression is necessary. That is why this type of losses are neglected.
The gas load flow (4.17) is implemented and evaluated to ensure that there is never an overloading of gas pipes. The network is designed for the worst case, this means, overloading due to loads is not possible. The optimisation has the ability to place Gas-to-Power systems. This could cause overloads. $P_{l,g}(t)$ is the line load for the time step t, *ref* is the reference node (slack), n_g is the total number of gas nodes, $P_{i,g}(t)$ is the node load of node i and $P_{l_{max}}$ is the maximal possible pipe power.

$$P_{l,g}(t) = \sum_{\substack{i=1 \\ i \neq \text{ref}}}^{n_g} L_{g_{li}} \cdot P_{i,g}(t) \leq P_{l_{max}} \tag{4.17}$$

The gas load flow calculation is not only used to ensure that there is no overloading of the pipes, it is also used to determine the amount of hydrogen H_2, which can be fed directly into the network. As mentioned in section 3.2.2, the H_2-concentration should not exceed the 4% limit. This is important since the optimisation can place Power-to-Gas technologies, and one possible path is Power-to-Hydrogen.

These technologies are more common in the range of several tens of kilowatt to megawatt, therefore it is not realistic that such a system is placed at nodes, which represent a single household. That is why one constraint is the placement of the Power-to-Gas technologies only at the slack node.

4.3.3 Thermal Network - Implementation

There are several options for the optimisation to satisfy the thermal demand. In the rural areas heat pumps or gas burners can be used. The urban/suburban area has additionally the option of a district heating grid. How it is modelled is mentioned in section 3.2.3. The district heating system is a centralised system; the heat has to be transferred from the place of production to the buildings. This includes losses for the hot water transport in the network. These losses are considered as following in the optimisation.
Compared to the electric grid, where the load network losses depend on the load ($P_{loss,e} \propto I^2$), for the thermal system this is not the case. To ensure that customers have access to hot water any time, it is necessary to circulate water permanently; this is demand independently. Because of this a correlation like ($P_{loss,t} \propto$ thermal demand) is not possible. If there is no network/network-segment the losses are zero, if the pipe is used the losses are existent at full extent. That is why each network segment (pipe) has a binary effect to the losses. Such binary decisions at linear optimisation are not possible, as this would lead to a Binary Linear Optimisation Problem (BLOP). One solution would have been to say that either the whole thermal network is existing and used, or that there is no thermal network at all. Because a thermal system where the residual waste of the whole region is burned, just to attach one or two buildings, would not be realistic. In this case, the investment costs of the power plant bears no relation to the possible earnings for the sold thermal energy. To ensure the freedom of the optimisation, to decide what the best way of thermal supply is, the following workaround is used. The generation and demand data are ideal forecasts, because they are available for the three representative weeks. With the load flow matrix $\boldsymbol{L}_t$ the load flow calculation is carried out and the maximal transported power for each branch is determined beforehand. This is equivalent to the electric load flow calculation shown in (4.14). With this beforehand calculation it is possible to determine the maximal power load $P_{th_{\mu,max}}$ for each branch μ. With this coefficient it is possible to calculate the utilisation for each branch $P_{th_\mu}(t) \cdot \frac{1}{P_{th_{\mu,max}}}$ at each time step. The losses are calculated as shown in (4.18). There is no 0/1-correlation any more. This approximation is accurate if the branch load is close to zero or close to full load. Then the product $P_{th_\mu}(t) \cdot \frac{1}{P_{th_{\mu,max}}}$ is nearly 0 or 1. That is why this is used as a workaround for the before mentioned binary correlation.

$$P_{loss_\mu}(t) = P_{th_\mu}(t) \cdot \frac{1}{P_{th_{\mu,max}}} \cdot \Phi_{tot} \cdot l_\mu \tag{4.18}$$

$P_{loss_\mu}(t)$	:	heat losses for branch μ and time step t	$[W]$
$P_{th_\mu}(t)$	:	pipe utilisation at time step t	$[W]$
$P_{th_{\mu,max}}$	:	maximum pipe utilisation	$[W]$
Φ_{tot}	:	total heat losses per pipe pair	$[W/m]$
l_μ	:	length of pipe/branch μ	$[m]$

The losses are dependent on the pipe length, temperatures (forward-, return-flow and ground) and heat loss coefficients (pipe, ground, etc.). According to [119, pp. 249–253] the losses per pipe pair can be calculated as following:

$$\begin{aligned} \Phi_f &= U_1(\vartheta_f - \vartheta_s) - U_2(\vartheta_r - \vartheta_s) \\ \Phi_r &= U_1(\vartheta_r - \vartheta_s) - U_2(\vartheta_f - \vartheta_s) \end{aligned} \tag{4.19}$$

This results in the following overall heat losses:

$$\Phi_{tot} = \Phi_f + \Phi_r = 2(U_1 - U_2)\left(\frac{\vartheta_f - \vartheta_r}{2} - \vartheta_s\right) \tag{4.20}$$

Φ_{tot}	:	total heat losses per pipe pair	$[W/m]$
Φ_f	:	losses of supply pipe	$[W/m]$
Φ_r	:	losses of return pipe	$[W/m]$
ϑ_f	:	temperature of supply pipe	[K]
ϑ_r	:	temperature of return pipe	[K]
ϑ_s	:	temperature of the undisturbed soil	[K]
$U_1,\ U_2$	:	heat loss coefficients	$[W/(mK)]$

For symmetric pipe constructions the overall heat loss coefficient is:

$$U_1 - U_2 = \frac{1}{R_s + R_i + R_h} \tag{4.21}$$

R_s	:	insulance of the soil	$[(mK)/W]$
R_i	:	insulance of the insulating material	$[(mK)/W]$
R_h	:	insulance of the heat exchange between supply and return pipe	$[(mK)/W]$

According to [120, p. 8], if both pipes have the same thermal isolation characteristics (4.20) can be simplified as follows, if the average thermal temperature ϑ_m of the forward and return flow temperature is used:

$$\begin{aligned} \Phi_{tot} &= U\left(\vartheta_f + \vartheta_r - 2\vartheta_s\right) \\ \text{with} \quad \vartheta_m &= \frac{\vartheta_f + \vartheta_r}{2} \\ \Phi_{tot} &= 2U\left(\vartheta_m - \vartheta_s\right) \end{aligned} \tag{4.22}$$

Figure 3.13 and 3.14 in section 3.2.3 illustrate the temperature values for forward and return flow. In order not to significantly over or underestimate the losses, the average values for forward and return temperature are used. This leads to the temperature values and losses shown in tab. 4.11, for the two thermal networks, one for the default/refurbished demand and one for the minimal thermal demand. $\varnothing\Phi_{tot}$ represents the losses per meter pipe pair, averaged over the whole network. Whereas $\Phi_{tot} \cdot l_{tot}$ represents the losses for the whole thermal network.

Table 4.11: Characteristics of the thermal network, which are used to calculate the thermal losses, for the two different network types "default/refurbished" and "minimal". Data for Φ modified according to [121, p. 7]

	Network	
	default/refurbished	minimal
ϑ_f	80 °C	80 °C
ϑ_r	35 °C	35 °C
ϑ_s	10 °C	10 °C
U	0.307 4 W/(mK) DN150 0.211 2 W/(mK) DN65 0.182 4 W/(mK) DN50	0.230 8 W/(mK) DN100 0.182 4 W/(mK) DN50 0.163 8 W/(mK) DN40
Φ single pipe	14.60 W/m DN150 10.03 W/m DN65 8.67 W/m DN50	10.96 W/m DN100 8.67 W/m DN50 7.78 W/m DN40
$\varnothing\Phi_{tot}$	20.62 W/m	17.22 W/m
$\Phi_{tot} \cdot l_{tot}$	37 406 W	31 226 W

Additionally to the calculation of the losses, the load flow matrix $\boldsymbol{L}_t$ is used to ensure that there is no overloading of pipes. The implementation is equivalent to the electric, or gas system ((4.14), (4.17)).
If the coverage of the thermal demand at the district heating grid with the biomass power plant and the burning of waste is not possible, it is assumed that the missing demand is covered via gas burning in a central power plant. This power plant is located at the same place as the other central thermal power plants (slack).

4.3.4 Storage - Implementation

Li-Ion and Lead-Acid batteries are available at small power and energy values and in some regions in Austria such storage systems in combination with PV-systems are promoted [122]. That is why it is assumed, that this storage types can be placed on each node in the network. In contrast, the Redox-Flow battery is not so commonly used so far and the existing systems are bigger, (several ten kilowatts up to megawatts). Because of this it is assumed as a restriction, that this technology can only be placed at the slack node.
From all the – in the previous section – mentioned technologies for thermal storage, the sensible storage tank with water is used in this work, because this technology is available from storage volumes of several 100 litres to 1 000 000 litres, is relatively easy to handle and is cheap. Due to the wide range of storage capacity this technology can be placed at each node on the network.
An important characteristic of batteries with built-in converters (Li-Ion, Lead-Acid) is the energy to power ratio (E/P-ratio). This provides an indication of whether it tends to be a short- or long-term storage. For Li-Ion and Lead-Acid batteries this ratio is typically relatively similar regardless of the design and size of the unit. The energy-performance ratio of 2 MWh/MW for a Lead-Acid battery means, that the battery can be fully charged or discharged within 2 h. In Redox-flow batteries however, the power can be dimensioned independently of the energy.
In context of the optimisation the specific storage characteristics of the different systems are not modelled in detail. This would cause non-linear effects which have to be modelled. This is not possible with a LOP. The consequence is an overestimation of the charge power for high SOC (>80 %) values. This issue is overcome with oversizing the storages in a way they are only operated at the linear SOC range. How this is implemented is described in section 4.3.7.
The E/P-factors listed in tab. 4.12 are guidance values. For Li-Ion and Lead-Acid batteries, a variety of different types exist, which differ especially in the E/P-ratio. For this reason, the here mentioned values are deputies of batteries with these properties. The efficiency values mentioned in tab. 4.12 are average values. Average values are used, to not significantly over or underestimate the capabilities of storages.

Table 4.12: Typical characteristics of the used storage technologies; Modified according to [37, p. 97]

Technology	E/P-ratio	Efficiency Roll-In	Efficiency Roll-Out	Nodes
Li-Ion	0.4 h	92.5%	97%	all
Lead-Acid	2.0 h	90%	91%	all
Redox-Flow	free	76%	88%	Slack
Thermal	free	89%	89%	all

The modelling of storages is carried out with the current energy content E(t), which is limited in terms of its value and the change rate (power). To be able to model the roll-in- and roll-out-efficiency these two operations are modelled separately (fig. 4.12). The sum of roll-in and roll-out energy represents the current storage content. For each time step this has to be greater or equal to zero and less or equal to the installed energy:

$$0 \leq E(t) = E_{out}(t) + E_{in}(t) \leq E_{inst}. \tag{4.23}$$

The electrical terminal power is calculated via the energy change rate (4.24), where

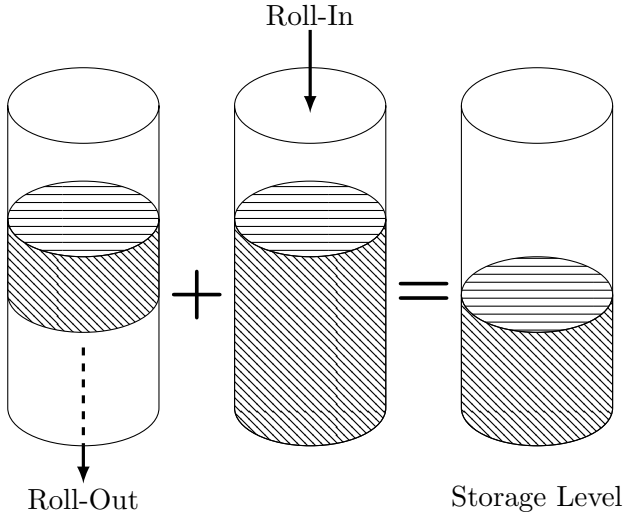

Figure 4.12: Modelling of the Roll-Out and Roll-In process of storages; Modified according to [43, p. 82]

$P_{el}(t)$ is the charge or discharge power. This resulted in a significantly reduced and sparse degree of the constraint matrix and allows the use of sparsely populated matrices, which significantly reduce the computational effort [37, p. 98].

$$\begin{aligned} P_{el}(t) > 0 \Rightarrow -P_{el}(t) \cdot \Delta t \quad &= \eta_{out} \cdot [E(t) - E(t-1)] \\ P_{el}(t) < 0 \Rightarrow -P_{el}(t) \cdot \Delta t \cdot \eta_{in} = \quad &[E(t) - E(t-1)] \end{aligned} \tag{4.24}$$

The parameter Δt describes the time step size of the simulation. As a constraint, at any time, the instantaneous power must be less or equal to the installed storage power. Thermal storages are modelled with the same approach. Part of the optimisation is to determine the installation size (energy and power) for each node and each storage technology and to determine a matched operation (energy content at any time) based on the installed size.

For storages there is one more effect that has to be considered. As mentioned in section 3.3, the simulation is based on representative weeks. There is one week which represents winter, one for summer and one for the transition (autumn, spring) period. The optimisation shall give conclusions for a period of one year. For none overlapping systems (systems without memory), such as loads, or conversion technologies, the simulation of just representative weeks is no problem to derive annual conclusions. But for systems with memory behaviour, it is a problem to derive annual conclusions by just simulating single weeks. It is not useful to simulate the representative weeks seventeen- or nine-times, since this would not give additional information but increase the computation requirements, that is why in the first place the reduction to representative weeks was done and why only one week for each period is simulated. The results of the storages for the representative weeks are then increased by a factor of 17 or 9, to derive annual results, this is shown in fig. 4.13. The difference between the SOC at the beginning and end of the representative week is multiplied with its occurrence in the VDEW-profile, to derive the beginning SOC of the following representative week.

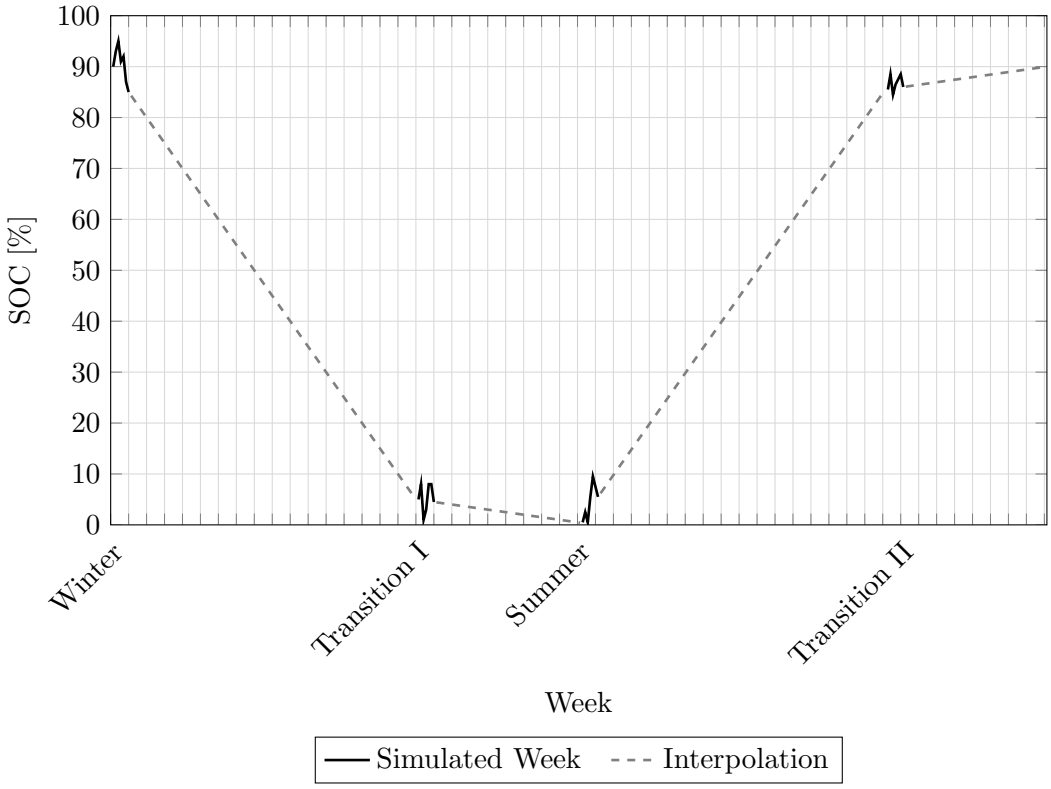

Figure 4.13: Projection of the simulation weeks of storages to an annual period. The continuous line segments represent the simulated weeks and the dashed line the interpolation of the results; Modified according to [37, p. 93]

With this approach it is possible to simulate the SOC-changes of storages in detail on a basis of single weeks and derive long term informations (seasonal) at the same time. The continuous lines in fig. 4.13 represent the simulated weeks and the dashed lines the interpolation, if the result of the week is multiplied by a factor of 17 or 9, to derive the start value for the next season. An additional constraint guarantees the same storage stocklevel at the beginning and end of the year. To guarantee a useful storage management, which goes beyond the one year period.

4.3.5 Conversion Technology - Implementation

Power-to-gas, heat pumps and gas burners/heaters are the three conversion technologies used in this work. The basics about Power-to-Gas technologies are mentioned earlier in section 4.2.5 and also the three possible paths with this technology, the direct infeed of H_2 (4% limit) or CH_4 into the gas network, or the separate storage of H_2 and direct reconversion in a fuel cell, all this is illustrated at the beginning of this section in fig. 4.10.
Conversion technologies are characterised by many characteristics, for example dynamic behaviour, needed space, need of special geological conditions (pumped storage). The most important is the efficiency which determines, how much energy arrives at the target energy form and how big are the losses during the conversion. Table 4.13 lists the used efficiency parameters, these are average parameters from the determined values (tab. 4.6, 4.7, 4.8, 4.9), only the H_2 storage is assumed ideal, the losses depend on the storage time and the diffusion rate. For stationary H_2 storages, there is no discrepancy between tight construction and low weight. That is, why a tight storage construction with a neglected diffusion rate is assumed.

Table 4.13: Used efficiencies for conversion technologies

Technology	Efficiency
Electrolysis	62 %
Methanation	77 %
Fuel-Cell	45 %
H_2-Storage	100 %

For methanation the gathering of the CO_2 is one important aspect. It can be extracted from air or from a preceding process such as a biomass power plant, a gas power plant, steelworks and so on. Basically each process which has a huge CO_2 output ideally with a rather high concentration is suitable. The CO_2-source is one major discussed problem, when it comes to methanation and so far no ideal solution has been found, that is why this point is excluded from this study and it is assumed that the CO_2 can be provided in an appropriate form. This study should show if Power-to-Gas at the level of a low voltage region is competitive to other storage systems. That is why the exclusion of the CO_2 gathering is chosen.

4.3.6 Infeed Power Limiting

With infeed power limiting, the active power reduction from supply-dependent producers, such as PV systems, is meant. In the case of PV systems this can be achieved by moving away from the Maximum Power Point (MPP). This is implemented in the optimisation with an additional slack variable for each node. This power reduction for each time step can be between zero (no change) and the current instantaneous infeed power. Depending on the objective (see section 4.3.7) this negative-adjustment has a negative impact on the objective function value. From the perspective of the model region, this causes a reduction in the export refund, or higher imports since the limited energy cannot be stored. Nevertheless, the instrument of limitation represents an important solution. On the one hand, this ensures that high input powers do not lead to unacceptable line loads. On the other hand, the maximum storage power not necessarily has to be dimensioned to fit the maximum installed production power.

4.3.7 Objective Function

So far all the technologies and the implementations are described. Since it is not possible to compare different parameters such as one kilowatt-hour storage capacity and one kilowatt-hour of electric energy consumption, a special parameter is needed to correlate these parameters. This parameter is the price, since everything is traded and therefore it is possible to price everything. The two basic price parameters, used to compare everything, are €/kW and €/kWh.
The objective of the optimisation in all scenarios is the minimisation of the overall, annual system cost.
With overall system costs, the costs for the entire model region is understood. The considered costs do not cover all considered costs for CAPEX or OPEX, since the depreciations and maintenance costs are not included.
The following list contains the components considered in the overall system cost and thus the objective function value:

- Installation costs for decentralised storage (Li-Ion, Lead-Acid)
- Installation costs for centralised storage (Redox-Flow)
- Installation costs for electrolysis
- Installation costs for methanation
- Installation costs for H_2-storage
- Installation costs for Fuel-Cell
- Installation costs for thermal storage
- Installation costs for heat-pump

- Loses of decentralised storage
- Loses of centralised storage
- Loses of H_2-storage
- Loses of thermal storage
- Loses of Fuel-Cell
- Loses at the electric network
- Loses at the thermal network
- Loses due to infeed limitations

- Revenues/costs for electricity exchange at the MV/LV-transformer
- Revenues for H_2 infeed
- Revenues for CH_4 infeed
- Costs for CH_4 import

Figure 4.14 shows the above mentioned list in context of the model region. Arrows and labels in red represent implemented costs and the green arrows show implemented revenues. With different costs/revenues, it is possible to set different goals for the optimisation, such as minimal energy import, or minimal storage implementation. That is why different costs represent different scenarios; they are described in the next chapter, chapter 5.
Since the minimisation of the annual system costs is the objective function, it is necessary to derive all the costs on an annual basis. For energy costs this is no problem, the price for one kilowatt-hour times the kilowatt-hours consumed in one year represents this type of costs. The following prices for the energy import and export are used. According to [123] the price of electricity for household consumers is in a range of about 15 cents/kWh to 19 cents/kWh. The price consists of three equivalent parts [124], one-third of the price is for the energy, one for the network charges and one is for taxes. It is assumed that all the households are equally spread over the price range, therefore the average of 17 cents/kWh for the electricity consumption is used. For the infeed of electricity in the power grid at network levels 6 and 7, the energy is repaid with about 6 cents/kWh. In this case, only the price of energy is used, because it is not realistic that the price for the usage of the network, or taxes is refunded. The electric power losses represents the loss of energy as a result of energy transport in the electrical grid, and therefore have to be additionally obtained, that is why they are priced with the price for the energy consumption with 6 cents/kWh.
For the gas consumption the price is between 5 cents/kWh to 7 cents/kWh. The average of 6 cents/kWh is used. The via power-to-gas produced gases, Synthetic Natural Gas (SNG) and H_2 are refunded with 23 cents/kWh or 15 cents/kWh [125, p. 31]. The thermal power loss at the district heating system is priced according to the energy purchase price for gas, with 6 cents/kWh. This means, the loss of energy as a result of energy transport in the district heating system is substituted in the form of additional gas purchases and burning in the central heating power plant.

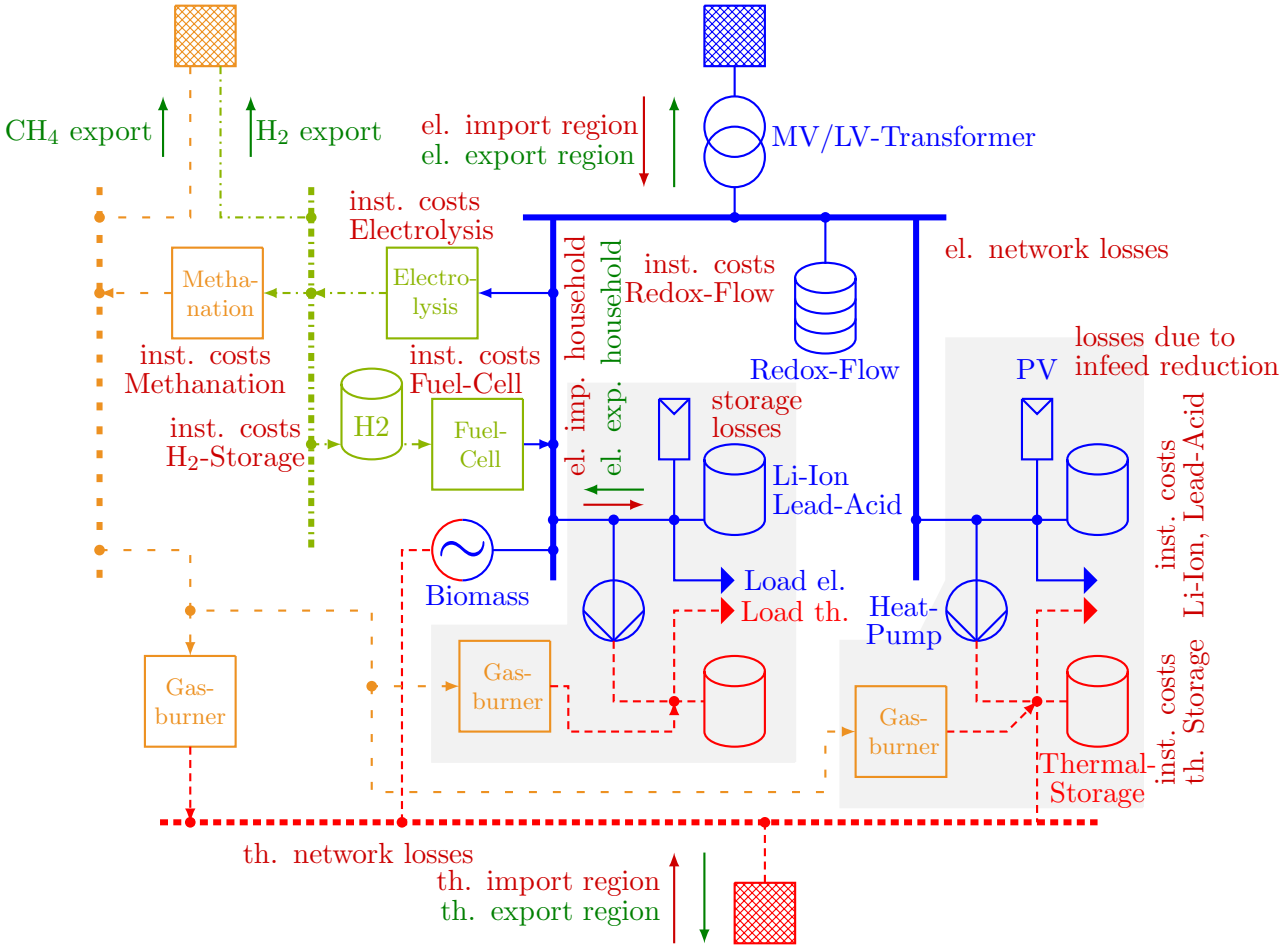

Figure 4.14: Considered costs/revenues in the optimisation model. Arrows and labels in red represent costs, green arrows are revenues.

For investment costs it is more difficult to derive costs on a annual period, since the lifetime of storage- and conversion-technologies is several decades. That is why an approach is necessary to break the one time investment costs down to equal annual costs. The annuity factor (4.25) is used to determine these annual costs.

$$A = I_0 \frac{(q-1) \cdot q^n}{q^n - 1} \tag{4.25}$$

A	:	annuity factor	[€]
I_0	:	initial investment	[€]
q	:	interest rate	[%]
n	:	lifetime	[a]

The initial investment costs vary for different technologies. According to [95, p. 20] an interest rate of 8 % is used. The lifetime n, especially for batteries, depends on the number of charge and discharge cycles. The maximum possible number of cycles for both technologies (Li-Ion, Lead-Acid), with a discharge depth of 80 %, is used to calculate the life time. For Li-Ion batteries 3 160 and for Lead-Acid battery a maximum of 1 500 cycles is used. The optimisation experiences from the project "SYMBIOSE" [37] showed, that 267 cycles/a are a suitable assumptions. The consideration behind this is that decentralised storages are only installed if they are used extensively. In this regard, it is assumed that the battery is used with a full cycle every day during the summer and transition (spring/autumn) period. In the winter time, the duration of a full cycle is roughly 3 days, therefore the days of the winter time are weighted with a factor of 0.3. The season assignment according to VDEW [64] is used for this approach. The charge characteristics of the Li-Ion (fig. 4.6) and Lead-Acid batteries (fig. 4.7) are not linear over the full State of Charge (SOC)-range. They are linear over a SOC-range of approximately 0 % to 80 %. To be able to use the batteries in the linear optimisation over a SOC-range of 0 % to 100 %, the investment costs of the batteries are increased by 25 %. This simplification is chosen for reducing the size and complexity of the optimisation model.
The literature research (tab. 4.2, 4.3 and 4.4), showed a wide range of storage costs. That is why, different storage prices are used as one variable to derive different scenarios, to be able to see, how storage technologies are used, based on different prices. Only the cost of thermal storage, hydrogen storage and methanation are kept constant for all scenarios. Because the first two technologies are well developed and no drastic further price change is assumed. Methanation is in an early research state and further price developments strongly depend on uncertain technology developments, that is why the costs are kept constant.
With all these cost and revenue parameters it is possible to optimise the whole region, how these parameters are varied to derive different scenarios, is described in the next chapter, chapter 5.

5 Scenarios

In the previous chapter, the implementation of the different parts in the optimisation is described. Depending on what technologies are considered and which costs are used for different technologies/energies, it is possible to optimise with different goals.
The following parameters have characteristics of binary variables. These parameters can be considered or not. If they are considered, they are weighted with their associated costs:

- storage costs,
- costs for heat-pumps,
- revenues/costs for electricity exchange at the MV/LV-transformer,
- revenues/costs for gas export/import,
- storage losses,
- electric network losses,
- thermal network losses,
- electric power limitation at building nodes

and the following parameters can be set to different values:

- electric load increase rate,
- thermal demand,
- storage/conversion-technology costs.

5.1 Basic Cases

With these parameters, it is possible to distinguish between three basic cases. The Technical (TE)-case where only the technically relevant parameters (line loads, transformer load, etc.) are considered. This does not include energy import/export costs. This scenario represents the stakeholder "system operator". With storage usage, the network

losses and the exceedance of threshold values (line loads, voltage limits, etc.) can be avoided. Furthermore it is interesting to keep replacement payments due to infeed curtailments low. Infeed curtailments can be considered – in combination with storages – as another remedy to meet the technical system requirements. The technical limitations, such as maximum line load, voltage-band, maximum transformer load, etc. are considered at all scenarios or sub-scenarios.
The case "Whole Region" (WR) corresponds to an overall system optimisation of the complete region. Here, especially the connections to the overall networks (electricity, gas) are important interfaces. Depending on the cost spread for imported and exported energy a more or less "autonomous" model region be derived.
The aim of the "Ecological Region" (ER)-scenario is the minimisation of the total energy imports (electricity and gas) while meeting the energy needs of the region. Essentially, this scenario corresponds to the "Whole Region"-scenario, but with high energy import costs. Due to high energy import costs, indirectly the pricing of CO_2-emissions for the imported electricity and gas is possible. This leads to the preferred usage of, renewable energy produced within the region. In addition the form of energy import is chosen, which satisfies the total consumption best.
Table 5.1 lists the considered parameters for the three basic cases.

Table 5.1: Considered cost-parameters for the three basic cases

Szenario	Technical	Whole Region (WR)	Ecological Region (ER)
Storage	✓	✓	✓
Heat-Pump	✓	✓	✓
Import/Export at Transformer		✓	✓
Import/Export for Gas		✓	✓
Storage losses	✓		
Losses el. Network	✓		
Losses th. Network	✓		

5.2 Further variations

An additional possibility is the variation of cost parameters. This and the usage of infeed curtailment leads to sub-scenarios.
The electric load increasing rate is another variation. In Austria the electric energy increase between 1990 and 2010 was up to 2 %/a [126]. That is why the following three annual electricity increase rates are used, to determine the influence of different electric load scenarios (tab. 5.2). Because of the reduced economic growth in the last years and consequential a reduced energy demand increase, values between 0.5 % to 1.5 % are used.

Table 5.2: Scenario variations due to annual electric load increase

Name	Increase
min	0.5 %/a
med	1 %/a
max	1.5 %/a

The thermal load scenarios are already described in section 3.3.2. They are:

- the default scenario, where no refurbishment of buildings had been done so far,
- the refurbished scenario, where the usual refurbishment had been done
- and the minimal scenario, where all buildings are constructed with a low-, lowest- or passive-house-standard.

The cost variation of the storage or conversion technology is one additional variation, which defines sub-scenarios. Table 5.3 lists the three used variations. They are derived from the possible cost ranges for the individual technologies, mentioned in section 4.2. To be able to determine the sensitivity depending on storage- and conversion- technology costs, minimal, medium and maximal costs are used for the technologies listed in tab. 5.3. The cost of thermal storage, hydrogen storage and methanation are kept constant for all scenarios. Thermal and hydrogen storages are regular tanks and a huge further product and therefore price development is not assumed. Methanation is at an early research state and further price developments are nearly impossible. They are strongly depending on a technological breakthrough. Which can not be predicted form today's perspective. For Li-Ion and Lead-Acid batteries, in this thesis, the energy-power-ratio (E/P-ratio) is constant, therefore the power depending costs are converted to energy related installation costs and only one value is given in tab. 5.3. For Redox-flow-batteries and Power-to-Gas conversions there is no constant E/P-ratio and the power- and energy-depending-prices are listed separately. Additionally to all the above mentioned variables, a few further variations are included. If not specially highlighted in the scenarios the following limitations are set to values, where they do not influence the maximum demand or infeed.
Optimisation results for the technical case showed the need of storages placement due to voltage-band (V-Band) violations at high PV-infeed. The maximum load is never a problem in the investigated scenarios and network set-ups. The maximum line load depending on the line never exceeded 10 % to 50 % of the maximum thermal possible line load. To see how the optimisation solves the problem if the thermal line loading is the limitation, the maximum permissible thermal line load is reduced to 25 %. For this case it is assumed that the same lines are used (same electrical characteristics) with lower thermal maximum current. Otherwise the characteristics of the whole network would have changed and a comparison between scenarios would not be possible. As voltage-band violation, the line load reduction is a local problem, where a solution for individual nodes has to be found.

Table 5.3: Annual storage and conversion technology costs for different scenarios; Modified according to [37, p. 86]

Technology	minimal costs (min)		medium costs (med)		maximal costs (max)	
	E_{inst} €/kWh/a	P_{inst} €/kW/a	E_{inst} €/kWh/a	P_{inst} €/kW/a	E_{inst} €/kWh/a	P_{inst} €/kW/a
Li-Ion	79.7		126.3		405.7	
Lead-Acid	29.9		35.9		95.5	
Redox-Flow	15.3	71.1	20.4	83.3	50.9	331.4
Electrolysis		114.8		131.7		151.2
H_2-Storage (30 bar)	1.2		1.2		1.2	
Fuel-Cell		101.2		216.3		331.4
Methanation		158.6		158.6		158.6
thermal Storage	0.0198	0.00198	0.0198	0.00198	0.0198	0.00198

In contrast to this, the limitation of the MV/LV-transformer leads to a centralised problem (slack located problem). For most cases a commonly used 630 kVA transformer is implemented, which is never a limitation factor in the investigated networks and scenarios. The maximum power demand is roughly 100 kW, therefore a 250 kVA transformer is implemented instead of the 630 kVA used in scenario TE01. From a load perspective the smaller transformer is no problem either, but for the PV-production it is, since the maximum production power exceeds the maximum load power by a factor of six. This variation is chosen to see, how the optimisation overcomes a central located limitation problem.
Another variation is the maximum allowable power (load/infeed) at nodes where buildings are located. This resembles a "power flat rate"-scenario, the power demand or infeed up to the limit is free of costs and beyond this limit it is extremely expensive (in case of this thesis, infinitely).
Since at the default model region set-up the renewable production power is more than six times the demand, reduced productions scenarios are analysed too. These scenarios are characterised with the suffix "red" in the scenario listing in tab. 5.4. The total PV size and biomass production is scaled with 29.4 % to derive an equal annual electricity production and demand.

5.3 Selected scenarios

If all combinations of the above mentioned variables are observed, several thousand combinations are possible. One optimisation takes one to several hours, which is why, it is not possible to analyse all scenarios. Because of this, the Technical (TE)-scenario (TE01) is defined as basic case, since the load and cost parameters are medium values and all other cases are derived from this scenario:
TE01 is the scenario with medium electric load increase, medium storage/conversion-technology costs and the refurbished thermal demand and all the technical requirements (line loads, V-Band, transformer limits, etc.) have to be fulfilled.
In total 31 scenarios are analysed, table 5.4 lists the considered parameters for each scenario.
Between the scenarios TE01 to TE03 everything is kept the same except the thermal demand which varies between all three possible options (refurbished, minimal and default). This is chosen to determine the influence of the thermal demand or building standards on technical requirements. TE04 is the basic scenario TE01 where additionally infeed curtailment is allowed, to see if the power reduction of renewable sources (PV and biomass) is a better option to fulfil all technical requirements, instead of storage installations. Compared to TE01, TE05 and TE06 are extreme situations, either everything is set to minimum or maximum.

Table 5.4: Analysed scenarios for the three different basic cases (Technical, Whole Region, Ecological Region)

Scen.	Description	el. Laod Increase	Storage Cost	th. Load Scen.	Load Flow			V-Band	MV/LV-Transf. Limit	Node Limit	Infeed Limiting	el. Cost SLACK	Cost gas Import
					el.	th.	gas						
TE01	Basic tech. case	med	med	ref	✓	✓	✓	✓	✓				
TE01-red	reduced PV and biomass	med	med	ref	✓	✓	✓	✓	✓				
TE02		med	med	min	✓	✓	✓	✓	✓				
TE03		med	med	max	✓	✓	✓	✓	✓				
TE04	T01 with infeed curt.	med	med	ref	✓	✓	✓	✓	✓		✓		
TE05		min	min	min	✓	✓	✓	✓	✓				
TE06		max	max	def	✓	✓	✓	✓	✓				
TE07	T01 with 250kVA transf.	med	med	ref	✓	✓	✓	✓	✓				
TE08	T07 with infeed curt.	med	med	ref	✓	✓	✓	✓	✓		✓		
TE09	T01 with 25% el. line load	med	med	ref	✓	✓	✓	✓	✓				
TE10	T09 with infeed curt.	med	med	ref	✓	✓	✓	✓	✓		✓		
TE11	T01 with $P_{max.Node} = P_{max.load}$	med	med	ref	✓	✓	✓	✓	✓	✓			
TE12	T01 with $P_{max.Node} = E_{year}/8760$	med	med	ref	✓	✓	✓	✓	✓	✓			
TE13	T01 with $P_{max.Node} = E_{year}/8760\text{-}50\,W$	med	med	ref	✓	✓	✓	✓	✓	✓			
TE14	T11 with infeed curt.	med	med	ref	✓	✓	✓	✓	✓	✓	✓		
TE15	T12 with infeed curt.	med	med	ref	✓	✓	✓	✓	✓	✓	✓		
TE16	T13 with infeed curt.	med	med	ref	✓	✓	✓	✓	✓	✓	✓		
WR01	Basic Whole Region case	med	med	ref	✓	✓	✓	✓	✓			✓	✓
WR01-red	reduced PV and biomass	med	med	ref	✓	✓	✓	✓	✓			✓	✓
WR02		med	med	min	✓	✓	✓	✓	✓			✓	✓
WR03		med	med	def	✓	✓	✓	✓	✓			✓	✓
WR04	WR01 with infeed curt.	med	med	ref	✓	✓	✓	✓	✓		✓	✓	✓
WR05		min	min	min	✓	✓	✓	✓	✓			✓	✓
WR06		max	max	def	✓	✓	✓	✓	✓			✓	✓
ER01	Basic Ecological Region case	med	med	ref	✓	✓	✓	✓	✓			✓	✓
ER01-red	reduced PV and biomass	med	med	ref	✓	✓	✓	✓	✓			✓	✓
ER02		med	min	ref	✓	✓	✓	✓	✓			✓	✓
ER03		med	max	ref	✓	✓	✓	✓	✓			✓	✓
ER04		max	min	def	✓	✓	✓	✓	✓			✓	✓
ER05		max	max	def	✓	✓	✓	✓	✓			✓	✓
ER06	ER01 with infeed curt.	med	med	ref	✓	✓	✓	✓	✓		✓	✓	✓

For the scenario TE07, as mentioned earlier, the reduced MV/LV-transformer (250 kVA instead of 630 kVA) is implemented. TE08 is the extension of TE07 with infeed curtailment. TE09 is the scenario where the line loading is reduced to 25 % of its normal thermal transfer capabilities and TE10 is the extension with infeed curtailment.
TE11 to TE13 are scenarios where the node power of each household node is reduced. At TE11 the node power is reduced to the maximum power demand. This means the power demand is never a problem and can be fulfilled any time. But, the PV-infeed is not always possible. Especially around noon the PV-power exceeds the maximum load power several times and therefore the node limits set at TE11 are exceeded. This case is equal to a flat rate, where the power demand up to the maximum load power is free and everything beyond is infinitely expensive. For scenario TE12 the threshold at each node is the average annual power demand. This is the annual consumed energy divided by 8 760 h. In this case, it would be possible to place storages with suitable size at each node. The storages could be charged if the current power demand is lower as the threshold (average value) and discharged, if the current power demand is beyond the threshold. At this scenario, a power supply without decentralised production still would be possible. At TE13 the threshold is set lower than the average annual power demand. The average annual power demand at the nodes is between 700 W to 5 000 W. A reduction value of 50 W is used at each node. This represents a average annual node power reduction of 1 % to 7 %. This reduction value does not significantly reduce the threshold value. But still limits the optimisation in such way, that decentralised production is necessary, since the annual energy import cannot fulfil the annual demand anymore. The cases TE14 to TE16 are extensions of TE11 to TE13 where infeed curtailment is allowed again.
The infeed curtailment scenarios for all cases are chosen to see, which path is best, either to use the same storage capacities as without curtailment, or reduced storage capacities and a reduction of decentralised infeed.
For the "Whole Region" (WR), the scenarios WR01 to WR06 are the same as for the TE-case, additionally the costs for electricity import/export (electricity costs at slack) and costs for gas import/export (gas costs at slack) are considered.
The scenario ER01 for the "Ecological Region" (ER)-case is equivalent to WR01. The used import costs for electricity and gas are the differences. They are 100 times higher as in the WR-case, to force the optimisation to use as much as possible of the decentralised renewable produced energy, and import as little as possible. Results show, that for the scenario ER01 the energy import is negligible. That is why a demand variation is not useful for this investigation cases. It is more interesting which export- or storage-path (electric, Power-to-Gas) is chosen depending on different storage/conversion-technology costs. That is why for ER02 and ER03 the storage/conversion-technology costs are set to minimal or maximal. ER05 and ER06 are extreme situations. The demand (el./th.) is a maximum and the technology costs are changed between minimum and maximum. At these two scenarios compared to other possible load scenarios most of the energy is used within the region. This maximises the need of energy storage/shifting. ER06 is the extension of ER01 with infeed curtailment, to see, if even in the case of high import costs power reduction of renewable sources is a more ideal option, compared to the case without infeed curtailment.

In the next chapter (chapter 6-"Results") the results for all scenarios are compared.

6 Results

In this chapter, firstly, the energetic and power characteristics for the different load scenarios, as well as the energy production are shown. Followed by the storage and conversion technology results for the 31 scenarios, the resulted up-scaling of interesting scenarios to the size of Austria concludes this chapter.
For all scenarios, some important optimisation results are listed in the appendix in tab. B.6 to B.8.
As already mentioned at the beginning of chapter 4, "centralised" and "decentralised" technologies should not be seen in context of the whole Austrian energy system. In context of this thesis "centralised" technologies are technologies only located at the slack node of the model region whereas "decentralised" technologies can be located at each node in the model region.

6.1 Energies and Powers

At this work, for the electric and thermal load three different cases are considered. Table 6.1 shows some characteristics for the different options. For the electric case, the power and energy increase between the three options is roughly 6 %. The Full Load Hours (FLH) are around 3 710 h. This is equivalent to an annual energy consumption with maximum power P_{max} within a five month period. Expressed differently, a constant average power demand P_{avg} of 43 kW to 48 kW for 8 760 h would lead to the same annual energy demand, and the factor between average power and maximum power is roughly 237 %.

For the thermal loads, the increase between the scenarios is more drastic and between 86 % to 125 %. Since the FLHs are in the same range as in the electric case, the ratio between P_{max} and P_{avg} is in the same percentage range from 240 % to 285 %. The

Table 6.1: Power and energy values for different load scenarios

	electric			thermal		
	min	med	max	min	ref	def
P_{max} [kW]	102	109	114	180	405	755
E_{annual} [MWh]	378	403	424	554	1 432	2 760
T_{FLH} [h]	3 710	3 710	3 710	3 530	3 530	3 530
P_{avg} [kW]	43	46	48	63	163	315

following table (tab. 6.2) lists the characteristics for renewable productions (PV, biomass and waste burning). Because all of the renewable production potentials are exhausted by 100 %, the result are very high production-powers and -energies. Compared to the electric load – independent of the scenario – the PV-power exceeds the maximum electric load by a factor of six and in terms of energy by a factor of more than two. The energetic, electric biomass potential is in the same energy range as the electric load. Therefore, from an energetic perspective biomass would be sufficient enough to supply the whole region with electricity. From an energetic and power perspective the thermal biomass production, including waste burning, is only sufficient for the minimal thermal load scenario.

Table 6.2: Power and energy values for renewable production

	electric		thermal	
	PV	Biomass	Biomass	Waste
P_{max} [kW]	618	80	174	29.6
E_{annual} [MWh]	929	441	968	259
T_{FLH} [h]	1 140	5 488	5 581	2×4 380 [1]
P_{avg} [kW]	106	50	111	29.6

In the next section, the results of the 31 scenarios are discussed. The high power- and energy-ratios between the demand and the renewable production are especially important for the optimisation result, and that is why there is a focus on this aspect.

[1] For the optimisation only the produced power/energy is important. The amount of therefore installed turbines has no influence on the optimisation results. Since waste arises the whole year, it is assumed, that two turbines – each of them dimensioned to use the average arising waste potential of 29.6 kW– are installed in the model region. They operate up to half the power as long as one is not in revision. This allows 8 760 h (whole year) of continuous waste burning.

6.2 Scenario Comparison

As mentioned in the previous chapter (chapter 5), TE01 is the basic scenario and all other scenarios, especially for the technical case, are derived from this scenario.
That is why many comparisons are between TE01 and other scenarios, and the optimisation results of TE01 are described in detail now.
The medium electric and refurbished thermal load parameters are listed in the previous section in tab. 6.1 and the electric and thermal production parameters are listed in tab. 6.2. The electric load- and production-profiles lead to over-voltages at certain nodes. The node-voltages for some representative 15 min values before the optimisation are shown in fig. 6.1 (each "cross" is one voltage values caused by one load/infeed situation - 15 min-step). If the slack voltage for the infeed case, according to the standard DIN EN50160 [116], is set to 107 %, due to infeed situations the relative voltage at some nodes reaches 115 %, while the maximum voltage drop due to load situations is always below 2 %. The corresponding node names are listed in fig. 6.2. Most of the rural-nodes (except AC_01 and the bus-bars BB_06 to BB_08) exceed the 110 % voltage band, and because of the huge PV-penetration even the right ring section of the urban area (node DH_05) exceeds this upper limit. The line loads and transformer loads are no problem

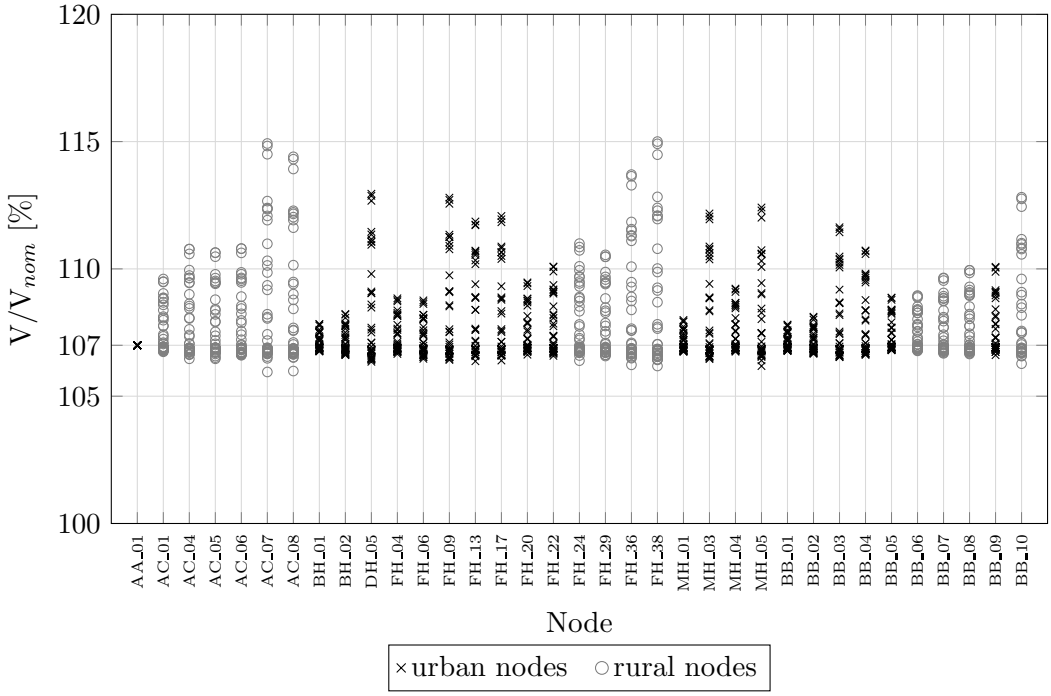

Figure 6.1: Voltage-Band for the representative summer week of the TE01-scenario before the optimisation

for this scenario. Because of the over-voltage the optimisation has to place storages to avoid these violations. The resulting storage placement and dimensioning is shown in

fig. 6.2. The blue rectangles represent electric storages and the red rectangle the placed thermal storage at the slack node (AA_01). Besides the mentioned power and energy values for each storage, the rectangle width indicates the installed power and the filled area the installed energy, compared to the maximum installed type (e.g. Lead-Acid P_{max}=59.2 kW and E_{max}=118.4 kWh).
From all of the possible electric storage options (Li-Ion, Lead-Acid, Redox-Flow) only Lead-Acid batteries are used. Since the voltage-band violations are local problems a centralised storage solution at the slack node, such as a Redox-Flow battery would not be sufficient in solving this problem. That is why this storage type is not used and because of the E/P-ratio of 2 h for Lead-Acid batteries – compared to 0.4 h for Li-Ion – Lead-Acid batteries are preferred. In total, 396 kW with 738 kWh are installed and a total energy of 258 MWh/a is stored and rolled-out. This means 350 cycles/a or a full charge-discharge cycle almost each day. These storages are only placed at nodes, where the high PV-infeed causes voltage problems. The thermal storage is only placed at the slack node, where the thermal biomass and waste burning infeed takes place. The thermal storage capacity is 106 MWh, which is 10 % of the annual thermal demand of the district heating area (urban and suburban). In total, 154 MWh are stored and rolled-out, and it is used as a long term storage, where the discharge process takes place in winter and interestingly in summer too. The thermal summer surplus energy is less than the surplus at the transition periods because of the missing biomass production. That is why the summer period is also used for discharging the thermal storage. Otherwise the installation of a bigger storage capacity would be necessary and this would lead to additional installation costs.
With these storage operations, 27 % of the electricity produced from renewables is used directly within the region. This leads to an degree of electric autonomy of 94.9 %. The thermal autonomy is 74.6 % and the total energetic autonomy (electric and thermal combined) is 79 %.

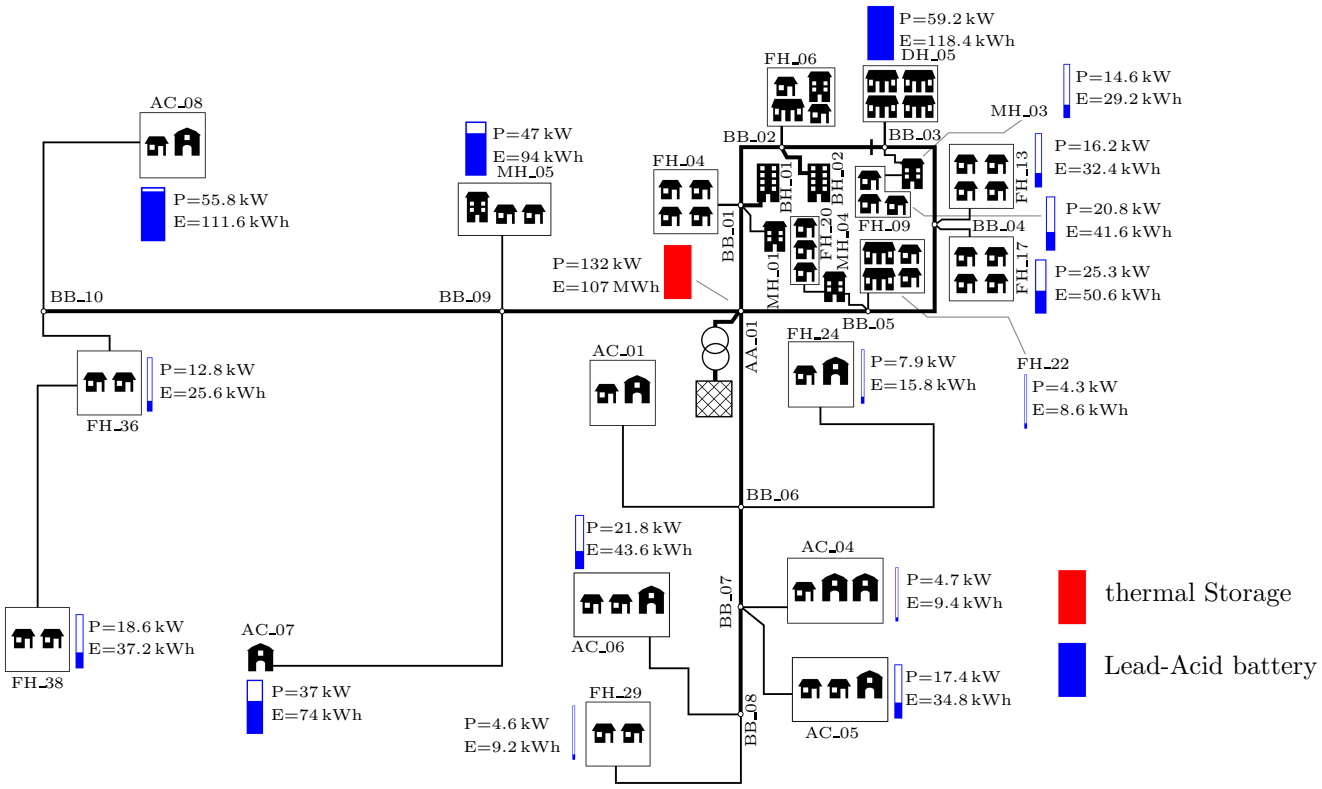

Figure 6.2: Storage distribution for the technical scenario TE01. Only Lead-Acid batteries and a thermal storage are used.

Furthermore, due to the electric storage operation no voltage violation is caused anymore, as shown in fig. 6.3, which represents the voltage values for the different nodes after the optimisation. The maximum related voltage is always beneath 110 %, the minimum voltage is also increased. Because the load cases are used to discharge the storages and the maximum resulting load (load power plus storage power) is decreased, compared to the "before the optimisation"-case. This can be seen, if the voltage values of node AC_07 and AC_08 between the range from 105 % to 107 % in fig. 6.1 and fig. 6.3 are compared.

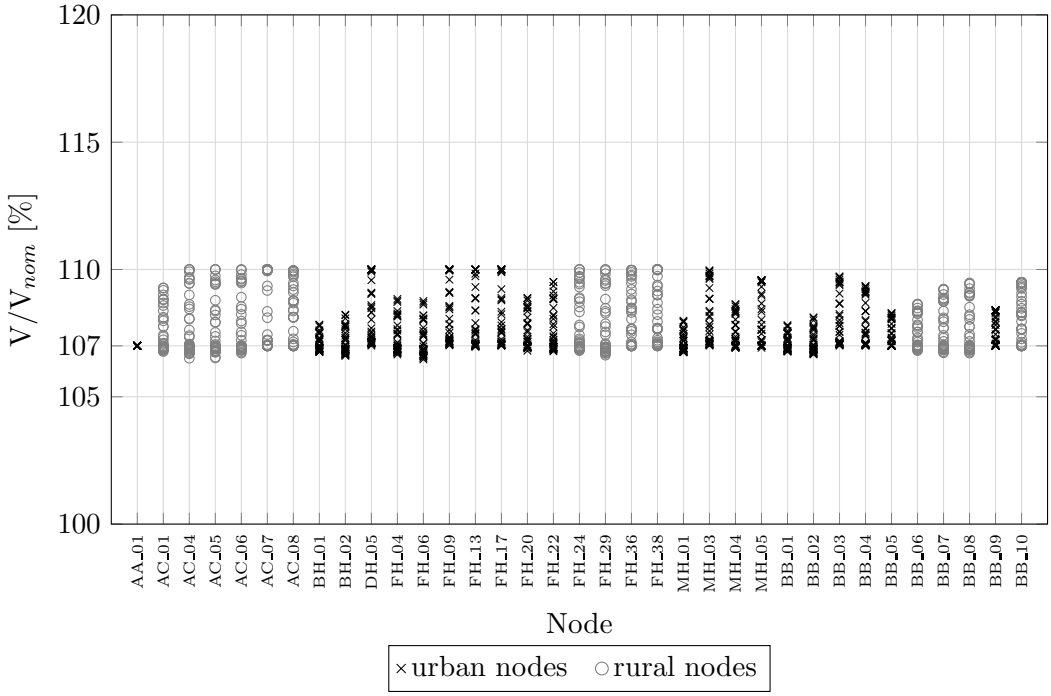

Figure 6.3: Voltage-Band for the representative summer week of the TE01-scenario after the optimisation

Since the characteristics of the basic scenario TE01 are described it is possible to compare this scenario with other scenarios and derive the differences.

6.2.1 Comparison-Thermal Variation

This leads to the first comparison of TE01, TE02 and TE03, where only the thermal demand is changed between refurbished, minimal and default. This has no impact on the electrical results whatsoever, as the electric storages installed by the optimisation turn out to be the same.
But the behaviour of the thermal system changes dramatically. For the scenario TE02 where the thermal demand is a minimum, the installed thermal storage power is 714 kW and the capacity is 88.4 kWh. Compared to TE01 this is a power increase of more than five times and a capacity reduction of 1 200. This drastic change is caused by a totally different storage requirement and operation: the storage is no longer used as seasonal storage, since the thermal energy production at each season exceeds the thermal demand and therefore the storage is used for daily balancing. In the TE03-scenario, the thermal storage has 67.9 kW and 28.5 MWh. This results from the fact that the storage is only charged during summer and it does not make sense to install larger storage, since the summer surplus energy in the district heating region is only 28.5 MWh. Over the other three seasons the storage is discharged.

The storages behaviour for the three scenarios and different seasons is shown in fig. 6.4. For comparison reasons the energies are normalised for each scenario to the maximum stored energy. It has to be considered, that the energetic difference between the beginning and end of the seasons, times the corresponding VDEW weeks number of this season, results in the start value of the next season. This is illustrated in fig. 4.13. Since only the four representative weeks (Transition I is equal Transition II) and not the extrapolation to the whole season is shown, there are gaps between the seasons, for example at the end of "Winter" and the beginning of "Transition I".

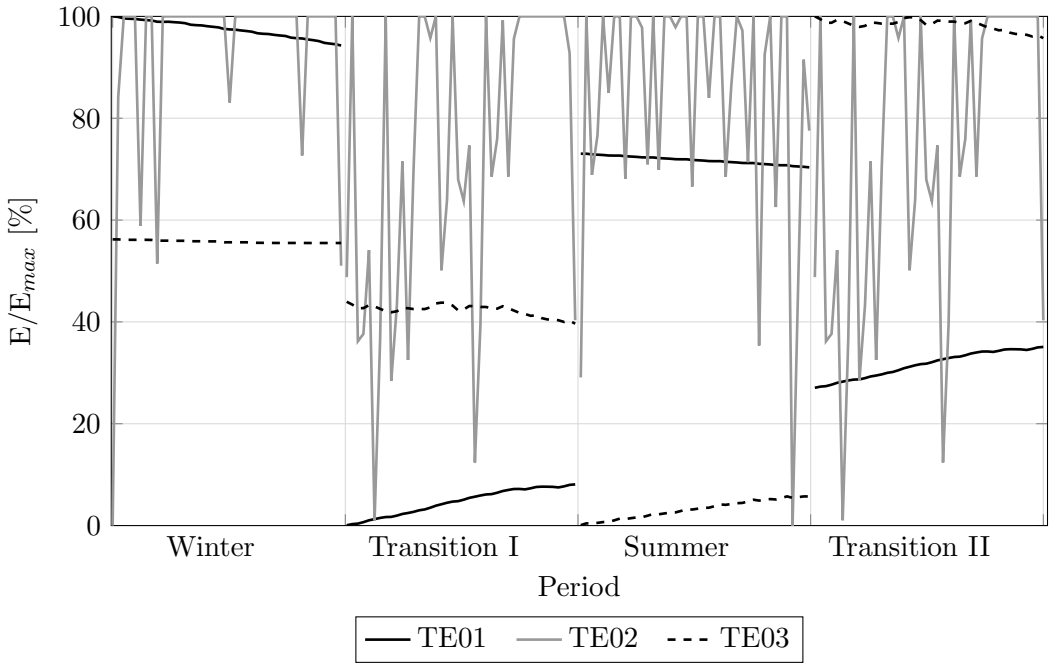

Figure 6.4: Charge/Discharge-characteristics of thermal storages for different seasons for the three scenarios TE01, TE02 and TE03

The TE01, TE02, TE03 comparison shows a big influence off the thermal load/production ratio on the thermal storage operation. If there is a seasonal gap of surplus energy (overproduction in one and demand in another season) the storage is proportioned and operated to shift as much energy between seasons and is fully charged and discharged only few times a year. If each season can energetically balance itself (TE02), the thermal storage is used for daily balancing and is therefore – from a capacity perspective [MWh] – proportioned much smaller.

6.2.2 Comparison-Extreme Cases

The optimisation results for the extreme scenarios TE05 (everything minimal) and TE06 (maximal), are almost identical to TE01 from an electric storage-placement and -operation point of view. The variation of the installed Lead-Acid battery capacities, between the extreme scenarios and TE01, is only a few percentage points. The thermal characteristics of TE05 and TE06, are identical to TE02 or TE03. That means, low demands and low storage/conversion technology prices or high demands and high storage/conversion technology prices, have no influence on storage placement and only little influence on the sizing. The sizing influence is caused by the demand variation. If the demand is increased the maximum surplus power and energy is reduced, which causes the need of smaller storage dimensioning, or vice versa.

6.2.3 Comparison-Central/Decentral Limitation

The voltage-band violation constitutes local limitations, additionally line current reductions to 25 % compared to its default values causes further local problems too. This limitation is represented with scenario TE09. Figure 6.5 shows the result of the relative line loadings before the optimisation and for scenario TE09. The line names follow the convention: "start node"-"end node", e.g. AA_01-BB_01. Positive values are due to load situations and negative due to PV-infeed. Without the reduced limitation, neither the load- or infeed-powers are problems. They are always within the ±100 %-range. With the reduced thermal line power, some of the infeed situations exceed the -25 % before the optimisation. Afterwards, the storages are placed and operated in a way to avoid these violations. For TE09, only decentralised storages in the form of Lead-Acid batteries are used. The total installed power and capacity compared to TE01 is increased by 55 % and more energy is stored and rolled-out: 486 MWh compared to 258 MWh in TE01. This increases the average storage usage from almost one to 1.2 full charge/discharge-cycles a day and the degree of electric autonomy is increased from 94.9 % to 98.4 %. The Lead-Acid batteries are placed at the same nodes as in TE01, since the problem of the thermal line overload is caused by the same reason as the voltage-band violation: the high PV-infeed.

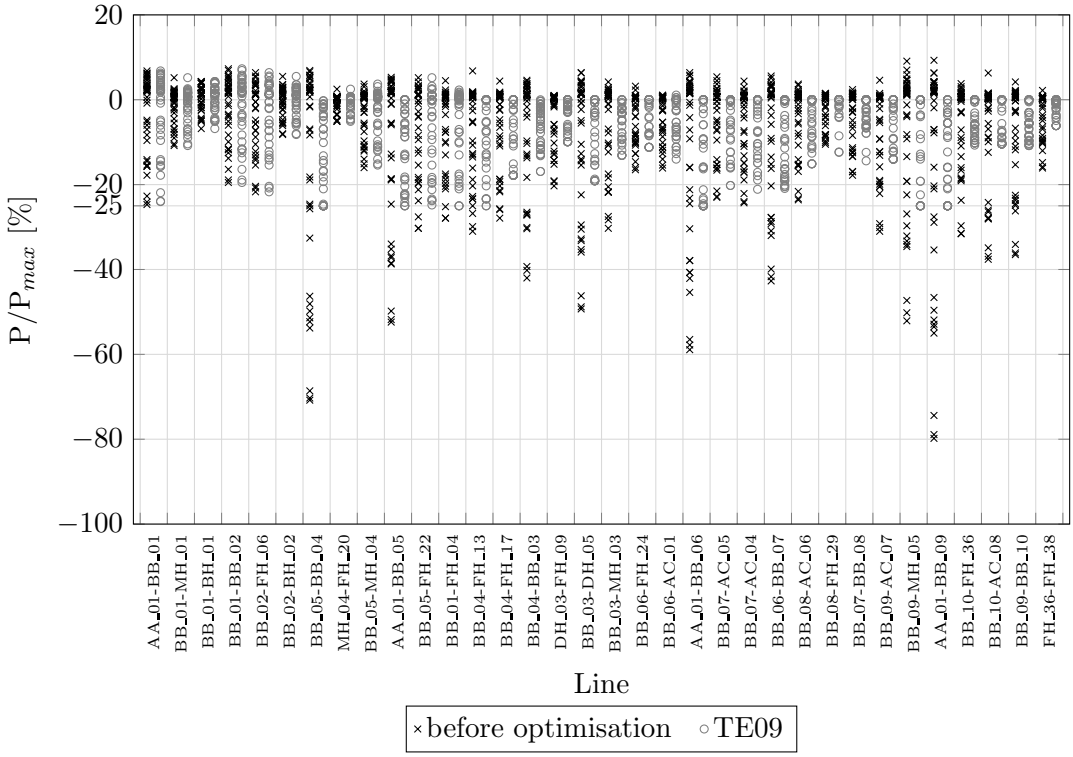

Figure 6.5: Relative line loadings before the optimisation and for scenario TE09. Positive values are due to loads and negative due to PV-infeed

As a counterpart it is interesting to see how the optimisation solves a problem located at the slack node (central problem). Therefore the MV/LV-transformer power is decreased from originally 630 kVA to 250 kVA as is modelled with scenario TE07.
Both limitations (TE07 and TE09) have no direct effect on the thermal system and therefore the optimisation result of the thermal storage placement, sizing and operation is the same as in TE01.
For scenario TE07 compared to TE01, decentralised electric storage (Lead-Acid) is increased to 412 kW and 824 kWh. This is an increase of 12 %.
Obviously since the problem is now centralised, a central solution would make sense. With the storage placement assumptions within this thesis, this can be realised by either a Redox-flow battery or the Power-to-Gas path. Under the model assumptions the optimisation did not use Redox-flow batteries, only the Power-to-Gas path is used. The reason is, for Power-to-Gas in this case for Power-to-H_2, only power depending installation cost occur, since the gas grid is used as storage system. For a Redox-flow battery both costs for power and energy would arise. That is why the Power-to-H_2 path is cheaper for this scenario. In TE01 942 MWh electricity is exported. This is reduced to 551 MWh, the other surplus energy is exported via Power-to-Gas with an amount of 400 MWh in the form of H_2.

This leaves the following conclusion: if the problem occurs at one certain point and the energy to power ratio is high (energy which has to be exported compared to the therefore necessary installation power of the system), it is useful to use a system where no energy depending installation costs arise, in the case of this thesis this is a shift to a different energy form (gas).

6.2.4 Comparison-Flat rate

All three flat-rate scenarios (power limit at each node; TE11: $P_{max} = P_{max,load}$, TE12: $P_{max} = E_{annual}/8\,760\,\text{h}$ and TE13: $P_{max} = E_{annual}/8\,760\,\text{h} - 50\,\text{W}$) have no direct influence in the thermal system and therefore the optimisation results for the thermal system are the same as in TE01.
In the electric system the changes are rather drastic. Almost all of the electric demand is supplied from sources within the region. In TE11 the electric autonomy is 98.9 %, for TE12 and TE13 the autonomy is 100 %. This results in an electric autarchy. The dimensions of decentralised storages are increased by 200 % (743 kW) for TE11 or 328 % (1 200 kW) for TE12 and TE13. The maximum PV production is only 618 kW, this means the installed storage power is higher than the maximum PV-production, which would not make sense, since not more than the maximum power in the system can be stored simultaneously. This indicates the storage capacity as a driving force and due to the fixed E/P-ratio with higher capacity requirements the installed power has to be increased as well. Figure 6.6 shows the Lead-Acid battery operation for the three scenarios TE01, TE11 and TE13 (there is no recognisable difference between TE12 and TE13, which is why it is skipped in the figure). For comparison reasons the stored energy is normalised with the maximum stored energy. Although the problem between TE01 and TE11 or TE01 and TE13 is completely different, which causes the use of storages, the storage operation is very similar. Even if the differences are small, TE13 has the most moderate storage cycles. For TE13, compared to TE11, the energy range is smaller, this is because of the additional -50 W limitation, which limits the storage even more with its charge or discharge power. The flat rate limitation requires larger decentralised storage dimensions, it does not influence the placement, which is the same as in TE01.

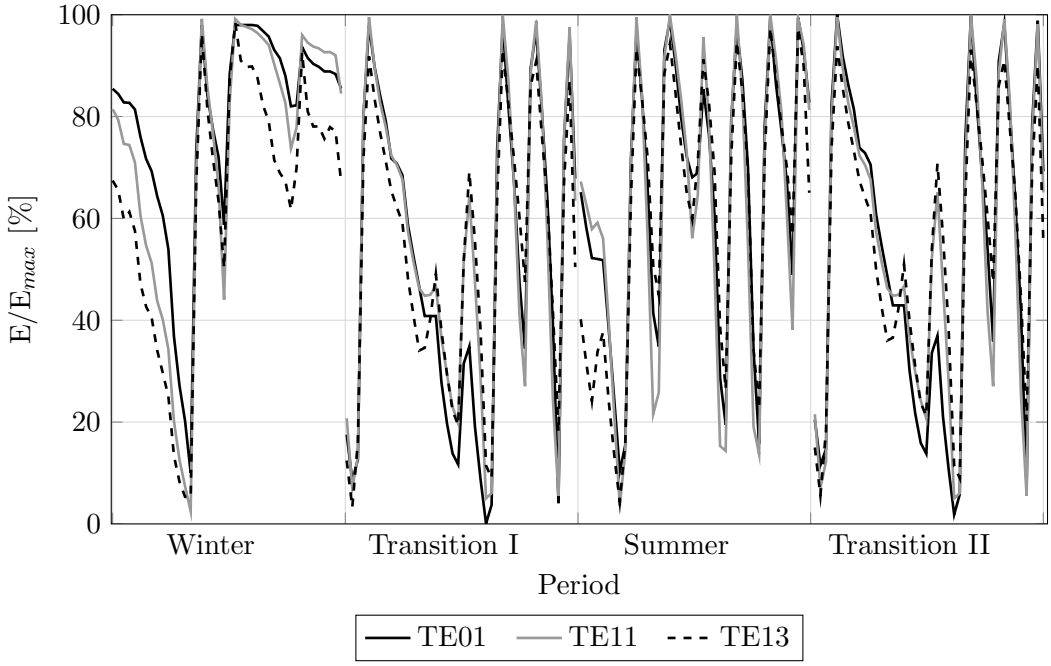

Figure 6.6: Charge/Discharge-characteristics of Lead-Acid batteries for different seasons for the three scenarios TE01, TE11 and TE13

The not allowed infeed limitation is why such huge storage capacities have to be installed, the effect of infeed curtailment is discussed in the next section.

6.2.5 Comparison-Infeed curtailment

In all previously discussed scenarios, infeed curtailment was not allowed. This has the consequence, that all the surplus energy which can not be exported due to different technical limitations (lines, transformer or flat rate) has to be wasted in storages. This is done by charging and discharging at the same time. Since the conversion efficiencies are <100 %, energy is wasted. That is why infeed curtailment is used as option to overcome the odd storage energy elimination.
For the infeed curtailment scenarios all parameters are kept unchanged except for the allowed curtailment.

This leads to the following counterpart scenarios (left without curtailment, right with curtailment):

- TE01 – TE04
- TE07 – TE08
- TE09 – TE10
- TE11 – TE14
- TE12 – TE15
- TE13 – TE16

It is interesting to see how much energy/power is limited and what influence this limitation has to the installed storages. The results are shown in tab. 6.3. The infeed curtailment with a range of 13.7 % to 52.4 % is rather high. It has to be considered, that the unlimited PV-production is 2.3 times the energy demanded and even after the PV-reduction of 52.4 %, the produced energy is still 110 % of the demand. The consequence of the infeed curtailment is a drastic reduction of installed decentralised storages between 61.7 % to 86.6 %. Since the flat rate scenarios (TE11 to TE16) are the ones with the strictest node power limitation, these scenarios benefit most from the infeed curtailment. The PV-duration curves for the basic scenario (TE01-no curtailment), TE04, TE08, TE16 and the load duration curve are shown in fig. 6.7.

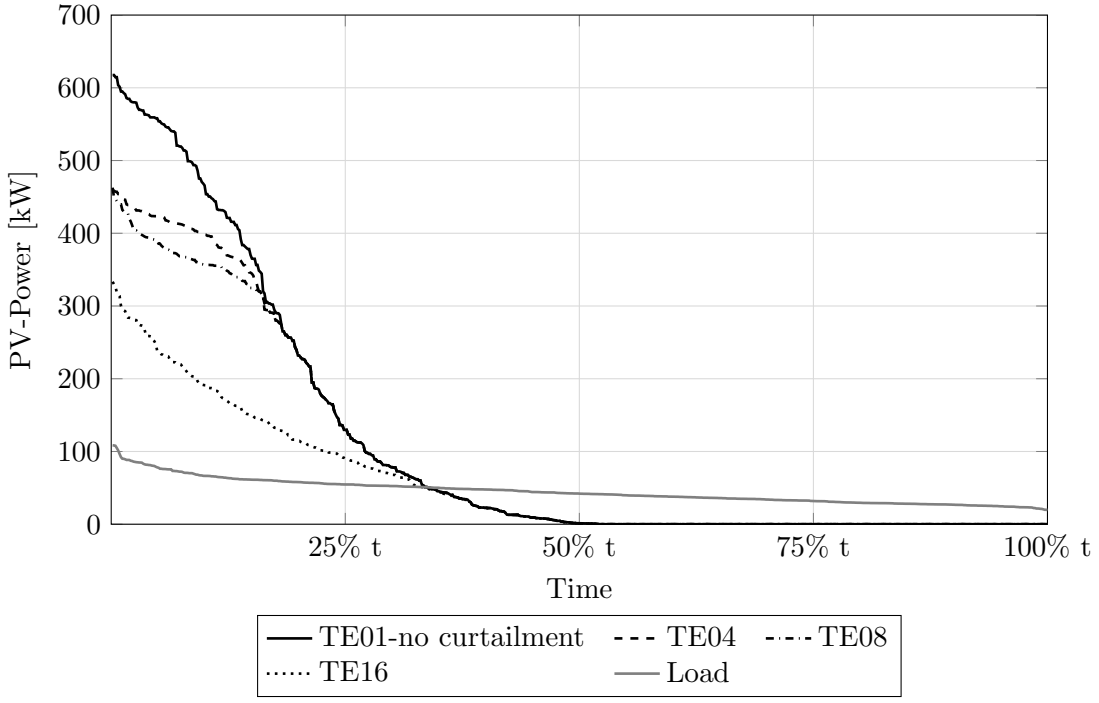

Figure 6.7: Annual load- and PV-duration curve for different PV-curtailment scenarios

As mentioned already even for the most drastic limitation scenario TE16 the annual energy production exceeds the annual demand and the peak power still exceeds the maximum demand by a factor of three. For scenario TE14 where the node threshold is set to the maximum node power, the maximum summed node power is 203 kW, the maximum PV-power with infeed curtailment exceeds this limit by a factor of almost 2.5. For TE16 the maximum summed node power for the whole region is 44.8 kW and the PV-power exceeds this limit by a factor of more than six (fig. 6.7). As a result, all of the power that exceeds the threshold limit has to be stored and rolled-out in demand situations. For TE11 this is roughly 20 % of the time and for TE16 this is the case for 30 % to 35 % of the time.
Except for scenario TE08 the autonomy is reduced due to the infeed curtailment, which obviously makes sense, since the imported or exported energy does not cost anything. Therefore, there is no need to supply the region as much as possible with its own resources; these targets are pursued at the ecological case. The reason why between TE07 and TE08 the autonomy is increased, is the export path. In TE07 double the energy is exported via Power-to-Gas and even with the curtailment in TE08, in TE07 more electricity has to be imported again.

The optimisation results for the curtailment scenarios shows the following:

- At scenarios with allowed infeed curtailment, the total decentralised (local) placed storages are reduced by a factor between 2.6 to 8.0. Compared to the counterparts without curtailment.
- At some scenarios with curtailment (TE04, TE08 and TE10), at some nodes no storages are placed from the optimisation. Compared to the counterpart scenarios without curtailment. These nodes are especially AC_04, AC_05, AC_06, FH_24 and FH_29. At the scenarios without curtailment the necessary storages at these nodes are already rather small. With curtailment (TE04, TE08 and TE10) it is possible to avoid technical violations even without storage placement at these nodes.
- The operation of local placed storages for all curtailment scenarios is similar to the basic scenario TE01.

The consequence of these results is: the large decentralised (local) storage dimensioning at technical scenarios without curtailment is mostly necessary for wasting energy to avoid violations of technical limitations. The storage dimensioning is only partly necessary due to energy shifting.

Table 6.3: Amount and consequences of infeed curtailment for different scenarios

	TE01	TE04	TE07	TE08	TE09	TE10	TE11	TE14	TE12	TE15	TE13	TE16
PV-production without curtailment	929.27 MWh											
PV-curtailment	-	128 MWh	-	158 MWh	-	206 MWh	-	280 MWh	-	479 MWh	-	487 MWh
Relative curtailment	-	13.7 %	-	17.0 %	-	22.2 %	-	30.1 %	-	51.5 %	-	52.4 %
dec. Storage reduction	-	86.6 %	-	87.6 %	-	76.2 %	-	73.4 %	-	62.3 %	-	61.7 %
el. Autonomy	94.9 %	88.7 %	83.2 %	92.9 %	98.4 %	92.3 %	98.9 %	94.5 %	100 %	99.6 %	100 %	99.7 %
resulting E_{PV}/E_{Demand}	231 %	199 %	231 %	191 %	231 %	180 %	231 %	161 %	231 %	112 %	231 %	110 %

6.2.6 Comparison-Technical/Whole Region

In the scenarios WR01–WR06, the slack connections are the interesting interfaces. The scenarios are identical to TE01–TE06 and consider all the technical limitations. Additionally costs and revenues at the slack node are taken into account. The considered costs/revenues are for energy import and export, which were neglected in the technical cases. The "Whole Region" (WR) case loosely represents a public service that holds all infrastructures.
From a thermal perspective there is no difference between the six technical and whole region scenarios. At the WR scenarios, compared to the TE counterpart scenarios (e.g. WR01 and TE01), the same amount of district heating and the same thermal storage power and capacity is used/installed from the optimisation.
Also WR01–WR06 do not use Redox-Flow batteries and except WR04 the installed decentralised storages have the same dimension as the counterparts in technical scenarios. Different storage usage is the reason why TE04 and WR04 have different installed decentralised storage dimensions. In WR04 the storage is charged during the day, and then on the one hand discharged at night to fulfil the load needs and then on the other hand it is discharged before the sunrise to enable an earlier H_2-production. Both circumstances can be seen in fig. 6.8. Positive values represent production or storage discharge, negative values are demands.

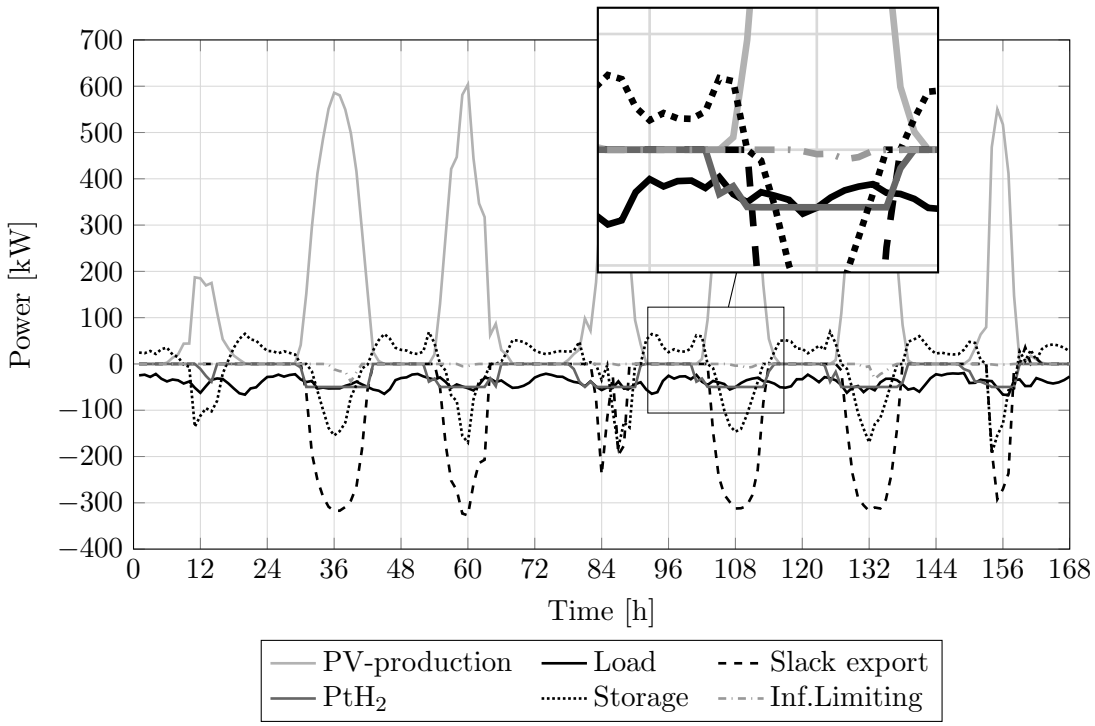

Figure 6.8: Optimisation result for the representative summer week for the whole region of the WR04-scenario.

The difference between the technical- and WR-case is, how parts of the surplus energy are exported. In the technical cases, direct electricity export is the path of choice, since no import/export costs are considered and the installation of Power-to-Gas systems does cause costs. For the whole region, part of the electric surplus energy is exported via Power-to-Gas in the form of H_2 and CH_4. Because – as mentioned in section 4.3.7 – at this work it is assumed, that one kilowatt-hour of electricity is refunded with 6 cents, one kilowatt-hour of H_2 with 15 cents and one kilowatt-hour of CH_4 with 23 cents. Because of the high amount of surplus energy it is worth to install Power-to-Gas systems, depending on the scenario with an electrolyser power range of 41 kW to 78 kW and a methanation power range of 23 kW to 28 kW. The export of H_2 is between 6 MWh to 91 MWh and CH_4 has an export range of 128 MWh to 164 MWh.
The consideration of energy import/export costs has almost no influence on the storage placement, dimensioning and operation. But it does influence the path, how the surplus energy is exported from the region. The gap between the export revenues for electricity or gas, the necessary installation power for the system and the system price determine the best path of export. For the chosen values, Power-to-Gas is more lucrative than the direct electricity export.

6.2.7 Comparison-Technical/Ecological Region

From a financial perspective the "Ecological Region" (ER) case is extreme because of the change of the import costs. They are assumed 100 times higher than in the WR cases. From an electrical point the WR cases are already 100 % autonomous. That is why for many ER-cases there are not many optimisation result changes to WR01. In fact this is the case for ER01, ER02 and ER03. Almost the same amount of decentralised storages is installed, and no central storage is implemented. The slack import is zero for all cases and the export is between 510 MWh and 585 MWh. In the WR cases gas import is used to cover the thermal demand at nodes which are not connected to the district heating grid. Since importing gas is expensive in ER cases, instead of gas heating, heat-pumps are installed and all ER-scenarios have a 100 % electric and almost 100 % thermal autonomy. From the total thermal demand of 1 431 MWh or 2 760 MWh (depending on the scenario) only 0.03 % of the demand is covered with gas imports (374 kWh to 610 kWh). To give a comparison, an old (constructed before 1919) and unrenovated building needs this amount of annual heating energy to heat several square-metres. This gas import amount for one year and the whole region is negligible.
Figure 6.9 shows the storage and heat pump placement for the ER01 scenario. Heat pumps are only located at nodes, which are not supplied via the district heating system. The power and energy values next to the heat pump rectangles are the thermal parameters. The electricity parameters can be derived by considering the Coefficient of Performance (COP) of 3.75.
The two extreme scenarios ER04 and ER05 use different export approaches. The direct electricity export is only one third compared to ER01. They do use the Power-to-Gas path but do not produce CH_4. Instead they store H_2 and use fuel cells for the conver-

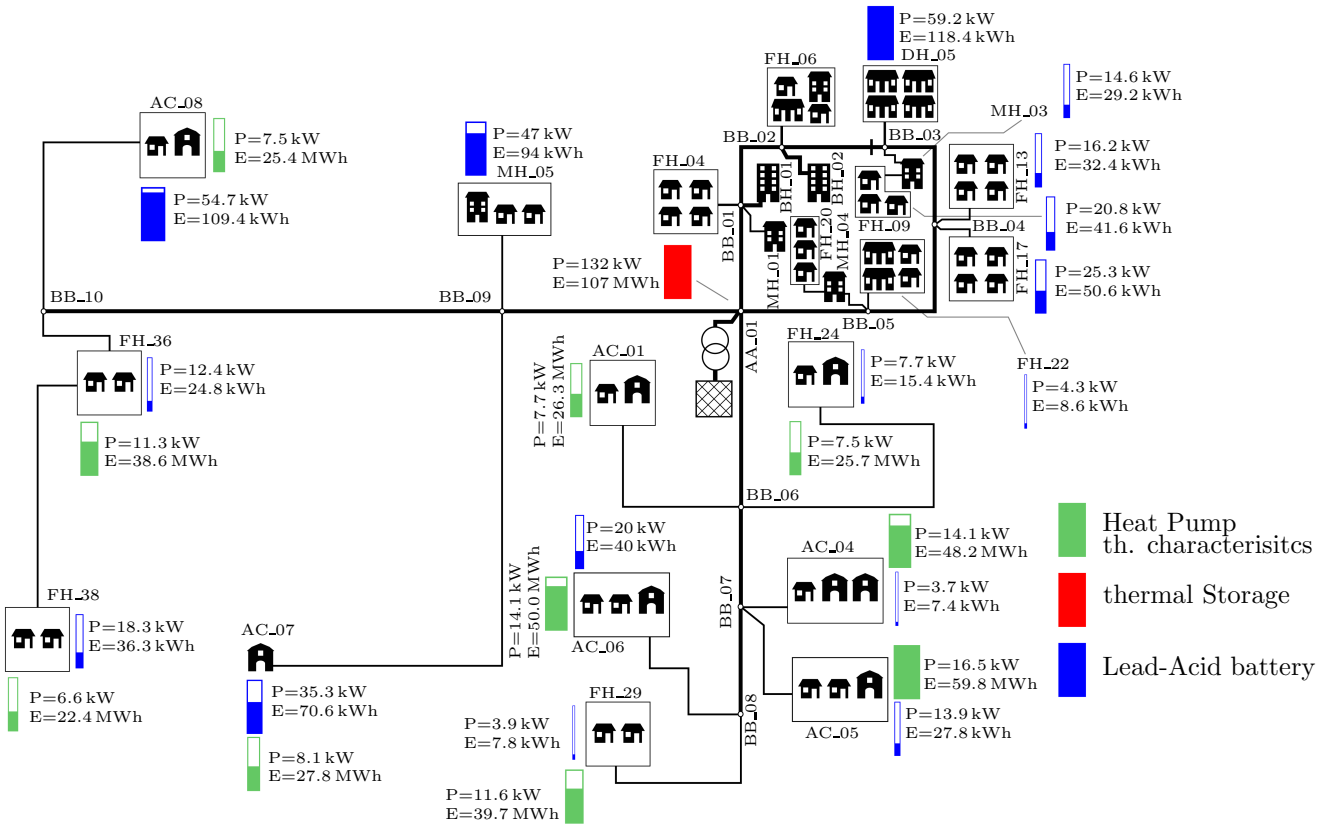

Figure 6.9: Storage and heat pump distribution for the ecological scenario ER01.

sion back to electricity. But the installed fuel cell powers of 1.1 kW or 8.4 kW are small. The installed H_2 storage is fully charged and discharged only once (ER04) or 1.3 times (ER05). The reason why the additional conversion path from H_2 to CH_4 is not used, is because of the high thermal demand. There is not much electric surplus energy that can be exported, since most of the electricity, which originally is not used by the electric system, is covered by heat pumps. Compared to ER01, 4.7 times the heat pump power is installed and the produced heat pump energy increase is in the same range. The total produced energy (electricity and thermal) in the model region is 2 598 MWh, while in ER01 the total demand (electricity and thermal) is 1 834 MWh and 3 184 MWh in ER04 or ER05. At a first glance it looks like, in ER04 or ER05, energy has to be imported to cover the demand. But since the optimisation uses heat pumps for the thermals demand, with the electric surplus energy a heat demand up to 8 152 MWh could be fulfilled

without the need of any energy import. That is why, there is still some electricity left for export.
In the scenario ER06 infeed curtailment is allowed so the optimisation makes use of this option, since the region is easily capable to fulfil the total demand (electric and thermal) and still can export some energy. The reductions are minimal: the electric energy curtailment is 0.4 % and the energetic thermal curtailment is 6 %.

So far all scenarios are compared and important results are highlighted. In the next section, some of the results are up-scaled to the size of Austria.

6.3 Up-Scaling

In this section, some of the scenarios are up-scaled from the model region to the scale of Austria and the impact in the energy system is shown. It has to be considered, that only loads and production which are modelled in the region are up-scaled. This up-scaling does not take the industry impact or centralised power plants (e.g. pumped storage) into account. Not all scenarios are up-scaled since many have similar slack characteristics (imports, exports). That is why the following basic scenarios TE01, WR01 and ER01 are used for the up-scaling. Additionally, the infeed curtailment counterparts ER04 and WR04 are also up-scaled. ER06 which is ER01 with infeed curtailment is skipped, since the curtailment is negligible. In all of the above mentioned scenarios, much more energy is produced than consumed. That is why for each basic case (TE01, WR01 and ER01) the reduced sub-scenarios (TE01-red, WR01-red and ER01-red) are used for up-scaling too. For these sub-scenarios, the electricity production (PV and biomass) is downscaled to 29.4 %, to derive an equal annual energy demand and production.
As mentioned in chapter 3. For the design of the model region, the population ratio of 28 359 between the model region population (300) and Austria's population (8 507 786 [84]) is used to determine the decentralised production characteristics of the model region. That is why the results are up-scaled using this ratio.
Figure 6.10 compares the up-scaled storage powers and the Austrian pumped storage power (4.8 GW). The pumped storage power is just for comparison reasons. Even if the power is sufficient enough for some cases, the centralised pumped storage power plants are no alternative to the storages which need to be implemented in the model region. Due to the decentralised voltage-band problem, this is what the storages are used for to overcome this problem. For the reduced cases, TE01-red and WR01-red, almost no storages are needed, the optimisation only places a small storage at node (AC_08). This is because no voltage-band violation occurs at other nodes. Scenario ER01-red does still use storages to limit the import, because of the high import costs. The total installed up-scaled storage power, even if it is double the current installed pumped storage power, is within a range of which is technically feasible.

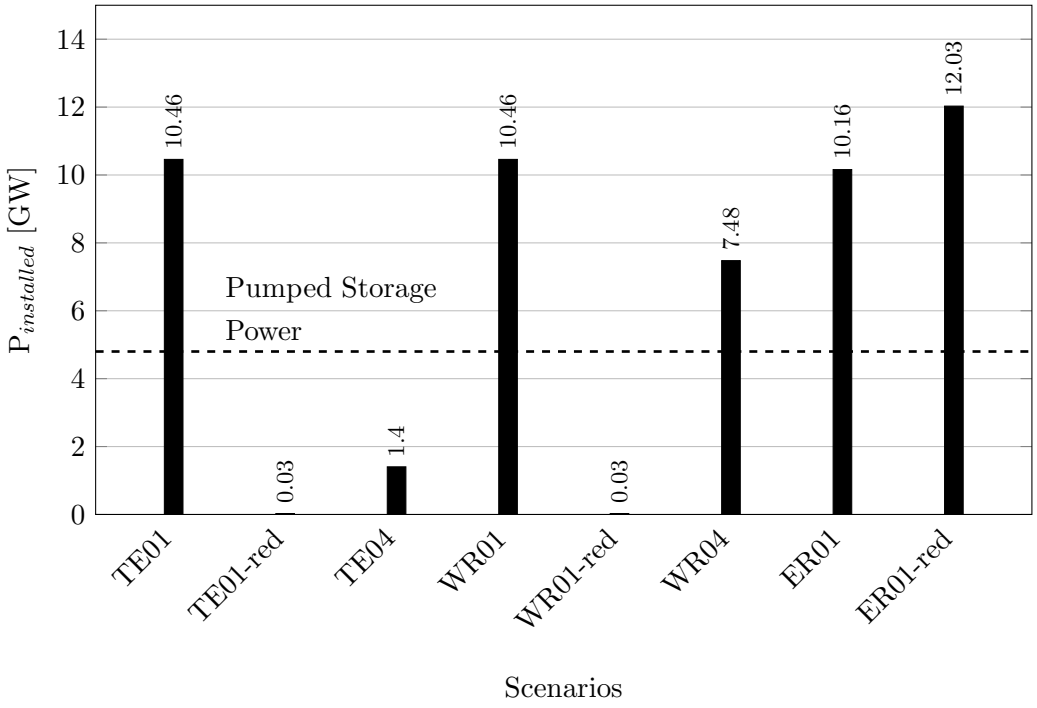

Figure 6.10: Installed decentralised storage (Lead-Acid) power and the Austrian pumped storage power; Pumped storage power from [77, p. 76]

Decentralised storages in this work are characterised with a fixed E/P-ratio, which is why a reduced installed power leads to the same installed energy reduction. The energetic characteristics are shown in fig. 6.11. The reversible Austrian installed pumped storage energy (140 000 MWh) is shown for comparison reason again. Again, even if the reversible pumped storage energy is almost seven times the maximum storage demand, for the purposes of the decentralised storages it would not help to use the capacity of the pumped storages.
If it is considered, that the price for one kilowatt-hour of decentralised storage is several hundred Euros. The model region realisation on an Austrian scale, in terms of the needed storage capacity of 20 919 MWh for some scenarios would cost several billion of Euros.
To reduce the storage demand, infeed curtailment is the solution of choice. The question now is how this influences energy imports and exports. This is answered in fig. 6.12. For the technical case, infeed curtailment doubles the electricity imports (TE01 versus TE04) but does not significantly reduce the exports. Compared to the annual Austrian electricity demand of 62 000 GWh in the year 2013, 27 % of this demand is accounted by households, which is 16 700 GWh/a [127]. The up-scaled model region demand, depending on the scenario, is between 11 000 GWh/a to 12 000 GWh/a. If only the import is taken into account. Which, in the case of the model region having to be supplied from power plants outside of the region, the external energy demand is only

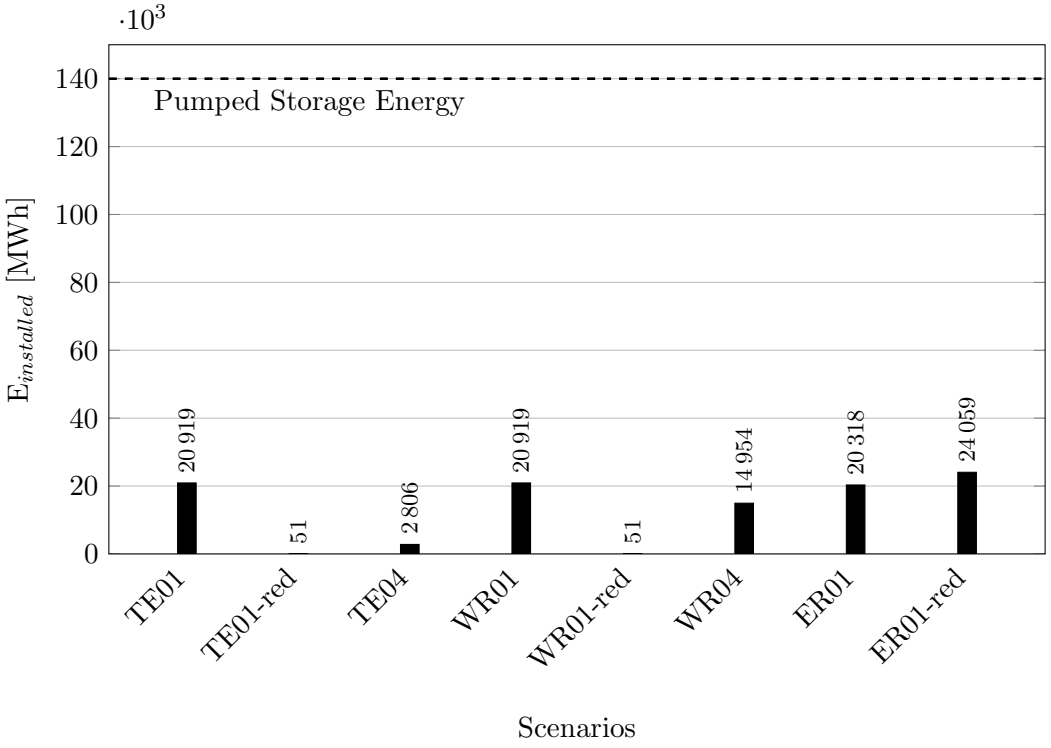

Figure 6.11: Installed decentralised storage (Lead-Acid) energy and the reversible Austrian pumped storage energy; Pumped storage energy from [77, p. 76]

594 GWh/a to 7 193 GWh/a. This illustrates, that even the reduced scenarios have a very small energetic system requirement. The ER01-red requires most electricity, this is because of the thermal demand coverage with heat pumps, and therefore it imports almost no gas. In Austria, in the year 2014, 15 940 GWh of electricity was produced via caloric power plants [128, p. 20]. If the electricity exports in fig. 6.12 are considered, in some of the scenarios this production could be replaced with the exports. But it has to be considered, that this statement is only valid for an energetic view. For reasons like network stability, load flow distribution or heat extraction this substitution might not be possible.

For the CO_2-emission calculation, it is necessary to determine the relevant emissions for electricity and gas. For gas this is rather simple. The energy density of CH_4 and the molar mass ratio between CH_4 and O_2 can be used to calculate the emissions per kilowatt-hour, which are 180 gCO_2/kWh [37, p. 232]. For exported H_2 the same value of 180 gCO_2/kWh is used, because one kilowatt-hour of H_2 in the gas network substitutes the use of one kilowatt-hour of CH_4.

For electricity the used CO_2-factor depends on the used energy mix. The Austrian mix emits 103.33 gCO_2/kWh and the ENTSO-e mix emits 363.28 gCO_2/kWh [129, pp. 13, 33]. The question is where to draw the system boundaries. If one additional kilowatt-

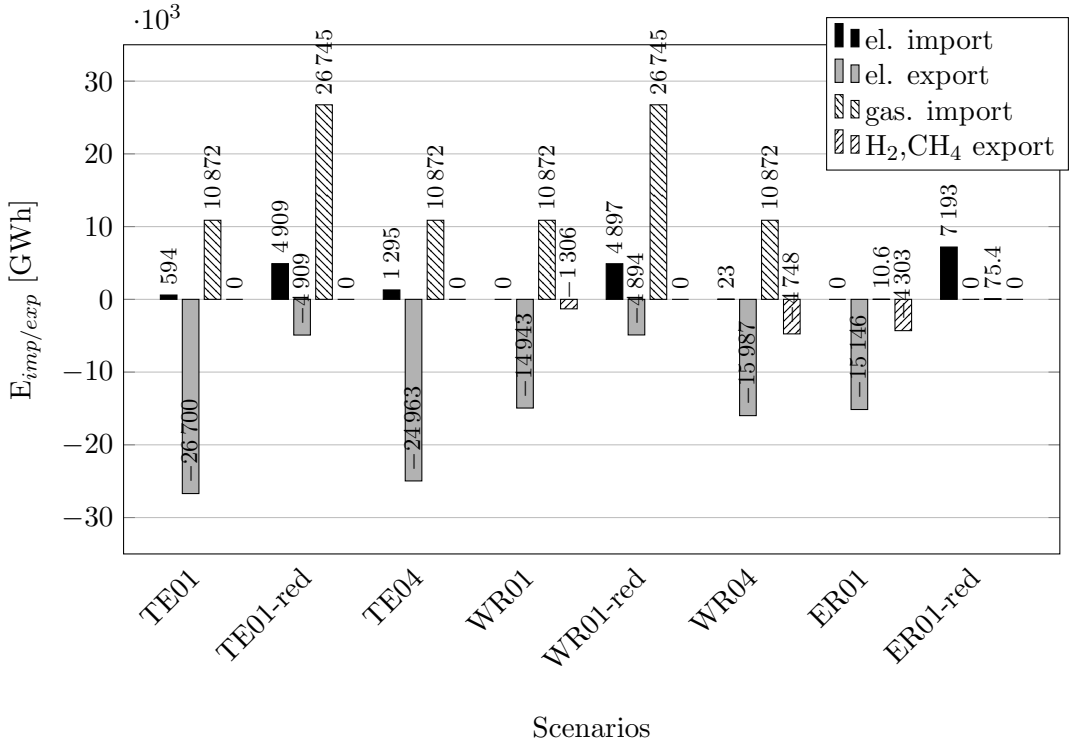

Figure 6.12: Electricity and gas import/export for the scenarios up-scaled to the size of Austria

hour of electricity is imported, is it possible to produce this additional unit with the Austrian power plant mix, or is this production resource exhausted and the energy is produced at an ENTSO-e scale and is imported to Austria? The same question has to be answered with the substitution of exported electricity.
Since the up-scaling shall deliver results for Austria, the Austrian mix is used. The results are shown in fig. 6.13. Since there is a linear correlation between energy import/export and emitted CO_2, fig. 6.13 is similar to fig. 6.12. The basic scenarios TE01, WR01 and ER01 have a positive CO_2 balance, they save more CO_2 due to the energy export than they emit due to imports. According [130], 2010 households in Austria caused $16\,727 \times 10^3$ t of CO_2-emissions. Even in the reduced scenarios, where almost no energy export takes place – the emissions due to electricity- and gas-import are five to twenty times smaller than the 2010 Austrian household emissions. This is due to still rather high renewable energy production and usage within the region.

Summarised it can be said, that even if it would be possible to use the Austrian pumped storage potentials, instead of the needed decentralised storages – which is not due to the local voltage-band problem – the Austrian pumped storage power does not fulfil the requirements of most scenarios. In terms of energy, the pumped storage power plants would be sufficient enough. The up-scaled electricity import, even for the reduced

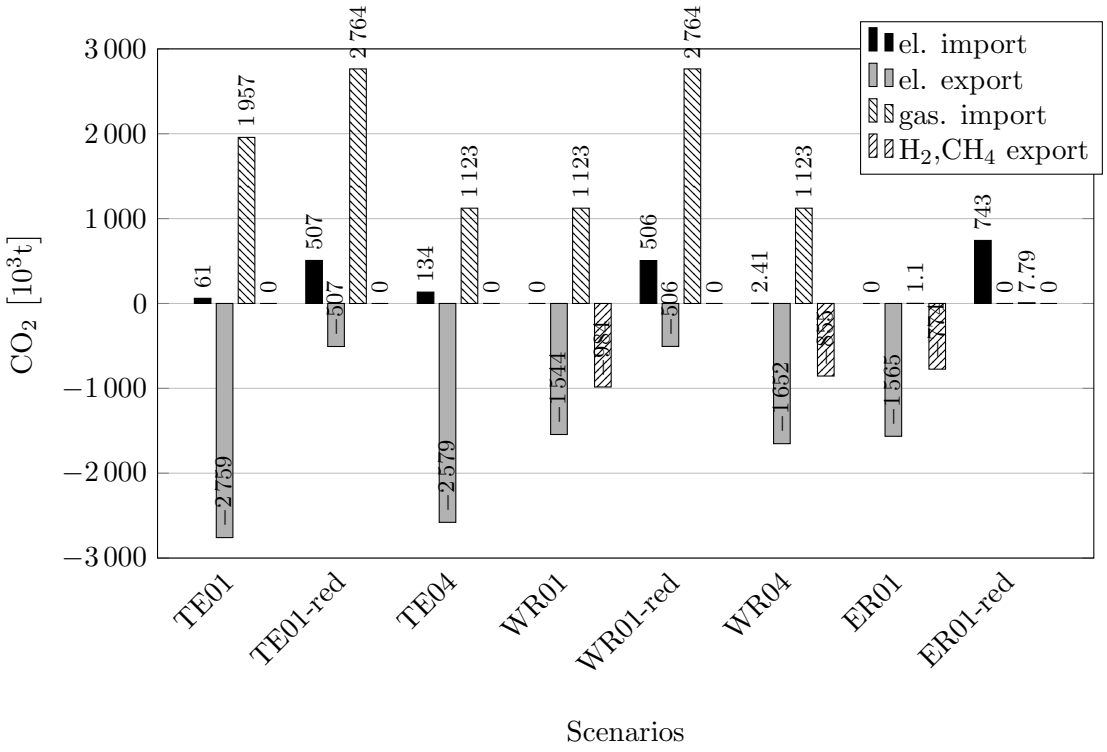

Figure 6.13: CO_2 emissions and savings due to electricity and gas import/export

scenarios, is small compared to the electricity demand of households in the year 2013. This results also in high CO_2 emission reductions, compared to the current emissions. Even if the CO_2 emission reductions due to renewable energy exports are not taken into account. This is because of the very high exploitation of renewable energies in the model region and the high usage of this energy, even in the reduced scenarios.

7 Conclusions/Outlook

Firstly, this chapter sums up the characteristics of the model region, followed by key results derived at scenarios and via direct scenarios comparison. This is then followed by showing key results gathered from scenario up-scaling to Austrian conditions. Finally, possible further steps that could be implemented or extended for a more comprehensive model are listed.

Conclusion
In total, 31 scenarios for three different cases (technological, whole region and ecological region) are analysed. The installed decentralised, renewable energy production in form of PV- and biomass-systems exploits the potential 100 %. This is why the electric production exceeds the maximum electric load in terms of power by a factor of six and in terms of energy by a factor of 3.4. For the thermal system, from the power perspective the situation is reversed, the demand exceeds the production by a factor of two. Energetically it is depending on the load-scenario if the production exceeds the demand or vice versa.
Because of this high decentralised production penetration technical limitation violations occur. In the technical basic case (scenario TE01) these are voltage-band violations. With downscaling technical infrastructure (transformer power, thermal line load), some scenarios are designed to add a centralised problem (at the slack node), or to increase the decentralised problem (at each node).
For the characteristics of the model region the following results can be summarised:

- Electric decentralised storages are always installed at nodes where voltage-band violation occurs, independent if additionally a centralised technical limitation is implemented. If so, the decentralised storages are partly operated to prevent or reduce the problem at the central node.
- Electric centralised storages are almost not used and if, their installed dimension is small compared to the sum of installed decentralised storages.

- One reason for the centralised storage avoidance is due to the biomass production at the slack node, which produces three-fourths of the year continuously electricity and heat.
- Because of the high energetic storage needs only batteries are used, which have a higher energy/power-ratio. In case of this work these are Lead-Acid batteries due to the modelled E/P of 2 h compared to the 0.4 h of Li-Ion batteries.
- Because of the high surplus energy, at centralised problems it is more useful to use the Power-to-Gas path and export energy this way. Because the investment costs for this technology only depend on the installation power and the big export of surplus energy covers this investment costs. Redox-Flow batteries face both costs – installed power and energy – that is why this technology is not used and the circumstance, that the stored energy would be no longer needed in the region.
- Only with high energy import costs are heat pumps used for nodes without district heating connections, otherwise gas heating is preferred.
- Thermal storages are only placed at nodes where thermal biomass production takes place (at this work this is the slack node).

Even if it would be possible to use the Austrian pumped storage power plants – which it is not, because of the local voltage-band violation – to fulfil the storage needs, from a power perspective, they are not sufficient. Energetically the pumped storage power plants exceed the up-scaled need almost seven times. Scenarios where the annual electricity production is equal to the demand (reduced scenarios), have almost no need for storage implementation and still only require 4 897 GWh/a to 7 193 GWh/a electricity import. Which is small compared to 16 700 GWh [127] of what the Austrian households in the year 2013 accounted for. This is a reduction of a factor of 2.3 to 3.4. Even if the scenarios are very sustainable it is questionable if such a system from a cost perspective would be realisable, since the model region realisation at an Austrian scale, only taking the storage costs into account, would cost more than several billion Euros. This does not even include installation costs for PV- and biomass-systems.

Outlook

The model region is designed to represent Austria. During the design process much attention was paid to differentiations of load profiles. Electric loads for each household are derived for example from individually created profiles, based on statistical parameters. However there are still only households represented in the region and they only account for 27 % of the total Austrian electricity demand. An extension with other load types, industrial and commercial would be interesting. The risks of such implementations are already mentioned in the motivation chapter. Such risks are, e.g. profile inhomogeneity for these load types. This implies the need of measuring a huge number of profiles to be able to derive statistical parameters and create representative load profiles.
Electric vehicles are predicted to become popular and commonly used. Because of that, it would be interesting to model the car behaviour, especially the parking place/time and State of Charge (SOC) of car batteries. The current energy prices do not cover the

costs for battery deterioration due to vehicle-to-grid usage. But, it would be interesting to investigate if the vehicle batteries could help to avoid violations of technical limitation in the grid or which business models are necessary for economically attractive vehicle-to-grid usages in a highly renewable supplied system.
Since the three load flow calculations (electric, gas, thermal) are non-linear, the non-linear modelling of these systems and the usage of other than linear optimisation methods would be interesting. This would enable a direct network loss calculation and consideration in the optimisation and objective function.
The implementation of several network levels (especially for electricity and gas) would be another interesting extension. This would enable simulations and energy exchange investigations of larger scales. This might require a cascaded optimisation process, where in a first step with higher granularity a rough pre-optimum is derived and this optimum is then optimised in detail. Granularity in this context could be a change of resolution, either in time or geographically.

Appendix A

List of Abbreviations

AC	Alternating Current
ACLF	AC Load Flow
ADRES	Autonome Dezentrale Regenerative Energie Systeme
aDSM	aktives Demand-Side-Management durch Einspeiseprognose
AEL	Alkaline Electrolysis
AHD	Annual Heating Demand
AI	Artificial Intelligence
BLOP	Binary Linear Optimisation Problem
CHP	Combined Heat and Power plant
COP	Coefficient of Performance
DA	Durchmesser Außen
DC	Direct Current
DCLF	Direct Current Load Flow
DN	Diameter Nominal
DSM	Demand Side Management
DVGW	German Technical and Scientific Association for Gas and Water
ER	"Ecological Region"

EU European Union

FLH Full Load Hours

GA Genetic Algorithm

GFA Gross Floor Area

GLOP Game Linear Optimisation Problem

HDD Heating Degree Days

HESS Hybrid Energy Storage System

HEV Hybrid Electric Vehicle

HP High Pressure

HRES Hybrid Renewable Energy System

HTEL High Temperature Electrolysis

ILOP Integer Linear Optimisation Problem

LCE Levelised Cost of Energy

LOLP Loss of Load Probability

LOP Linear Optimisation Problem

LP Low Pressure

LVG Low Voltage Grid

MILOP Mixed Integer Linear Optimisation Problem

MINLOP Mixed Integer Nonlinear Optimisation Problem

MOP Maximum Operating Pressure

MP Medium Pressure

MPP Maximum Power Point

MVG Medium Voltage Grid

NPS Nominal Pipe Size

OVGW Austrian Association for Gas and Water

PDCS Power Distribution Control Strategy

PE Polyethylene

PEMEL Proton Exchange Membrane Electrolysis

PR Power Resistance

PSO Particle Swarm Optimisation

PV Photovoltaic

PVC Polyvinyl Chloride

RAM Random Access Memory

SDR Standard Dimension Ratio

SET Strategic Energy Technology

SF Simultaneity Factor

SNG Synthetic Natural Gas

SOC State of Charge

SPE Solid Polymer Electrolyte

SPF Seasonal Performance Factor

TE Technical

UC Ultra-Capacitor

V2G Vehicle-to-Grid

VDEW Verband der Elektrizitätswirtschaft

WR "Whole Region"

List of Nomenclature

For better differentiation between real and complex variables, complex variables are marked with an underscore. Vectors and matrices are represented with bold letters.

$\delta_{\nu\mu}$	voltage angle between certain nodes (e.g. ν, μ)
η	dynamic viscosity
η_{in}	efficiency charge
η_{out}	efficiency discharge
$\boldsymbol{\vartheta}$	voltage angle vector
$\boldsymbol{\vartheta}'$	reduced voltage angle vector
ϑ	temperature
ϑ_ν	voltage angle at certain node (e.g. ν)
ϑ_e	standard ambient temperature
ϑ_f	temperature (e.g. f...supply pipe; r...return pipe; s...undisturbed soil; m...average between forward and return pipe)
ϑ_{em}	average daily temperature
$\vartheta_{int,i}$	standard internal temperature; room i
ϑ_{out_i}	outside air temperature for time step i
$\boldsymbol{\Theta}_l$	node angle difference matrix

λ_k pipe friction coefficient at pipe k

ν kinematic viscosity

ρ density

φ_ν electric potential at certain node (e.g. ν)

Φ_{HL} heating power demand (e.g. *SU*...total heat demand; *HL*...heating demand; *DHW*...hot water; *AS*...affiliated systems)

Φ_{tot} heat losses (e.g. *tot*...total per pipe pair; f...supply pipe; r...return pipe)

Ω asymptotic lower optimisation bound

a_k pipe resistance at certain pipe (e.g. k)

$\boldsymbol{A}$ branch-node incidence matrix or constraint matrix

$\boldsymbol{A'}$ reduced branch-node incidence matrix

A annuity factor

A area, cross section

$\boldsymbol{b}$ constraint vector

$\boldsymbol{B}$ susceptance matrix

$\boldsymbol{B'}$ reduced susceptance matrix

$\boldsymbol{B}_l$ branch susceptance matrix

$\underline{B}_{\nu\mu}$ element of susceptance matrix

$\boldsymbol{c}$ objective vector

c_{p,H_2O} specific thermal capacity for water

$\boldsymbol{C}$ coupling matrix of energy hub

d_{ik} inner pipe diameter at certain pipe (e.g. k)

$E(t)$ energetic storage state

E_i internal energy at fluid element

E_{annual} annual energy consumption

f_{HL} heating demand design factor (e.g. *HL*...heating demand; *DHW*...hot water; *AS*...affiliated systems)

F	force
F_g	gravitational force
F_i	force due to internal friction
F_p	compressive force
F_w	force due to wall friction
g	gravity acceleration
$\underline{G}_{\nu\mu}$	element of conductance matrix
H	transmission heat loss coefficient
$\boldsymbol{I}$	current vector
$\boldsymbol{I}_{qn}$	node source current vector
I	impulse
I_0	initial investment
I_ν	current at certain node (e.g. ν)
j	imaginary unit
k_v	internal friction coefficient
k_{sk}	pipe roughness at certain pipe (e.g. k)
$\boldsymbol{L}$	output parameter of energy hub
$\boldsymbol{L}_e$	electric load flow matrix
$\boldsymbol{L}_g$	gas load flow matrix
$\boldsymbol{L}_h$	district heating load flow matrix
m	mass
M	mating pool
n	lifetime
n_k	node number
n_l	line/branch number
O	asymptotic upper optimisation bound
$\boldsymbol{p}$	active power matrix

$\boldsymbol{p'}$ reduced active power matrix

p or p_e pressure

p_h geodetic fluid pressure

p_v fluid pressure due to pipe friction

p_{kin} dynamic fluid pressure

p_{stat} static fluid pressure

$\boldsymbol{P}$ input parameter of energy hub

P individual population for genetic search

P' slightly changed individual population for genetic search

P_ν active power injection at certain node (e.g. ν)

$P_{\nu\mu}$ active power flow between certain nodes (e.g. ν, μ)

$P_{D,\nu}$ active power demand at certain node (e.g. ν)

P_{el} charge or discharge power

$P_{G,\nu}$ active power generation at certain node (e.g. ν)

P_{HW_i} heating power for hot water demand for time step i

$P_{i,e}$ electric node load of node i

$P_{i,g}$ gas node load of node i

$P_{l,e_{max}}$ maximum electric line load

$P_{l,e}$ electric line load

$P_{l,g}$ gas pipe load

$P_{l_{max}}$ maximum gas pipe load

$P_{loss,cur}$ current depending line power loss

P_{maxHH} maximal heat demand (e.g. *HH*...household, *DH*...district heating system)

$P_{su/di}$ dissipated power at fluid element

q interest rate

Q_ν reactive power injection at certain node (e.g. ν)

$Q_{D,\nu}$ reactive power demand at certain node (e.g. ν)

$Q_{G,\nu}$ reactive power generation at certain node (e.g. ν)

$\boldsymbol{R}$ resistance matrix

R' resistance load per unit length

R_s insulance (e.g. s...soil; i...pipe insulating material; h...between supply and return pipe)

Re Reynolds' number

t time

U thermal transmittance

U' average thermal transmittance

U_1 or U_2 heat losses coefficient

$\bar{v}_k$ average flow at certain pipe (e.g. k)

v speed

$\boldsymbol{V}$ voltage vector

$\boldsymbol{V}_n$ node voltage vector

$\underline{V}_\nu$ voltage at certain node (e.g. ν)

V_n nominal voltage

$V_{\nu\mu}$ voltage between certain nodes (e.g. ν, μ)

V_{tap_i} water flow rate for time step i

w objective function dual problem

$\boldsymbol{x}$ decision vector

x_j decision variable

X optimisation search space

$\boldsymbol{y}$ decision vector

y_i decision variable

$\boldsymbol{Y}$ admittance matrix

$\underline{Y}_{\nu\mu}$ element of admittance matrix

z objective function primal problem or day number

$\underline{Z}_{\nu\mu}$ element of impedance matrix

List of Figures

List of Tables

Bibliography

[1] J. Schindler and W. Zittel, "Zukunft der weltweiten Erdölversorgung." http://www.energywatchgroup.org/fileadmin/global/pdf/2008-05-21_EWG_Erdoelstudie_D.pdf, 2008. [Online]; accessed 2012-07-18.

[2] Statisitk Austria, "Energiestatistik: Energiebilanzen österreich 1970 bis 2010." http://www.statistik.at/web_de/statistiken/energie_und_umwelt/energie/energiebilanzen/index.html, 2011. [Online]; accessed 2012-07-23.

[3] M. Gege, *Erfolgsfaktor Energieeffizienz - Investitionen, die sich lohnen: Wie Unternehmen und öffentliche Einrichtungen Energie und Kosten einsparen können.* München: oekom-Verl., 2011.

[4] T. Reuters, "Workbook Contents-Spot Prices for Crude Oil and Petroleum Products." http://www.eia.gov/dnav/pet/pet_pri_spt_s1_d.htm, 2012. [Online]; accessed 2012-07-18.

[5] International Energy Agency, "World energy outlook 2008," 2008. Paris.

[6] A European Stratecig Energy Plan, "A European Stratecig Energy Plan (SET-PLAN)," 2007. Brussels.

[7] Bundesministerium für Wirtschaft, Familie und Jugend, "EnergieStrategie österreich Maßnahmenvorschläge," 2010. Vienna.

[8] A. Schuster, "Electric Mobility Model Region VLOTTE in Austria: Scientific Accompanying Research: Presentation at the The 25th World Battery, Hybrid and Fuel Cell Electric Vehicle Symposium & Exhibition," 2010-11-01. Shenzhen.

[9] W. Gawlik, M. Litzlbauer, A. Schuster, H. Koller, M. Reinthaler, K. Norman, N. Waldbauer, A. Bolzer, and M. Leitner, "Zukünftige Energienetze mit Elektromobilität: ZENEM," 2013. Vienna.

[10] W. Prüggler, R. Rezania, M. Litzlbauer, A. Schuster, C. Leitunger, M. Kloess, D. Burnier De Castro, H. Brunner, T. Rieder, and R. Pointner, "V2G-Strategies: Konzeption von Vehicle to Grid bezogenen Entwicklungsstrategien für österreichische Entscheidungsträger," 2013.

[11] Bundesverband der Energie- und Wasserwirtschaft e.V., "Energieverbrauch im Haushalt," 2010. Berlin.

[12] OENORM H 5055, "Energy certificate for buildings," 2008-02-01.

[13] Energie Tirol, "Energieausweis: Energiebilanz ziehen! Wie viel Heizenergie verbraucht ein Gebäude? Ob Haus oder Wohnung – der Energieausweis schafft Klarheit."

[14] C. Pöhn, *Bauphysik*, vol. 1,1 of *Baukonstruktionen*. Wien [u.a.]: Springer, 2007.

[15] Statisitk Austria, "Wohnungen, Gebäude." `http://www.statistik.at/web_de/statistiken/wohnen_und_gebaeude/`. [Online]; accessed 2015-04-29.

[16] W. Gawlik, C. Groiß, M. Litzlbauer, C. Maier, A. Schuster, F. Zeilinger, A. Kann, I. Meirold-Mautner, G. Günther, C. Eugster, R. Nenning, C. Kamer, and G. Wolfram, "aDSM - Aktives Demand-Side-Management durch Einspeiseprognose," 2014. Vienna.

[17] M. K. Deshmukh and S. S. Deshmukh, "Modeling of hybrid renewable energy systems," *Renewable and Sustainable Energy Reviews*, vol. 12, no. 1, pp. 235–249, 2008.

[18] B. Bhandari, K.-T. Lee, G.-Y. Lee, Y.-M. Cho, and S.-H. Ahn, "Optimization of Hybrid Renewable Energy Power Systems: A Review," in *International Journal of Precision Engineering and Manufacturing-Green Technology*, vol. 2, pp. 99–112.

[19] Fathima, A. Hina and K. Palanisamy, "Optimization in microgrids with hybrid energy systems – A review," *Renewable and Sustainable Energy Reviews*, vol. 45, pp. 431–446, 2015.

[20] J. L. Bernal-Agustín and R. Dufo-López, "Simulation and optimization of stand-alone hybrid renewable energy systems," *Renewable and Sustainable Energy Reviews*, vol. 13, no. 8, pp. 2111–2118, 2009.

[21] M. Amer, A. Namaane, and N. K. M'Sirdi, "Optimization of Hybrid Renewable Energy Systems (HRES) Using PSO for Cost Reduction," *Mediterranean Green Energy Forum 2013: Proceedings of an International Conference MGEF-13*, vol. 42, pp. 318–327, 2013.

[22] M. Sharafi and T. Y. ELMekkawy, "Multi-objective optimal design of hybrid renewable energy systems using PSO-simulation based approach," *Renewable Energy*, vol. 68, pp. 67–79, 2014.

[23] S. Ashok, "Optimised model for community-based hybrid energy system," *Renewable Energy*, vol. 32, no. 7, pp. 1155–1164, 2007.

[24] M. Geidl, *Integrated Modeling and Optimization of Multi-Carrier Energy Systems*. PhD thesis, ETH Zurich, Zurich, 2007.

[25] M. Berger, *Validierung des Energy Hub Konzepts mittels einer Fallstudiein Baden-Dättwil*. PhD thesis, ETH Zurich, Zurich, 2011.

[26] A. Shabanpour-Haghighi and A. R. Seifi, "Energy Flow Optimization in Multicarrier Systems," *IEEE Transactions on Industrial Informatics*, no. 99, p. 1, 2015.

[27] R. Niemi, J. Mikkola, and P. D. Lund, "Urban energy systems with smart multicarrier energy networks and renewable energy generation," *Renewable Energy*, vol. 48, pp. 524–536, 2012.

[28] M. Schulze and P. C. Del Granado, "Optimization modeling in energy storage applied to a multi-carrier system," in *Energy Society General Meeting*, (Minneapolis and MN), pp. 1–7.

[29] T. Krause, F. Kienzle, S. Art, and G. Andersson, "Maximizing exergy efficiency in multi-carrier energy systems," in *Energy Society General Meeting*, (Minneapolis and MN), pp. 1–8.

[30] *IEEE Power and Energy Society general meeting, 2010: IEEE PES-GM 2010 ; 25 - 29 July 2010, Minneapolis, Minnesota, USA*. Piscataway and NJ: IEEE, 2010.

[31] M. Geidl and G. Andersson, "Operational and topological optimization of multicarrier energy systems," in *2005 International Conference on Future Power Systems* (IEEE, ed.), (Amsterdam), pp. 6 pp–6, 2005.

[32] "2005 International Conference on Future Power Systems," (Amsterdam), 2005.

[33] S. Pazouki and M.-R. Haghifam, "Impact of energy storage technologies on multi carrier energy networks," in *2014 Smart Grid Conference (SGC)*, (Tehran), pp. 1–6.

[34] *Smart Grid Conference (SGC), 2014*. [S.l.]: [s.n.], 2014.

[35] R. Schultz, ed., *Innovative Modellierung und Optimierung von Energiesystemen*, vol. Bd. 26 of *Umwelt- und Ressourcenökonomik*. Berlin and Münster: Lit, 2009.

[36] M. Masih-Tehrani, M.-R. Ha'iri-Yazdi, V. Esfahanian, and A. Safaei, "Optimum sizing and optimum energy management of a hybrid energy storage system for lithium battery life improvement," *16th International Meeting on Lithium Batteries (IMLB)*, vol. 244, pp. 2–10, 2013.

[37] W. Gawlik, S. Begluk, M. Boxleitner, C. Groiß, M. Heimberger, C. Maier, R. Schlager, H. Walter, M. Lauermann, R. Eisl, K.-W. Schenzel, W. Neyer, H. Buzanich, J. Böckle, C. Eugster, and S. Hartmann, "Systemübergreifende optimale dezentrale Hybridspeicher: SYMBIOSE," 2014. Vienna.

[38] W. Gawlik, "Dezentrale, Energieträger-übergreifende Speicher im Universal Grid," *e & i Elektrotechnik und Informationstechnik*, vol. 2013, no. 130, pp. 145–147, 2013.

[39] *Gebäude- und Wohnungszählung 2001.* Wien: Statistik Austria, 2004.

[40] H. Seifi and M. S. Sepasian, *Electric power system planning: Issues, algorithms and solutions.* Power systems, Heidelberg: Springer, 2011.

[41] W. Gawlik, "Energieversorgung: Script for lecture." Script for lecture, 2014.

[42] W. Wellßow, *Ein Beitrag zur Zuverlässigkeitsberechnung in der Netzplanung.* PhD thesis, Darmstadt, Darmstadt, 1986.

[43] C. Groiß, *Maximierung des regenerativen Erzeugungsanteils an der österreichischen Elektrizitätsversorgung.* PhD thesis, Vienna University of Technology, Vienna, 2013.

[44] SimTec GmbH, "PSS-SINCAL 10.0 Gas Calculations in Pipe Networks."

[45] G. Cerbe, ed., *Grundlagen der Gastechnik: Gasbeschaffung - Gasverteilung - Gasverwendung ; mit 102 Beispielen, 66 Aufgaben.* München and Wien: Hanser, 7., vollst. neu bearb. aufl ed., 2008.

[46] German Institute for Standardization, "Gaseous fuels and other gases; types, constituents, application," 1990-12-01.

[47] DVGW, "Gasbeschaffenheit: Technische Regel - Arbeitsblatt: DVGW G 260," *DVGW Regelwerk*, 2013.

[48] Österreichische Vereinigung für das Gas- und Wasserfach, "Natural gas pipelines made of PE - Special requirements for design, construction and initial testing of natural gas pipelines made of PE," 2011.

[49] Österreichische Vereinigung für das Gas- und Wasserfach, "Natural gas pipelines - General requirements for design, construction and initial testing of natural gas pipelines," 2011.

[50] J. Rüdiger, *Gasnetzsimulation durch Potentialanalyse.* PhD thesis, Universität der Bundeswehr Hamburg, Dresden, 2009.

[51] SWM Services GmbH, "Erdgasqualität im Verteilungsnetz des Großraumes München." `http://www.swm.de/dms/swm/dokumente/schulen/downloads/erdgas-qualitaet.pdf`, 2015. [Online]; accessed 2015-05-13.

[52] A. Prechtl, "Elektrotechnik 2: Ergänzende Unterlagen zu den Lehveranstaltungen." Vienna, 2003.

[53] German Institute for Standardization, "Heating systems in buildings - Design for water-based heating systems," 2014.

[54] German Institute for Standardization, "Heating systems in buildings Method for calculation of the design heat load," 2003.

[55] idm energie, "Norm-Außentemperatur." `http://www.idm-energie.at/media/normaussentemp_de.pdf`. [Online]; accessed 2015-07-25.

[56] German Institute for Standardization, "Central heat-water-installations; rules for the determination of the water-heat-demand in dwelling-houses," 1994.

[57] U. Jordan and K. Vajen, "DHWcalc: Tool for the Generation of Domestic Hot Water (DHW) Profiles on a Statistical Basis." `http://solar.umwelt-uni-kassel.de/downloads.en.html`, 2013.

[58] "Möglichkeiten der technologischen und wirtschaftlichen Optimierung von Biomasse-Nahwärme- und Mikronetzen," (Salzburg), 1997.

[59] B. Glück, *Heizwassernetze für Wohn- und Industriegebiete*. Frankfurt (Main): Verlags- und Wirtschaftsges. d. Elektrizitätswerke, 1985.

[60] Wien Energie GmbH, "Technische Auslegungsbedingungen," 2013. Vienna.

[61] ISOPLUS, "Starre Verbundsysteme: Einzelrohr Konti." `http://www.isoplus.de/fileadmin/data/downloads/documents/germany/products/isoplus-EinzelrohrKONTI-Detail.pdf`, 2011. [Online]; accessed 2015-07-31.

[62] A. Leder, "Grundlagen der Strömungsmechanik." `http://www.lsm.uni-rostock.de/uploads/media/GSMUmdruck-Teil1-Uebersichten.pdf`. [Online]; accessed 2015-07-29.

[63] D. Rotsch, *Zuverlassigkeit von rohrleitungssystemen: Fernwarme und wasser*. [S.l.]: Springer, 2012.

[64] VDEW M-32/99, "Repräsentative VDEW-Lastprofile," 1999.

[65] F. Zeilinger, *Simulation von Demand Side Management mit frequenzabhängigen Lastprofilen in Inselnetzen*. Master's thesis, Vienna University of Technology, Vienna, 2010.

[66] F. Zeilinger, "Simulation of the effect of demand side management to the power consumption of households," in *3rd International Youth Conference on Energetics 2011*, ([Piscataway and N.J.]), [IEEE], 2011.

[67] A. Einfalt, A. Schuster, C. Leitinger, D. Tiefgraber, M. Litzlbauer, S. Ghaemi, D. Wertz, A. Frohner, and C. Karner, "Konzeptentwicklung für ADRES - Autonome Dezentrale Regenerative EnergieSysteme: ADRES-Concept," 2012. Vienna.

[68] A. Wegscheider-Pichler, "Strom- und Gastagebuch 2008: Strom- und Gaseinsatz sowie Energieeffizienz österreichischer Haushalte Auswertung Gerätebestand und Einsatz," 2009. Vienna.

[69] C. Groiß, *Power Demand Side Management - Potentiale und technische Realisierbarkeit im Haushalt*. Master's thesis, Vienna University of Technology, Vienna, 2008.

[70] S. Stukelj, *Photovoltaikstrom-Eigenverbrauchsoptimierung mit aktivem Demand Side Management auf Siedlungsebene*. Master's thesis, Vienna University of Technology, Vienna, 2014.

[71] Statisitk Austria, "Wohnungs- und Gebäudebestand." `http://www.statistik.at/web_de/statistiken/menschen_und_gesellschaft/wohnen/wohnungs_und_gebaeudebestand/index.html`, 24.06.2015. [Online]; accessed 2015-07-01.

[72] "EPISCOPE, TABULA." `http://episcope.eu/index.php?id=97`, 2014. [Online]; accessed 2015-07-10.

[73] OENORM B 8135, "Simplified calculation of the time related loss of heat (heating load) of buildings," 1978.

[74] R. Bointner, T. Bednar, S. Eikemeier, S. Ghaemi, R. Haas, C. Harreiter, H. Huber-Fauland, C. Ipser, K. Krec, M. Leeb, K. Ponweiser, T. Steiner, K. Stieldorf, P. Wegerer, and D. Wertz, "Gebäude maximaler Energieeffizienz mit integrierter erneuerbarer Energieerschließung," 2012. Vienna.

[75] H. Recknagel, E. Sprenger, and E.-R. Schramek, *Taschenbuch für Heizung und Klimatechnik: Einschließlich Warmwasser- und Kältetechnik*. München [etc.]: Oldenbourg Industrieverlag, 74. aufl. ed., op. 2009.

[76] E. Schiefl, *Modellierung der Entwicklung von Treibhausgasemissionen und Energieverbrauch für Raumwärme und Warmwasser im österreichischen Wohngebäudebestand unter der Annahme verschiedener Optimierungsziele*. PhD thesis, Vienna University of Technology, Vienna, 2007.

[77] M. Boxleitner, C. Groiß, M. Chochole, G. Brauner, J. Hiebl, C. Springer, G. Blöschl, C. Maier, and H. Schmöller, "Super-4-Micro-Grid: Nachhaltige Energieversorgung im Klimawandel," 2011. Vienna.

[78] Österreichischer Städtebund and Statisitk Austria, "Österreichs Städte in Zahlen 2011." `http://www.statistik.at/web_de/nomenu/suchergebnisse/index.html`, 2011. [Online]; accessed 2015-06-15.

[79] M. Lödl, G. Kerber, R. Witzmann, C. Hoffmann, and M. Metzger, "Abschätzung des Photovoltaik-Potentials auf Dachflächen in Deutschland," 2010. Graz.

[80] R. Schlager, M. Boxleitner, S. Begluk, M. Heimberger, H. Buzanich, W. Neyer, and W. Gawlik, "Möglichkeiten und Anforderungen an Speichertechnologien im Verteilnetz bei einem starken Ausbau dezentraler Erzeugungseinheiten," 2013. Vienna.

[81] "Monitoring der PV-Anlage Zwentendorf - Wirkungsgradanalyse der Umwandlungskette," Wissen für Profis, (Regensburg), OTTI, 2013.

[82] Wien Energie GmbH, "Wien Energie Jahrbuch 2011/12," 2012. Vienna.

[83] Statisitk Austria, "Bevölkerung im Jahresdurchschnitt." `http://www.statistik.at/web_de/statistiken/menschen_und_gesellschaft/bevoelkerung/bevoelkerungsstand_und_veraenderung/bevoelkerung_im_jahresdurchschnitt/index.html`, 2015. [Online]; accessed 2015-06-29.

[84] Statisitk Austria, "Bundesländer." `http://www.statistik.at/web_de/klassifikationen/regionale_gliederungen/bundeslaender/index.html`. [Online]; accessed 2015-06-29.

[85] G. Stanzer, N. Stephanie, C. Spanring, H. Schaffer, H. Dumke, S. Plha, M. Kirtz, and P. Biermayr, "REGIO Energy: Regionale Szenarien erneuerbarer Energiepotenziale in den Jahren 2012/2020." `http://regioenergy.oir.at/sites/regioenergy.oir.at/files/uploads/pdf/REGIO-Energy_Endbericht_201013_korr_Strom_Waerme.pdf`, 2010.

[86] F. Rothlauf, *Design of modern heuristics: Principles and application*. Natural computing series, Berlin and New York: Springer, 2011.

[87] N. Kumar, "D Nagesh Kumar, IISc Optimization Methods: M1L3 Introduction and Basic Concepts: Classifigation of Optimization Problems." `http://www.nptel.ac.in/courses/105108127/pdf/Module_1/M1L3slides.pdf`, 23.09.2015.

[88] G. Hurlbert, *Linear optimization: A Simplex workbook*. Undergraduate texts in mathematics, New York: Springer, 2010.

[89] M. Papageorgiou, *Optimierung: Statische, dynamische, stochastische Verfahren*. Berlin: Springer, 3., neu bearb. und erw. aufl ed., 2006.

[90] M. Sterner and I. Stadler, *Energiespeicher - Bedarf, Technologien, Integration*. SpringerLink : Bücher, Berlin: Springer Vieweg, 2014.

[91] E. Rummich, *Energiespeicher: Grundlagen, Komponenten, Systeme und Anwendungen ; mit 22 Tabellen*. Renningen: expert-Verl, 2009.

[92] A. Jossen and W. Weydanz, *Moderne Akkumulatoren richtig einsetzen: 36 Tabellen*. Neusäß: Ubooks, 1. aufl. ed., 2006.

[93] U. Brünger, F. Crotogino, S. Donadei, C. Gatzen, W. Glaunsinger, M. Kleinmaier, M. Könemund, and H. Landinger, "Energiespeicher in Stromversorgungssystemen mit hohem Anteil erneuerbarer Energieträger: Bedeutung, Stand der Technik, Handlungsbedarf." Frankfurt.

[94] E. Mahnke and J. Mühlenhoff, "Strom speichern," *Renews Spezial*, no. 57, 2012.

[95] D. U. Sauer, M. Leuthold, D. Magnor, and B. Lunz, "Dezentrale Energiespeicherung zur Steigerung des Eigenverbrauches bei netzgekoppelten PV-Anlagen," 2011. Aachen.

[96] Siemens AG, "SIESTORAGE: The modular energy storage system for a reliable power supply." `http://w3.siemens.com/powerdistribution/global/SiteCollectionDocuments/en/mv/power-supply-solutions/siestorage/brochure-siestorage_en.pdf`, 2014. [Online]; accessed 2015-08-27.

[97] Saft, "Evolion Li-ion battery," 2013. Bagnolet.

[98] Energy Storage Association, "Energy Storage Technologies — Energy Storage Association." `http://energystorage.org/energy-storage/energy-storage-technologies`. [Online]; accessed 2015-08-27.

[99] IEK9, "Quartett: Energie sticht!." `http://www.fz-juelich.de/SharedDocs/Downloads/IEK/IEK-9/DE/Batteriequartett.pdf?__blob=publicationFile`, 2014. [Online]; accessed 2015-09-08.

[100] C. Blanc, *Modeling of a Vanadium Redox Flow Battery Electricity Storage System*. PhD thesis, Politechnique federale del Lausanne, Lausanne, 2009.

[101] P. de Boer and J. Raadschelders, "Flow batteries: Briefing Paper." `http://www.leonardo-energy.org/sites/leonardo-energy/files/root/pdf/2007/Briefing%20paper%20-%20Flow%20batteries.pdf`, 2007. [Online]; accessed 2015-07-06.

[102] M. Bodach, *Energiespeicher im Niederspannungsnetz zur Integration dezentraler, fluktuierender Energiequellen*. PhD thesis, Technischen Universität Chemnitz, Chemnitz, 2006.

[103] M. Dennenmoser, K. Bromberger, F. Oßwald, K. Korring, T. Schwind, T. Smolinka, and M. Vetter, "Design, characterisation and operation strategies of 1 KW all-vanadium redox flow battery," 2011. Edinburgh.

[104] R. Rezanla and W. Prüggler, "Wirtschaftliche Bewertung der Teilnahme eines stationären Speichersystems an den Regelenergiemärkten österreichs," *Informatik-Spektrum*, vol. 2013, no. 36, pp. 69–77, 2013.

[105] T. M. Masaud, K. Lee, and P. K. Sen, "An overview of energy storage technologies in electric power systems: What is the future?," in *2010 North American Power Symposium (NAPS 2010)*, (Arlington and TX and USA), pp. 1–6, 2010.

[106] *North American Power Symposium (NAPS), 2010: Date:26-28 Sept. 2010*. [Piscataway and N.J.]: IEEE, 2010.

[107] I. Dinçer and M. A. Rosen, "Thermal Energy Storage and Energy Savings," in *Thermal Energy Storage* (İ. Dinçer and M. A. Rosen, eds.), pp. 211–231, Chichester and UK: John Wiley & Sons, Ltd, 2010.

[108] İ. Dinçer and M. Rosen, *Thermal energy storage: Systems and applications*. Hoboken and N.J.: Wiley, 2nd ed. ed., 2011.

[109] J.-C. Hadorn, D. Chuard, P. Jaboyedoff, and P. Chuard, "Guid to Seasonal Heat Storage." `ftp://ftp.tech-env.com/pub/ENERGY/ATESSTES/guide_to_seasonal_heat_storage.pdf`, 1987. [Online]; accessed 2015-09-08.

[110] A. Hauer, M. Specht, and M. Sterner, "Energiespeicher – Steigerung der Energieeffizienz und Integration erneuerbarer Energien." `http://www.fvee.de/fileadmin/publikationen/Themenhefte/th2010-2/th2010_13_01.pdf`, 2010. [Online]; accessed 2015-09-17.

[111] B. Hey, *Power-to-Gas als Möglichkeit zur Speicherung eines Energieüberangebots und als Bestandteil eines flexiblen Demand Side Managements*. Master's thesis, Hochschue für angewandte Wissenschaften Hamburg, Hamburg, 2012.

[112] H. Hubert, P. Schöfmann, and A. Zott, "Wärme!pumpen: zur energieeffizienten Wärmeversorgung," 2014. Vienna.

[113] Wärmepumpe Austria, "Förderungsliste Länder." `http://www.waermepumpe-austria.at/fileadmin/user_upload/Bilder_WPA/foerderung/Foerderliste_WPA_laender.pdf`. [Online]; accessed 2015-09-14.

[114] A. Nietlisbach and C. Gmür, "Gasthermen im Test," vol. 2000, no. 25, pp. 33–34, 2000.

[115] OCE Austrian Electrotechnical Association, "CENELEC standard voltages," 2012. Vienna.

[116] German Institute for Standardization, "Merkmale der Spannung in öffentlichen Elektrizitätsversorgungsnetzen," 2011.

[117] A. Hinz, "Der regelbare Ortsnetztransformator im Verteilungsnetz – Lösung aller Spannungsbandprobleme?," 2013. Aachen.

[118] B. R. Oswald, "Verlust- und Verlustenergieabschätzung: für das 380-kV-Leitungsbauvorhaben Wahle – Mecklar," 2007. Hannover.

[119] German Institute for Standardization, "Design and installation of preinsulated bonded pipe systems for district heating," 2010.

[120] Kunstoffwerk GesmbH, "Fernwärme-Rohrsystem," 2006. Linz.

[121] ISOPLUS, "Kontirohrtechnik." http://www.isoplus.de/fileadmin/data/downloads/documents/germany/products/Kontirohr-8-Seiten_DEUTSCH_Web.pdf, 2015. [Online]; accessed 2015-09-01.

[122] Energie AG, "Sonnenstrom-Speicherpaket." http://www.energieag.at/eag_at/resources/339536908088248262_1074326016693987141_2YB0wJEm.pdf, 08.07.2015. [Online]; accessed 2015-10-28.

[123] e control, "Strom- und Gaspreise." http://www.e-control.at/de/preismonitor, 2015. [Online]; accessed 2015-09-21.

[124] e control, "Preiszusammensetzung." http://www.e-control.at/de/konsumenten/strom/strompreis/preiszusammensetzung, 2015. [Online]; accessed 2015-09-21.

[125] D. Stolten, "Power to Gas," 2013-08-20. Bregenz.

[126] Umweltbundesamt, "Energieeinsatz in österreich." http://www.umweltbundesamt.at/umweltsituation/energie/energie_austria/, 2011. [Online]; accessed 2015-09-30.

[127] Statisitk Austria, "Energiebilanzen." http://www.statistik.at/web_de/statistiken/energie_umwelt_innovation_mobilitaet/energie_und_umwelt/energie/energiebilanzen/index.html, 2015. [Online]; accessed 2015-10-21.

[128] W. Boltz and M. Graf, "Statistikbroschüre 2015," 2015. Vienna.

[129] W. Boltz and M. Graf, "Stromkennzeichnungsbericht 2014," 2014. Vienna.

[130] Statisitk Austria, "Presse." http://www.statistik.at/web_de/presse/066950.html. [Online]; accessed 2015-10-21.

Appendix B

Households

PV Power

Table B.1: Classification of the PV power and profile to each household; Modified according to [16]

Household (HH)	PV Power [kW_p]	PV Profile	HH	PV Power [kW_p]	PV Profile	HH	PV Power [kW_p]	PV Profile
001	21.7	33	043	11.5	23	085	2.8	16
002	21.7	33	044	11.5	56	086	2.8	29
003	43.4	25	045	11.5	28	087	2.8	41
004	11.5	32	046	11.5	25	088	2.8	43
005	11.5	41	047	11.5	40	089	1.2	39
006	11.5	38	048	11.5	41	090	1.2	42
007	11.5	33	049	11.5	36	091	1.2	53
008	11.5	35	050	11.5	16	092	1.2	13
009	11.5	36	051	11.5	25	093	1.2	38
010	11.5	55	052	11.5	23	094	1.2	32
011	11.5	20	053	11.5	27	095	1.2	24
012	11.5	25	054	11.5	24	096	1.2	41
013	11.5	13	055	11.5	38	097	1.2	33
014	11.5	33	056	11.5	45	098	1.2	47
015	5.8	44	057	11.5	30	099	1.2	21
016	5.8	27	058	11.5	39	100	1.2	23
017	5.8	27	059	11.5	42	101	1.2	38
018	5.8	30	060	11.5	35	102	1.2	23
019	5.8	31	061	11.5	30	103	1.2	34
020	5.8	45	062	2.8	27	104	1.2	28
021	5.8	33	063	2.8	20	105	1.2	46
022	5.8	27	064	2.8	30	106	1.2	38
023	5.8	40	065	2.8	35	107	1.2	28
024	5.8	17	066	2.8	31	108	1.2	26
025	5.8	40	067	2.8	36	109	1.2	28
026	5.8	31	068	4.1	34	110	1.2	61
027	5.8	58	069	4.1	41	111	1.2	32
028	5.8	26	070	4.1	26	112	1.2	31
029	11.5	38	071	4.1	32	113	2.0	31
030	11.5	34	072	3.3	36	114	2.0	51
031	11.5	21	073	3.3	29	115	2.0	13
032	11.5	43	074	3.3	36	116	2.0	46
033	11.5	7	075	3.3	13	117	2.0	25
034	11.5	11	076	3.3	38	118	2.0	30
035	11.5	18	077	2.8	38	119	2.0	41
036	11.5	48	078	2.8	33	120	2.0	22
037	11.5	44	079	2.8	29	121	2.0	38
038	11.5	19	080	2.8	28	122	2.0	32
039	11.5	31	081	2.8	13	123	2.0	17
040	11.5	24	082	2.8	46	124	2.0	35
041	11.5	36	083	2.8	40	125	2.0	40
042	11.5	57	084	2.8	20	126	2.0	40

Building Parameters

Table B.2: The square meter, construction year or type and the thermal heating demand for each household for the three different scenarios (Default, Refurbished and Minimal), HH...household, HD...Heating Demand; 1/4

HH	Size	Default		Refurbished		Minimal	
	[m^2]	Year/Type	HD [kWh/a]	Year/Type	HD [kWh/a]	Year/Type	HD [kWh/a]
001	131	1981-1990	19184	1981-1990	10085	low	6574
002	163	1981-1990	23823	1981-1990	12524	low	8164
003	88	>2001	8649	>2001	8649	low	4395
004	102	>2001	10079	>2001	10079	low	5121
005	172	1961-1970	47457	1961-1970	18055	lowest	4311
006	101	1981-1990	14800	1981-1990	7780	lowest	2536
007	112	1961-1970	30710	1961-1970	11684	passive	1116
008	107	>2001	10564	>2001	10564	passive	1074
009	106	>2001	10400	>2001	10400	lowest	2642
010	135	1961-1970	37232	1961-1970	14165	low	6765
011	76	1961-1970	20877	1961-1970	7942	low	3793
012	155	<1919	61768	<1919	25685	lowest	3868
013	179	<1919	71504	<1919	29734	lowest	4478
014	174	1981-1990	25388	1981-1990	13346	passive	1740
015	133	1981-1990	19360	1981-1990	10178	passive	1327
016	125	1919-1944	43718	1919-1944	13356	passive	1251
017	179	1919-1944	62503	1919-1944	19094	passive	1788
018	172	1981-1990	25138	1981-1990	13215	lowest	4307
019	162	1981-1990	23602	1981-1990	12408	lowest	4044
020	146	<1919	58336	<1919	24258	passive	1461
021	87	<1919	34765	<1919	14456	passive	871
022	154	1919-1944	53772	1919-1944	16427	passive	1538
023	177	1919-1944	62019	1919-1944	18946	passive	1774
024	158	<1919	62925	<1919	26166	lowest	3941
025	50	1919-1944	17382	1919-1944	5310	low	2486
026	133	1961-1970	36671	1961-1970	13952	low	6663
027	151	>2001	14862	>2001	14862	passive	1510
028	139	>2001	13677	>2001	13677	lowest	3475
029	121	>2001	11886	>2001	11886	lowest	3020
030	95	<1919	37832	<1919	15732	low	4739
031	123	1971-1980	33826	1971-1980	12869	lowest	3073
032	145	1981-1990	21127	1981-1990	11106	lowest	3620
033	117	1991-2000	11995	1991-2000	9697	low	5862
034	84	1981-1990	12238	1981-1990	6434	passive	839
035	105	<1919	41952	<1919	17445	lowest	2627

Table B.3: The square meter, construction year or type and the thermal heating demand for each household for the three different scenarios (Default, Refurbished and Minimal), HH...household, HD...Heating Demand; 2/4

HH	Size	Default		Refurbished		Minimal	
	[m^2]	Year/Type	HD [kWh/a]	Year/Type	HD [kWh/a]	Year/Type	HD [kWh/a]
036	120	<1919	47921	<1919	19927	low	6002
037	126	<1919	50214	<1919	20880	passive	1258
038	174	1981-1990	25366	1981-1990	13335	passive	1739
039	160	<1919	63678	<1919	26479	low	7976
040	157	1991-2000	16092	1991-2000	13009	lowest	3933
041	134	1961-1970	36946	1961-1970	14056	lowest	3356
042	158	1945-1960	34100	1945-1960	11966	lowest	3941
043	99	1991-2000	10159	1991-2000	8213	lowest	2483
044	111	1961-1970	30513	1961-1970	11609	low	5544
045	151	1981-1990	22024	1981-1990	11578	low	7548
046	140	1981-1990	20491	1981-1990	10772	passive	1404
047	173	1971-1980	47503	1971-1980	18072	lowest	4315
048	159	1991-2000	16222	1991-2000	13114	low	7929
049	143	1991-2000	14658	1991-2000	11849	passive	1433
050	179	>2001	17592	>2001	17592	low	8939
051	133	<1919	52947	<1919	22017	passive	1326
052	95	1971-1980	26114	1971-1980	9935	passive	949
053	160	1945-1960	34654	1945-1960	12160	passive	1602
054	160	>2001	15793	>2001	15793	low	8025
055	74	1945-1960	16104	1945-1960	5651	lowest	1861
056	62	>2001	6058	>2001	6058	low	3078
057	39	1971-1980	7868	1971-1980	2884	lowest	985
058	53	1971-1980	10604	1971-1980	3887	lowest	1327
059	95	1971-1980	18873	1971-1980	6918	lowest	2363
060	29	1971-1980	5817	1971-1980	2132	lowest	728
061	128	1971-1980	25621	1971-1980	9391	lowest	3207
062	76	1971-1980	15149	1971-1980	5553	lowest	1896
063	122	1961-1970	33651	1961-1970	12803	low	6114
064	173	1981-1990	25188	1981-1990	13242	low	8632
065	133	1971-1980	36626	1971-1980	13934	lowest	3327
066	154	<1919	61436	<1919	25547	low	7695
067	139	1919-1944	48566	1919-1944	14836	passive	1389
068	69	1981-1990	8219	1981-1990	3574	low	3430
069	69	1981-1990	8295	1981-1990	3608	low	3462
070	51	1981-1990	6102	1981-1990	2654	low	2547

Table B.4: The square meter, construction year or type and the thermal heating demand for each household for the three different scenarios (Default, Refurbished and Minimal), HH...household, HD...Heating Demand; 3/4

HH	Size	Default		Refurbished		Minimal	
	[m^2]	Year/Type	HD [kWh/a]	Year/Type	HD [kWh/a]	Year/Type	HD [kWh/a]
071	52	1981-1990	6243	1981-1990	2715	low	2606
072	48	1945-1960	10815	1945-1960	5245	lowest	1193
073	67	1945-1960	15081	1945-1960	7314	lowest	1664
074	65	1945-1960	14718	1945-1960	7138	lowest	1624
075	48	1945-1960	10919	1945-1960	5296	lowest	1205
076	98	1945-1960	22270	1945-1960	10801	lowest	2457
077	97	1981-1990	11580	1981-1990	5036	passive	967
078	108	1981-1990	12919	1981-1990	5619	passive	1078
079	85	1981-1990	10231	1981-1990	4449	passive	854
080	76	1981-1990	9099	1981-1990	3957	passive	760
081	102	1981-1990	12199	1981-1990	5305	passive	1018
082	77	1981-1990	9228	1981-1990	4013	passive	770
083	73	1945-1960	16480	1945-1960	7993	passive	727
084	112	1945-1960	25404	1945-1960	12321	passive	1121
085	67	1945-1960	15292	1945-1960	7416	passive	675
086	51	1945-1960	11494	1945-1960	5574	passive	507
087	121	1945-1960	27487	1945-1960	13331	passive	1213
088	158	1945-1960	35773	1945-1960	17350	passive	1579
089	27	1991-2000	2330	1991-2000	1931	passive	272
090	64	1991-2000	5455	1991-2000	4520	passive	636
091	93	1991-2000	8022	1991-2000	6647	passive	935
092	95	1991-2000	8113	1991-2000	6723	passive	946
093	39	1991-2000	3325	1991-2000	2756	passive	388
094	61	1991-2000	5272	1991-2000	4368	passive	614
095	58	1991-2000	4945	1991-2000	4098	passive	576
096	87	1991-2000	7499	1991-2000	6214	passive	874
097	74	1991-2000	6369	1991-2000	5278	passive	742
098	99	1991-2000	8520	1991-2000	7060	passive	993
099	50	1991-2000	4267	1991-2000	3536	passive	497
100	58	1991-2000	4942	1991-2000	4095	passive	576
101	38	1991-2000	3288	1991-2000	2725	passive	383
102	36	1991-2000	3089	1991-2000	2560	passive	360
103	105	1991-2000	8994	1991-2000	7453	passive	1048
104	71	1991-2000	6118	1991-2000	5070	passive	713
105	67	1991-2000	5749	1991-2000	4764	passive	670

Table B.5: The square meter, construction year or type and the thermal heating demand for each household for the three different scenarios (Default, Refurbished and Minimal), HH...household, HD...Heating Demand; 4/4

HH	Size	Default		Refurbished		Minimal	
	[m^2]	Year/Type	HD [kWh/a]	Year/Type	HD [kWh/a]	Year/Type	HD [kWh/a]
106	39	1991-2000	3315	1991-2000	2747	passive	386
107	92	1991-2000	7879	1991-2000	6529	passive	918
108	64	1991-2000	5476	1991-2000	4538	passive	638
109	58	1991-2000	4993	1991-2000	4137	passive	582
110	88	1991-2000	7527	1991-2000	6237	passive	877
111	77	1991-2000	6579	1991-2000	5452	passive	767
112	36	1991-2000	3049	1991-2000	2527	passive	355
113	55	1961-1970	7810	1961-1970	3725	low	2731
114	48	1961-1970	6802	1961-1970	3244	low	2378
115	97	1961-1970	13871	1961-1970	6615	low	4850
116	31	1961-1970	4380	1961-1970	2089	low	1532
117	32	1961-1970	4579	1961-1970	2184	low	1601
118	46	1961-1970	6597	1961-1970	3146	low	2307
119	87	1961-1970	12434	1961-1970	5930	low	4348
120	82	1961-1970	11797	1961-1970	5626	low	4125
121	74	1961-1970	10599	1961-1970	5055	low	3706
122	73	1961-1970	10388	1961-1970	4954	low	3632
123	73	1961-1970	10433	1961-1970	4976	low	3648
124	49	1961-1970	7048	1961-1970	3362	low	2464
125	75	1961-1970	10689	1961-1970	5098	low	3737
126	52	1961-1970	7458	1961-1970	3557	low	2608
Total	12 708	-	2 546 417	-	1 209 594	-	329 968
Avg.	100.85	-	200.38	-	95.18	-	25.97

The following code shows the settings for the tap profile generation with the tool DHW-calc [57].

```
LOGFILE  MFH126_log.txt

  for a multi-family house with 126 households


  Total duration:         365 days
  Start day :             1. day of the year
  Mean daily draw-off vol.: 13500 l/day
  No. of categories:      4
  Time step duration:     15 min


 FLOW RATE SETTINGS

  Categories:              1    2     3     4

  Mean flow Rate:         4   24   480   160  l/h
  Duration of draw-off:   15     15     15     15  min
  portion:                14    36    10    40  %
  sigma:                  8   8   8   8  l/h
  min. flow rate:         1 l/h
  max. flow rate:         151200 l/h


 PROBABILITY FUNCTION SETTINGS

  Standard probability distribution
  Ratio of the mean daily draw-off volume tapped
    on weekend-days/on weekdays: 120 %
  Seasonal Variations:
    Sine amplitude: 10 %
    Day of sine maximum: 45
  Holiday Periods:
  Relative consumption during holiday periods:  0 %
```

Optimisation Results

Table B.6: Optimisation Results 1/3

Scenario	TE01	TE01-red	TE02	TE02-1	TE03	TE04	TE05	TE06	TE07	TE08	TE09
$P_{el.,load,max}$ [MW]	0.1086	0.1086	0.1086	0.1086	0.1086	0.1086	0.1019	0.1143	0.1086	0.1086	0.1086
$E_{el.,load}$ [MWh]	402.8	402.8	402.8	402.8	402.8	402.8	378.1	424.1	402.8	402.8	402.8
$T_{FLH,load}$ [h]	3711	3711	3711	3711	3711	3711	3711	3711	3711	3711	3711
$P_{el,prod.,max}$ [MW]	0.6871	0.2020	0.6871	0.6871	0.6871	0.6871	0.6871	0.6871	0.6871	0.6871	0.6871
$E_{el.,prod}$ [MWh]	1370.1	402.9	1370.1	1370.1	1370.1	1370.1	1370.1	1370.1	1370.1	1370.1	1370.1
$T_{FLH,prod.}$ [h]	1994	1994	1994	1994	1994	1994	1994	1994	1994	1994	1994
Prod./Load	3.40	1.00	3.40	3.40	3.40	3.40	3.62	3.23	3.40	3.40	3.40
$P_{BIO,max}$ [MW]	0.080	0.024	0.080	0.080	0.080	0.080	0.080	0.080	0.080	0.080	0.080
E_{BIO} [MWh]	440.8	129.6	440.8	440.8	440.8	440.8	440.8	440.8	440.8	440.8	440.8
$T_{FLH,BIO}$ [h]	5488	5488	5488	5488	5488	5488	5488	5488	5488	5488	5488
$P_{PV,max}$ [MW]	0.6175	0.1816	0.6175	0.6175	0.6175	0.6175	0.6175	0.6175	0.6175	0.6175	0.6175
E_{PV} [MWh]	929.3	273.2	929.3	929.3	929.3	929.3	929.3	929.3	929.3	929.3	929.3
$T_{FLH,PV}$ [h]	1505	1505	1505	1505	1505	1505	1505	1505	1505	1505	1505
$P_{th.,load,max}$ [MW]	0.4052	0.4052	0.1795	0.1795	0.7550	0.4052	0.1795	0.7550	0.4052	0.4052	0.4052
$E_{load,th.}$ [MWh]	1431.5	1431.5	554.2	554.2	2759.8	1431.5	554.2	2759.8	1431.5	1431.5	1431.5
$T_{FLH,load,th.}$ [h]	3533	3533	3087	3087	3655	3533	3087	3655	3533	3533	3533
$P_{BIO,th.,max}$ [MW]	0.1735	0.0510	0.1735	0.1735	0.1735	0.1735	0.1735	0.1735	0.1735	0.1735	0.1735
$E_{BIO,th.}$ [MWh]	968.4	284.8	968.4	968.4	968.4	968.4	968.4	968.4	968.4	968.4	968.4
$T_{FLH,BIO,th.}$ [h]	5581	5581	5581	5581	5581	5581	5581	5581	5581	5581	5581
$E_{imp.Slack}$ [MWh]	-20.9	-173.1	-20.7	-20.9	-20.6	-45.7	-14.5	-22.5	-337.6	-145.8	-7.1
$E_{exp.Slack}$ [MWh]	941.5	173.1	941.2	941.4	941.2	880.2	954.5	924.1	551.0	642.0	886.3
$E_{imp.Gas}$ [MWh]	383.4	943.1	160.2	160.2	1627.6	383.4	160.2	1627.6	383.4	383.4	383.4
$E_{dist.Heating}$ [MWh]	1067.3	535.6	402.0	402.0	1213.6	1067.3	402.0	1213.6	1067.3	1067.3	1067.3
$P_{P2H,inst.}$ [MW]	0	0	0	0	0	0	0	0	0.1498	0.1098	0
P_{H2SNG} [MW]	0	0	0	0	0	0	0	0	0	0	0
$P_{HS,inst.}$ [MW]	0	0	0	0	0	0	0	0	0	0	0
$P_{FuelCell,inst.}$ [MW]	0	0	0	0	0	0	0	0	0	0	0
$E_{HSinst.}$ [MWh]	0	0	0	0	0	0	0	0	0	0	0
$E_{P2Hinst.}$ [MWh]	0	0	0	0	0	0	0	0	0	0	0
$E_{H2prod.}$ [MWh]	0	0	0	0	0	0	0	0	440.1	189.1	0
$E_{H2inf.}$ [MWh]	0	0	0	0	0	0	0	0	440.1	189.1	0
$E_{SNGinf.}$ [MWh]	0	0	0	0	0	0	0	0	0	0	0
$E_{HSrollin}$ [MWh]	0	0	0	0	0	0	0	0	0	0	0
$P_{cent.St.,inst}$ [MW]	0	0	0	0	0	0	0	0	0	0	0
$E_{cent.St.,inst}$ [MWh]	0	0	0	0	0	0	0	0	0	0	0
E/PcentS [h]	0	0	0	0	0	0	0	0	0	0	0
$E_{cent.rollin}$ [MWh]	0	0	0	0	0	0		0	0	0	0
$P_{dec.St.,inst}$ [MW]	0.369	0.001	0.369	0.369	0.369	0.049	0.386	0.368	0.412	0.051	0.571
$E_{dec.rollin}$ [MWh]	0.738	0.002	0.738	0.738	0.738	0.099	0.773	0.737	0.824	0.102	1.143
E/PdecS [h]	2	2	2	2	2	2	2	2	2	2	2
$E_{dec.rollin}$ [MWh]	258.1	0.1	258.1	258.1	258.1	27.1	287.1	245.9	243.4	45.5	486.4
$P_{heat.St.,inst}$ [MW]	0.1319	0.0368	0.7140	0.0368	0.0679	0.1009	0.7140	0.0679	0.1319	0.1009	0.1319
$E_{th.inst}$ [MWh]	106.61	28.49	0.09	0.09	28.49	106.61	0.09	28.49	106.61	106.61	106.61
$E_{th.rollin}$ [MWh]	771.68	40.72	3971.91	7.71	68.21	167.49	3971.91	68.21	771.68	228.32	771.68
$P_{HeatPump.,inst.el.}$ [MW]	0	0	0	0	0	0	0	0	0	0	0
$P_{HeatPump.,max.th.}$ [MW]	0	0	0	0	0	0	0	0	0	0	0
$E_{heatpump,th.}$ [MWh]	0	0	0	0	0	0	0	0	0	0	0
$T_{FLH,heatpump}$ [h]	0	0	0	0	0	0	0	0	0	0	0
$P_{infeedRed.}$ [MW]	0	0	0	0	0	0.188	0	0	0	0.293	0
$E_{infeedRed.}$ [MWh]	0	0	0	0	0	127.8	0	0	0	157.8	0
$P_{infeedRed.th.}$ [MW]	0	0	0	0.164	0	0.125	0	0	0	0.185	0
$E_{infeedRed.th.}$ [MWh]	0	0	0	824.2	0	125.6	0	0	0	113.0	0
$E_{loss,th.net.}$ [MWh]	0.1953	0.0495	0.0192	0.0192	0.2688	0.1953	0.0192	0.2688	0.1953	0.1953	0.1953

Table B.7: Optimisation Results 2/3

Scenario	TE10	TE11	TE12	TE13	TE14	TE15	TE16	WR01	WR02	WR03	WR04
$P_{el.,load,max}$ [MW]	0,1086	0,1086	0,1086	0,1086	0,1086	0,1086	0,1086	0,1086	0,1086	0,1086	0,1086
$E_{el.,load}$ [MWh]	402.8	402.8	402.8	402.8	402.8	402.8	402.8	402.8	402.8	402.8	402.8
$T_{FLH,load}$ [h]	3711	3711	3711	3711	3711	3711	3711	3711	3711	3711	3711
$P_{el,prod.,max}$ [MW]	0.6871	0.6871	0.6871	0.6871	0.6871	0.6871	0.6871	0.6871	0.6871	0.6871	0.6871
$E_{el.,prod}$ [MWh]	1370.1	1370.1	1370.1	1370.1	1370.1	1370.1	1370.1	1370.1	1370.1	1370.1	1370.1
$T_{FLH,prod.}$ [h]	1994	1994	1994	1994	1994	1994	1994	1994	1994	1994	1994
Prod./Load	3.40	3.40	3.40	3.40	3.40	3.40	3.40	3.40	3.40	3.40	3.40
$P_{BIO,max}$ [MW]	0.080	0.080	0.080	0.080	0.080	0.080	0.080	0.080	0.080	0.080	0.080
E_{BIO} [MWh]	440.8	440.8	440.8	440.8	440.8	440.8	440.8	440.8	440.8	440.8	440.8
$T_{FLH,BIO}$ [h]	5488	5488	5488	5488	5488	5488	5488	5488	5488	5488	5488
$P_{PV,max}$ [MW]	0.6175	0.6175	0.6175	0.6175	0.6175	0.6175	0.6175	0.6175	0.6175	0.6175	0.6175
E_{PV} [MWh]	929.3	929.3	929.3	929.3	929.3	929.3	929.3	929.3	929.3	929.3	929.3
$T_{FLH,PV}$ [h]	1505	1505	1505	1505	1505	1505	1505	1505	1505	1505	1505
$P_{th.,load,max}$ [MW]	0.4052	0.4052	0.4052	0.4052	0.4052	0.4052	0.4052	0.4052	0.1795	0.7550	0.4052
$E_{load,th.}$ [MWh]	1431.5	1431.5	1431.5	1431.5	1431.5	1431.5	1431.5	1431.5	554.2	2759.8	1431.5
$T_{FLH,load,th.}$ [h]	3533	3533	3533	3533	3533	3533	3533	3533	3087	3655	3533
$P_{BIO,th.,max}$ [MW]	0.1735	0.1735	0.1735	0.1735	0.1735	0.1735	0.1735	0.1735	0.1735	0.1735	0.1735
$E_{BIO,th.}$ [MWh]	968.4	968.4	968.4	968.4	968.4	968.4	968.4	968.4	968.4	968.4	968.4
$T_{FLH,BIO,th.}$ [h]	5581	5581	5581	5581	5581	5581	5581	5581	5581	5581	5581
$E_{imp.Slack}$ [MWh]	-30.8	-5.1	0	0	-22.3	-1.7	-1.4	0.0	0.0	0.0	-0.8
$E_{exp.Slack}$ [MWh]	778.9	840.9	558.1	553.1	689.2	464.7	462.3	526.9	526.9	526.9	563.7
$E_{imp.Gas}$ [MWh]	383.4	383.4	383.4	383.4	383.4	383.4	383.4	383.4	160.2	1627.6	383.4
$E_{dist.Heating}$ [MWh]	1067.3	1067.3	1067.3	1067.3	1067.3	1067.3	1067.3	1067.3	402.0	1213.6	1067.3
$P_{P2H,inst.}$ [MW]	0	0	0	0	0	0	0	0.0548	0.0548	0.0548	0.0497
P_{H2SNG} [MW]	0	0	0	0	0	0	0	0.0254	0.0254	0.0254	0.0237
$P_{HS,inst.}$ [MW]	0	0	0	0	0	0	0	0	0	0	0
$P_{FuelCell,inst.}$ [MW]	0	0	0	0	0	0	0	0	0	0	0
$E_{HSinst.}$ [MWh]	0	0	0	0	0	0	0	0	0	0	0
$E_{P2Hinst.}$ [MWh]	0	0	0	0	0	0	0	0	0	0	0
$E_{H2prod.}$ [MWh]	0	0	0	0	0	0	0	236.5	236.5	236.5	205.7
$E_{H2inf.}$ [MWh]	0	0	0	0	0	0	0	46.0	46.0	46.0	39.3
$E_{SNGinf.}$ [MWh]	0	0	0	0	0	0	0	146.6	146.6	146.6	128.1
$E_{HSrollin}$ [MWh]	0	0	0	0	0	0	0	0	0	0	0
$P_{cent.St.,inst}$ [MW]	0	0	0	0	0	0	0	0	0	0	0
$E_{cent.St.,inst}$ [MWh]	0	0	0	0	0	0	0	0	0	0	0
E/PcentS [h]	0	0	0	0	0	0	0	0	0	0	0
$E_{cent.rollin}$ [MWh]	0	0	0	0	0	0	0	0	0	0	0
$P_{dec.St.,inst}$ [MW]	0.136	0.743	1.194	1.206	0.198	0.450	0.462	0.369	0.369	0.369	0.264
$E_{dec.rollin}$ [MWh]	0.272	1.485	2.389	2.413	0.396	0.900	0.924	0.738	0.738	0.738	0.527
E/PdecS [h]	2	2	2	2	2	2	2	2	2	2	2
$E_{dec.rollin}$ [MWh]	75.0	726.5	2260.7	2288.1	110.0	215.5	217.4	325.5	325.5	325.5	323.5
$P_{heat.St.,inst}$ [MW]	0.1009	0.1319	0.1319	0.1319	0.1009	0.1009	0.1009	0.1319	0.7140	0.0679	0.1009
$E_{th.inst}$ [MWh]	106.61	106.61	106.61	106.61	106.61	106.61	106.61	106.61	0.09	28.49	106.61
$E_{th.rollin}$ [MWh]	147.97	771.68	771.68	771.68	147.53	141.46	146.14	771.68	3971.91	68.21	132.27
$P_{HeatPump.,inst.el.}$ [MW]	0	0	0	0	0	0	0	0	0	0	0
$P_{HeatPump.,max.th.}$ [MW]	0	0	2.25E-06	2.25E-06	0	0	0	0	0	0	2.25E-06
$E_{heatpump,th.}$ [MWh]	0	0	4.06E-05	4.06E-05	0	0	0	0	0	0	4.06E-05
$T_{FLH,heatpump}$ [h]	0	0	1.80E+01	1.80E+01	0	0	0	0	0	0	1.80E+01
$P_{infeedRed.}$ [MW]	0.286	0	0	0	0.355	0.479	0.487	0	0	0	0.121
$E_{infeedRed.}$ [MWh]	205.5	0	0	0	280.5	465.3	467.0	0	0	0	14.00
$P_{infeedRed.th.}$ [MW]	0.182	0	0	0	0.185	0.173	0.181	0	0	0	0.12
$E_{infeedRed.th.}$ [MWh]	129.7	0	0	0	129.8	131.0	130.0	0	0	0	132.93
$E_{loss,th.net.}$ [MWh]	0.1953	0.1953	0.1953	0.1953	0.1953	0.1953	0.1953	0.1953	0.0192	0.2688	0.1953

Table B.8: Optimisation Results 3/3

Scenario	WR05	WR06	ER01	ER01-1	ER01-red	ER02	ER03	ER04	ER05	ER06
$P_{el.,load,max}$ [MW]	0.1019	0.1143	0.1086	0.1086	0.1086	0.1086	0.1086	0.1143	0.1143	0.1086
$E_{el.,load}$ [MWh]	378.1	424.1	402.8	402.8	402.8	402.8	402.8	424.1	424.1	402.8
$T_{FLH,load}$ [h]	3711	3711	3711	3711	3711	3711	3711	3711	3711	3711
$P_{el,prod.,max}$ [MW]	0.6871	0.6871	0.6871	0.6871	0.2020	0.6871	0.6871	0.6871	0.6871	0.6871
$E_{el.,prod}$ [MWh]	1370.1	1370.1	1370.1	1370.1	402.9	1370.1	1370.1	1370.1	1370.1	1370.1
$T_{FLH,prod.}$ [h]	1994	1994	1994	1994	1994	1994	1994	1994	1994	1994
Prod./Load	3.62	3.23	3.40	3.40	1.00	3.40	3.40	3.23	3.23	3.40
$P_{BIO,max}$ [MW]	0.080	0.080	0.080	0.080	0.024	0.080	0.080	0.080	0.080	0.080
E_{BIO} [MWh]	440.8	440.8	440.8	440.8	129.6	440.8	440.8	440.8	440.8	440.8
$T_{FLH,BIO}$ [h]	5488	5488	5488	5488	5488	5488	5488	5488	5488	5488
$P_{PV,max}$ [MW]	0.6175	0.6175	0.6175	0.6175	0.1816	0.6175	0.6175	0.6175	0.6175	0.6175
E_{PV} [MWh]	929.3	929.3	929.3	929.3	273.2	929.3	929.3	929.3	929.3	929.3
$T_{FLH,PV}$ [h]	1505	1505	1505	1505	1505	1505	1505	1505	1505	1505
$P_{th.,load,max}$ [MW]	0.1795	0.7550	0.4052	0.4052	0.4052	0.4052	0.4052	0.7550	0.7550	0.4052
$E_{load,th.}$ [MWh]	554.2	2759.8	1431.5	1431.5	1431.5	1431.5	1431.5	2759.8	2759.8	1431.5
$T_{FLH,load,th.}$ [h]	3087	3655	3533	3533	3533	3533	3533	3655	3655	3533
$P_{BIO,th.,max}$ [MW]	0.1735	0.1735	0.1735	0.1735	0.0510	0.1735	0.1735	0.1735	0.1735	0.1735
$E_{BIO,th.}$ [MWh]	968.4	968.4	968.4	968.4	284.8	968.4	968.4	968.4	968.4	968.4
$T_{FLH,BIO,th.}$ [h]	5581	5581	5581	5581	5581	5581	5581	5581	5581	5581
$E_{imp.Slack}$ [MWh]	0	0	0	0	-253.6	0	0	0	0	0
$E_{exp.Slack}$ [MWh]	435.6	583.0	534.1	641.0	0	510.5	585.3	168.0	152.3	555.8
$E_{imp.Gas}$ [MWh]	160.2	1621.7	0.4	0.4	2.7	0.4	0.4	0.5	0.6	0.4
$E_{dist.Heating}$ [MWh]	402.0	1213.6	1067.3	1067.3	530.8	1067.3	1067.3	1094.8	1090.9	1067.3
$P_{P2H,inst.}$ [MW]	0.0784	0.0412	0.0441	0.0349	0	0.0499	0.0336	0.0474	0.0995	0.0416
P_{H2SNG} [MW]	0.0286	0.0244	0.0119	0.0094	0	0.0119	0.0129	0	0	0.0094
$P_{HS,inst.}$ [MW]	0	0	0	0.02	0	0	0	0.029	0.062	0
$P_{FuelCell,inst.}$ [MW]	0	0	0	0.01	0	0	0	0.001	0.008	0
$E_{HSinst.}$ [MWh]	0	0	0	0.26	0	0	0	1.882	37.036	0
$E_{P2Hinst.}$ [MWh]	0	0	0	12.13	0	0	0	64.0	600.6	0
$E_{H2prod.}$ [MWh]	304.0	189.8	172.9	129.0	0	187.1	142.6	154.8	184.3	156.9
$E_{H2inf.}$ [MWh]	90.9	6.1	80.7	62.5	0	95.2	43.3	152.9	135.2	87.2
$E_{SNGinf.}$ [MWh]	164.1	141.4	71.0	46.9	0	70.8	76.5	0	0	53.7
$E_{HSrollin}$ [MWh]	0	0	0	5.53	0	0	0	1.89	49.13	0
$P_{cent.St.,inst}$ [MW]	0	0	0	0.002	0	0	0	0	0.021	0
$E_{cent.St.,inst}$ [MWh]	0	0	0	0.032	0	0	0	0	0.128	0
E/PcentS [h]	0	0	0	17.1	0	0	0	0	6.08	0
$E_{cent.rollin}$ [MWh]	0	0	0	2.85	0	0	0	0	28.28	0
$P_{dec.St.,inst}$ [MW]	0.386	0.368	0.358	0.232	2.080	0.358	0.358	1.404	0.677	0.306
$E_{dec.rollin}$ [MWh]	0.773	0.736	0.716	0.465	0.848	0.716	0.716	2.808	1.354	0.611
E/PdecS [h]	2	2	2	2	0.407	2	2	2	2	2
$E_{dec.rollin}$ [MWh]	364.5	306.6	316.2	126.0	136.6	320.0	303.3	472.3	355.2	317.1
$P_{heat.St.,inst}$ [MW]	0.7140	0.0679	0.1319	0.1319	0.0834	0.1319	0.1319	0.3751	0.3560	0.1009
$E_{th.inst}$ [MWh]	0.09	28.49	106.61	106.61	56.68	106.61	106.61	556.08	563.24	106.61
$E_{th.rollin}$ [MWh]	3971.91	68.21	771.68	771.68	63.86	771.68	771.68	639.48	658.19	323.44
$P_{HeatPump.,inst.el.}$ [MW]	0	0.0002	0.0280	0.0280	0.0623	0.0280	0.0280	0.1334	0.1377	0.0280
$P_{HeatPump.,max.th.}$ [MW]	0	0.0007	0.1027	0.1027	0.2334	0.1027	0.1027	0.4745	0.4920	0.1027
$E_{heatpump,th.}$ [MWh]	0	5.6	363.9	363.9	898.2	363.9	363.9	1664.5	1668.3	363.9
$T_{FLH,heatpump}$ [h]	0	8179.8	3541.4	3541.4	3847.6	3541.4	3541.4	3507.7	3390.5	3541.4
$P_{infeedRed.}$ [MW]	0	0	0	0	0	0	0	0	0	0.0455
$E_{infeedRed.}$ [MWh]	0	0	0	0	0	0	0	0	0	3.928
$P_{infeedRed.th.}$ [MW]	0	0	0	0	0	0	0	0	0	0.185
$E_{infeedRed.th.}$ [MWh]	0	0	0	0	0	0	0	0	0	93.189
$E_{loss,th.net.}$ [MWh]	0.0192	0.2688	0.1953	0.1953	0.0660	0.1953	0.1953	0.5107	0.5076	0.1953